Advanced exchange-correlation functionals

Iurii Timrov

Paul Scherrer Institut (PSI), Switzerland

Advanced exchange-correlation functionals

Iurii Timrov
Paul Scherrer Institut (PSI), Switzerland

Arosa (Grisons, Switzerland), 27th December 1925

“At the moment I am struggling with a new atomic theory. I am very optimistic about this thing and expect that if I can only… solve it, it will be very beautiful”

Erwin Schrödinger

The Nobel Prize in Chemistry 1998

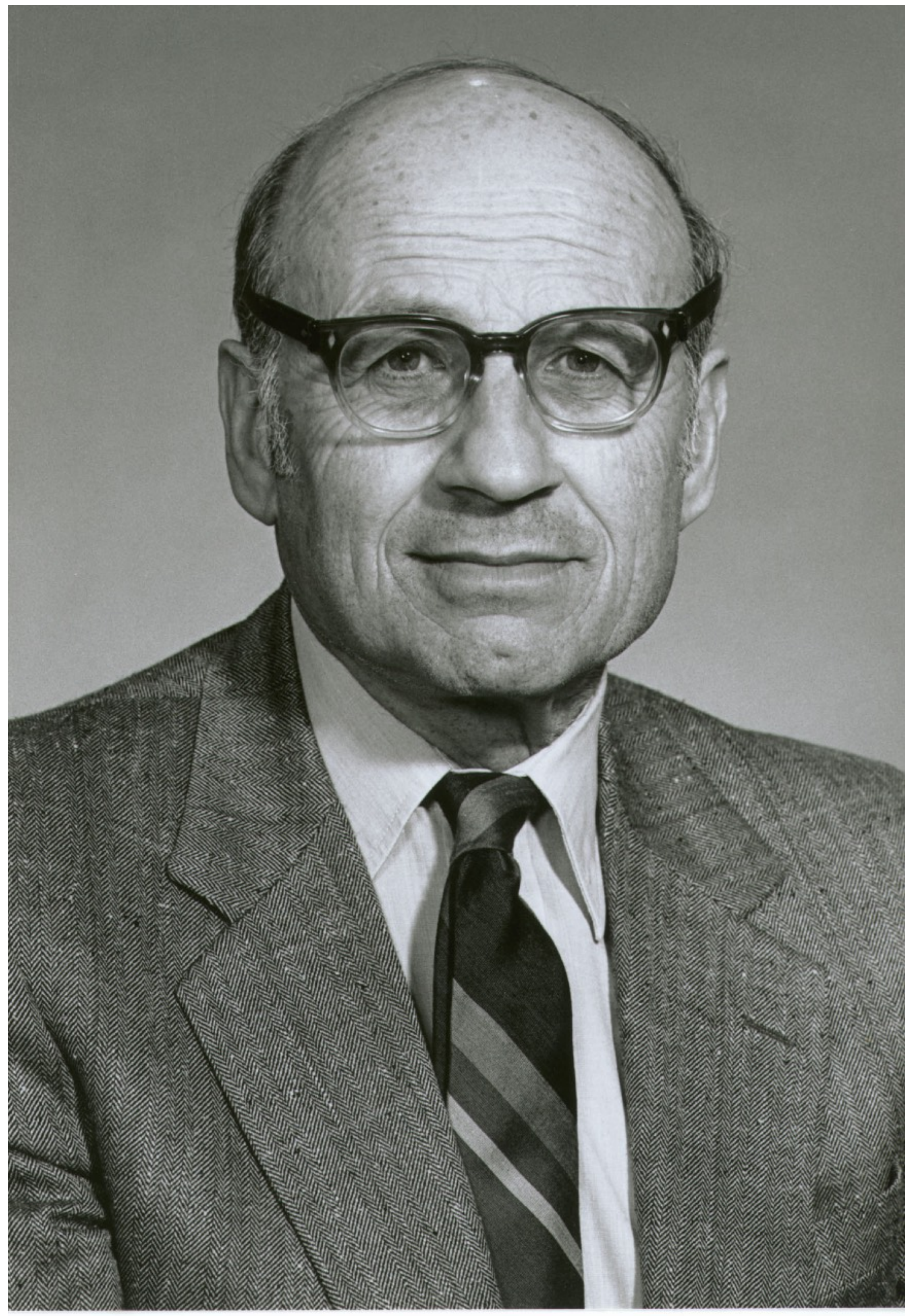

Walter Kohn
(1923 - 2016)

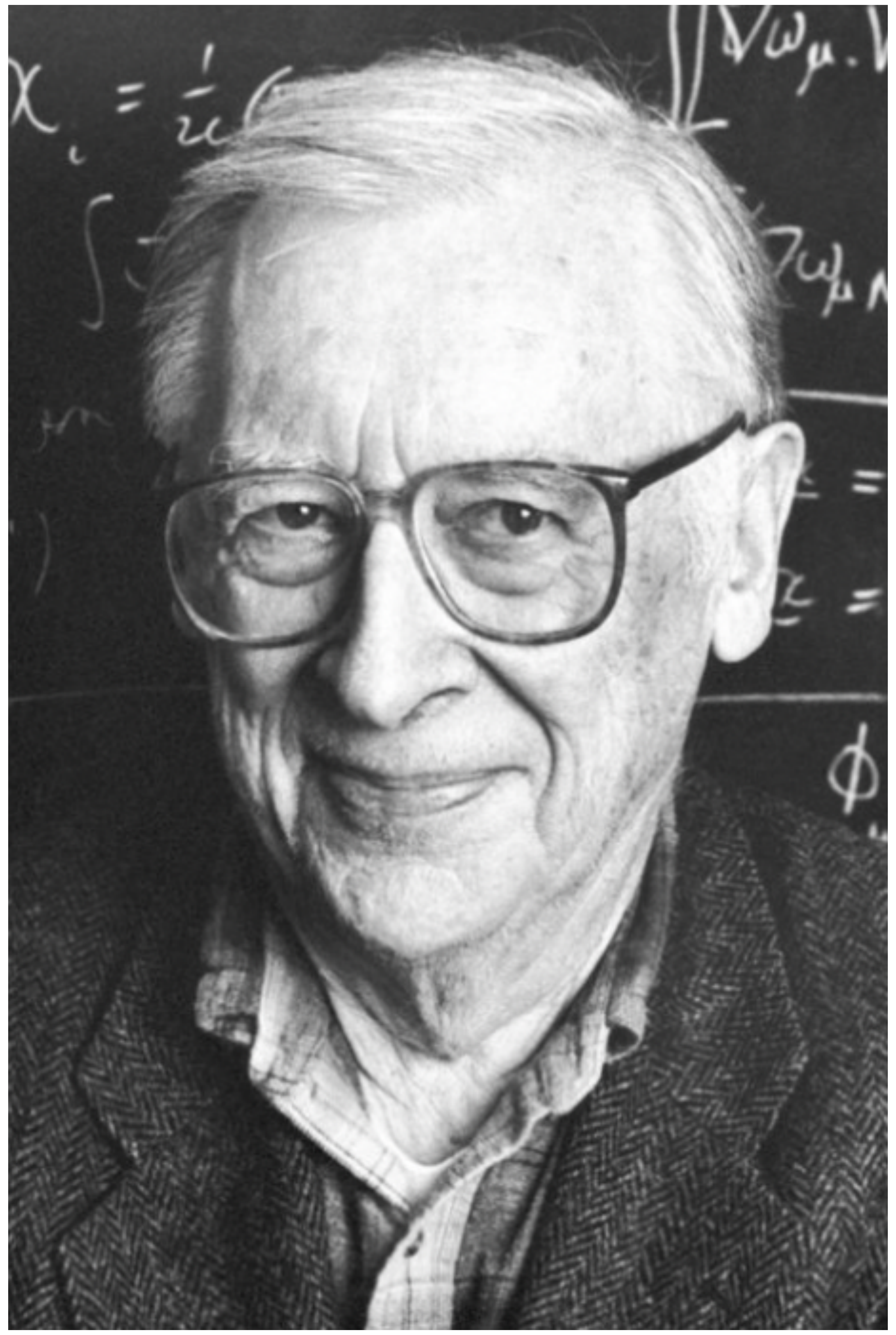

John A. Pople
(1925 - 2004)

The Nobel Prize in Chemistry 1998 was divided equally between Walter Kohn "for his development of the density-functional theory" and John A. Pople "for his development of computational methods in quantum chemistry"

Most cited papers in the history of the American Physical Society (from 1893)

	Journal	# cites	Title	Author(s)
1	PRL (1996)	78085	Generalized Gradient Approximation Made Simple	Perdew, Burke, Ernzerhof
2	PRB (1988)	67303	Development of the Colle-Salvetti Correlation-Energy …	Lee, Yang, Parr
3	PRB (1996)	41683	Efficient Iterative Schemes for Ab Initio Total-Energy …	Kresse and Furthmuller
4	PR (1965)	36841	Self-Consistent Equations Including Exchange and Correlation …	Kohn and Sham
5	PRA (1988)	36659	Density-Functional Exchange-Energy Approximation ...	Becke
6	PRB (1976)	31865	Special Points for Brillouin-Zone Integrations	Monkhorst and Pack
7	PRB (1999)	30940	From Ultrasoft Pseudopotentials to the Projector Augmented …	Kresse and Joubert
8	PRB (1994)	30801	Projector Augmented-Wave Method	Blochl
9	PR (1964)	30563	Inhomogeneous Electron Gas	Hohenberg and Kohn
10	PRB (1993)	19903	Ab initio Molecular Dynamics for Liquid Metals	Kresse and Hafner
11	PRB (1992)	17286	Accurate and Simple Analytic Representation of the Electron …	Perdew and Wang
12	PRB (1990)	15618	Soft Self-Consistent Pseudopotentials in a Generalized …	Vanderbilt
13	PRB (1992)	15142	Atoms, Molecules, Solids, and Surfaces - Applications of the …	Perdew, Chevary, …
14	PRB (1981)	14673	Self-Interaction Correction to Density-Functional Approx. …	Perdew and Zunger
15	PRB (1986)	13907	Density-Functional Approx. for the Correlation-Energy …	Perdew
16	RMP (2009)	13513	The Electronic Properties of Graphene	Castro Neto et al.
17	PR (1934)	12353	Note on an Approximation Treatment for Many-Electron Systems	Moller and Plesset
18	PRB (1972)	11840	Optical Constants on Noble Metals	Johnson and Christy
19	PRB (1991)	11580	Efficient Pseudopotentials for Plane-Wave Calculations	Troullier and Martins
20	PRL (1980)	10784	Ground-State of the Electron-Gas by a Stochastic Method	Ceperley and Alder

The top 100 papers

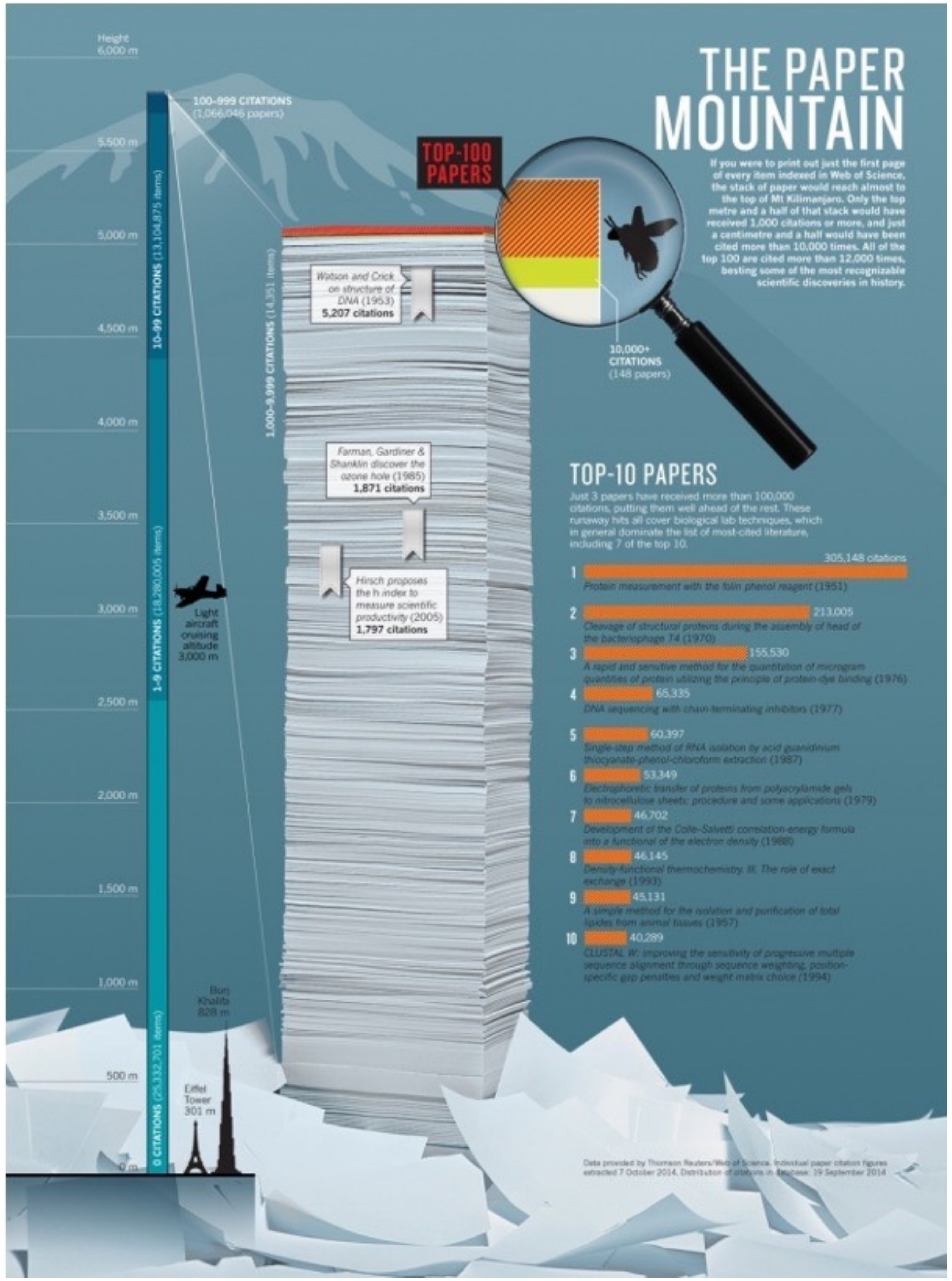

THE PAPER MOUNTAIN

If you were to print out just the first page of every item indexed in Web of Science, the stack of paper would reach almost to the top of Mt Kilimanjaro. Only the top metre and a half of that stack would have received 1,000 citations or more, and just a centimetre and a half would have been cited more than 10,000 times. All of the top 100 are cited more than 12,000 times, besting some of the most recognizable scientific discoveries in history.

Watson and Crick on structure of DNA (1953) **5,207 citations**

Farman, Gardiner & Shanklin discover the ozone hole (1985) **1,871 citations**

Hirsch proposes the h index to measure scientific productivity (2005) **1,797 citations**

TOP-10 PAPERS

Just 3 papers have received more than 100,000 citations, putting them well ahead of the rest. These runaway hits all cover biological lab techniques, which in general dominate the list of most-cited literature, including 7 of the top 10.

1 305,148 citations
Protein measurement with the folin phenol reagent (1951)

2 213,005
Cleavage of structural proteins during the assembly of head of the bacteriophage T4 (1970)

3 155,530
A rapid and sensitive method for the quantitation of microgram quantities of protein utilizing the principle of protein-dye binding (1976)

4 65,335
DNA sequencing with chain-terminating inhibitors (1977)

5 60,397
Single-step method of RNA isolation by acid guanidinium thiocyanate-phenol-chloroform extraction (1987)

6 53,349
Electrophoretic transfer of proteins from polyacrylamide gels to nitrocellulose sheets: procedure and some applications (1979)

7 46,702
Development of the Colle–Salvetti correlation-energy formula into a functional of the electron density (1988)

8 46,145
Density-functional thermochemistry. III. The role of exact exchange (1993)

9 45,131
A simple method for the isolation and purification of total lipides from animal tissues (1957)

10 40,289
CLUSTAL W: improving the sensitivity of progressive multiple sequence alignment through sequence weighting, position-specific gap penalties and weight matrix choice (1994)

Data provided by Thomson Reuters/Web of Science. Individual paper citation figures extracted 7 October 2014. Distribution of citations in database: 19 September 2014

12 papers on density functional theory in the top-100 most cited papers in the entire scientific, medical, engineering literature, ever.

Nature, Oct 2014

From a many-body to a one-body problem

$$\Psi(\mathbf{r}_1, \mathbf{r}_2, \ldots, \mathbf{r}_N)$$

$$\varphi(\mathbf{r})$$

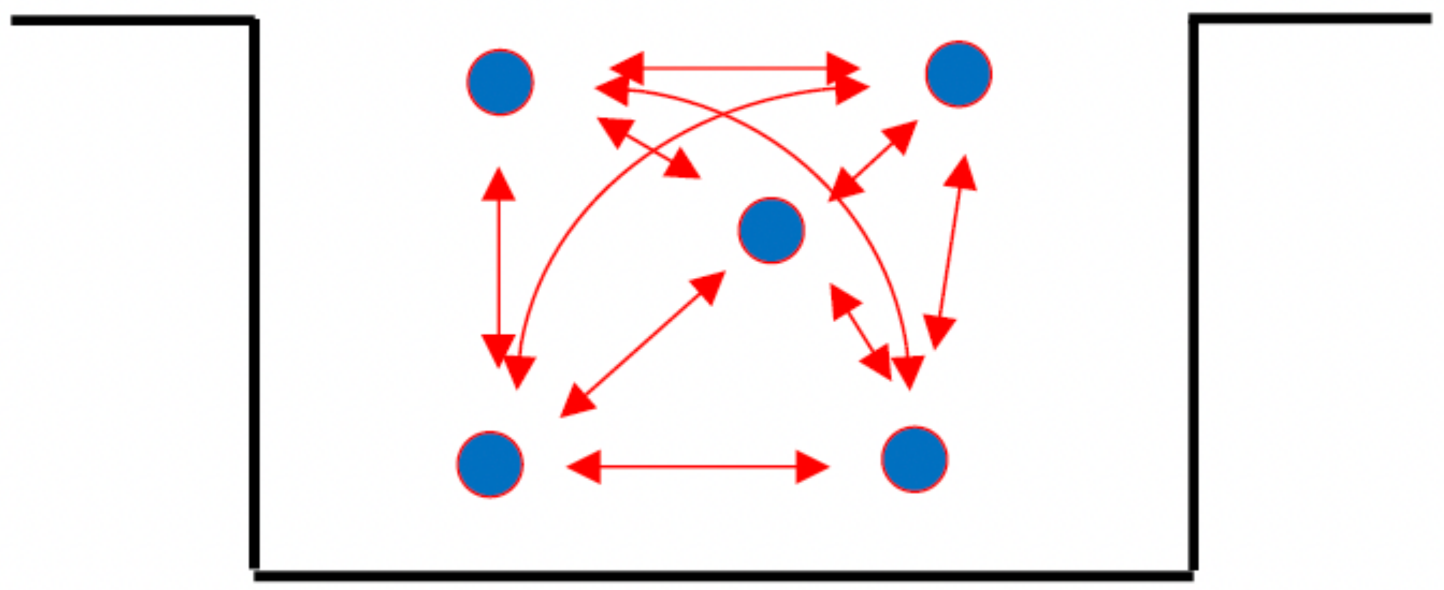

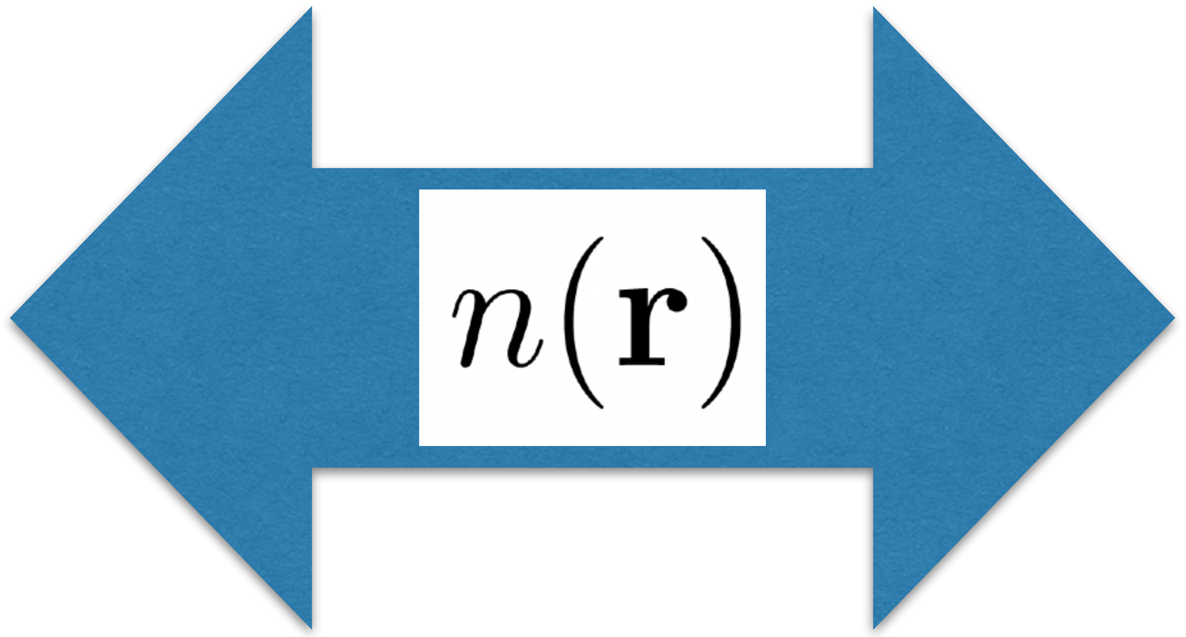

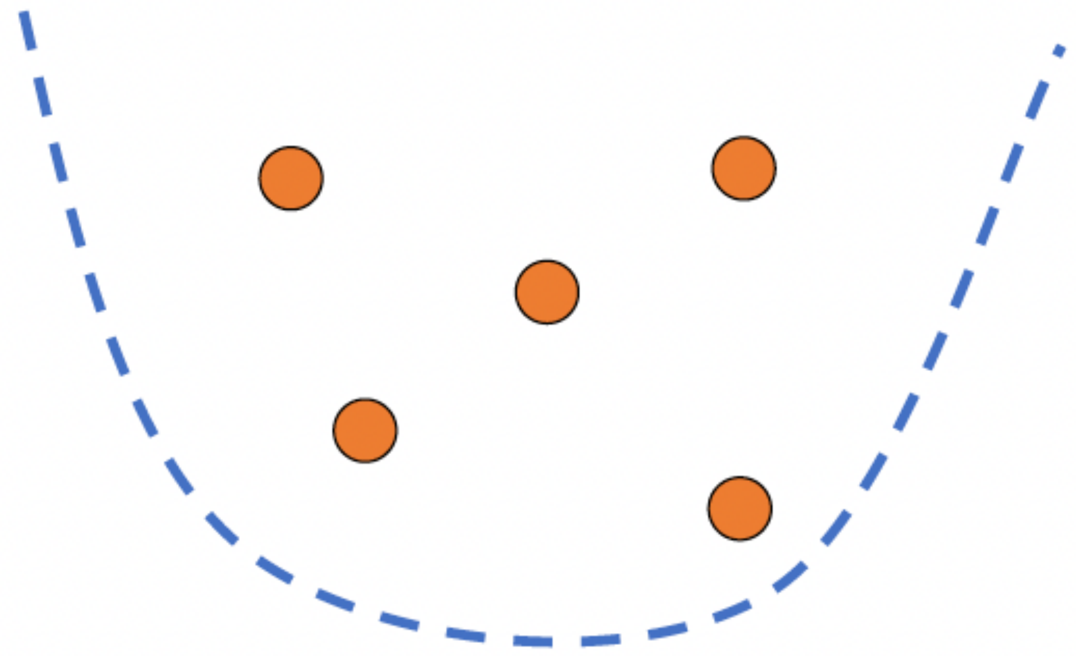

● electrons
↔ interaction
— external potential $v_{ext}(\mathbf{r})$

● Kohn-Sham particles (non-interacting)
- - - effective potential $v_{KS}(\mathbf{r})$

$$n(\mathbf{r}) = \sum_i^{occ} \int |\Psi_i(\mathbf{r}, \mathbf{r}_2, \ldots, \mathbf{r}_N)|^2 d\mathbf{r}_2 \ldots d\mathbf{r}_N$$

$$n(\mathbf{r}) = \sum_i^{occ} |\varphi_i(\mathbf{r})|^2$$

Density-functional theory

Kohn-Sham equation:

$$\boxed{\left(-\frac{\hbar^2}{2m_0}\nabla^2 + V_{KS}(\mathbf{r})\right)\varphi_i(\mathbf{r}) = \varepsilon_i\,\varphi_i(\mathbf{r})}$$

$$\begin{aligned} V_{KS}(\mathbf{r}) &= V_H(\mathbf{r}) + V_{\mathrm{xc}}(\mathbf{r}) + V_{ext}(\mathbf{r}) \\ &= e^2 \int \frac{n(\mathbf{r}')}{|\mathbf{r}-\mathbf{r}'|}\,d\mathbf{r}' + \underbrace{\frac{\delta E_{\mathrm{xc}}[n]}{\delta n(\mathbf{r})}}_{?} + V_{ext}(\mathbf{r}) \end{aligned}$$

Density-functional theory

Kohn-Sham equation:

$$\boxed{\left(-\frac{\hbar^2}{2m_0}\nabla^2 + V_{KS}(\mathbf{r})\right)\varphi_i(\mathbf{r}) = \varepsilon_i\,\varphi_i(\mathbf{r})}$$

$$\begin{aligned} V_{KS}(\mathbf{r}) &= V_H(\mathbf{r}) + V_{\mathrm{xc}}(\mathbf{r}) + V_{ext}(\mathbf{r}) \\ &= e^2\int \frac{n(\mathbf{r}')}{|\mathbf{r}-\mathbf{r}'|}\,d\mathbf{r}' + \underset{?}{\boxed{\frac{\delta E_{\mathrm{xc}}[n]}{\delta n(\mathbf{r})}}} + V_{ext}(\mathbf{r}) \end{aligned}$$

Local density approximation (LDA):

$$E_{\mathrm{xc}}^{LDA}[n] = \int \varepsilon_{\mathrm{xc}}^{hom}(n(\mathbf{r}))\,n(\mathbf{r})\,d\mathbf{r}$$

Generalized-gradient approximation (GGA):

$$E_{\mathrm{xc}}^{GGA}[n] = \int \varepsilon_{\mathrm{xc}}(n(\mathbf{r}),\nabla n(\mathbf{r}))\,n(\mathbf{r})\,d\mathbf{r}$$

PBE, PBEsol, …

Some drawbacks of LDA / GGA

- Self-interaction errors

Consequences:
- over-delocalization of electrons (*d* and *f*)
- incorrect description of charge transfer
- incorrect energetics of chemical reactions
- underestimation of the band gaps
- …

- Lack of non-locality

Consequences:
- incorrect description of weak long-range (Van der Waals) interactions
- inadequate description of bond breaking and formation
- no Rydberg series
- …

Self-interaction error

Self-interaction errors arrise from an incomplete cancellation of self-Coulomb terms by the approximate exchange-correlation energy terms

total charge density

Hartree potential
felt by each electron →

$$V_H(\mathbf{r}) = e^2 \int \frac{n(\mathbf{r}')}{|\mathbf{r} - \mathbf{r}'|} d\mathbf{r}'$$

An electron interacts with itself → self-interaction (unphysical)

A self-interaction problem in DFT

Due to approximations to the exchange-correlation energy E_{xc}, each electron interacts with itself (which is unphysical).

A self-interaction problem in DFT

Due to approximations to the exchange-correlation energy E_{xc}, each electron interacts with itself (which is unphysical).

Analogy: *A dog looking at a mirror and barking at its own reflection, thinking it's another dog.*

The dog doesn't realize it's barking at itself (i.e. “interacts with itself”), just like electrons in approximate DFT are interacting with themselves!

A self-interaction problem in DFT

Due to approximations to the exchange-correlation energy $E_{\rm xc}$, each electron interacts with itself (which is unphysical).

Analogy: *A dog looking at a mirror and barking at its own reflection, thinking it's another dog.*

The dog doesn't realize it's barking at itself (i.e. "interacts with itself"), just like electrons in approximate DFT are interacting with themselves!

Self-interaction error

The simplest example: the dissociation of H_2^+

The problem: approximate DFT gives only one solution - equal splitting of the charge

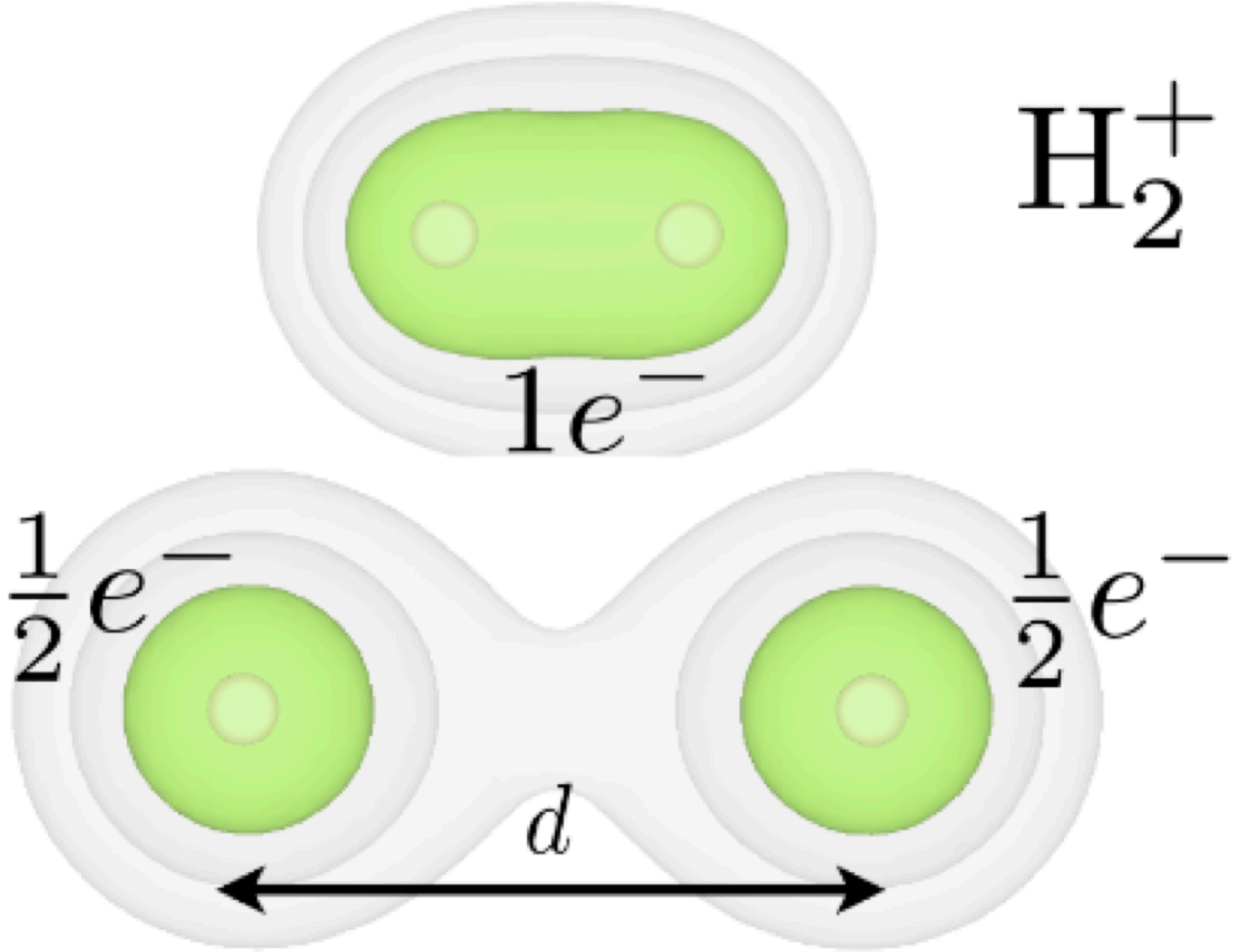

Perdew, Parr, Levy, Balduz, PRL (1982).

Self-interaction error

The simplest example: the dissociation of H_2^+

The problem: approximate DFT gives only one solution - equal splitting of the charge

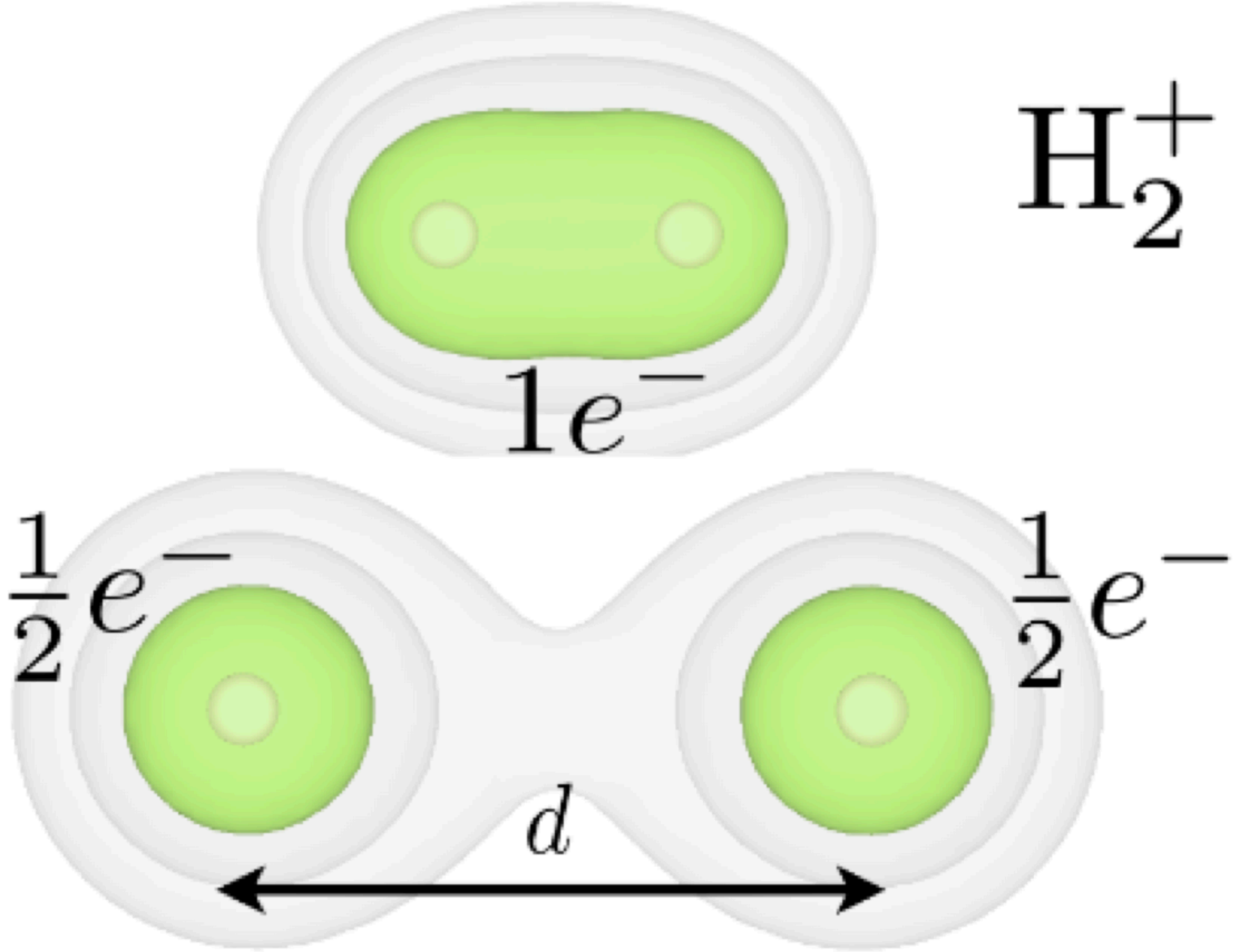

Perdew, Parr, Levy, Balduz, PRL (1982).

Origin of the problem: self-interaction error (**spurious quadratic energy change** when adding/removing a fraction of an electron)

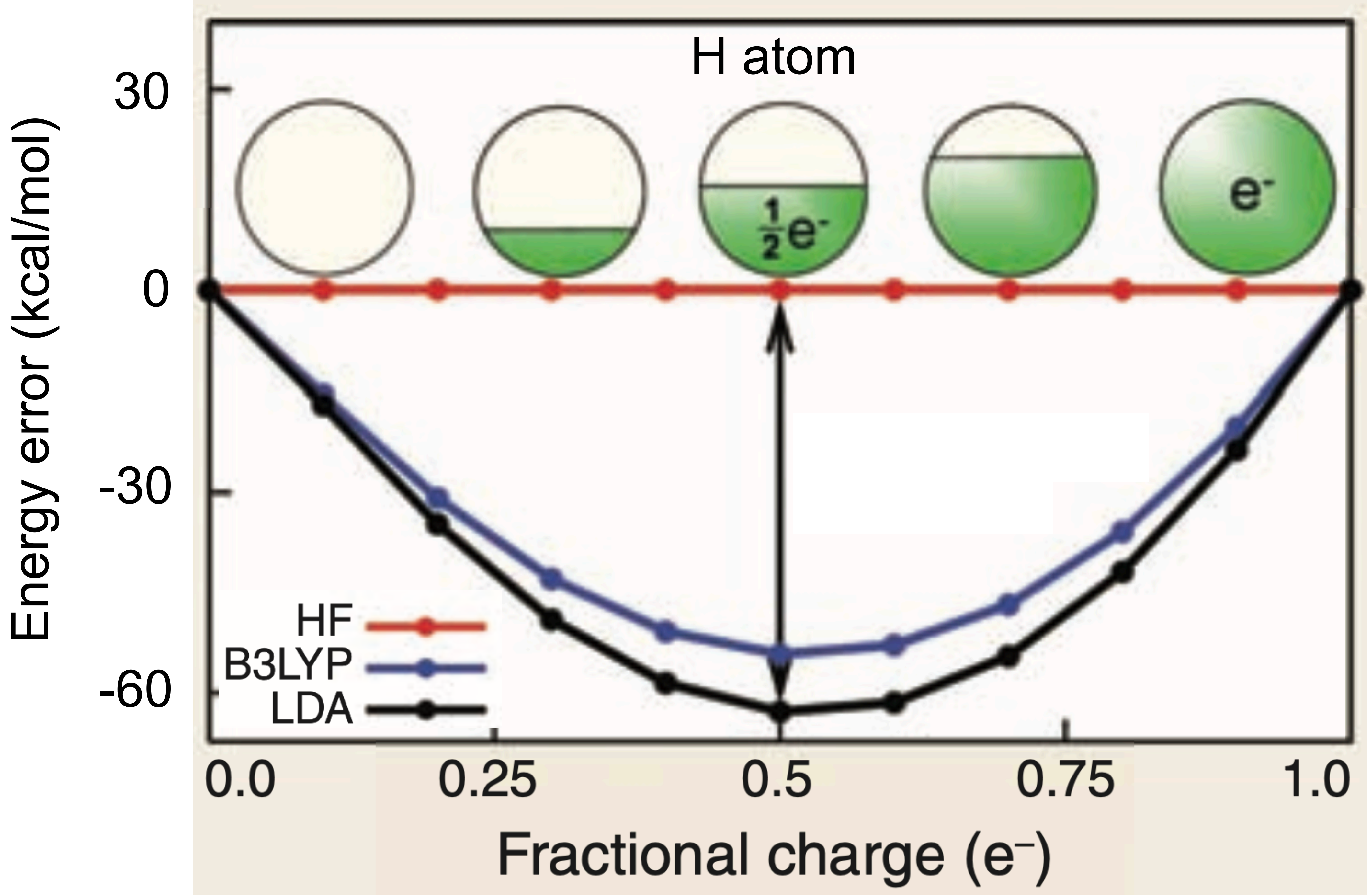

Cohen, Mori-Sanchez, Yang, Science (2008).

Some advanced exchange-correlation functionals

Advanced functionals

Hubbard functionals
(DFT+*U*, DFT+*U*+*V*,…)

Hybrid functionals
(B3LYP, PBE0, HSE06,…)

meta-GGA
(TPSS, SCAN, r2SCAN…)

van der Waals
(DFT-D, DFT-D3, TS, rVV10, …)

Self-interaction error in materials

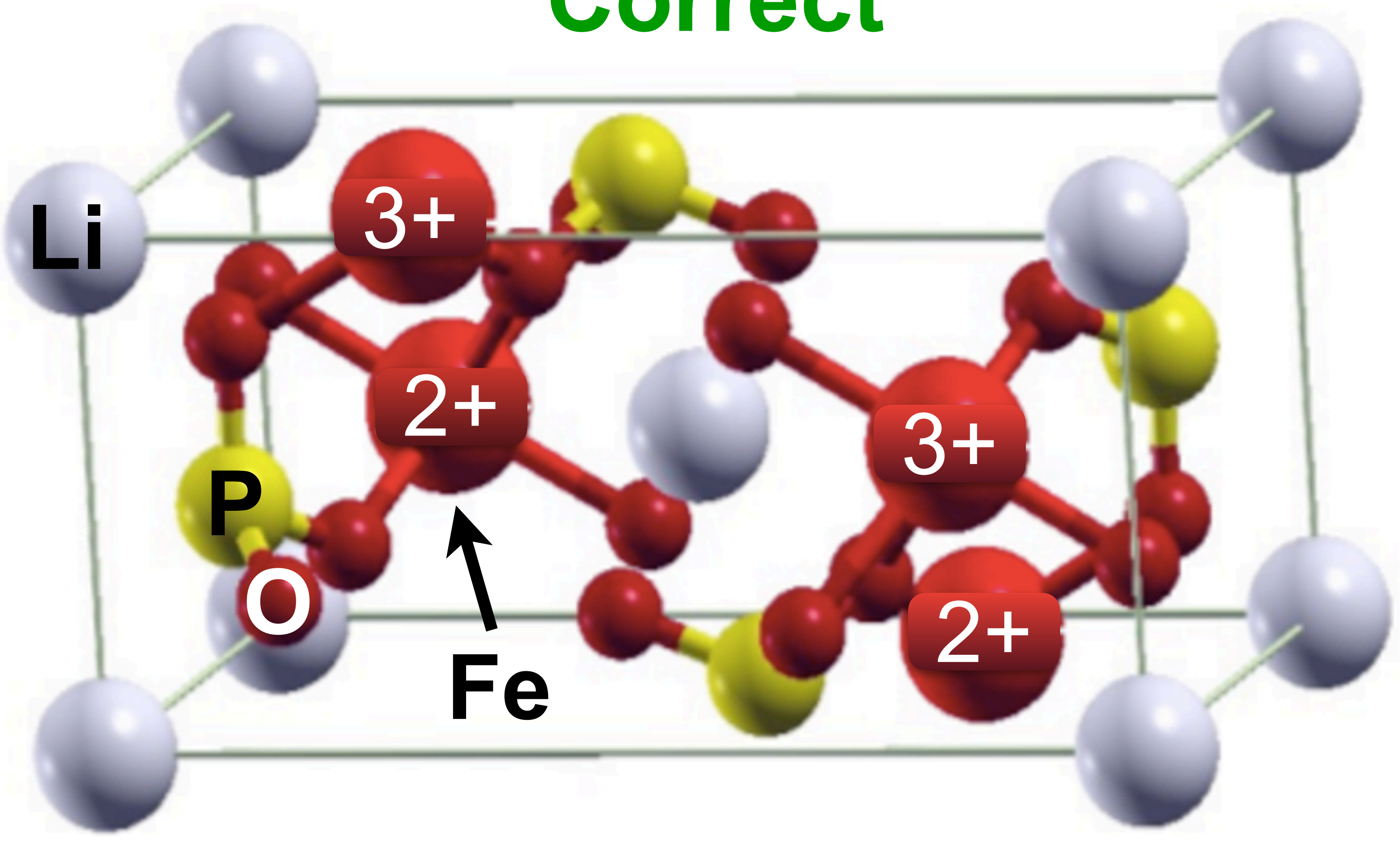

Correct

$Li_{0.5}FePO_4$

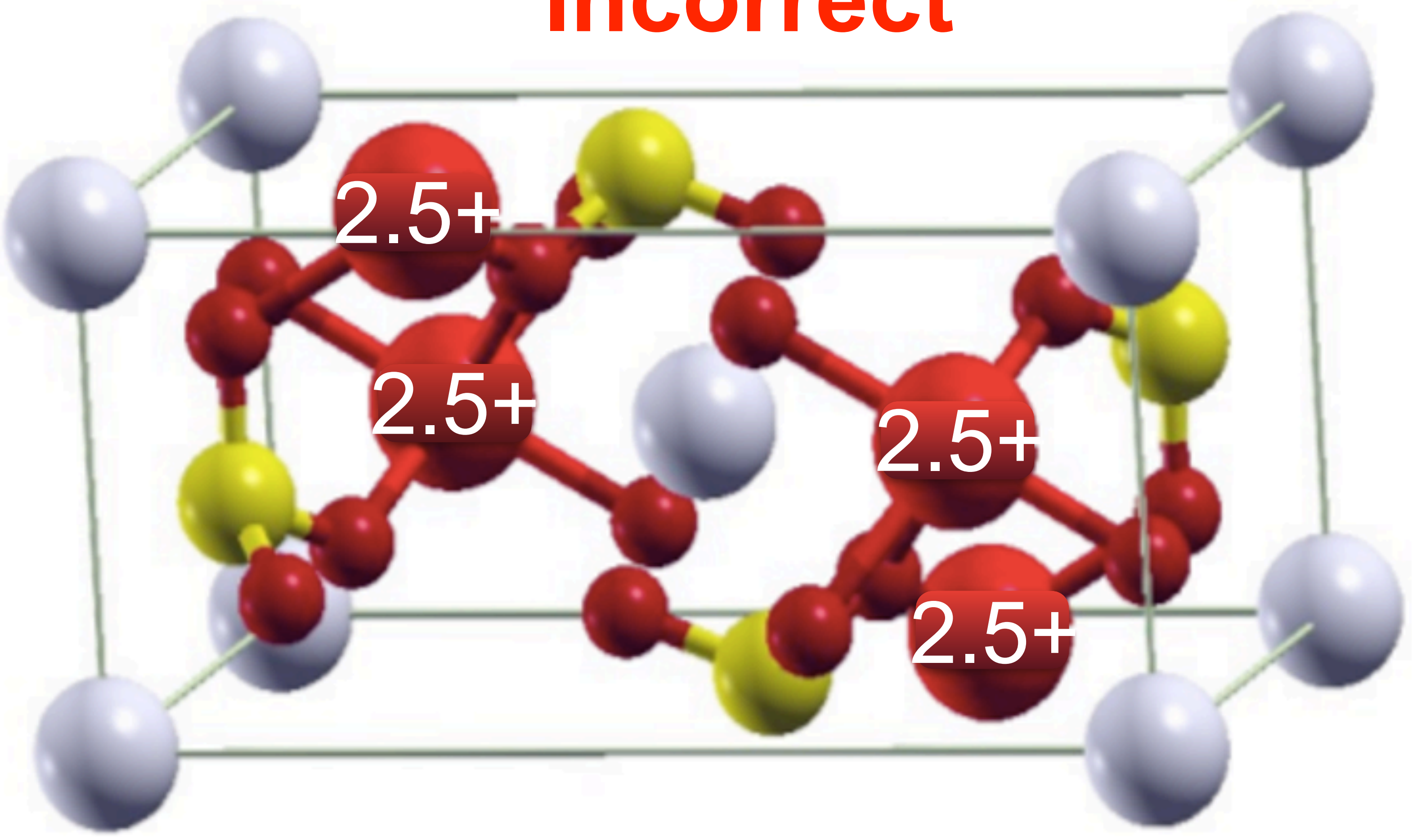

Incorrect

Self-interaction error in materials

Correct

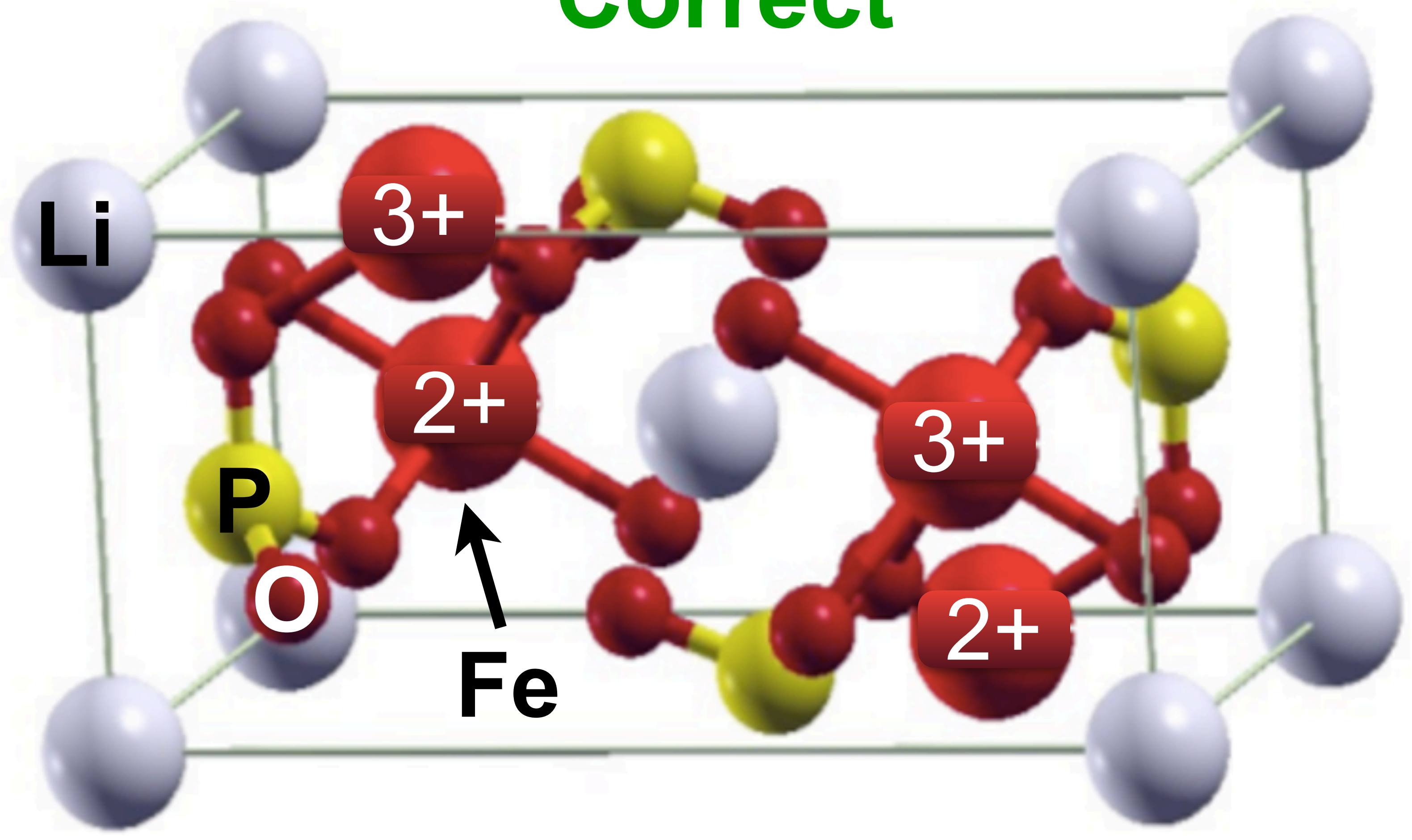

$Li_{0.5}FePO_4$

Incorrect

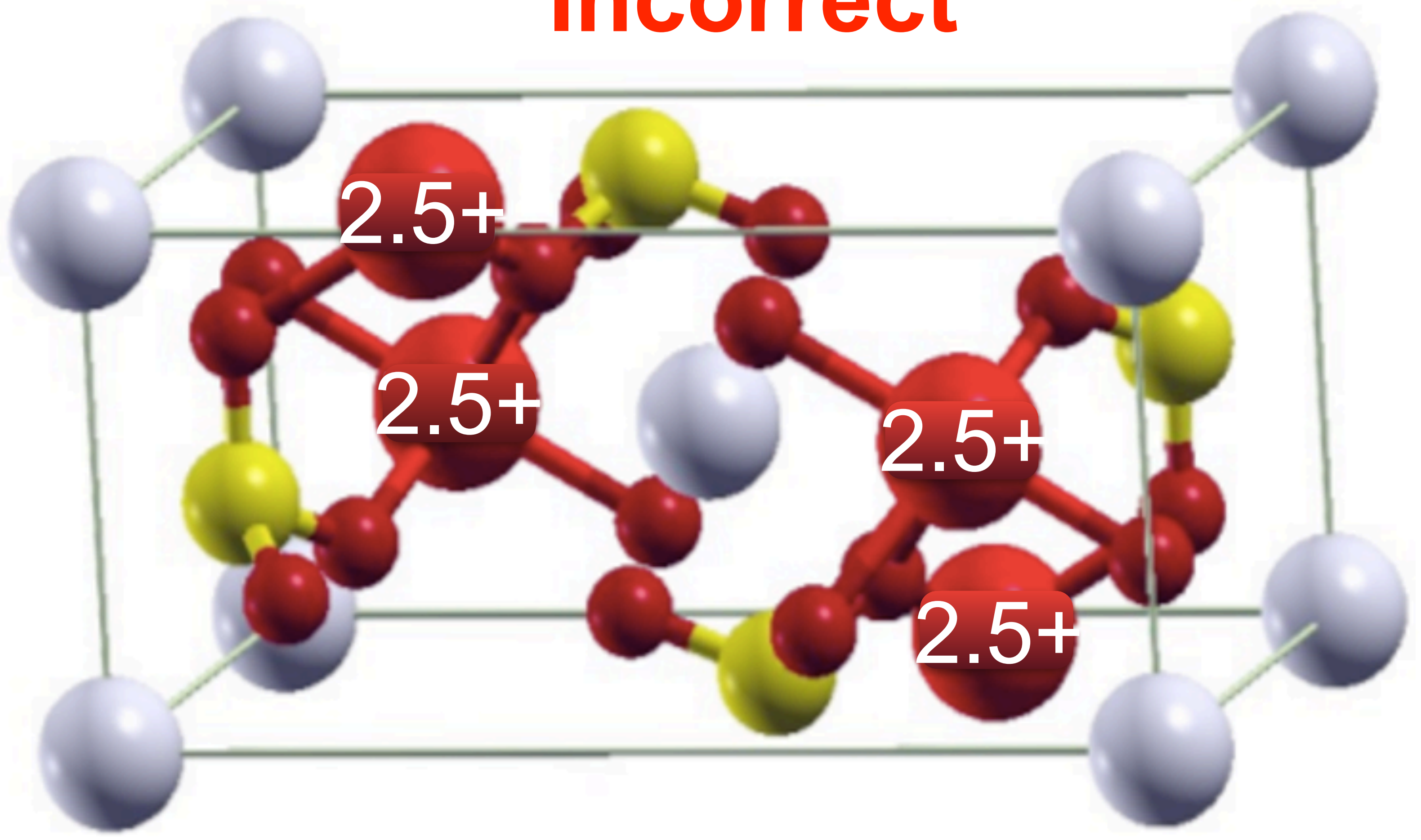

Fe^{2+}: $3d^6$

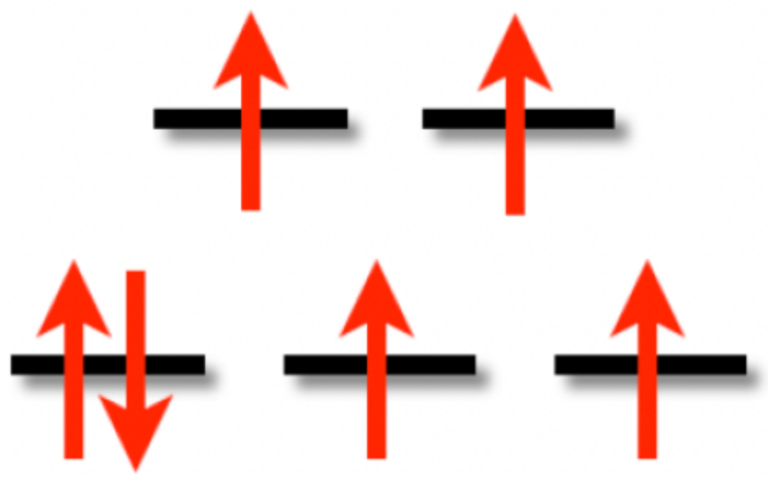

Fe^{3+}: $3d^5$

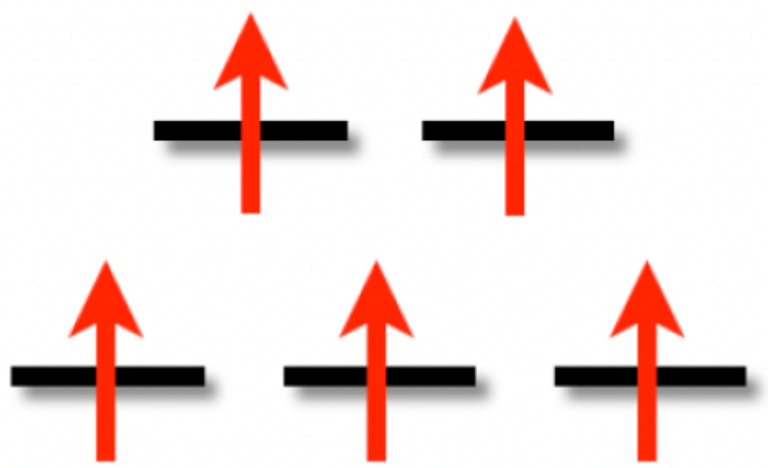

Self-interaction error in materials

Correct

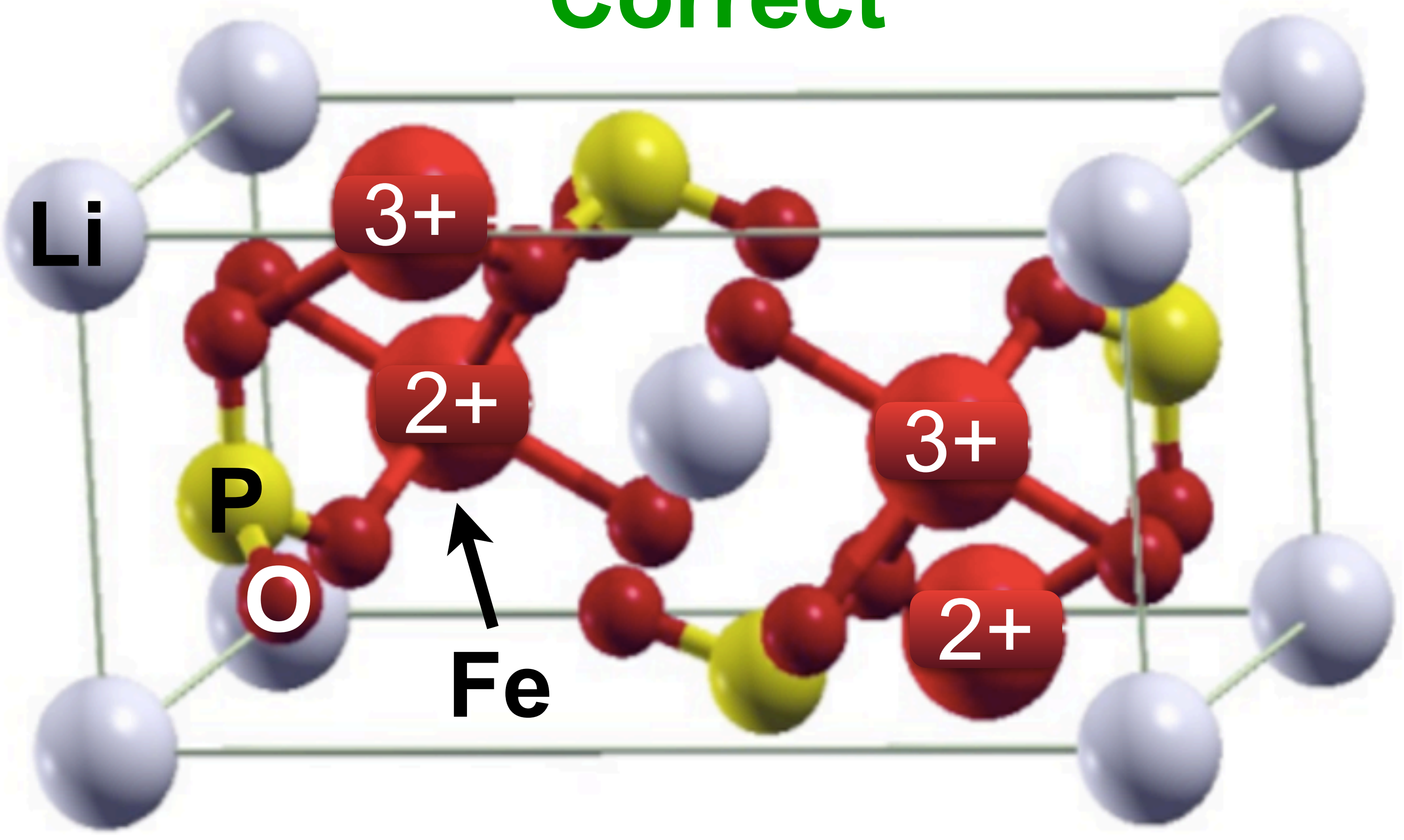

$Li_{0.5}FePO_4$

Incorrect

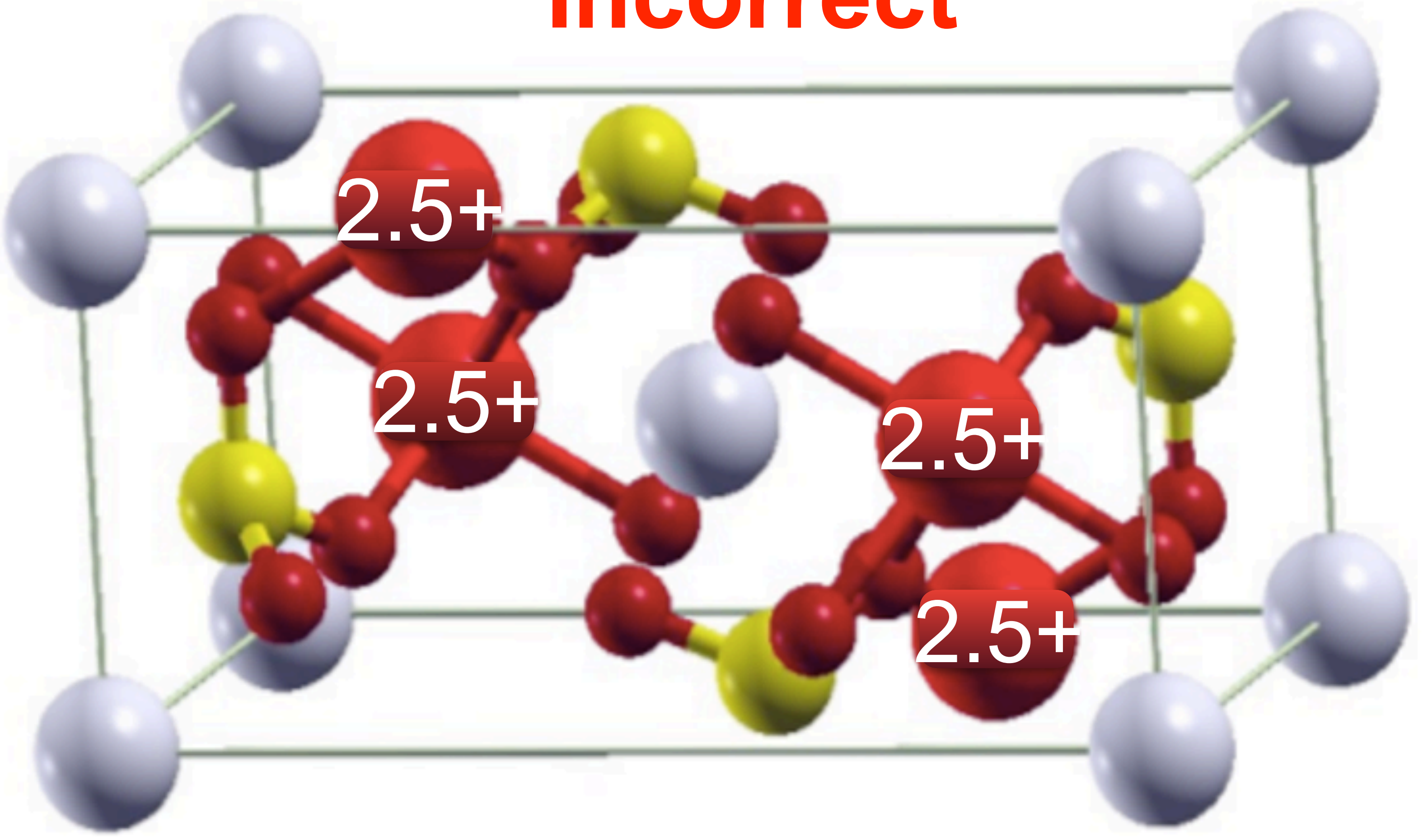

Self-interaction error

Fe-*3d* electrons are delocalized and spread around

Wrong average oxidation state of 2.5+ for Fe ions

Self-interaction error in materials

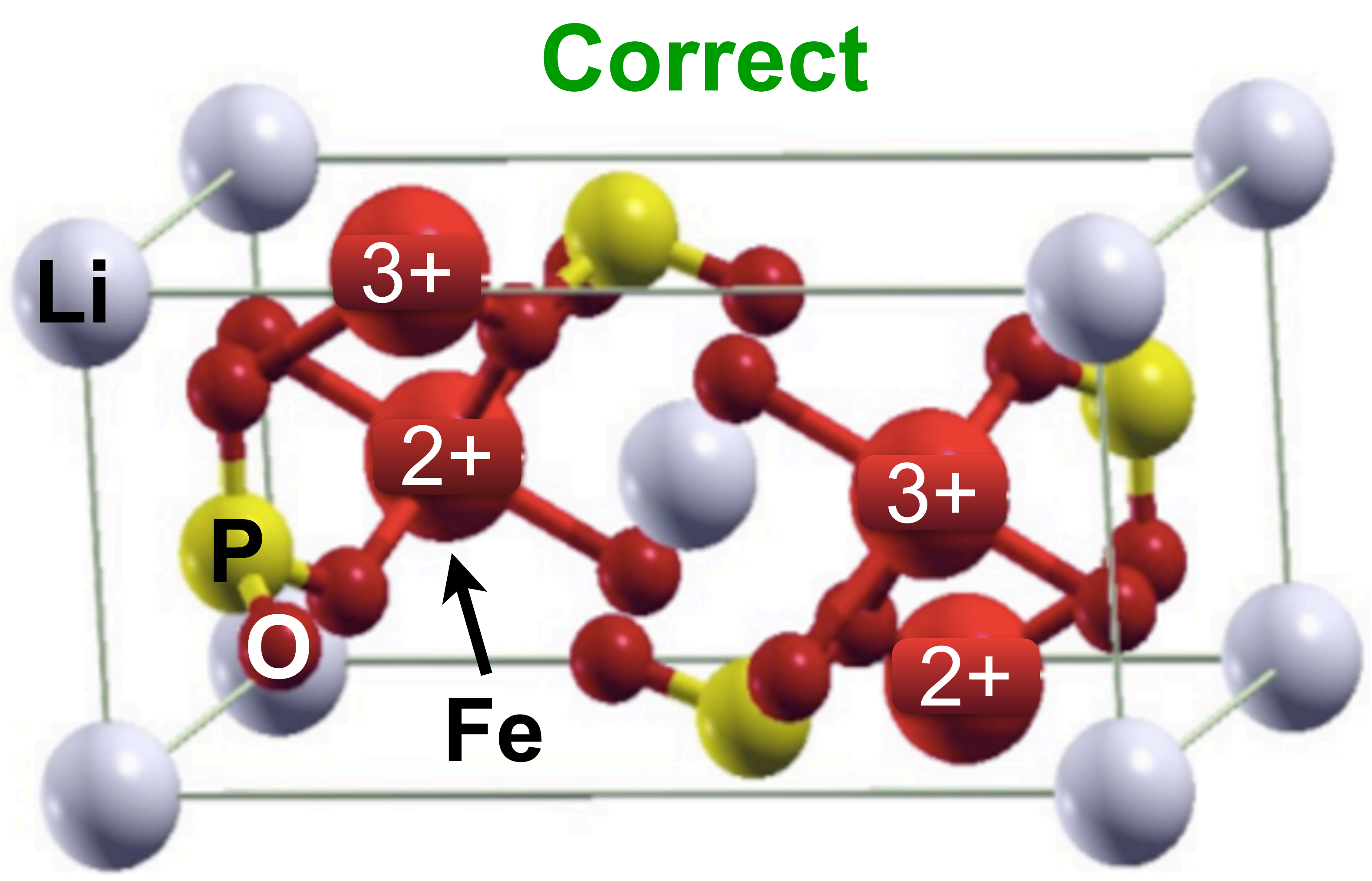

$Li_{0.5}FePO_4$

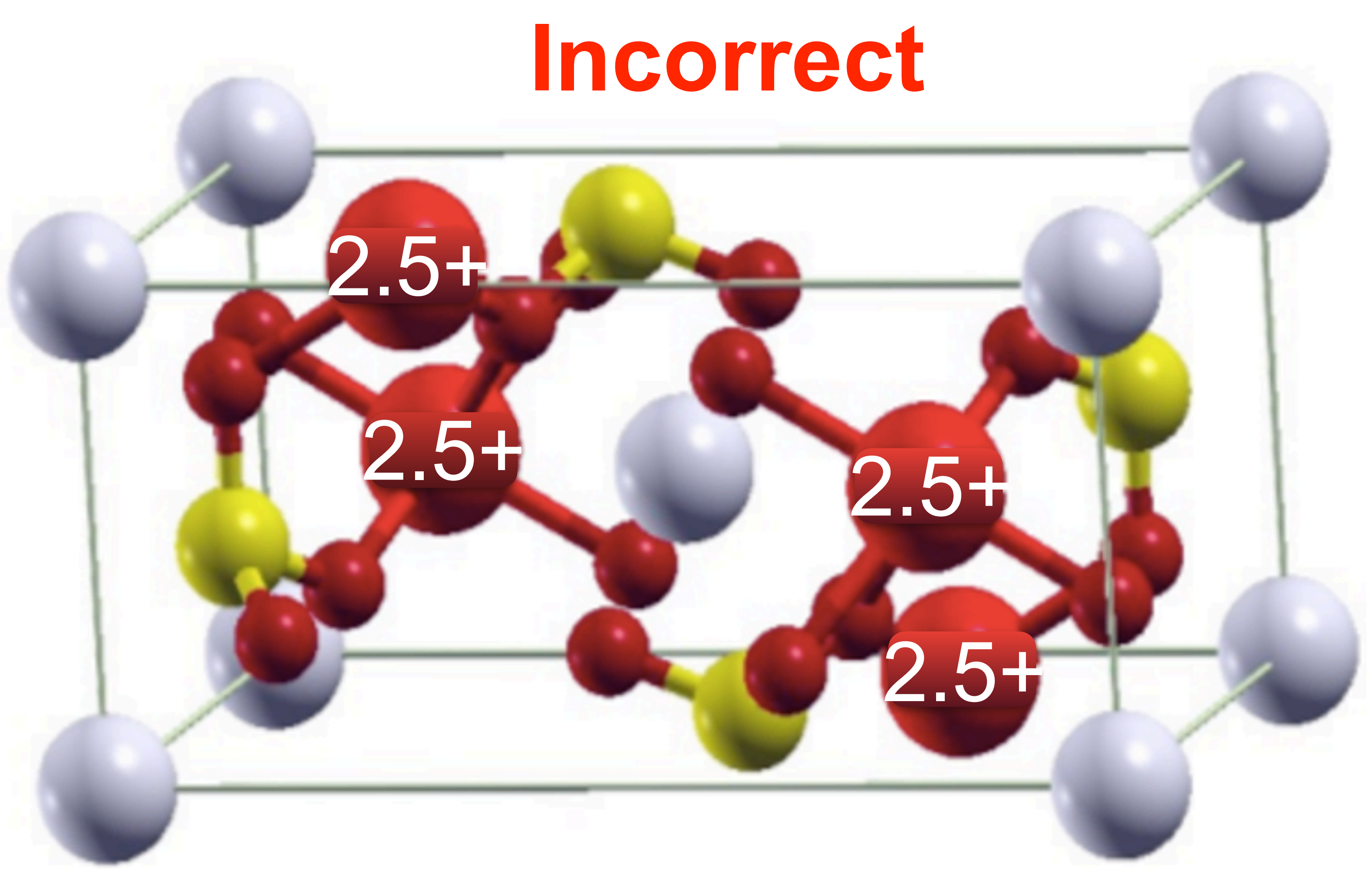

Spurious quadratic energy change when adding/removing a fraction of an electron to Fe

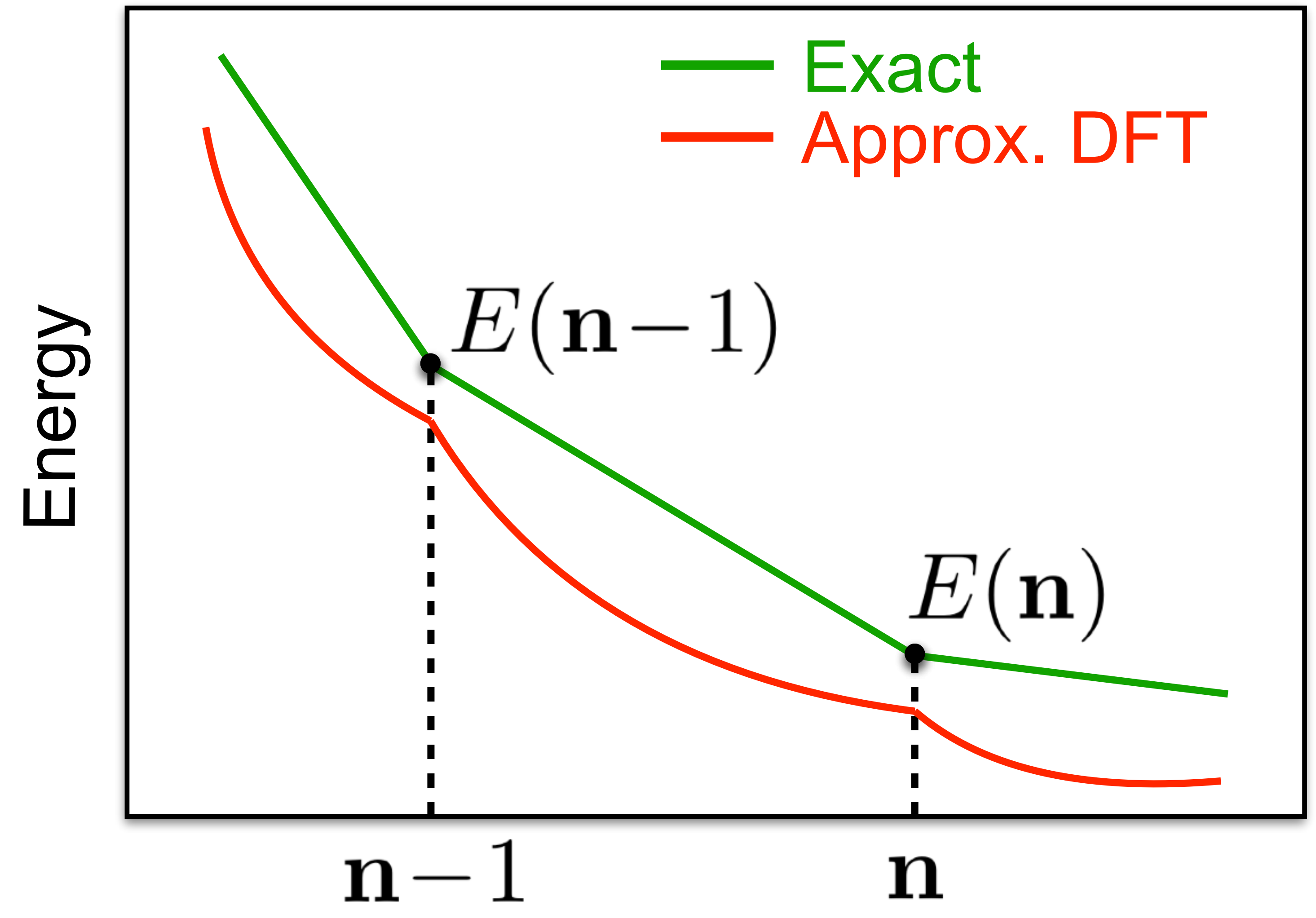

Self-interaction error

Fe-*3d* electrons are delocalized and spread around

Wrong average oxidation state of 2.5+ for Fe ions

Hubbard functionals (DFT+*U*)

When do we need DFT+*U*?

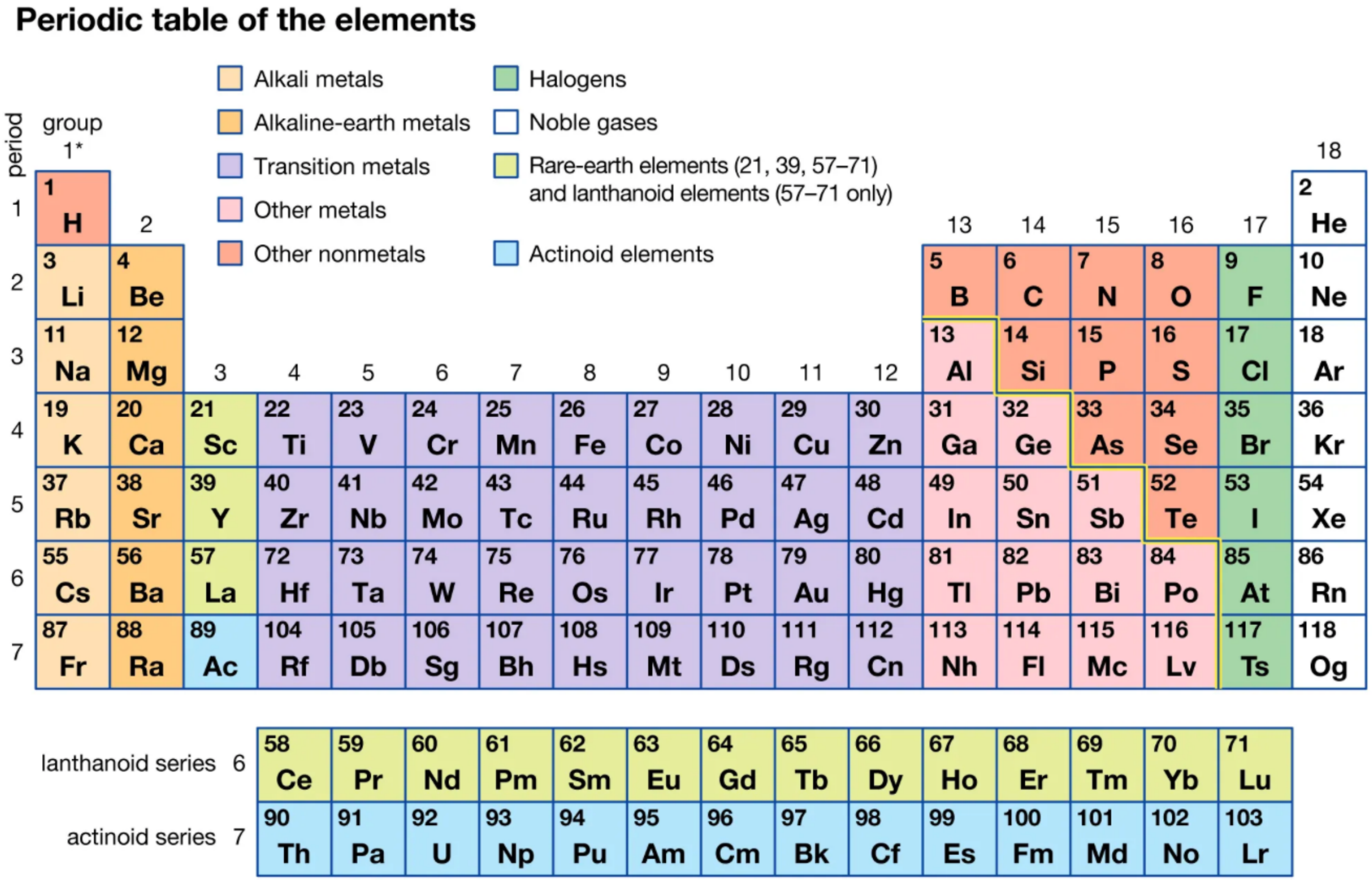

Periodic table of the elements

- Alkali metals
- Alkaline-earth metals
- Transition metals
- Other metals
- Other nonmetals
- Halogens
- Noble gases
- Rare-earth elements (21, 39, 57–71) and lanthanoid elements (57–71 only)
- Actinoid elements

period \ group	1*	2	3	4	5	6	7	8	9	10	11	12	13	14	15	16	17	18
1	1 H																	2 He
2	3 Li	4 Be											5 B	6 C	7 N	8 O	9 F	10 Ne
3	11 Na	12 Mg											13 Al	14 Si	15 P	16 S	17 Cl	18 Ar
4	19 K	20 Ca	21 Sc	22 Ti	23 V	24 Cr	25 Mn	26 Fe	27 Co	28 Ni	29 Cu	30 Zn	31 Ga	32 Ge	33 As	34 Se	35 Br	36 Kr
5	37 Rb	38 Sr	39 Y	40 Zr	41 Nb	42 Mo	43 Tc	44 Ru	45 Rh	46 Pd	47 Ag	48 Cd	49 In	50 Sn	51 Sb	52 Te	53 I	54 Xe
6	55 Cs	56 Ba	57 La	72 Hf	73 Ta	74 W	75 Re	76 Os	77 Ir	78 Pt	79 Au	80 Hg	81 Tl	82 Pb	83 Bi	84 Po	85 At	86 Rn
7	87 Fr	88 Ra	89 Ac	104 Rf	105 Db	106 Sg	107 Bh	108 Hs	109 Mt	110 Ds	111 Rg	112 Cn	113 Nh	114 Fl	115 Mc	116 Lv	117 Ts	118 Og
lanthanoid series 6				58 Ce	59 Pr	60 Nd	61 Pm	62 Sm	63 Eu	64 Gd	65 Tb	66 Dy	67 Ho	68 Er	69 Tm	70 Yb	71 Lu	
actinoid series 7				90 Th	91 Pa	92 U	93 Np	94 Pu	95 Am	96 Cm	97 Bk	98 Cf	99 Es	100 Fm	101 Md	102 No	103 Lr	

When do we need DFT+*U*?

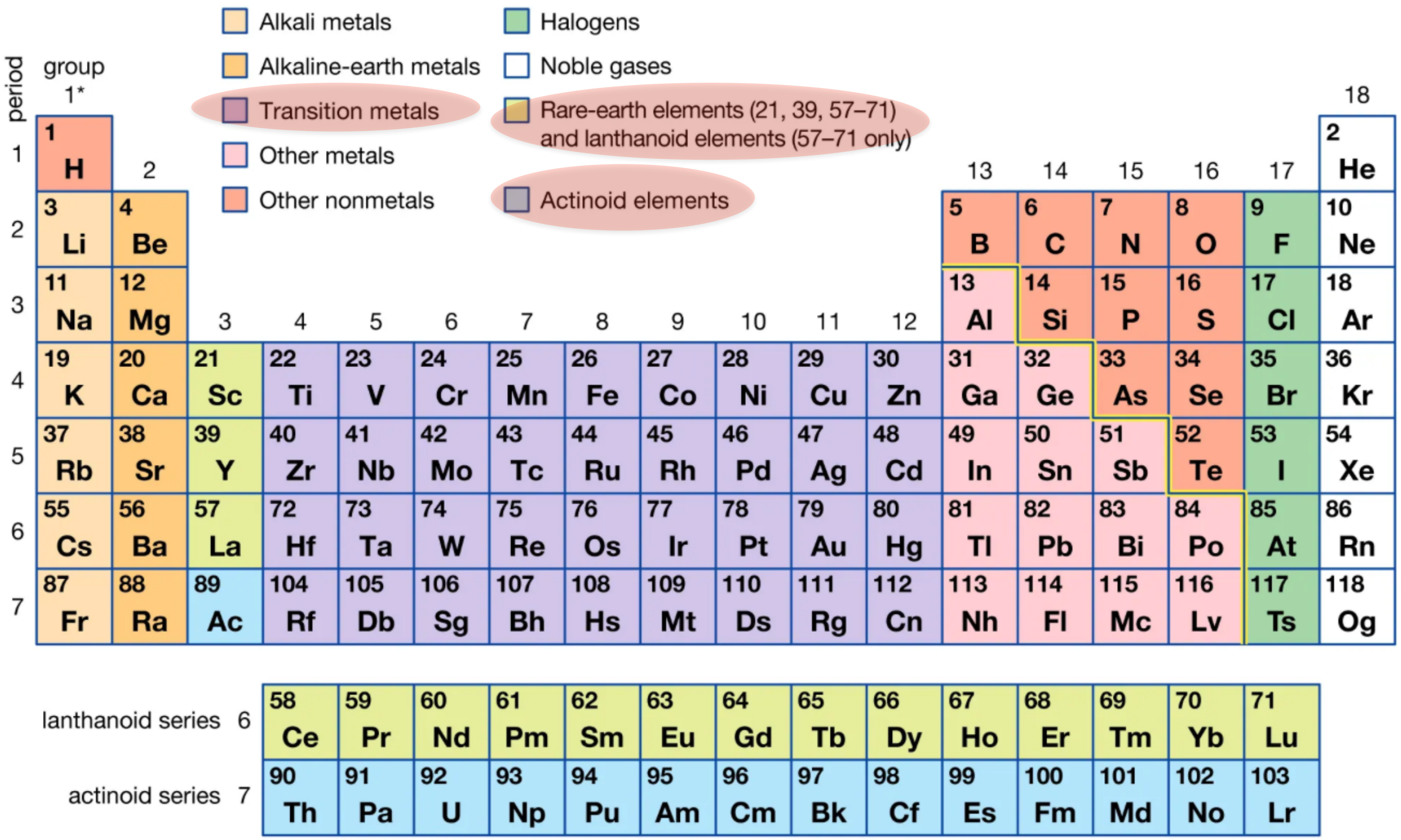

Periodic table of the elements

☐ Alkali metals
☐ Alkaline-earth metals
☐ Transition metals
☐ Other metals
☐ Other nonmetals
☐ Halogens
☐ Noble gases
☐ Rare-earth elements (21, 39, 57–71) and lanthanoid elements (57–71 only)
☐ Actinoid elements

period	group 1*	2	3	4	5	6	7	8	9	10	11	12	13	14	15	16	17	18
1	1 H																	2 He
2	3 Li	4 Be											5 B	6 C	7 N	8 O	9 F	10 Ne
3	11 Na	12 Mg											13 Al	14 Si	15 P	16 S	17 Cl	18 Ar
4	19 K	20 Ca	21 Sc	22 Ti	23 V	24 Cr	25 Mn	26 Fe	27 Co	28 Ni	29 Cu	30 Zn	31 Ga	32 Ge	33 As	34 Se	35 Br	36 Kr
5	37 Rb	38 Sr	39 Y	40 Zr	41 Nb	42 Mo	43 Tc	44 Ru	45 Rh	46 Pd	47 Ag	48 Cd	49 In	50 Sn	51 Sb	52 Te	53 I	54 Xe
6	55 Cs	56 Ba	57 La	72 Hf	73 Ta	74 W	75 Re	76 Os	77 Ir	78 Pt	79 Au	80 Hg	81 Tl	82 Pb	83 Bi	84 Po	85 At	86 Rn
7	87 Fr	88 Ra	89 Ac	104 Rf	105 Db	106 Sg	107 Bh	108 Hs	109 Mt	110 Ds	111 Rg	112 Cn	113 Nh	114 Fl	115 Mc	116 Lv	117 Ts	118 Og

lanthanoid series 6	58 Ce	59 Pr	60 Nd	61 Pm	62 Sm	63 Eu	64 Gd	65 Tb	66 Dy	67 Ho	68 Er	69 Tm	70 Yb	71 Lu
actinoid series 7	90 Th	91 Pa	92 U	93 Np	94 Pu	95 Am	96 Cm	97 Bk	98 Cf	99 Es	100 Fm	101 Md	102 No	103 Lr

Answer: For elements with partially filled *d* and/or *f* electrons

When do we need DFT+*U*?

When do we need DFT+*U*?

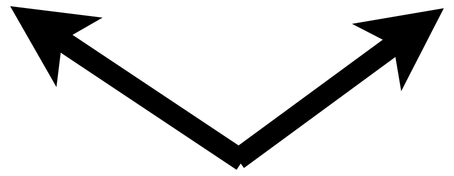

more localized = larger self-interactions
(delocalization) errors in LDA/GGA

apply +*U* correction (historically)

When do we need DFT+*U*?

nowadays, people apply +*U* correction even to s and p states…

more localized = larger self-interactions (delocalization) errors in LDA/GGA

apply +*U* correction (historically)

Mott-Hubbard and charge-transfer insulators

For some transition-metal and rare-earth compounds, DFT with LDA/GGA functionals predicts a metallic ground state, while in reality they are insulating.
Examples: CoO, FeO, …

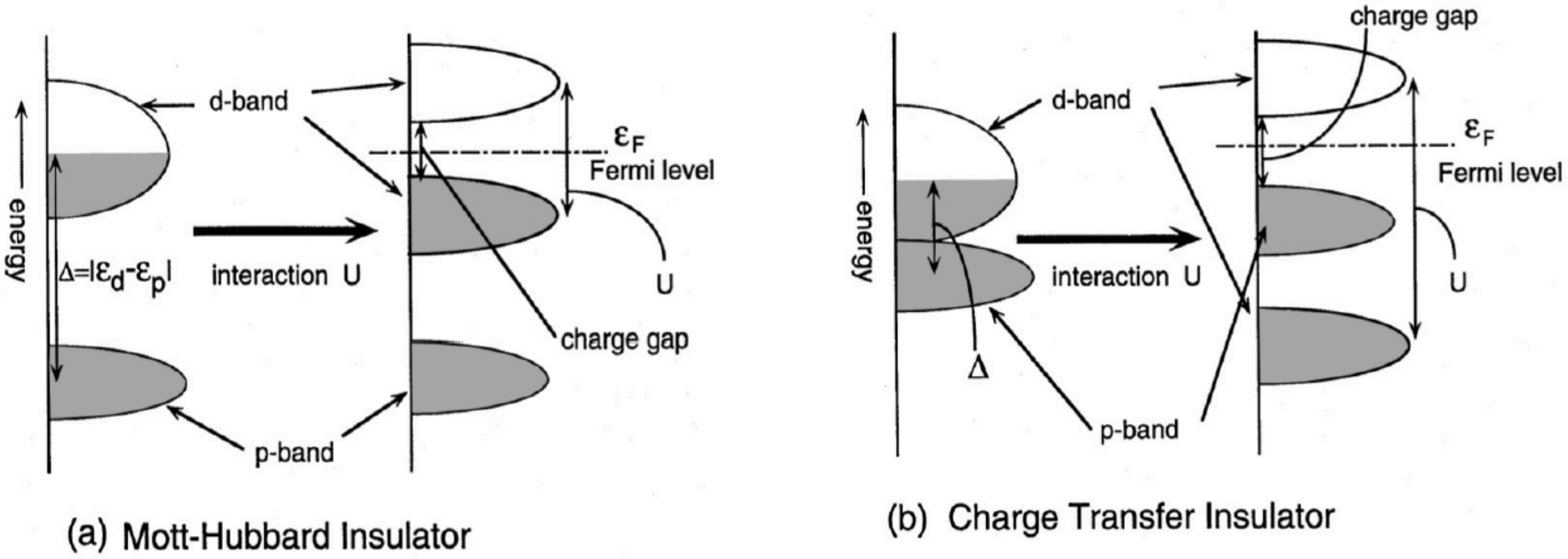

(a) Mott-Hubbard Insulator

(b) Charge Transfer Insulator

M. Imada *et al.*, Rev. Mod. Phys. **70**, 1039 (1998).

Technological importance of transition-metal and rare-earth compounds

Batteries for electric cars

Magnets for generators

Photocatalysis

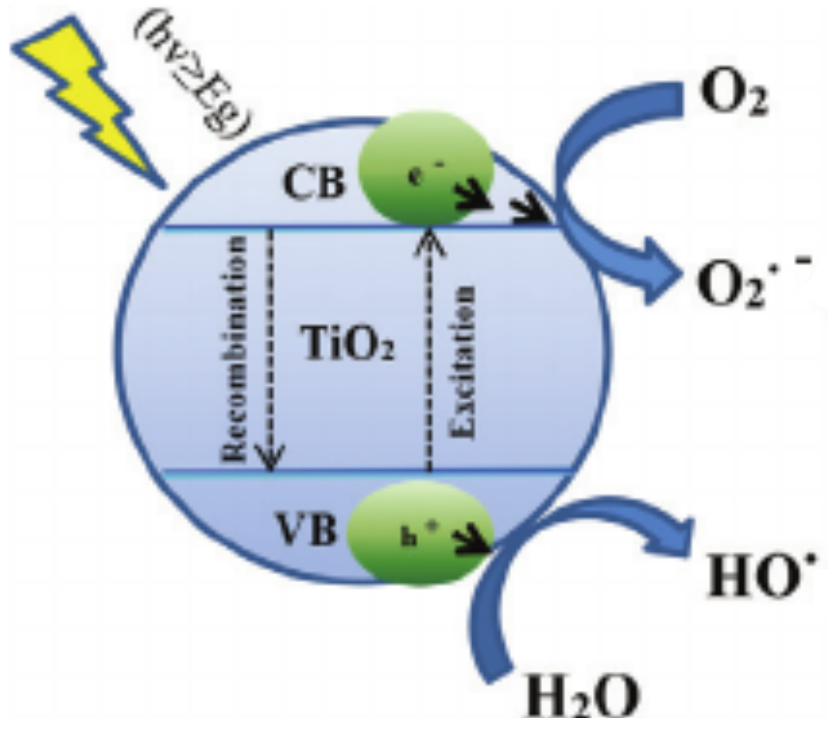

Spintronic devices

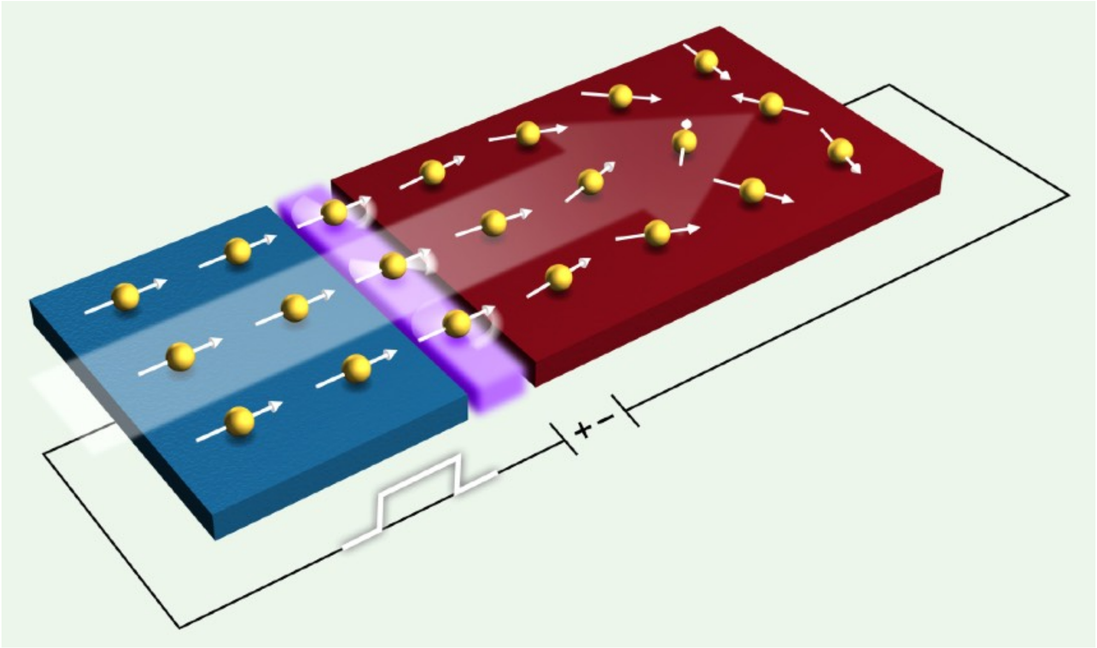

Inorganic perovskite solar cells

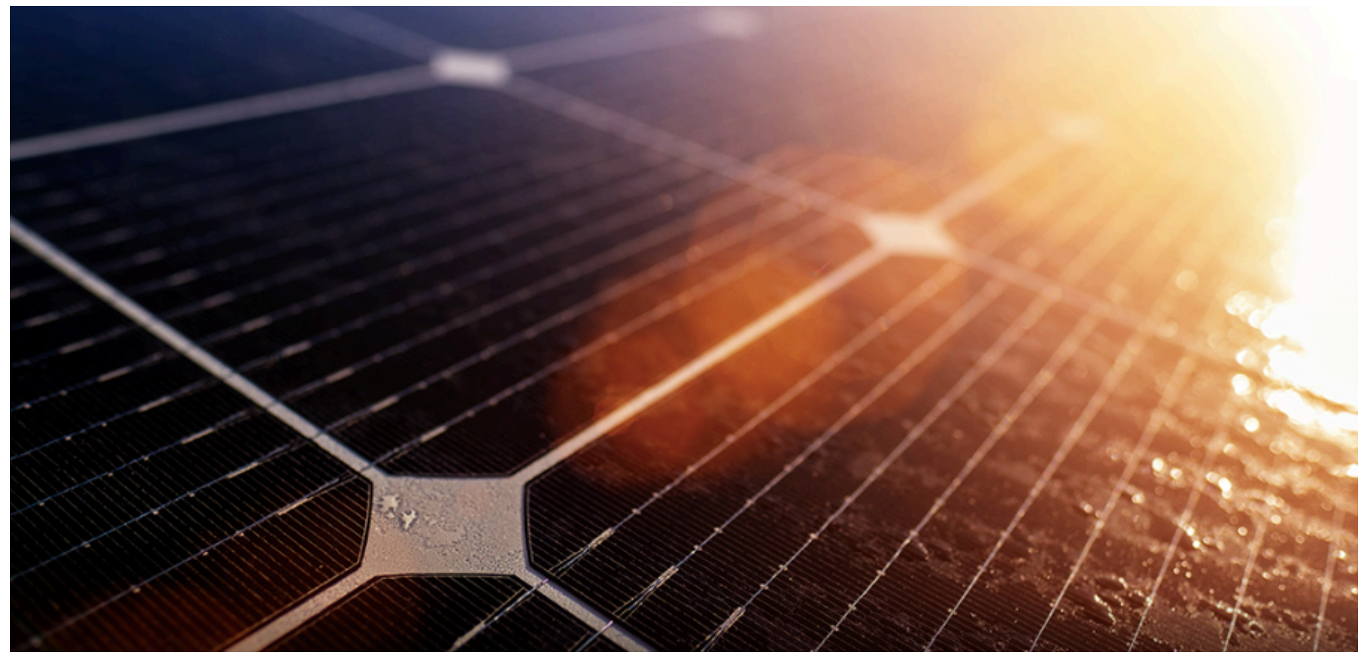

History of DFT+*U*

DFT

W. Kohn

(1964 - 1965)

The main idea:

$$\Psi(\mathbf{r}_1, \mathbf{r}_2, ..., \mathbf{r}_N) \Rightarrow \rho(\mathbf{r})$$

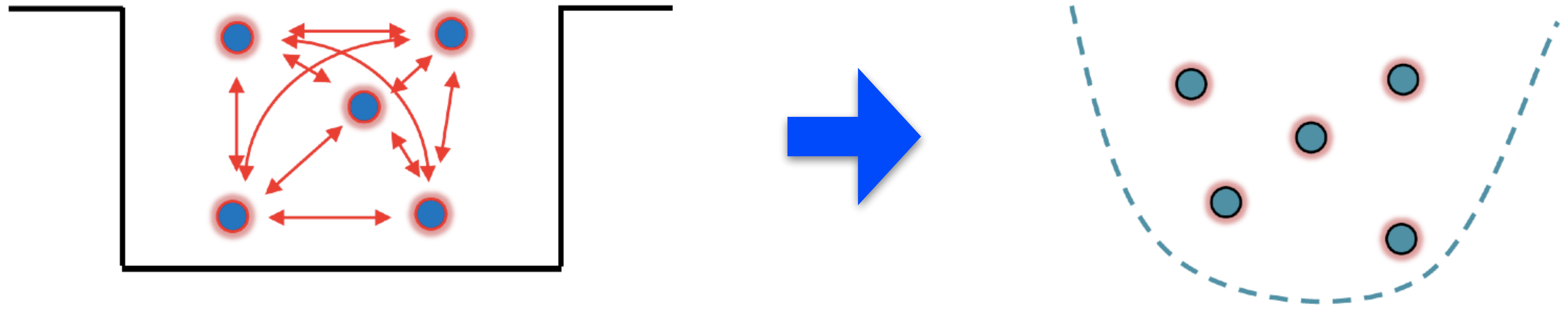

interacting electrons
in the external potential

noninteracting electrons
in the effective potential

The Hubbard model

(1963 - 1967)

J. Hubbard

The main idea:

$$\hat{H} = -\sum_{I\neq J,\sigma} t_{IJ}\, \hat{c}^\dagger_{I\sigma}\, \hat{c}_{J\sigma} + U\sum_{I} \hat{n}_{I\uparrow}\, \hat{n}_{I\downarrow}$$

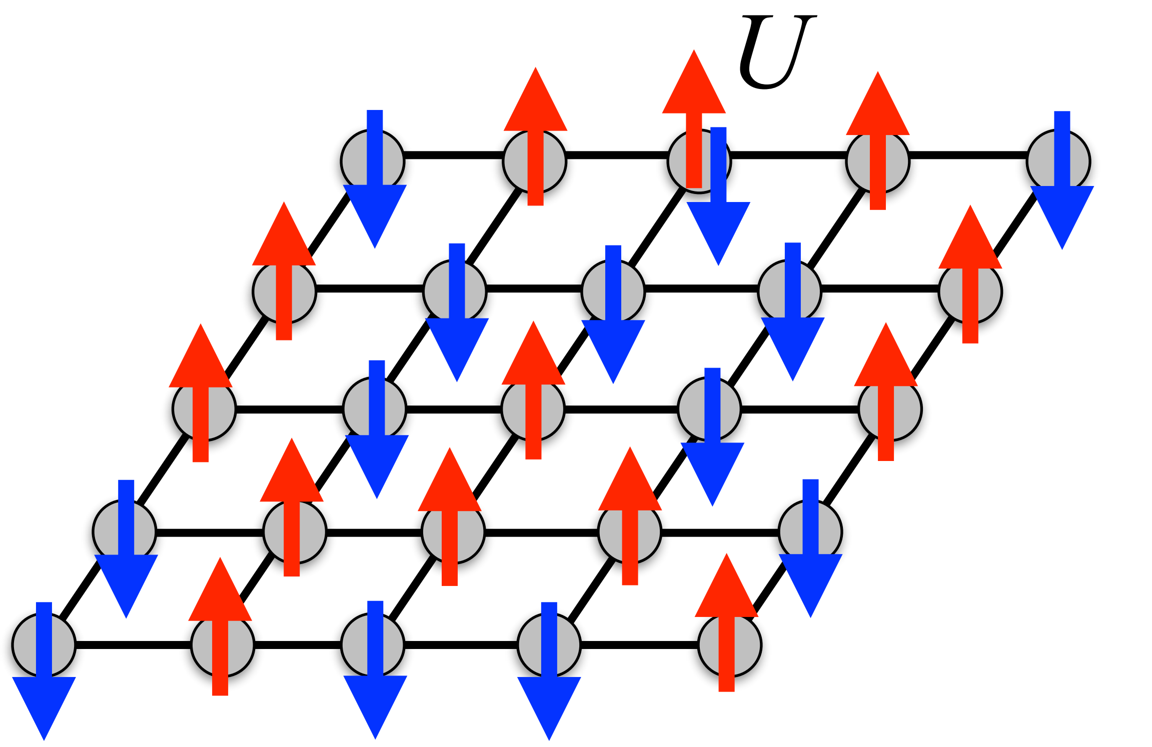

History of DFT+*U*

W. Kohn

DFT

(1964 - 1965)

The Hubbard model

(1963 - 1967)

J. Hubbard

~25 years

DFT+*U*

V.I. Anisimov, J. Zaanen, O.K. Andersen,
Phys. Rev. B **44**, 943 (1991)

The idea behind DFT+*U*

DFT total-energy functional is corrected by the Hubbard-like term.

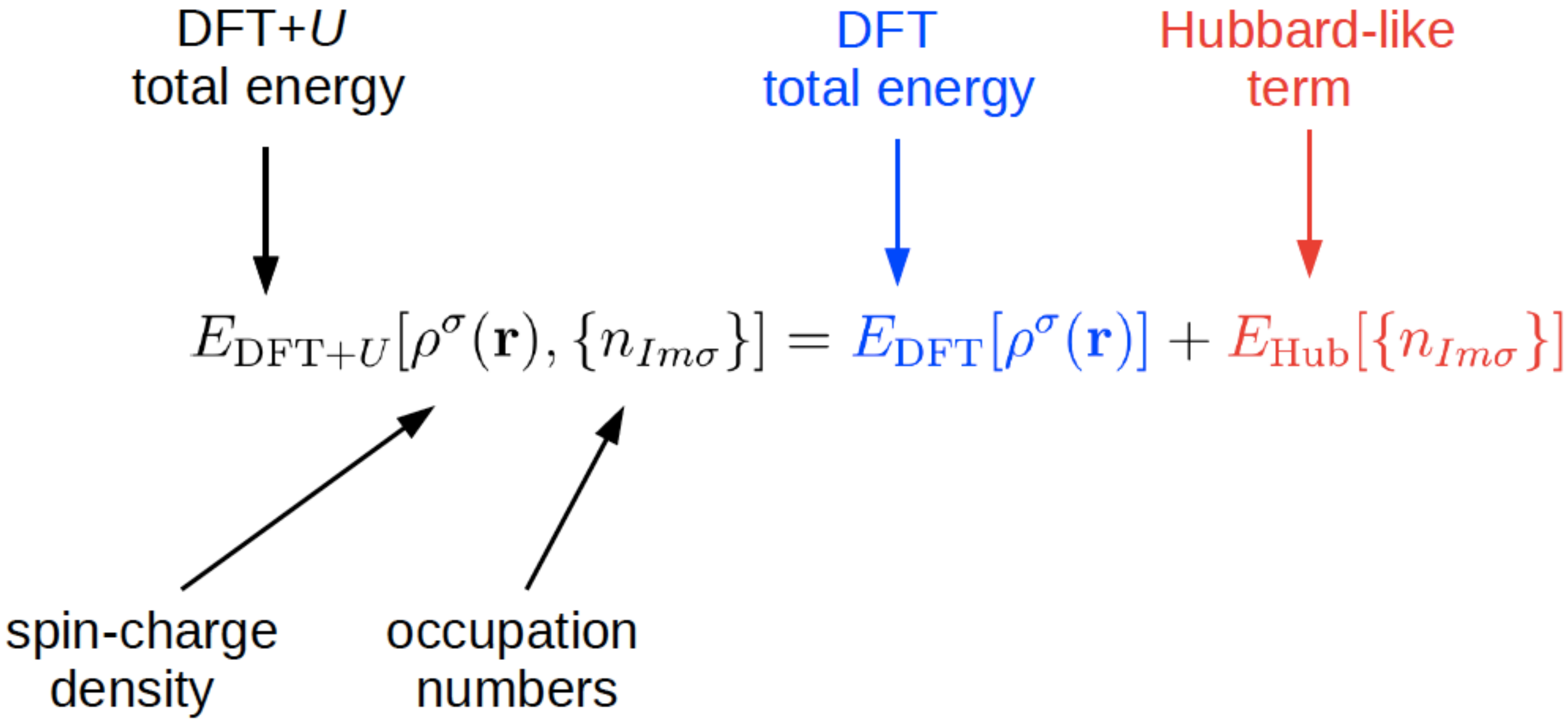

DFT+*U*
total energy

DFT
total energy

Hubbard-like
term

$$E_{\mathrm{DFT}+U}[\rho^{\sigma}(\mathbf{r}), \{n_{Im\sigma}\}] = E_{\mathrm{DFT}}[\rho^{\sigma}(\mathbf{r})] + E_{\mathrm{Hub}}[\{n_{Im\sigma}\}]$$

spin-charge
density

occupation
numbers

The idea behind DFT+*U*

DFT total-energy functional is corrected by the Hubbard-like term.

Double-counting problem: subtract a term describing interactions in DFT in some average way.

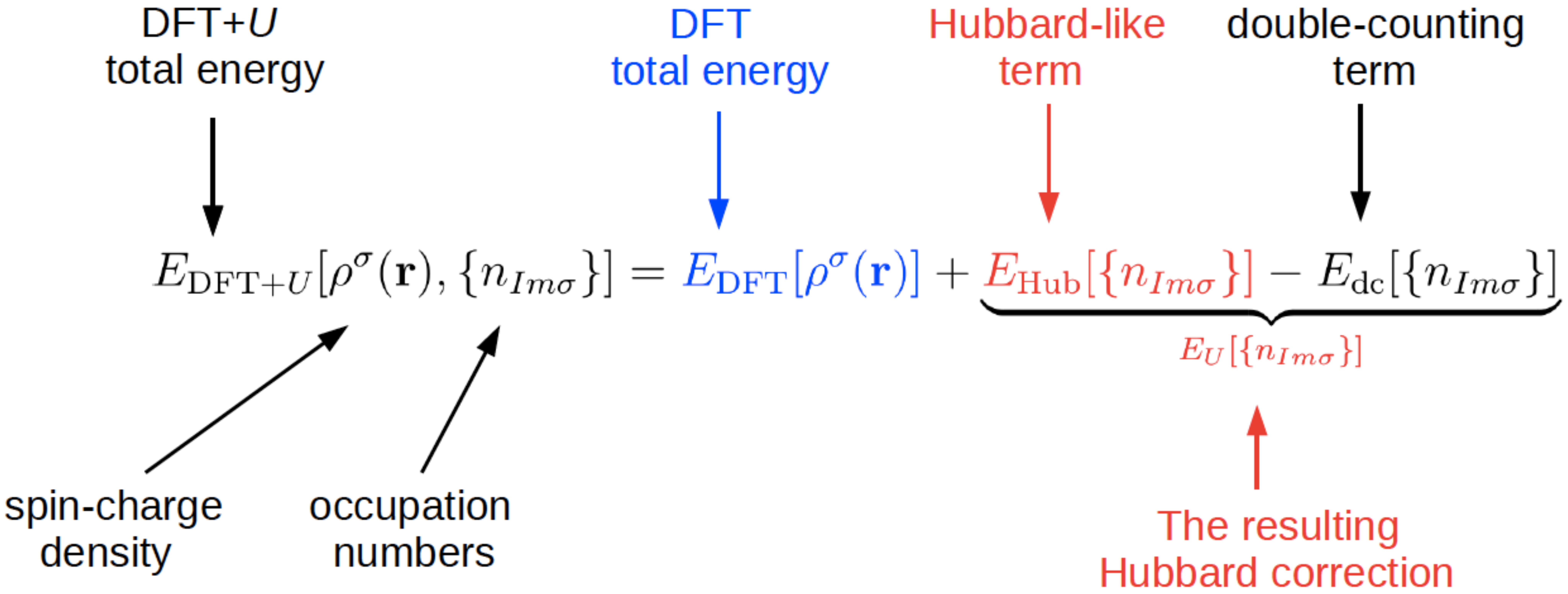

DFT+*U* total energy

DFT total energy

Hubbard-like term

double-counting term

$$E_{\mathrm{DFT+}U}[\rho^{\sigma}(\mathbf{r}),\{n_{Im\sigma}\}] = E_{\mathrm{DFT}}[\rho^{\sigma}(\mathbf{r})] + \underbrace{E_{\mathrm{Hub}}[\{n_{Im\sigma}\}] - E_{\mathrm{dc}}[\{n_{Im\sigma}\}]}_{E_U[\{n_{Im\sigma}\}]}$$

spin-charge density

occupation numbers

The resulting Hubbard correction

Total energy and atomic occupations in DFT+*U*

The DFT+*U* total energy:

$$E_{\text{DFT}+U} = E_{\text{DFT}} + E_U$$

The Hubbard correction energy:

$$E_U = \frac{1}{2} \sum_{I,m,m',\sigma} \underbrace{\left(U^I - J^I\right)}_{U^I_{\text{eff}}} \left(\delta_{mm'} - n^{I\sigma}_{mm'}\right) n^{I\sigma}_{m'm}$$

effective Hubbard parameter

The occupation matrix:

$$n^{I\sigma}_{mm'} = \sum_{v,\mathbf{k}} f^{\sigma}_{v\mathbf{k}} \langle \psi^{\sigma}_{v\mathbf{k}} | \varphi^{I}_{m'} \rangle \langle \varphi^{I}_{m} | \psi^{\sigma}_{v\mathbf{k}} \rangle$$

v is the band index
$\mathbf{k}$ is the k point in BZ

occupations of Kohn-Sham levels

Kohn-Sham wavefunctions

localized orbitals (e.g. atomic/Wannier)

$$n^I = \sum_{m,\sigma} n^{I\sigma}_{mm}$$ ← the total occupation of localized states (*d* or *f*) at site *I*

Total energy and atomic occupations in DFT+*U*

The DFT+*U* total energy:

$$E_{\mathrm{DFT}+U} = E_{\mathrm{DFT}} + E_U$$

The Hubbard correction energy:

$$E_U = \frac{1}{2} \sum_{I,m,m',\sigma} \underbrace{\left(U^I - J^I\right)}_{U^I_{\mathrm{eff}}} \left(\delta_{mm'} - n^{I\sigma}_{mm'}\right) n^{I\sigma}_{m'm}$$

effective Hubbard parameter

The total energy is minimized when *n* is idempotent, i.e., eigenvalues are 0 (i.e. fully unoccupied orbitals) or 1 (i.e. fully occupied orbitals).

- For **partial occupations** (e.g., eigenvalues like 0.5), the product *n*(1−*n*) is **maximal** at *n*=0.5 and **zero** at *n*=0 or 1.
- This makes the Hubbard correction energy E_U largest for partially occupied orbitals and zero for fully occupied or fully empty orbitals.
- DFT+*U* restores **localization** by energetically penalizing delocalized (fractionally occupied) states.

Kohn-Sham equations including the Hubbard potential

By taking a functional derivative of the DFT+U total-energy functional with respect to the complex-conjugate Kohn-Sham wavefunction, we obtain an expression for the **modified Kohn-Sham equations**:

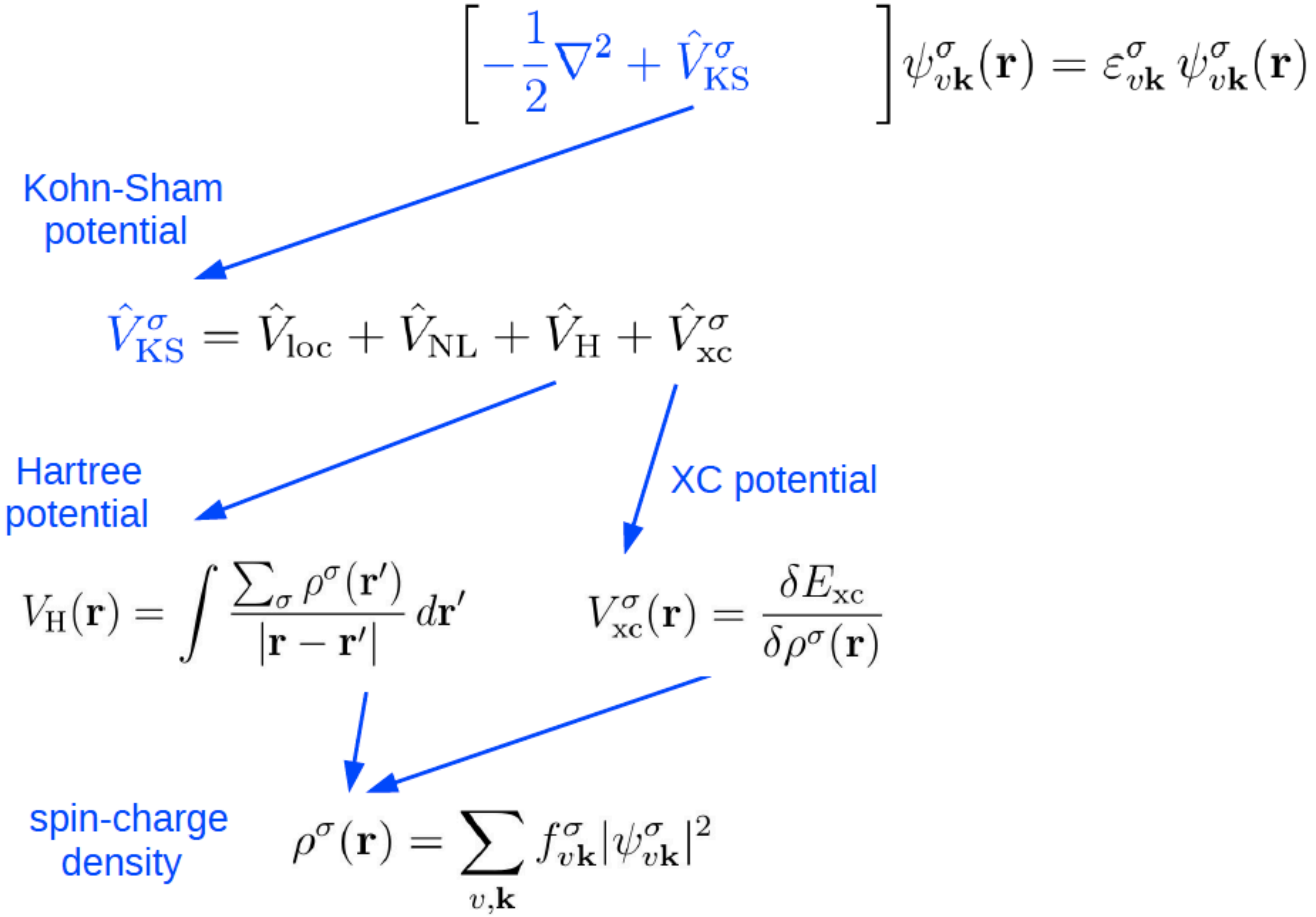

$$\left[-\frac{1}{2}\nabla^2 + \hat{V}^{\sigma}_{\mathrm{KS}} \qquad\qquad \right]\psi^{\sigma}_{v\mathbf{k}}(\mathbf{r}) = \varepsilon^{\sigma}_{v\mathbf{k}}\,\psi^{\sigma}_{v\mathbf{k}}(\mathbf{r})$$

Kohn-Sham potential

$$\hat{V}^{\sigma}_{\mathrm{KS}} = \hat{V}_{\mathrm{loc}} + \hat{V}_{\mathrm{NL}} + \hat{V}_{\mathrm{H}} + \hat{V}^{\sigma}_{\mathrm{xc}}$$

Hartree potential

XC potential

$$V_{\mathrm{H}}(\mathbf{r}) = \int \frac{\sum_{\sigma}\rho^{\sigma}(\mathbf{r}')}{|\mathbf{r}-\mathbf{r}'|}\,d\mathbf{r}' \qquad V^{\sigma}_{\mathrm{xc}}(\mathbf{r}) = \frac{\delta E_{\mathrm{xc}}}{\delta\rho^{\sigma}(\mathbf{r})}$$

spin-charge density

$$\rho^{\sigma}(\mathbf{r}) = \sum_{v,\mathbf{k}} f^{\sigma}_{v\mathbf{k}}|\psi^{\sigma}_{v\mathbf{k}}|^2$$

Kohn-Sham equations including the Hubbard potential

By taking a functional derivative of the DFT+U total-energy functional with respect to the complex-conjugate Kohn-Sham wavefunction, we obtain an expression for the **modified Kohn-Sham equations**:

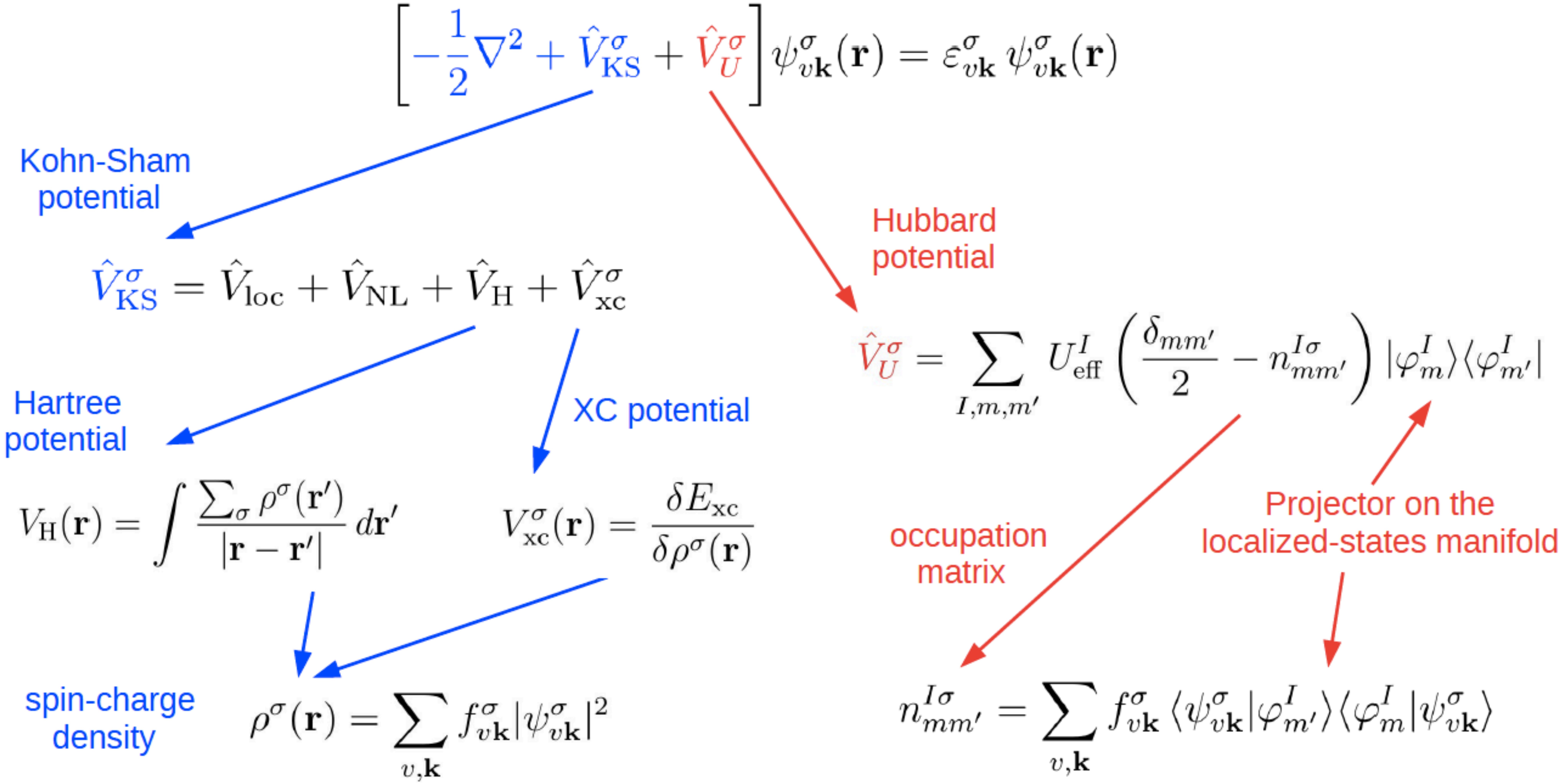

$$\left[-\frac{1}{2}\nabla^2 + \hat{V}^{\sigma}_{\mathrm{KS}} + \hat{V}^{\sigma}_{U}\right]\psi^{\sigma}_{v\mathbf{k}}(\mathbf{r}) = \varepsilon^{\sigma}_{v\mathbf{k}}\,\psi^{\sigma}_{v\mathbf{k}}(\mathbf{r})$$

Kohn-Sham potential

$$\hat{V}^{\sigma}_{\mathrm{KS}} = \hat{V}_{\mathrm{loc}} + \hat{V}_{\mathrm{NL}} + \hat{V}_{\mathrm{H}} + \hat{V}^{\sigma}_{\mathrm{xc}}$$

Hartree potential

XC potential

$$V_{\mathrm{H}}(\mathbf{r}) = \int \frac{\sum_{\sigma}\rho^{\sigma}(\mathbf{r}')}{|\mathbf{r}-\mathbf{r}'|}\,d\mathbf{r}'$$

$$V^{\sigma}_{\mathrm{xc}}(\mathbf{r}) = \frac{\delta E_{\mathrm{xc}}}{\delta\rho^{\sigma}(\mathbf{r})}$$

spin-charge density

$$\rho^{\sigma}(\mathbf{r}) = \sum_{v,\mathbf{k}} f^{\sigma}_{v\mathbf{k}}|\psi^{\sigma}_{v\mathbf{k}}|^2$$

Hubbard potential

$$\hat{V}^{\sigma}_{U} = \sum_{I,m,m'} U^{I}_{\mathrm{eff}}\left(\frac{\delta_{mm'}}{2} - n^{I\sigma}_{mm'}\right)|\varphi^{I}_{m}\rangle\langle\varphi^{I}_{m'}|$$

occupation matrix

Projector on the localized-states manifold

$$n^{I\sigma}_{mm'} = \sum_{v,\mathbf{k}} f^{\sigma}_{v\mathbf{k}}\,\langle\psi^{\sigma}_{v\mathbf{k}}|\varphi^{I}_{m'}\rangle\langle\varphi^{I}_{m}|\psi^{\sigma}_{v\mathbf{k}}\rangle$$

Kohn-Sham equations including the Hubbard potential

By taking a functional derivative of the DFT+U total-energy functional with respect to the complex-conjugate Kohn-Sham wavefunction, we obtain an expression for the **modified Kohn-Sham equations**:

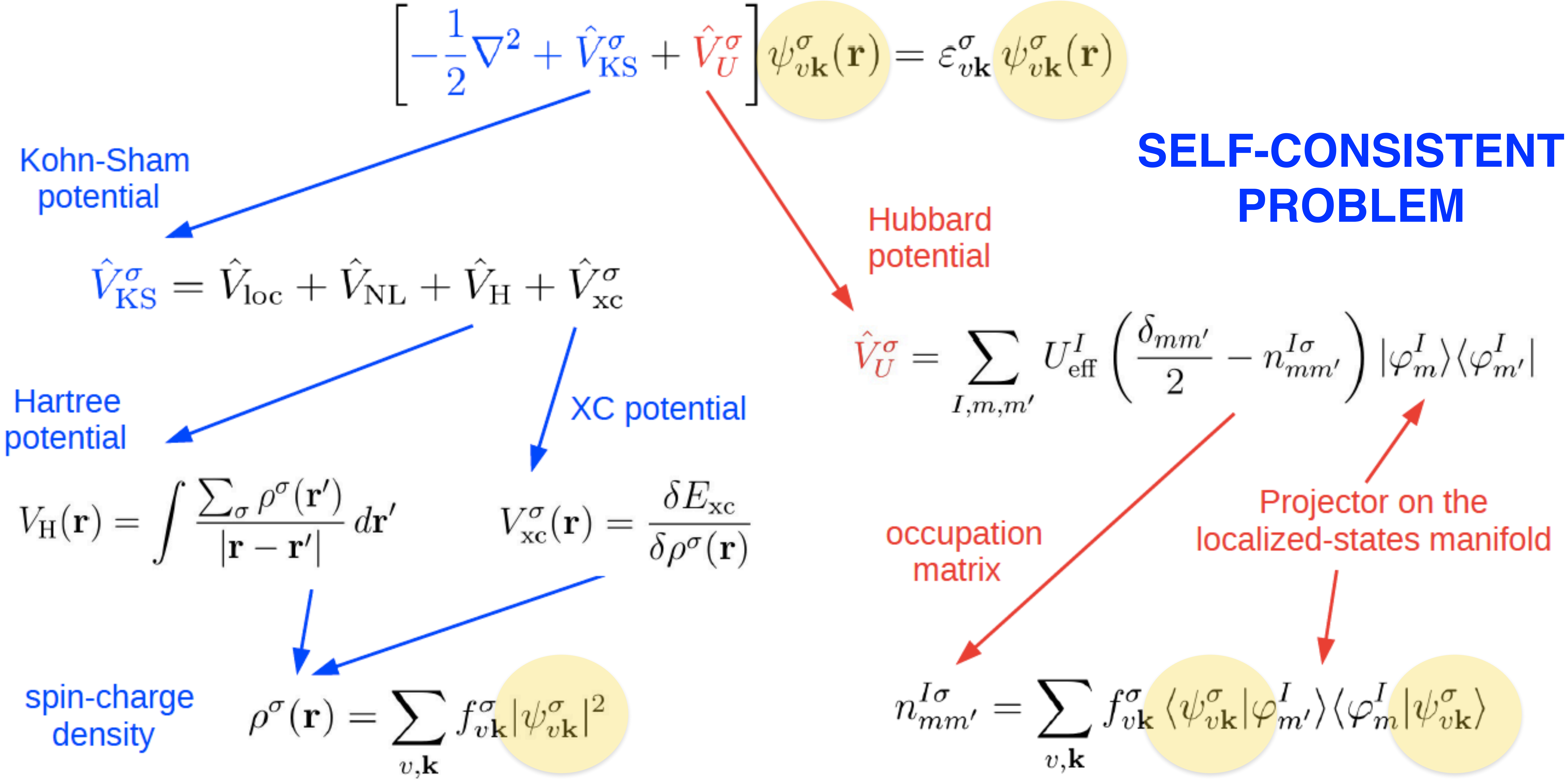

$$\left[-\frac{1}{2}\nabla^2 + \hat{V}^\sigma_{\mathrm{KS}} + \hat{V}^\sigma_U\right]\psi^\sigma_{v\mathbf{k}}(\mathbf{r}) = \varepsilon^\sigma_{v\mathbf{k}}\,\psi^\sigma_{v\mathbf{k}}(\mathbf{r})$$

Kohn-Sham potential

$$\hat{V}^\sigma_{\mathrm{KS}} = \hat{V}_{\mathrm{loc}} + \hat{V}_{\mathrm{NL}} + \hat{V}_{\mathrm{H}} + \hat{V}^\sigma_{\mathrm{xc}}$$

Hartree potential

XC potential

$$V_{\mathrm{H}}(\mathbf{r}) = \int \frac{\sum_\sigma \rho^\sigma(\mathbf{r}')}{|\mathbf{r}-\mathbf{r}'|}\,d\mathbf{r}' \qquad V^\sigma_{\mathrm{xc}}(\mathbf{r}) = \frac{\delta E_{\mathrm{xc}}}{\delta\rho^\sigma(\mathbf{r})}$$

spin-charge density

$$\rho^\sigma(\mathbf{r}) = \sum_{v,\mathbf{k}} f^\sigma_{v\mathbf{k}}|\psi^\sigma_{v\mathbf{k}}|^2$$

SELF-CONSISTENT PROBLEM

Hubbard potential

$$\hat{V}^\sigma_U = \sum_{I,m,m'} U^I_{\mathrm{eff}}\left(\frac{\delta_{mm'}}{2} - n^{I\sigma}_{mm'}\right)|\varphi^I_m\rangle\langle\varphi^I_{m'}|$$

occupation matrix

Projector on the localized-states manifold

$$n^{I\sigma}_{mm'} = \sum_{v,\mathbf{k}} f^\sigma_{v\mathbf{k}}\,\langle\psi^\sigma_{v\mathbf{k}}|\varphi^I_{m'}\rangle\langle\varphi^I_m|\psi^\sigma_{v\mathbf{k}}\rangle$$

Generalization of DFT+*U* to DFT+*U*+*V*

DFT+*U* : $$\boxed{E = E_{\mathrm{DFT}} + \frac{1}{2}\sum_{I,\sigma} U^I \,\mathrm{Tr}\left[\left(\mathbf{1} - \mathbf{n}^{I\sigma}\right)\mathbf{n}^{I\sigma}\right]} \qquad \left(\mathbf{n}^{I\sigma}\right)_{m_1 m_2} = \sum_i f_i \,\langle \psi_{i\sigma} | \varphi^I_{m_2} \rangle \langle \varphi^I_{m_1} | \psi_{i\sigma} \rangle$$

Anisimov et al., PRB (1991). *Liechtenstein et al., PRB (1995).* *Dudarev et al., PRB (1998).*

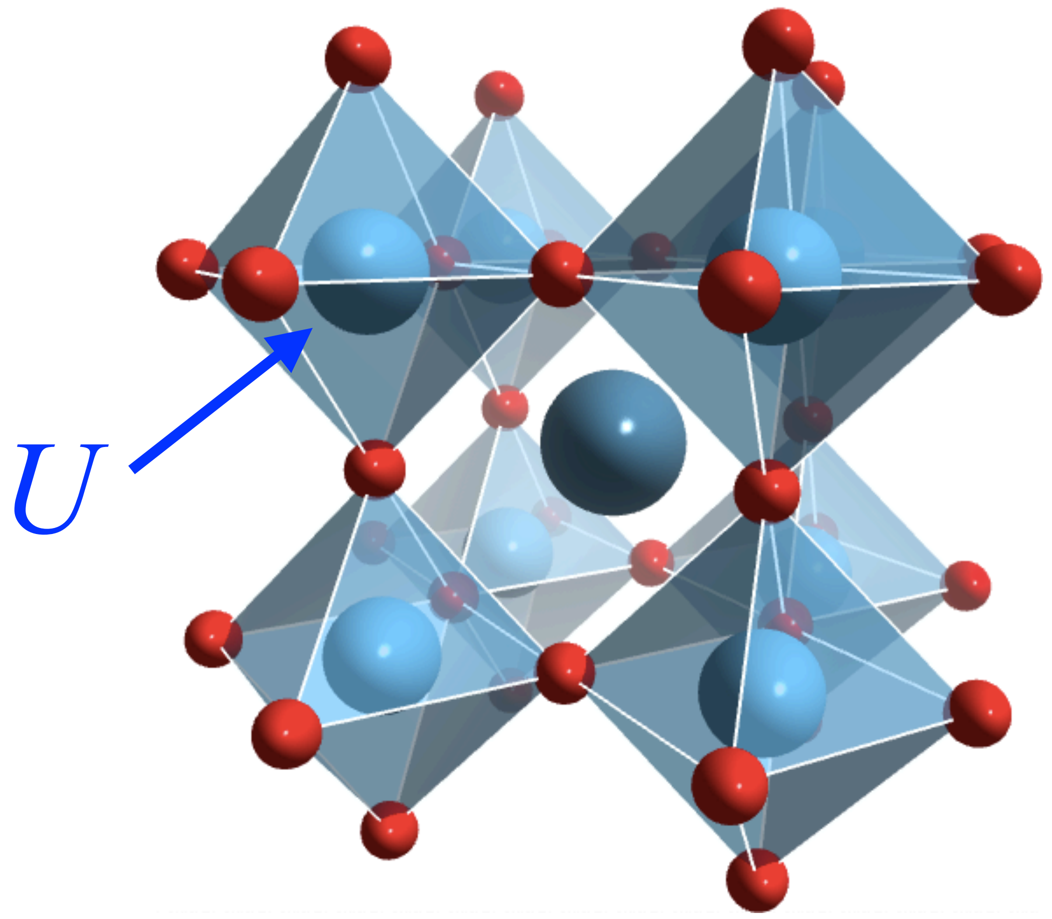

← **on-site localisation (*U*)**

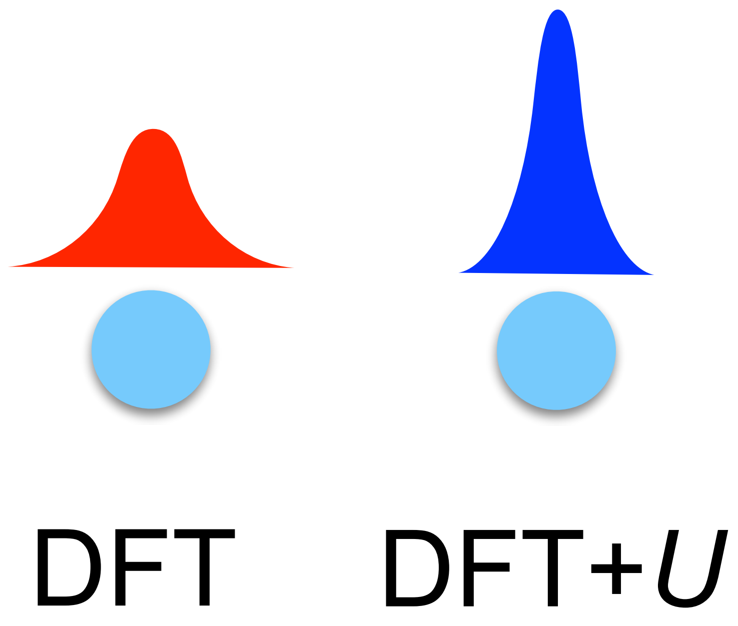

Generalization of DFT+*U* to DFT+*U*+*V*

DFT+*U* :

$$\boxed{E = E_{\mathrm{DFT}} + \frac{1}{2}\sum_{I,\sigma} U^I \,\mathrm{Tr}\left[\left(\mathbf{1} - \mathbf{n}^{I\sigma}\right)\mathbf{n}^{I\sigma}\right]} \qquad \left(\mathbf{n}^{I\sigma}\right)_{m_1 m_2} = \sum_i f_i \,\langle\psi_{i\sigma}|\varphi^I_{m_2}\rangle\langle\varphi^I_{m_1}|\psi_{i\sigma}\rangle$$

Anisimov et al., PRB (1991). *Liechtenstein et al., PRB (1995).* *Dudarev et al., PRB (1998).*

DFT+*U*+*V* :

$$\boxed{E = E_{\mathrm{DFT}} + \frac{1}{2}\sum_{I,\sigma} U^I \,\mathrm{Tr}\left[\left(\mathbf{1} - \mathbf{n}^{I\sigma}\right)\mathbf{n}^{I\sigma}\right] - \frac{1}{2}\sum_{I,J,\sigma} V^{IJ}\,\mathrm{Tr}\left[\mathbf{n}^{IJ\sigma}\mathbf{n}^{JI\sigma}\right]}$$

Campo Jr and Cococcioni, JPCM (2010).

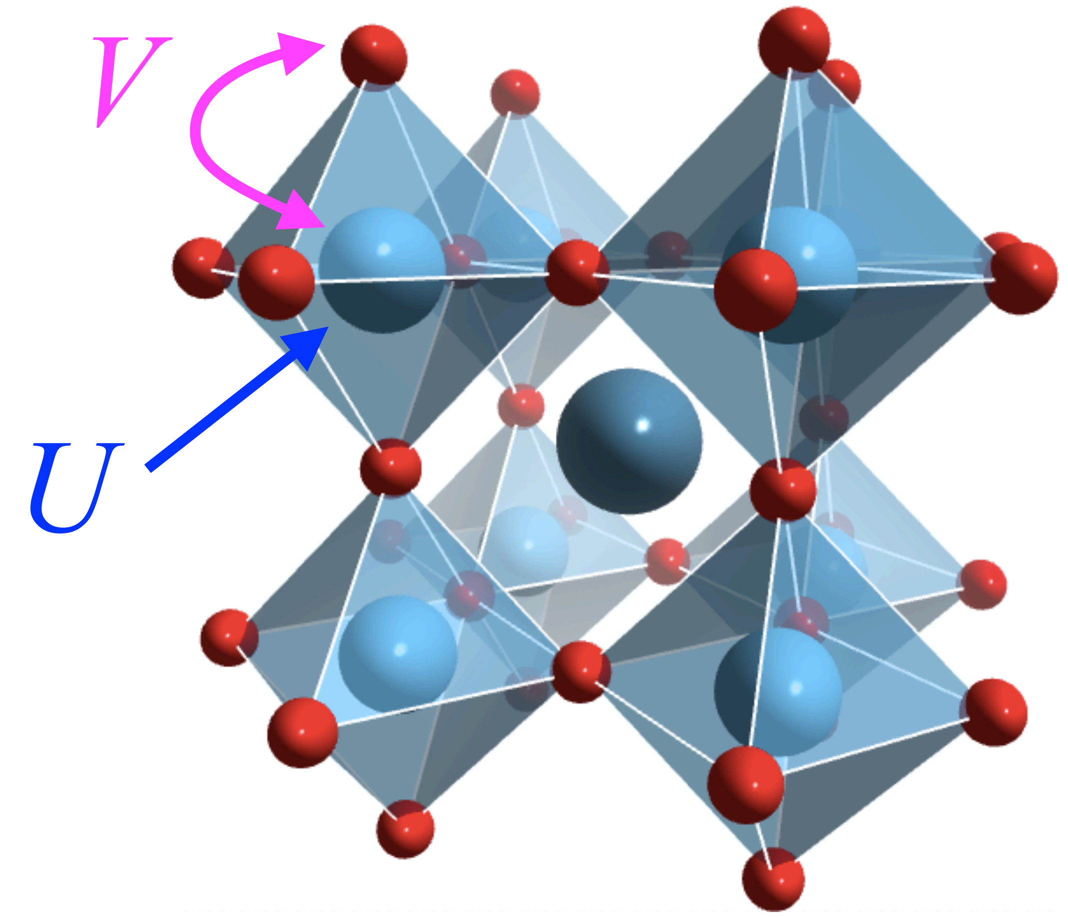

on-site localisation (*U*) &
inter-site hybridisations (*V*)

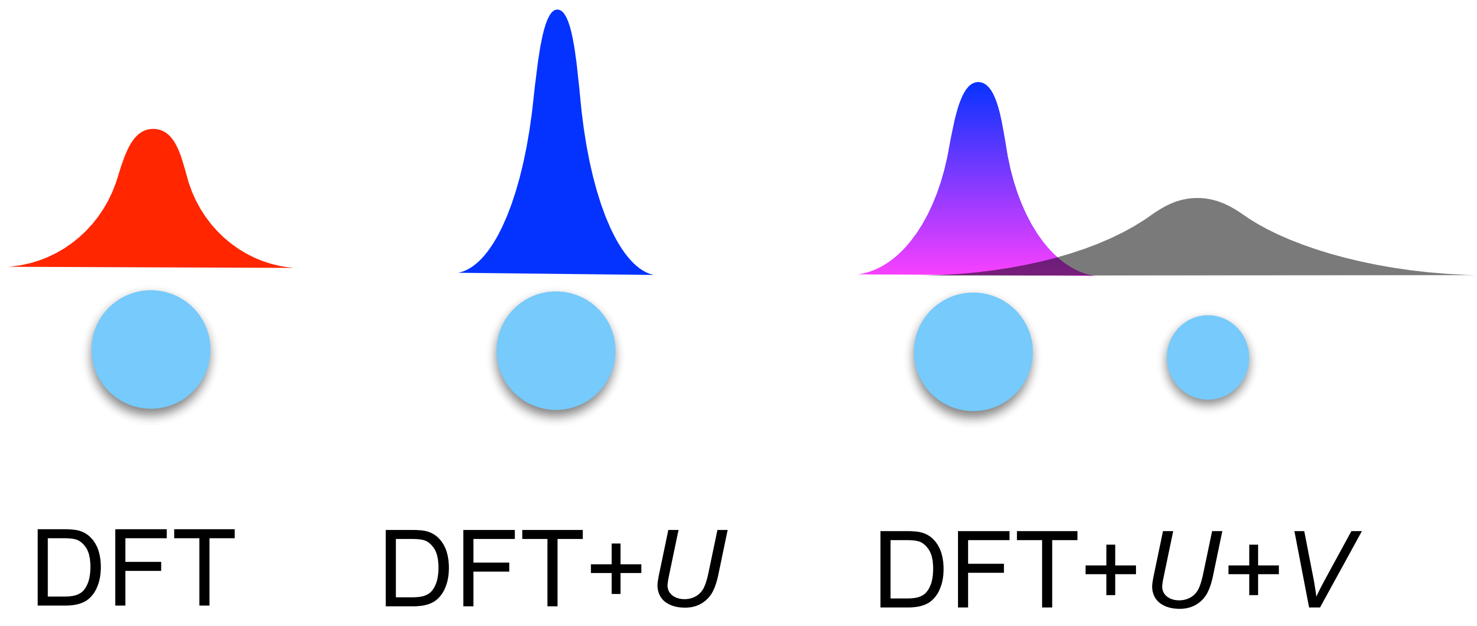

Two (strongly-interconnected) key aspects of DFT+*U*(+*V*)

$$E = E_{\mathrm{DFT}} + \frac{1}{2}\sum_{I,\sigma} U^I \,\mathrm{Tr}\left[\left(\mathbf{1} - \mathbf{n}^{I\sigma}\right)\mathbf{n}^{I\sigma}\right] - \frac{1}{2}\sum_{I,J,\sigma} V^{IJ}\,\mathrm{Tr}\left[\mathbf{n}^{IJ\sigma}\mathbf{n}^{JI\sigma}\right]$$

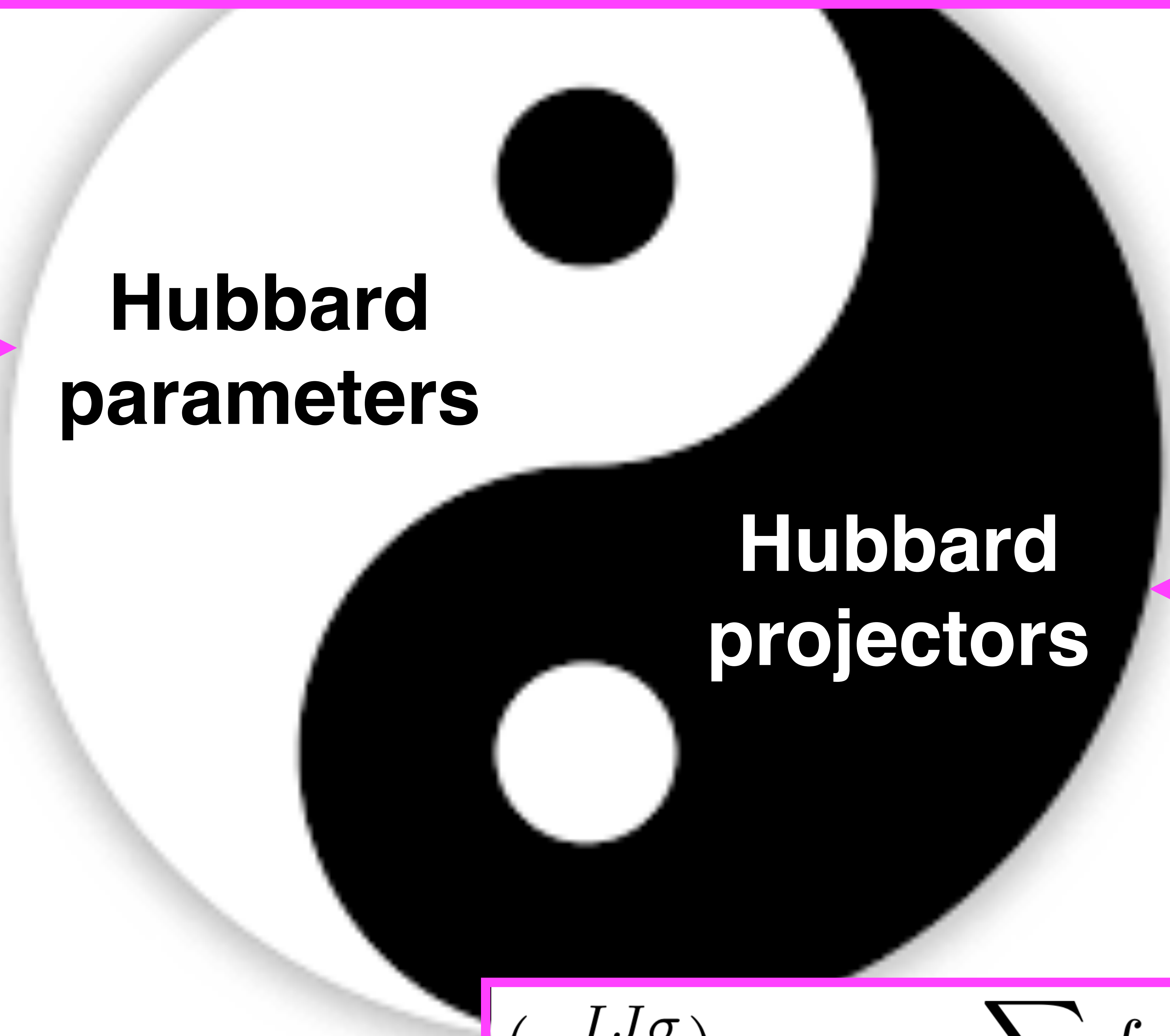

Hubbard parameters

Hubbard projectors

$$\left(\mathbf{n}^{IJ\sigma}\right)_{m_1 m_2} = \sum_i f_i \,\langle\psi_{i\sigma}|\varphi^J_{m_2}\rangle\langle\varphi^I_{m_1}|\psi_{i\sigma}\rangle$$

Which values for the Hubbard parameters?

The values of Hubbard parameters are not known *a priori*

Which values for the Hubbard parameters?

The values of Hubbard parameters are not known *a priori*

Two strategies

Which values for the Hubbard parameters?

The values of Hubbard parameters are not known *a priori*

Two strategies

(Semi-)empirical

Tune *U* to reproduce, for example:

- Band gaps
- Magnetic moments
- Lattice parameters
- Oxidation enthalpies
- …

Requires the availability of the experimental data!

Which values for the Hubbard parameters?

The values of Hubbard parameters are not known *a priori*

Two strategies

(Semi-)empirical

Tune *U* to reproduce, for example:

- Band gaps
- Magnetic moments
- Lattice parameters
- Oxidation enthalpies
- …

Requires the availability of the experimental data!

First-principles

- Constrained density-functional theory (cDFT)
- Constrained random phase approximation (cRPA)
- Hartree-Fock-based approaches (e.g. ACBN0)
- Linear-response theory

this talk

Hubbard parameters are not universal

Computed Hubbard parameters depend on:

- **Type of Hubbard projector functions**
  (e.g. atomic, orthogonalized atomic, maximally localized Wannier functions, etc.)

$$(\mathbf{n}^{I\sigma})_{m_1 m_2} = \sum_i f_i \, \langle \psi_{i\sigma} | \varphi^I_{m_2} \rangle \langle \varphi^I_{m_1} | \psi_{i\sigma} \rangle$$

- **Oxidation state of a pseudized atom (pseudopotentials)** [1]

- **Exchange-correlation functional** (e.g. LDA, GGA, etc.)

- **Self-consistency** (i.e. either “one-shot” or self-consistent)

[1] Kulik and Marzari, JCP (2008).

Hubbard parameters from linear-response theory

$$\boxed{E = E_{\mathrm{DFT}} + \frac{1}{2} U \, \mathrm{Tr}\left[(\mathbf{1} - \mathbf{n})\, \mathbf{n}\right]} \qquad \mathrm{n} = \mathrm{Tr}[\mathbf{n}]$$

The main idea: Hubbard corrections remove spurious curvature of the total energy

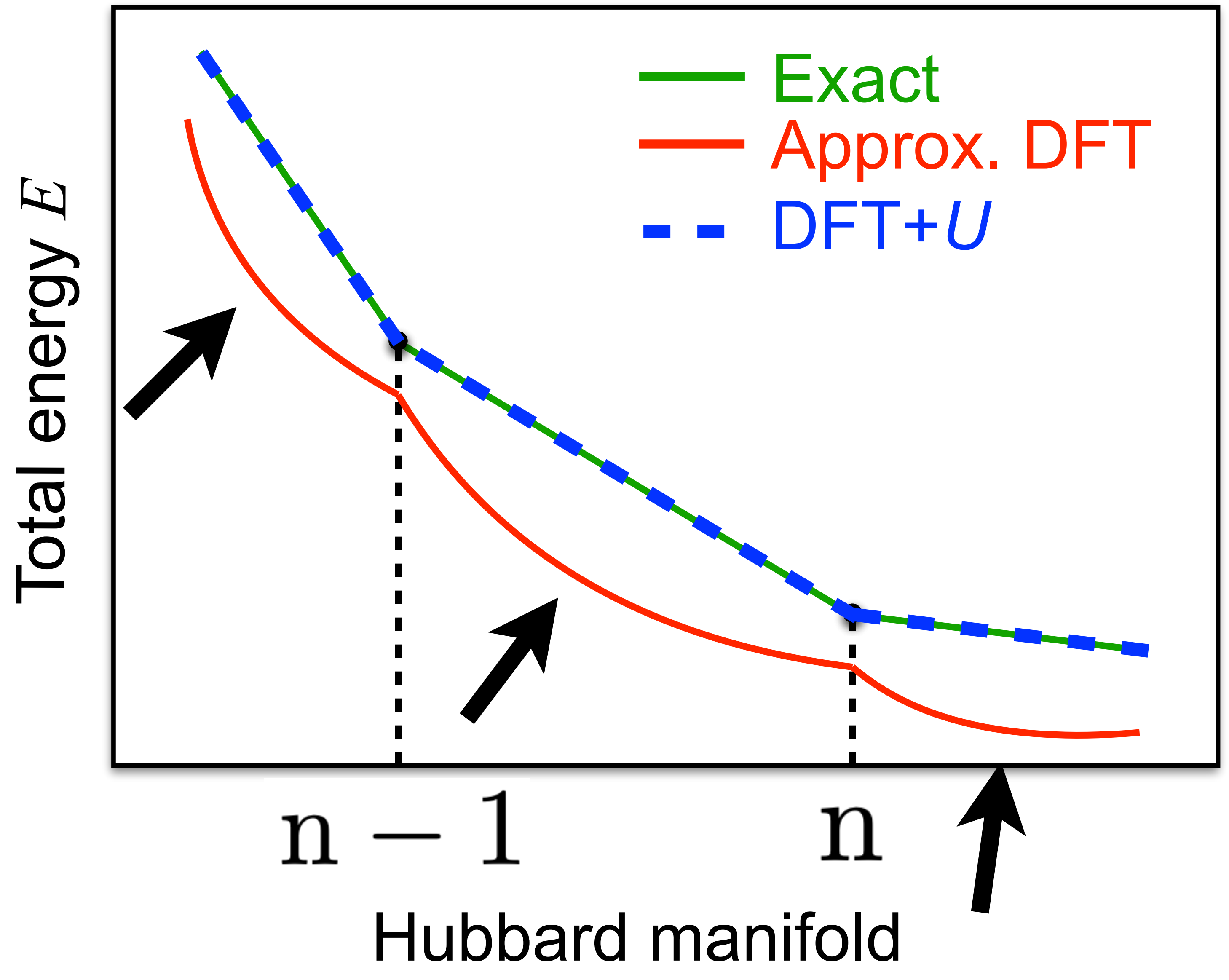

Note: There is no theorem for the piece-wise linearity of E in the Hubbard manifold (only for total number of electrons)

Hubbard parameters from linear-response theory

$$\boxed{E = E_{\mathrm{DFT}} + \frac{1}{2} U \,\mathrm{Tr}\left[(\mathbf{1} - \mathbf{n})\,\mathbf{n}\right]}$$

$$\mathrm{n} = \mathrm{Tr}[\mathbf{n}]$$

The main idea: Hubbard corrections remove spurious curvature of the total energy

Hubbard parameters can be obtained from the following condition:

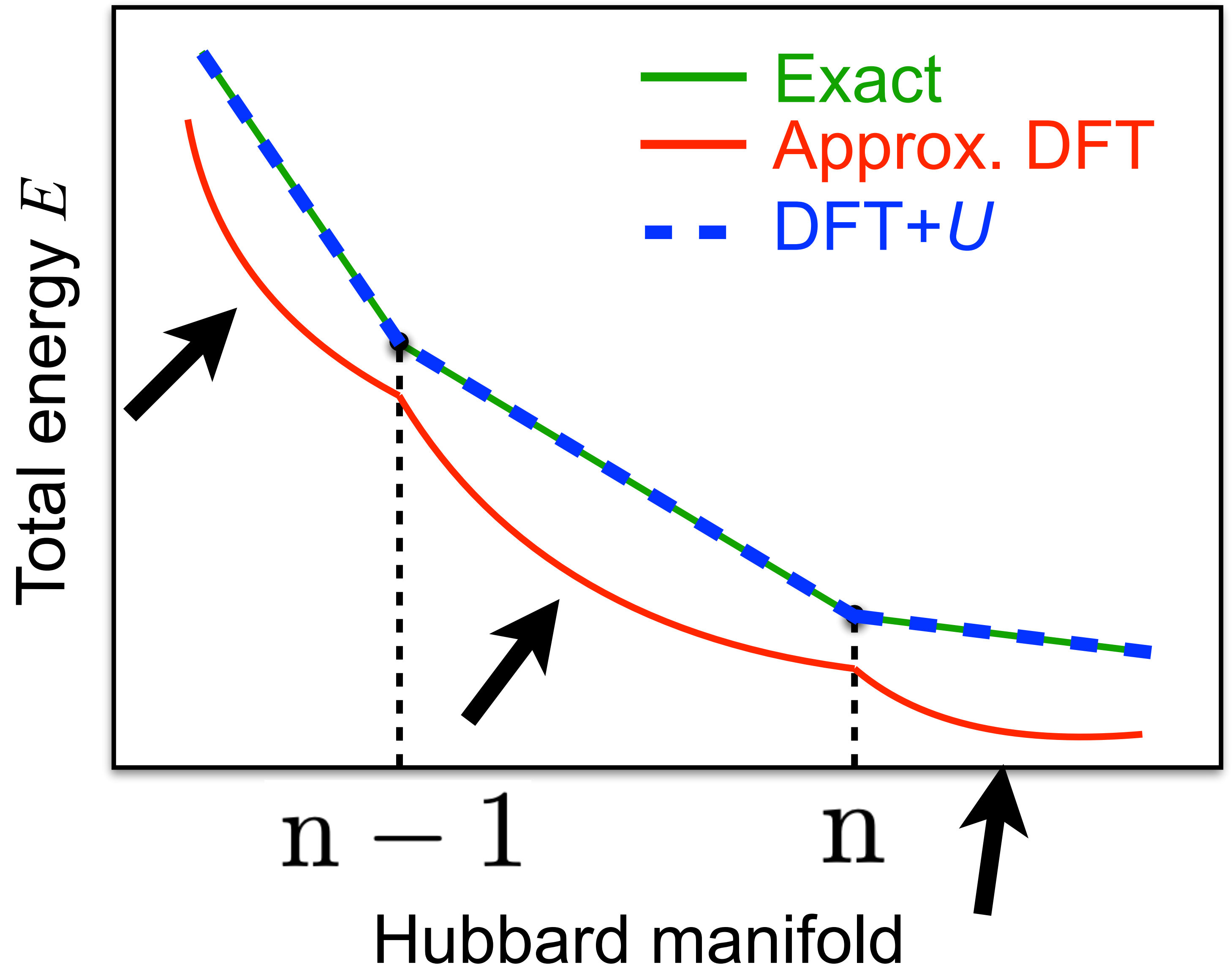

$$\boxed{\frac{d^2 E}{d\mathrm{n}^2} = 0}$$

$$\boxed{U = \frac{d^2 E_{\mathrm{DFT}}}{d\mathrm{n}^2}}$$

Note: There is no theorem for the piece-wise linearity of E in the Hubbard manifold (only for total number of electrons)

Cococcioni and de Gironcoli, PRB (2005).

Linear-response theory using supercells

Modified Kohn-Sham equations:

$$\left(\hat{H}_\sigma + \lambda^J \hat{V}^J_{\mathrm{pert}}\right)|\psi_{v\mathbf{k}\sigma}\rangle = \varepsilon_{v\mathbf{k}\sigma}|\psi_{v\mathbf{k}\sigma}\rangle$$

Perturbing potential:

$$\hat{V}^J_{\mathrm{pert}} = \sum_m |\varphi^J_m\rangle\langle\varphi^J_m|$$

Response matrices
(numerical derivative using finite differences)

$$\chi_{IJ} = \frac{\Delta n^I}{\Delta\lambda^J}$$

Hubbard parameters:

$$U^I = (\chi_0^{-1} - \chi^{-1})_{II} \quad V^{IJ} = (\chi_0^{-1} - \chi^{-1})_{IJ}$$

Cococcioni and de Gironcoli, PRB (2005).

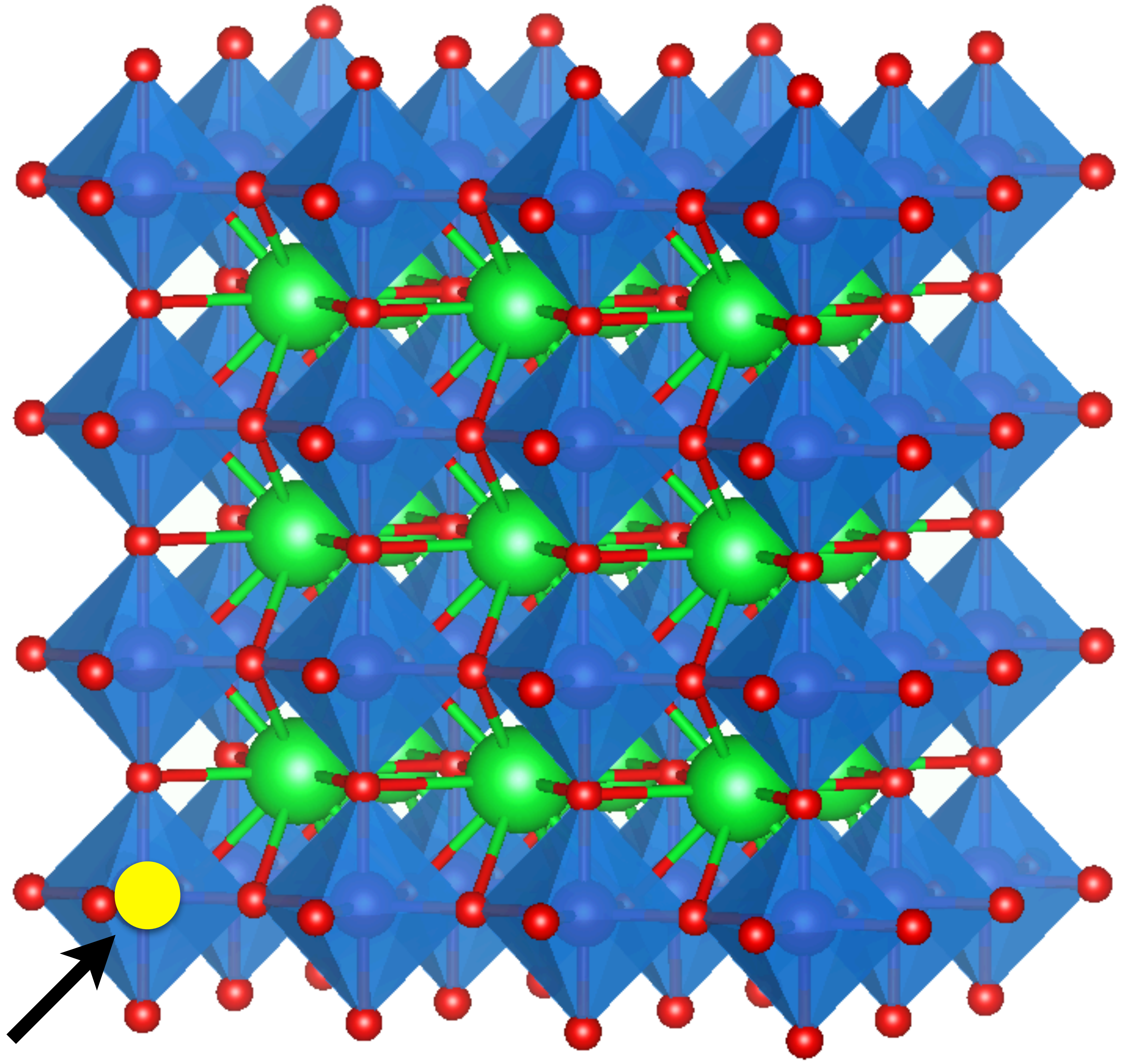

Perturbed
atom

- Computationally expensive
- Possible convergence issues when using large supercells
- Quite cumbersome to use

Linear-response theory: from supercells to primitive unit cells

Modified Kohn-Sham equations:

$$\left(\hat{H}_\sigma + \lambda^J \hat{V}^J_{\mathrm{pert}}\right)|\psi_{v\mathbf{k}\sigma}\rangle = \varepsilon_{v\mathbf{k}\sigma}|\psi_{v\mathbf{k}\sigma}\rangle$$

Perturbing potential:

$$\hat{V}^J_{\mathrm{pert}} = \sum_m |\varphi^J_m\rangle\langle\varphi^J_m|$$

Perturbation theory to 1st order:

$$(\hat{H}^\circ_\sigma - \varepsilon^\circ_{v\mathbf{k}\sigma})\left|\frac{d\psi_{v\mathbf{k}\sigma}}{d\lambda^J}\right\rangle = -\left(\frac{d\hat{V}_{\mathrm{Hxc},\sigma}}{d\lambda^J} - \frac{d\varepsilon_{v\mathbf{k}\sigma}}{d\lambda^J} + \hat{V}^J_{\mathrm{pert}}\right)|\psi^\circ_{v\mathbf{k}\sigma}\rangle$$

Cococcioni and de Gironcoli, PRB (2005).

Timrov, Marzari, and Cococcioni, PRB (2018), PRB (2021).

Linear-response theory: from supercells to primitive unit cells

Modified Kohn-Sham equations:

$$\left(\hat{H}_\sigma + \lambda^J \hat{V}^J_{\mathrm{pert}}\right)|\psi_{v\mathbf{k}\sigma}\rangle = \varepsilon_{v\mathbf{k}\sigma}|\psi_{v\mathbf{k}\sigma}\rangle$$

Perturbing potential:

$$\hat{V}^J_{\mathrm{pert}} = \sum_m |\varphi^J_m\rangle\langle\varphi^J_m|$$

Perturbation theory to 1st order:

$$(\hat{H}^\circ_\sigma - \varepsilon^\circ_{v\mathbf{k}\sigma})\left|\frac{d\psi_{v\mathbf{k}\sigma}}{d\lambda^J}\right\rangle = -\left(\frac{d\hat{V}_{\mathrm{Hxc},\sigma}}{d\lambda^J} - \frac{d\varepsilon_{v\mathbf{k}\sigma}}{d\lambda^J} + \hat{V}^J_{\mathrm{pert}}\right)|\psi^\circ_{v\mathbf{k}\sigma}\rangle$$

Potential in a supercell can be decomposed into a sum over **q** points for a primitive cell:

$$V(\mathbf{r}) = \sum_{\mathbf{q}} e^{i\mathbf{q}\cdot\mathbf{r}}\,\bar{V}_{\mathbf{q}}(\mathbf{r})$$

Cococcioni and de Gironcoli, PRB (2005).

Timrov, Marzari, and Cococcioni, PRB (2018), PRB (2021).

Linear-response theory: from supercells to primitive unit cells

Modified Kohn-Sham equations:

$$\left(\hat{H}_\sigma + \lambda^J \hat{V}^J_{\text{pert}}\right)|\psi_{v\mathbf{k}\sigma}\rangle = \varepsilon_{v\mathbf{k}\sigma}|\psi_{v\mathbf{k}\sigma}\rangle$$

Perturbing potential:

$$\hat{V}^J_{\text{pert}} = \sum_m |\varphi^J_m\rangle\langle\varphi^J_m|$$

Response matrices
(numerical derivative using finite differences)

$$\chi_{IJ} = \frac{\Delta n^I}{\Delta \lambda^J}$$

Hubbard parameters:

$$U^I = (\chi_0^{-1} - \chi^{-1})_{II} \quad V^{IJ} = (\chi_0^{-1} - \chi^{-1})_{IJ}$$

Perturbation theory to 1st order:

$$(\hat{H}^\circ_\sigma - \varepsilon^\circ_{v\mathbf{k}\sigma})\left|\frac{d\psi_{v\mathbf{k}\sigma}}{d\lambda^J}\right\rangle = -\left(\frac{d\hat{V}_{\text{Hxc},\sigma}}{d\lambda^J} - \frac{d\varepsilon_{v\mathbf{k}\sigma}}{d\lambda^J} + \hat{V}^J_{\text{pert}}\right)|\psi^\circ_{v\mathbf{k}\sigma}\rangle$$

Potential in a supercell can be decomposed into a sum over **q** points for a primitive cell:

$$V(\mathbf{r}) = \sum_{\mathbf{q}} e^{i\mathbf{q}\cdot\mathbf{r}}\,\bar{V}_{\mathbf{q}}(\mathbf{r})$$

Response occupation matrices
(from the iterative solution of the eq. above)

$$\frac{dn^{sl\sigma}_{m_1m_2}}{d\lambda^{s'l'}} = \frac{1}{N_{\mathbf{q}}}\sum_{\mathbf{q}}^{N_{\mathbf{q}}} e^{i\mathbf{q}\cdot(\mathbf{R}_l - \mathbf{R}_{l'})}\,\Delta^{s'}_{\mathbf{q}}\bar{n}^{s\sigma}_{m_1m_2}$$

Cococcioni and de Gironcoli, PRB (2005).

Timrov, Marzari, and Cococcioni, PRB (2018), PRB (2021).

Linear-response theory: from supercells to primitive unit cells

Density-functional perturbation theory (DFPT)

primitive cell

monochromatic perturbations

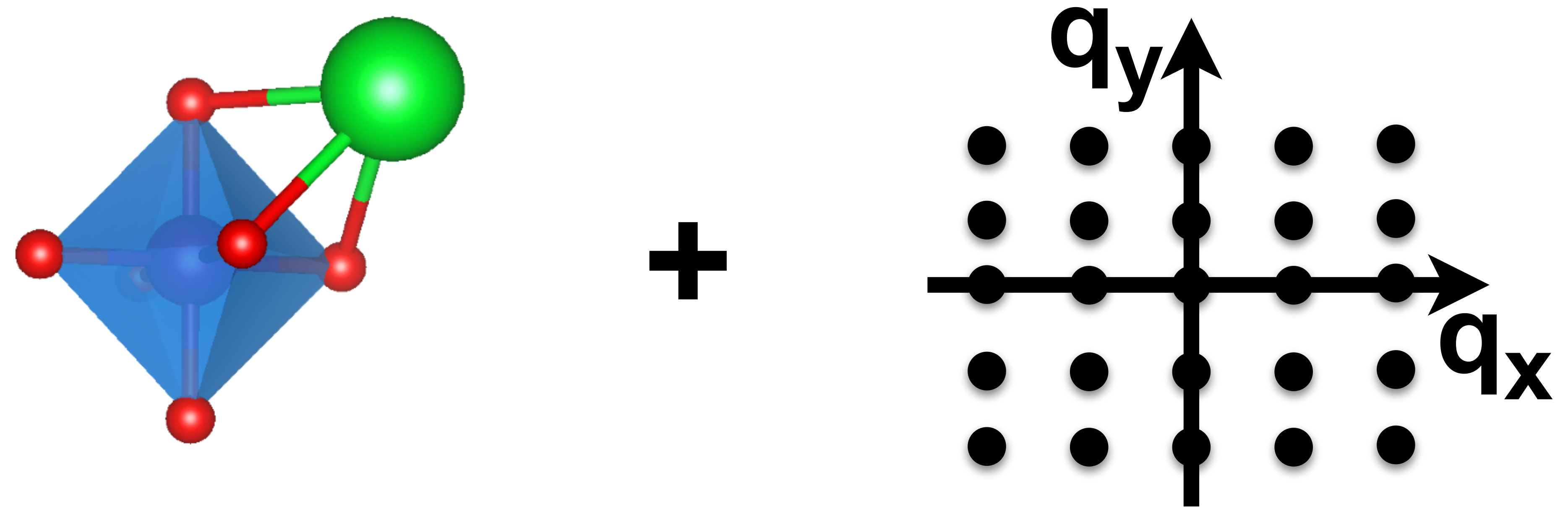

- Computationally much less expensive
- Easier convergence
- User-friendly and autonomous

Inspired by DFPT for phonons:

Baroni, de Gironcoli, Dal Corso, and Giannozzi, RMP (2001).

Perturbation theory to 1st order:

$$(\hat{H}^{\circ}_{\sigma} - \varepsilon^{\circ}_{v\mathbf{k}\sigma})\left|\frac{d\psi_{v\mathbf{k}\sigma}}{d\lambda^{J}}\right\rangle = -\left(\frac{d\hat{V}_{\mathrm{Hxc},\sigma}}{d\lambda^{J}} - \frac{d\varepsilon_{v\mathbf{k}\sigma}}{d\lambda^{J}} + \hat{V}^{J}_{\mathrm{pert}}\right)|\psi^{\circ}_{v\mathbf{k}\sigma}\rangle$$

Potential in a supercell can be decomposed into a sum over **q** points for a primitive cell:

$$V(\mathbf{r}) = \sum_{\mathbf{q}} e^{i\mathbf{q}\cdot\mathbf{r}}\,\bar{V}_{\mathbf{q}}(\mathbf{r})$$

Response occupation matrices (from the iterative solution of the eq. above)

$$\frac{dn^{sl\sigma}_{m_1m_2}}{d\lambda^{s'l'}} = \frac{1}{N_{\mathbf{q}}}\sum_{\mathbf{q}}^{N_{\mathbf{q}}} e^{i\mathbf{q}\cdot(\mathbf{R}_l-\mathbf{R}_{l'})}\,\Delta^{s'}_{\mathbf{q}}\bar{n}^{s\,\sigma}_{m_1m_2}$$

Timrov, Marzari, and Cococcioni, PRB (2018), PRB (2021).

Comparison of the “conventional” linear response and DFPT

Scaling

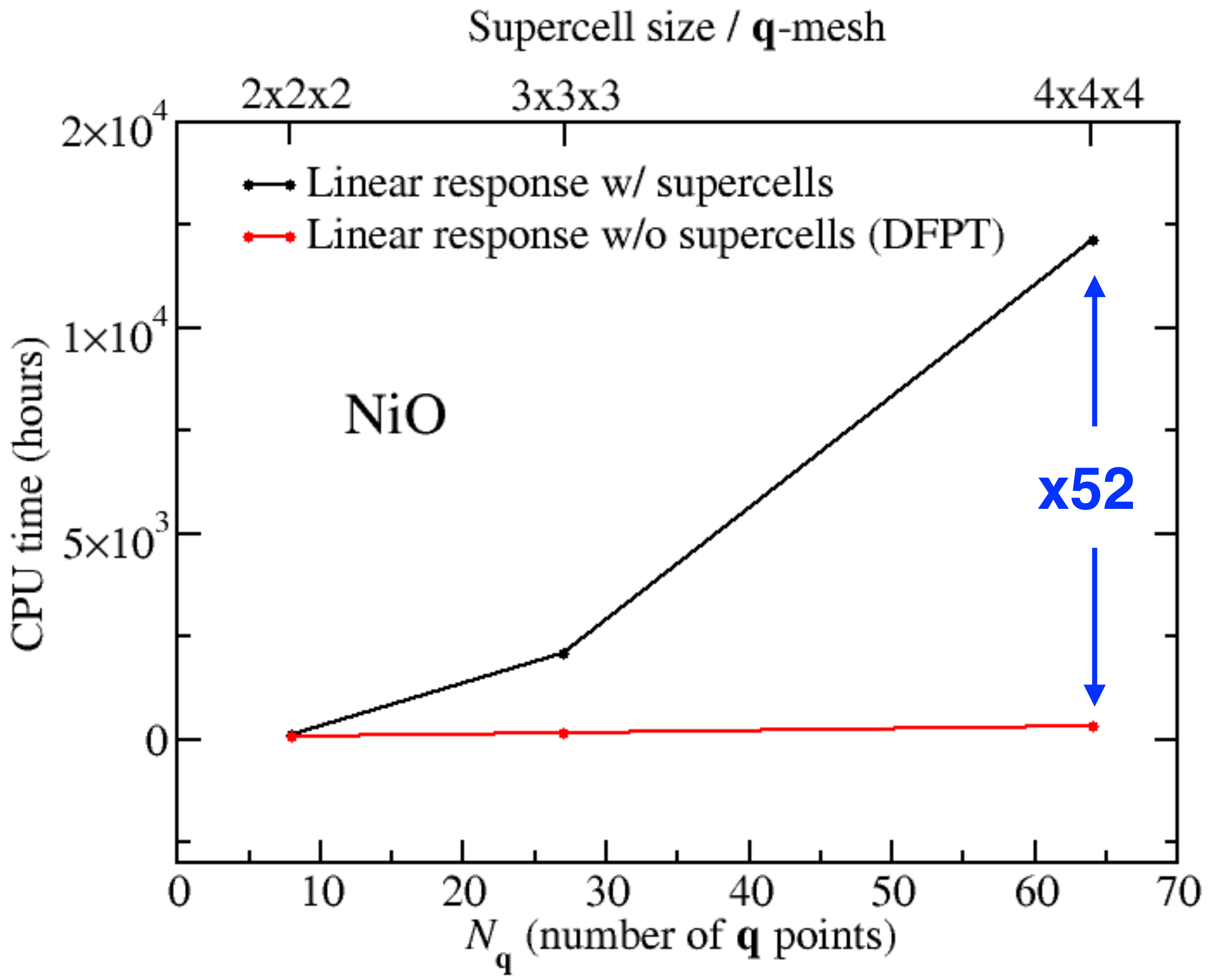

Benchmark of the equivalence between the two approaches

Method	**k**-mesh	SC-size/**q**-mesh	U(Ni-d)
LR-SC	$6\times6\times6$	$2\times2\times2$	7.895
DFPT	$12\times12\times12$		7.900
LR-SC	$4\times4\times4$	$3\times3\times3$	8.146
DFPT	$12\times12\times12$		8.149
LR-SC	$3\times3\times3$	$4\times4\times4$	8.168
DFPT	$12\times12\times12$		8.172

HP code is public and is part of

QUANTUM ESPRESSO

Symmetry → Reduction of $N_\mathbf{q}$ in DFPT

(no equivalence in the supercell approach)

Timrov, Marzari, and Cococcioni, PRB (2018), PRB (2021), CPC (2022).

The zoo of Hubbard projectors

1. Nonorthogonalized atomic orbitals

$\phi^I_{m_1}(\mathbf{r}-\mathbf{R}_I)$ (contained in pseudopotentials)

→

Drawback:
Application of Hubbard *U*
twice in the overlap regions

2. Orthogonalized atomic orbitals

$$\tilde{\phi}^I_{m_1}(\mathbf{r}-\mathbf{R}_I) = \sum_{Jm_2} \left(\hat{O}^{-\frac{1}{2}}\right)^{JI}_{m_2 m_1} \phi^J_{m_2}(\mathbf{r}-\mathbf{R}_J)$$

$$\left(\hat{O}\right)^{IJ}_{m_1 m_2} = \langle \phi^I_{m_1} | \phi^J_{m_2} \rangle$$

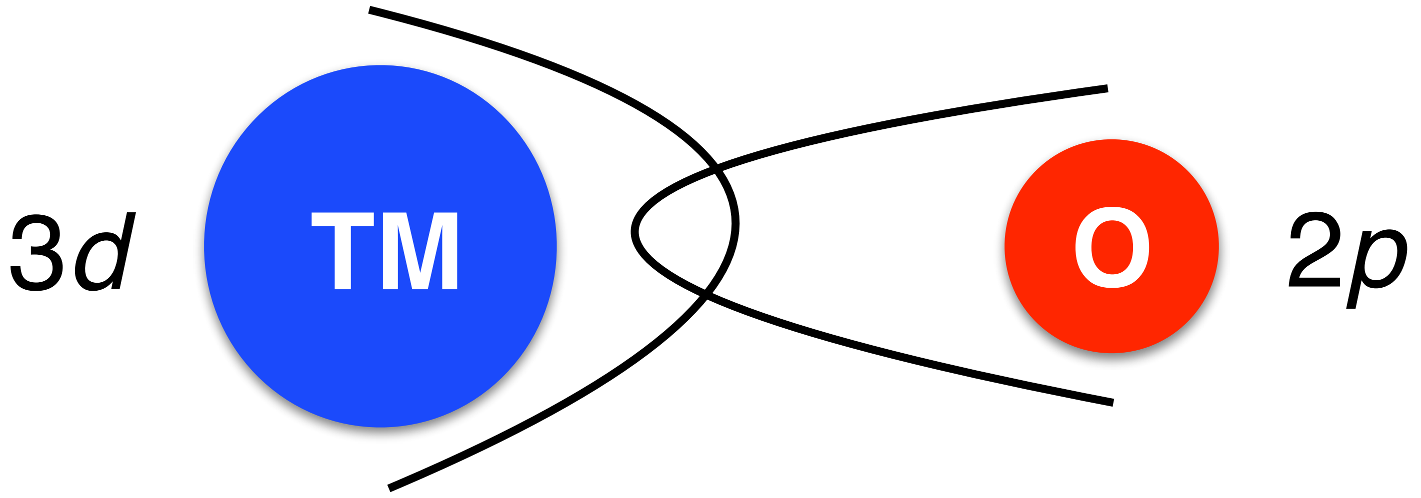

3. Maximally localized Wannier functions

$$w^I_{m_1}(\mathbf{r}-\mathbf{R}_I) = \frac{1}{\sqrt{N_\mathbf{k}}} \sum_{\mathbf{k}} e^{-i\mathbf{k}\cdot\mathbf{R}_I} \sum_{n}^{N_{\mathrm{KSbands}}} U^{(\mathbf{k})}_{nm_1} \psi_{n\mathbf{k}}(\mathbf{r})$$

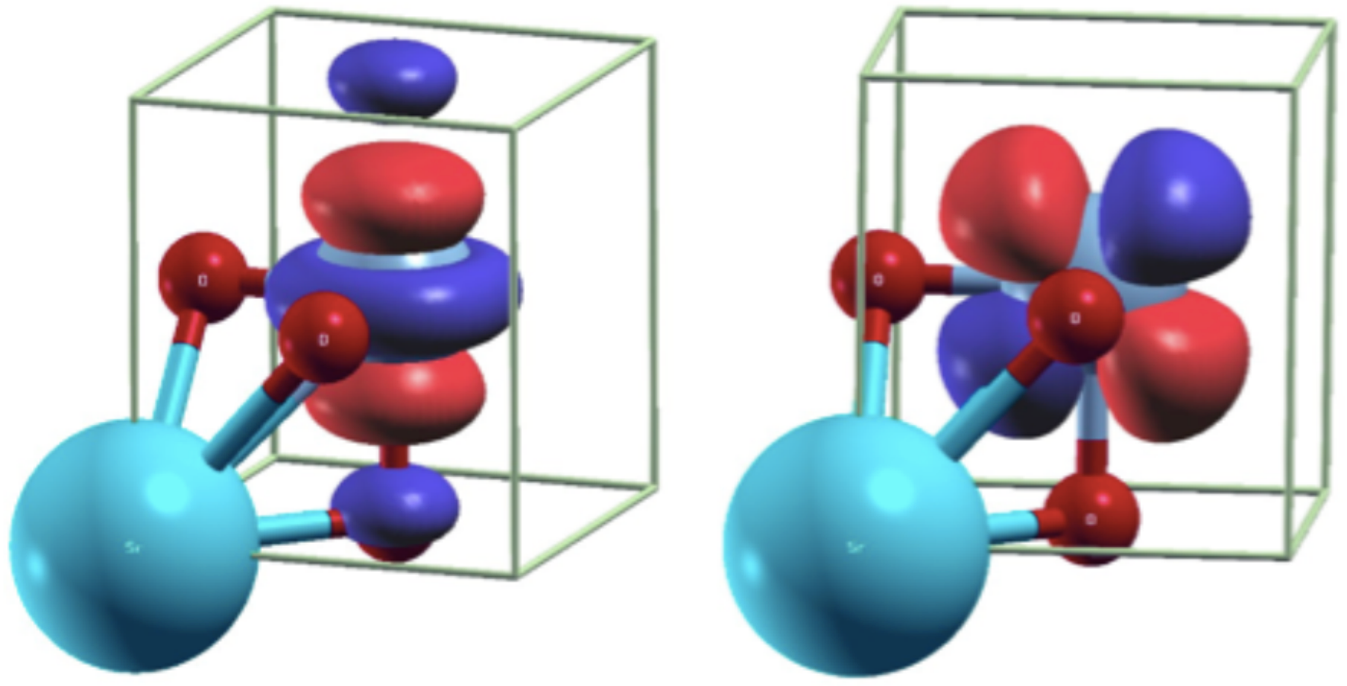

Self-consistent workflow of DFT+*U*+*V*

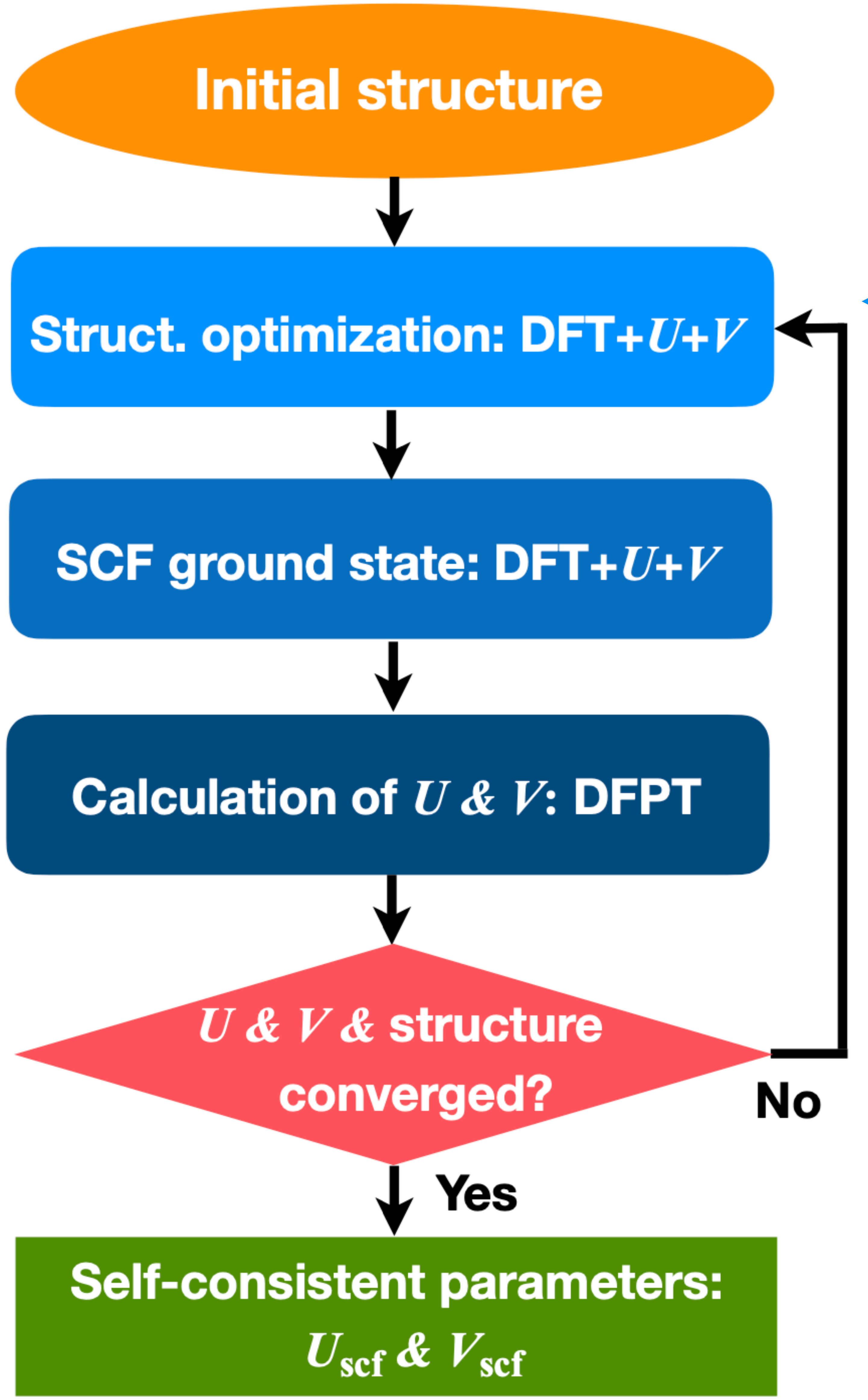

Initial structure

Struct. optimization: DFT+U+V

SCF ground state: DFT+U+V

Calculation of U & V: DFPT

U & V & structure converged?

No

Yes

Self-consistent parameters:
U_{scf} & V_{scf}

Structural optimization (needs Hubbard forces and stresses)

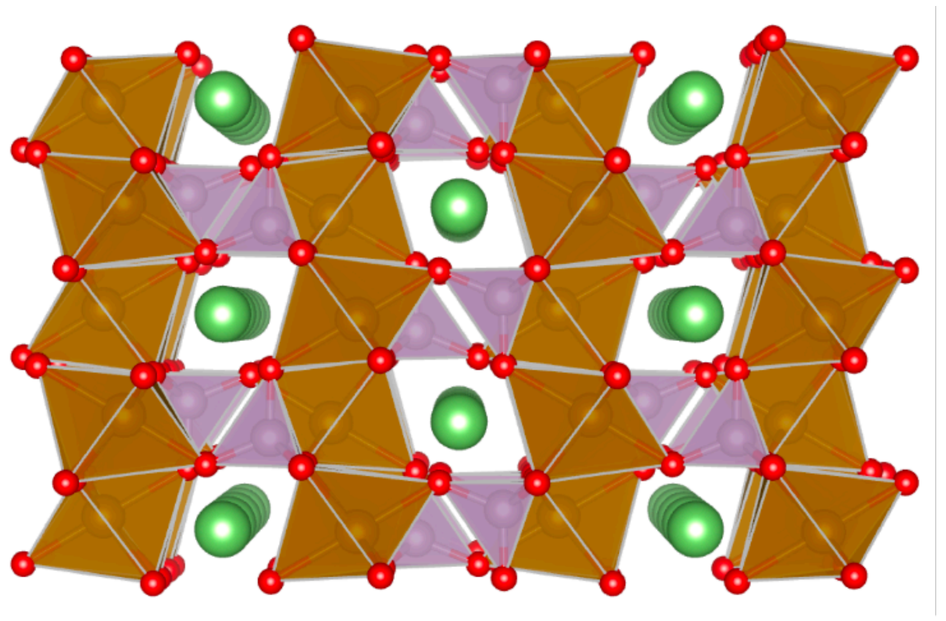

Calculation of Hubbard parameters

$$U^{I} = (\chi_0^{-1} - \chi^{-1})_{II}$$

$$V^{IJ} = (\chi_0^{-1} - \chi^{-1})_{IJ}$$

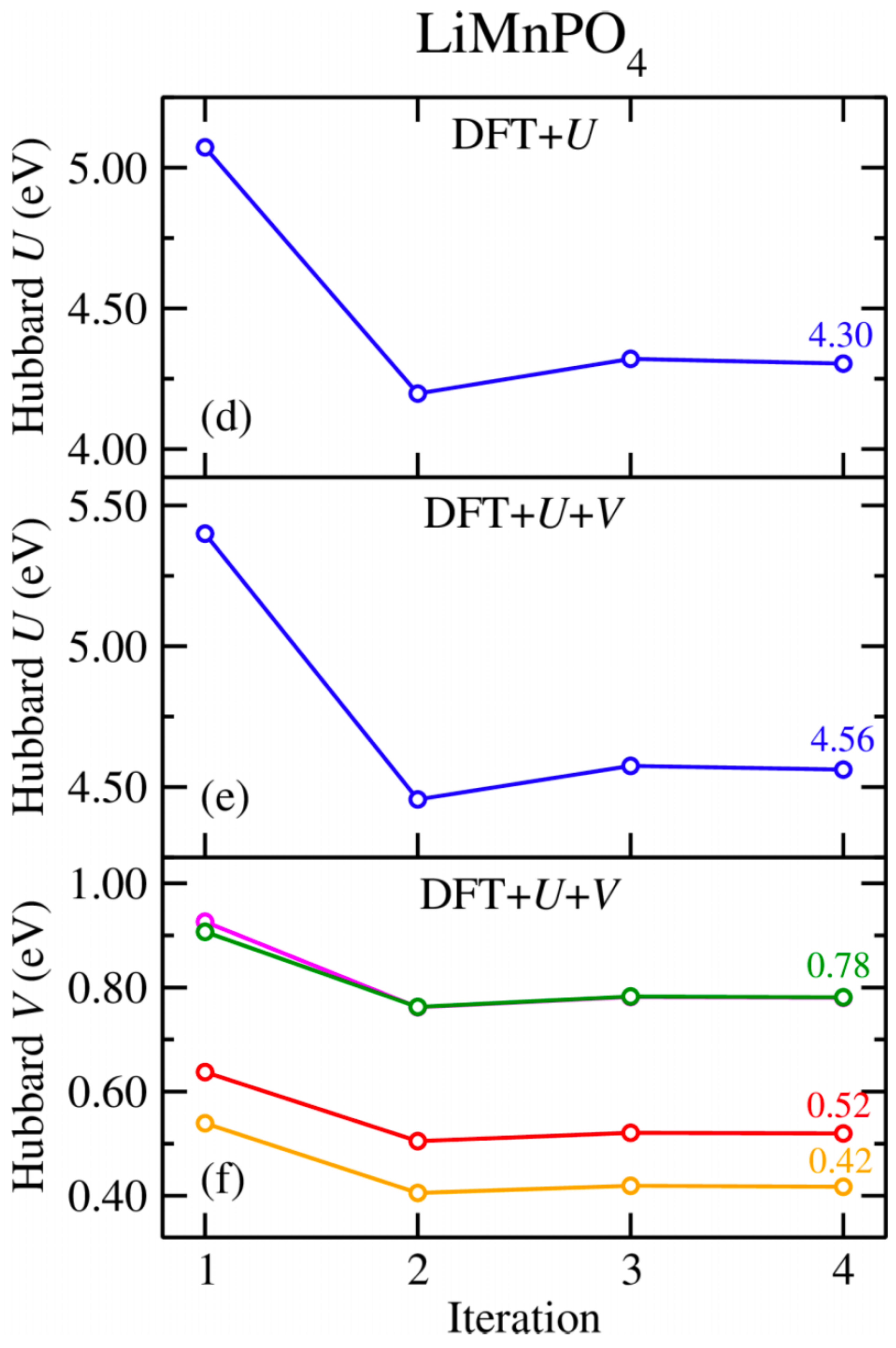

Timrov, Marzari, and Cococcioni, PRB (2021).

Applications

Defects in perovskites

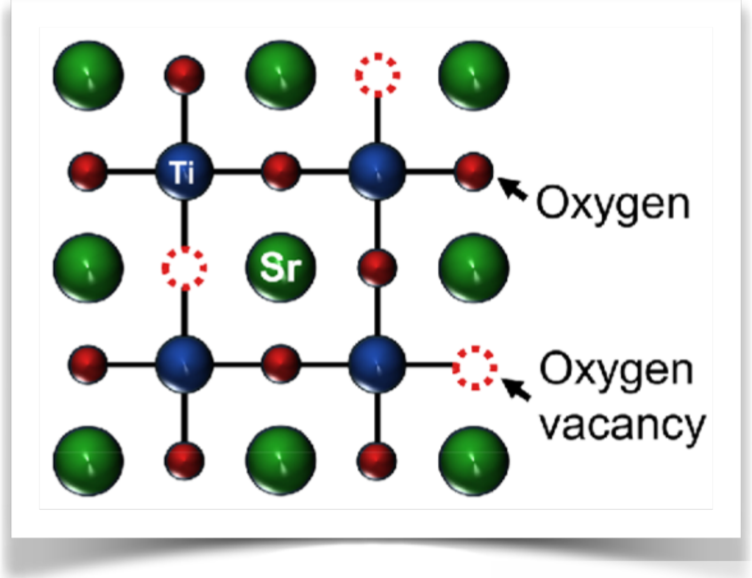

Photocatalytic water splitting

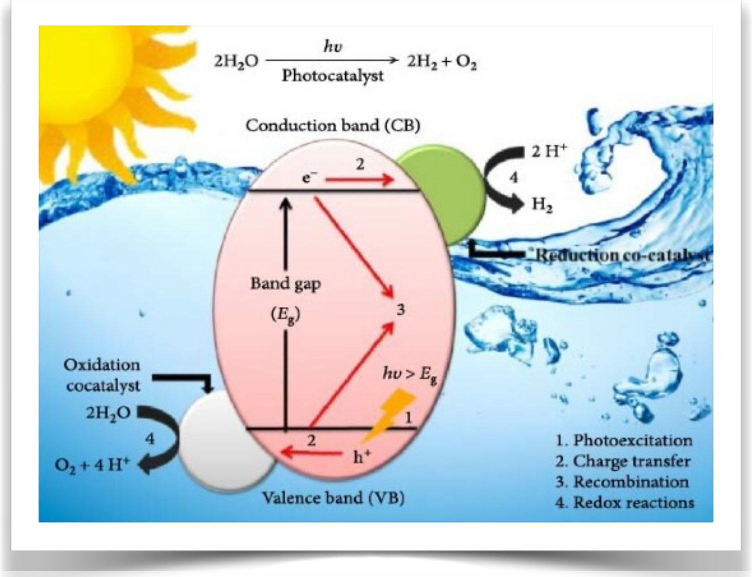

Muon spectroscopy

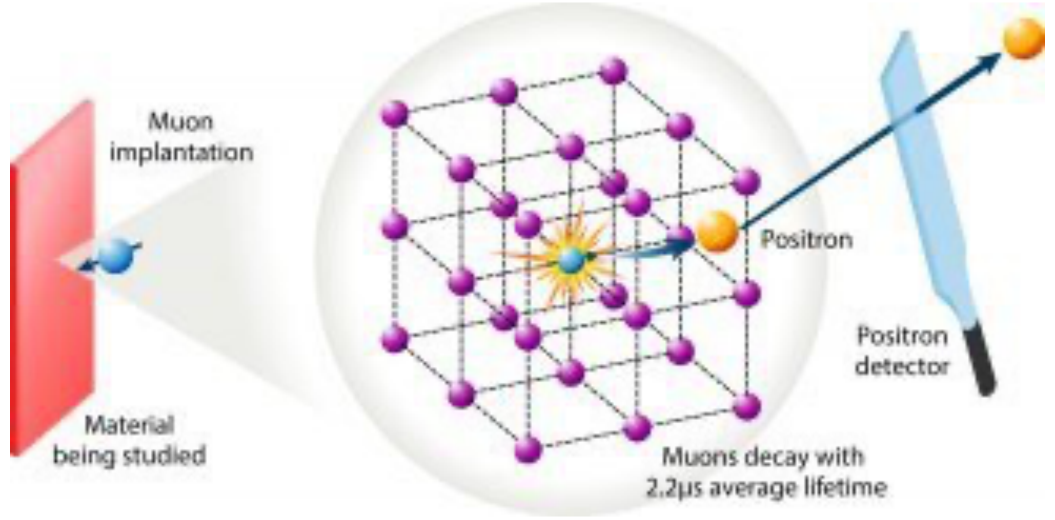

Phonons

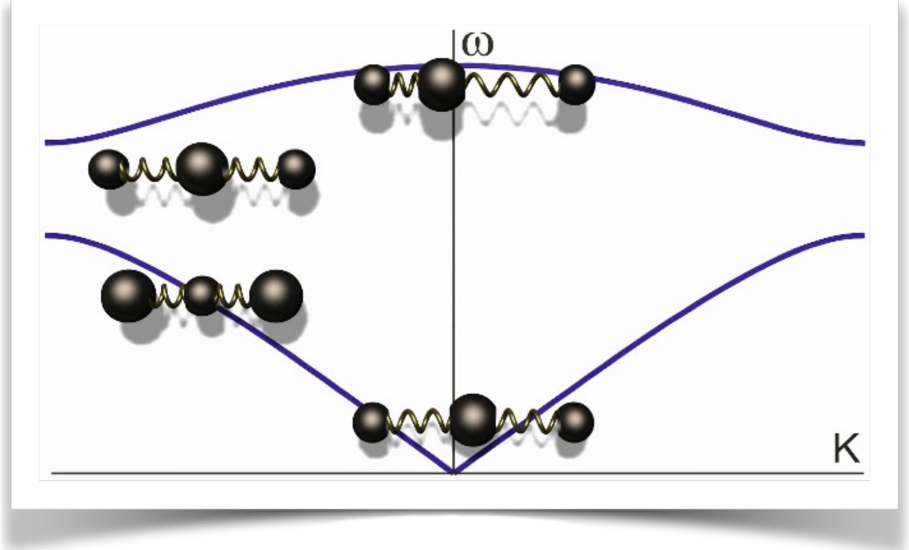

E-ph coupling

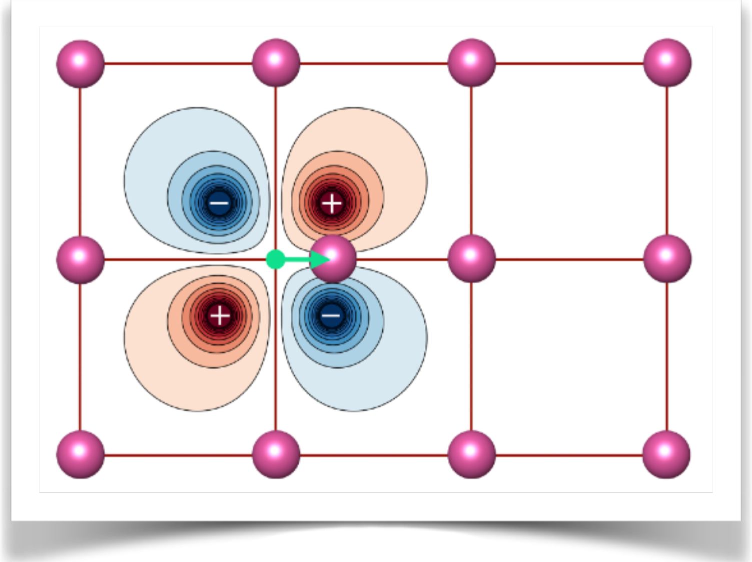

Li-ion batteries

Magnons

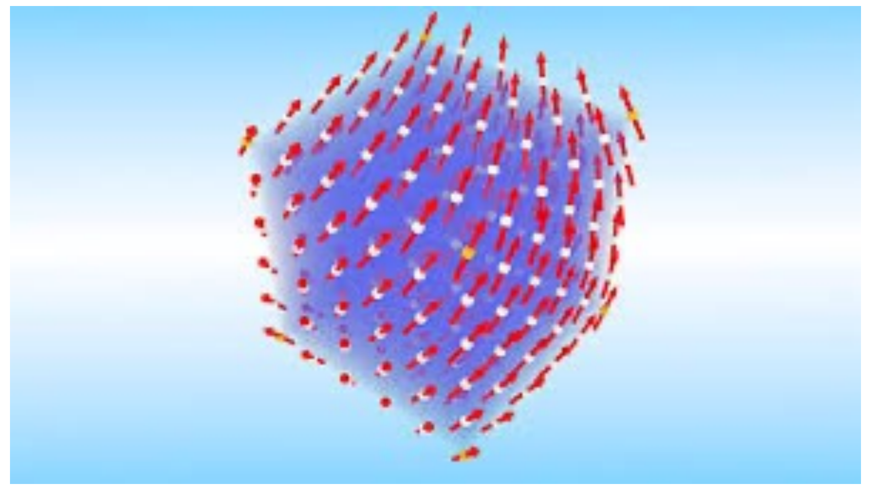

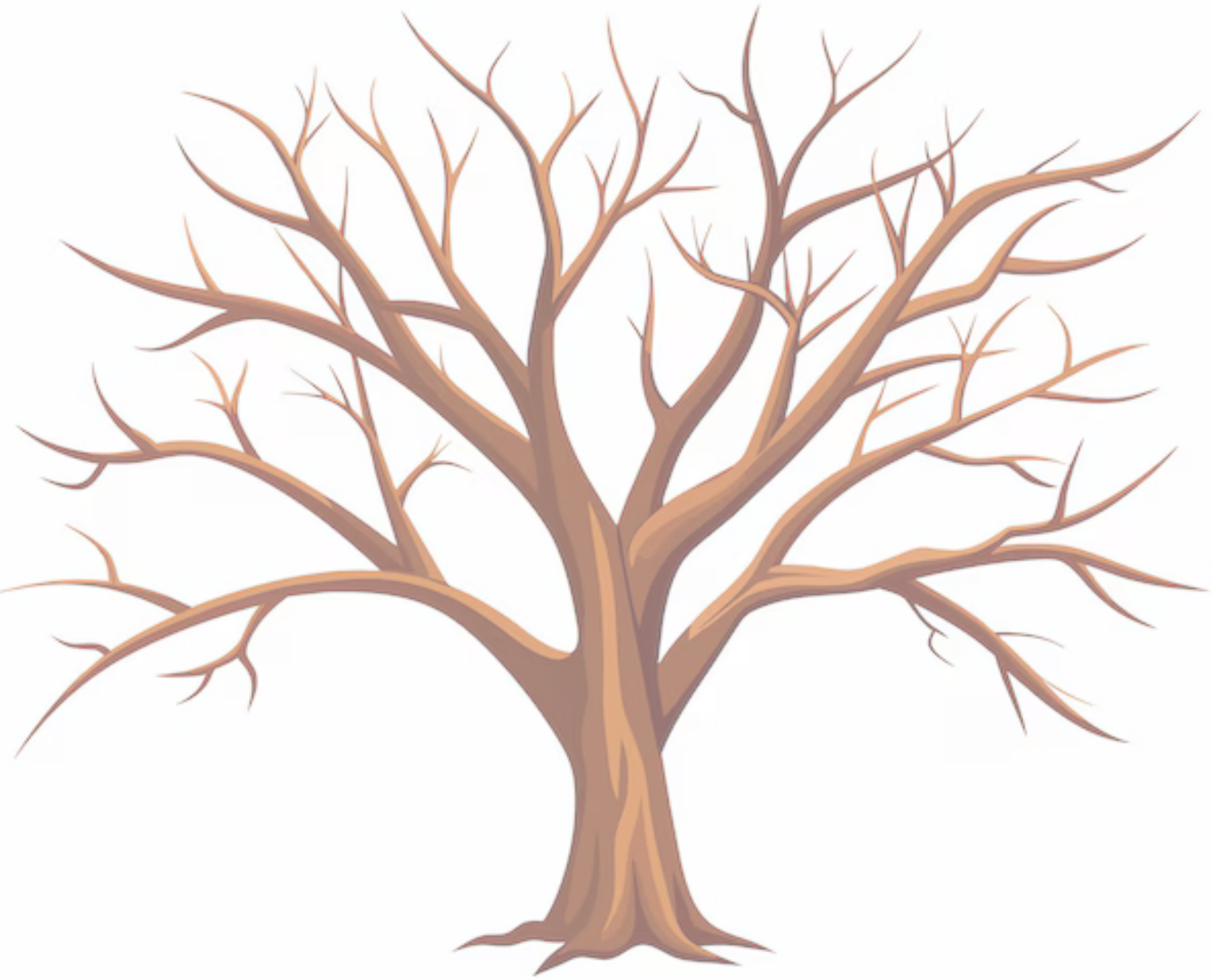

DFT+Hubbard

Modeling Li-ion battery cathode materials

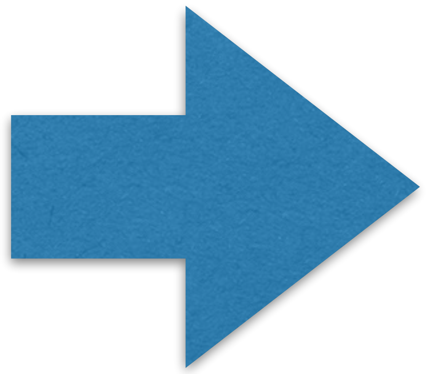

Discharging process

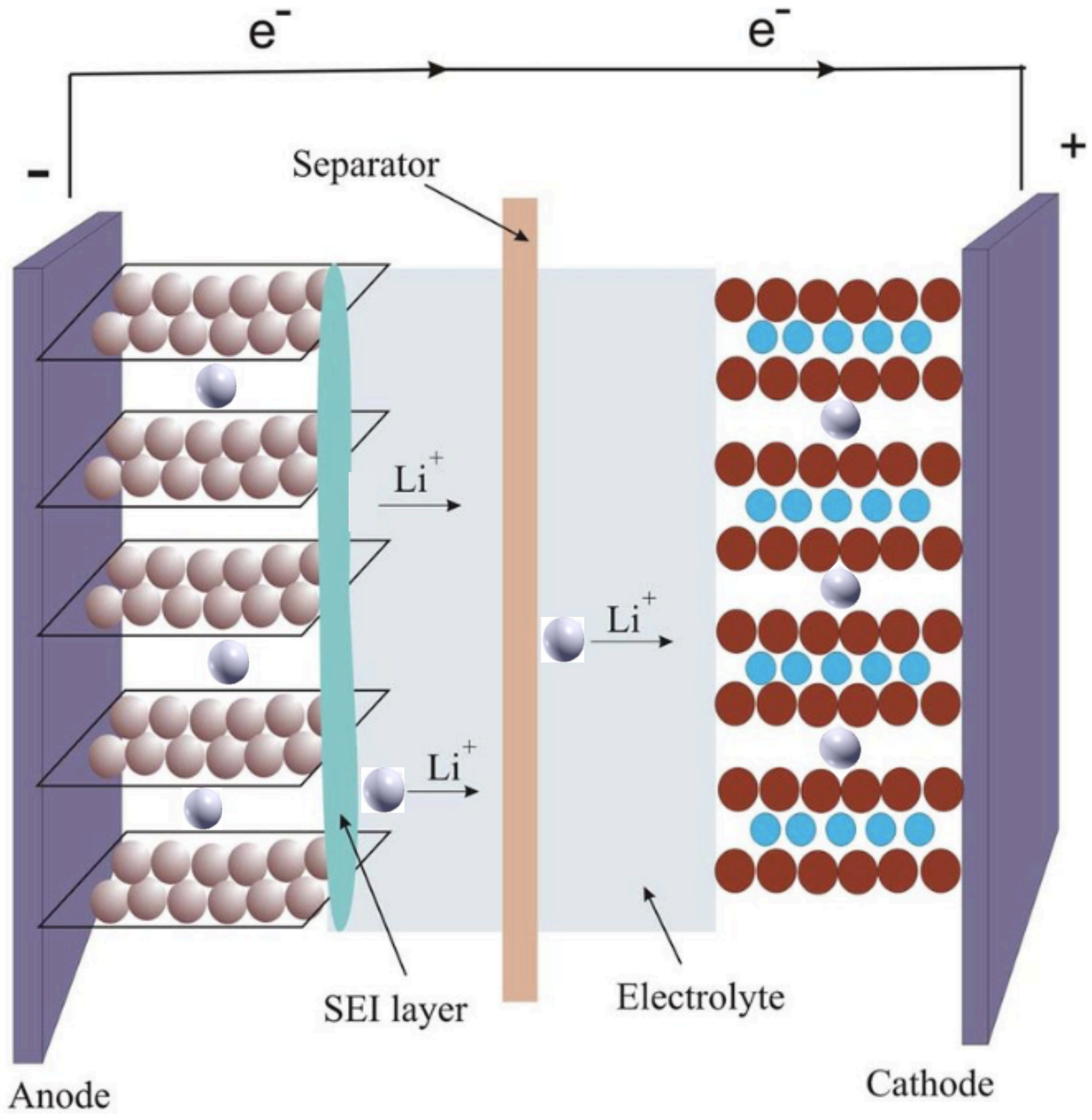

Li-ion batteries

Discharging process

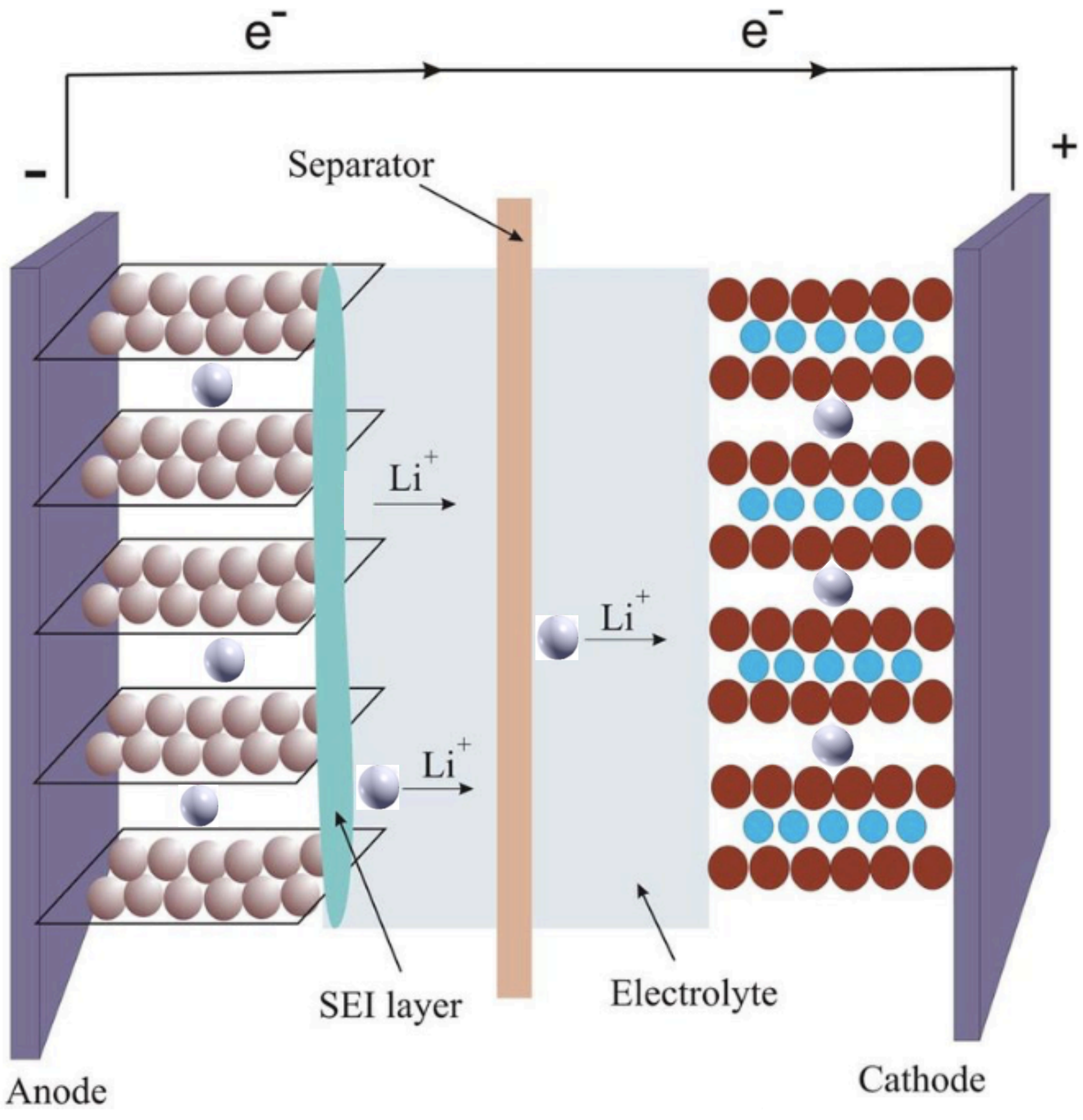

$FePO_4$

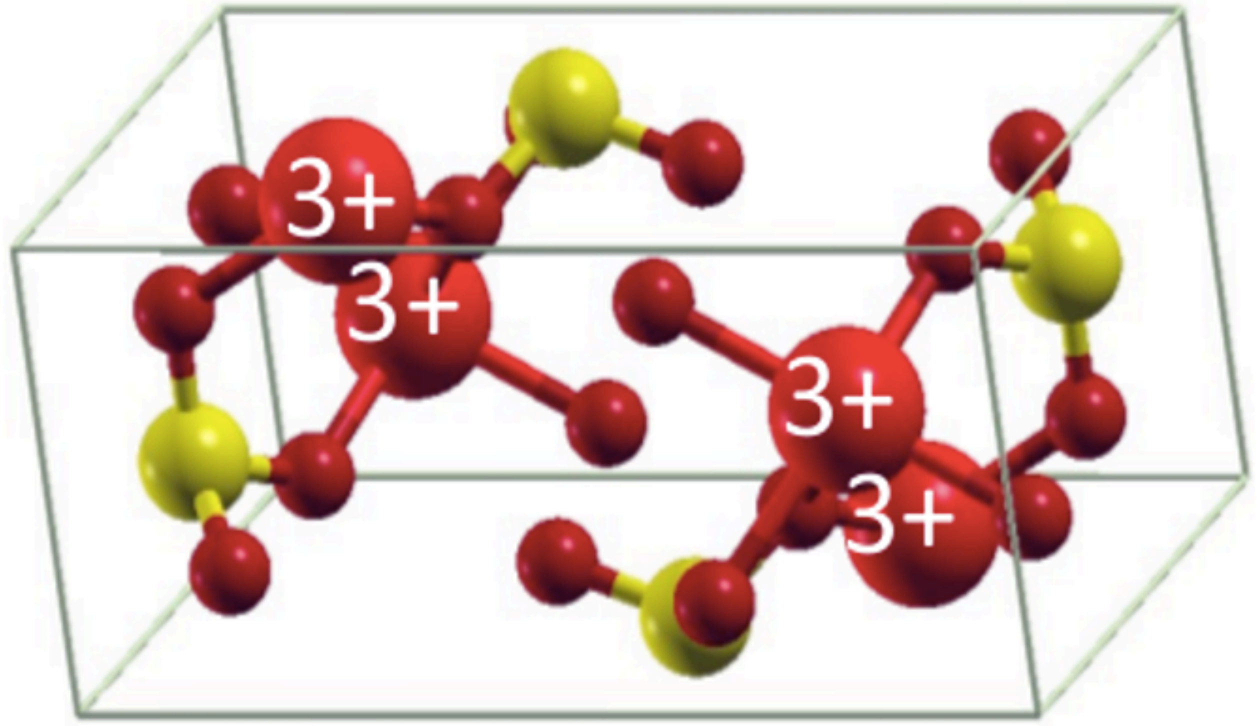

$Li_{0.5}FePO_4$

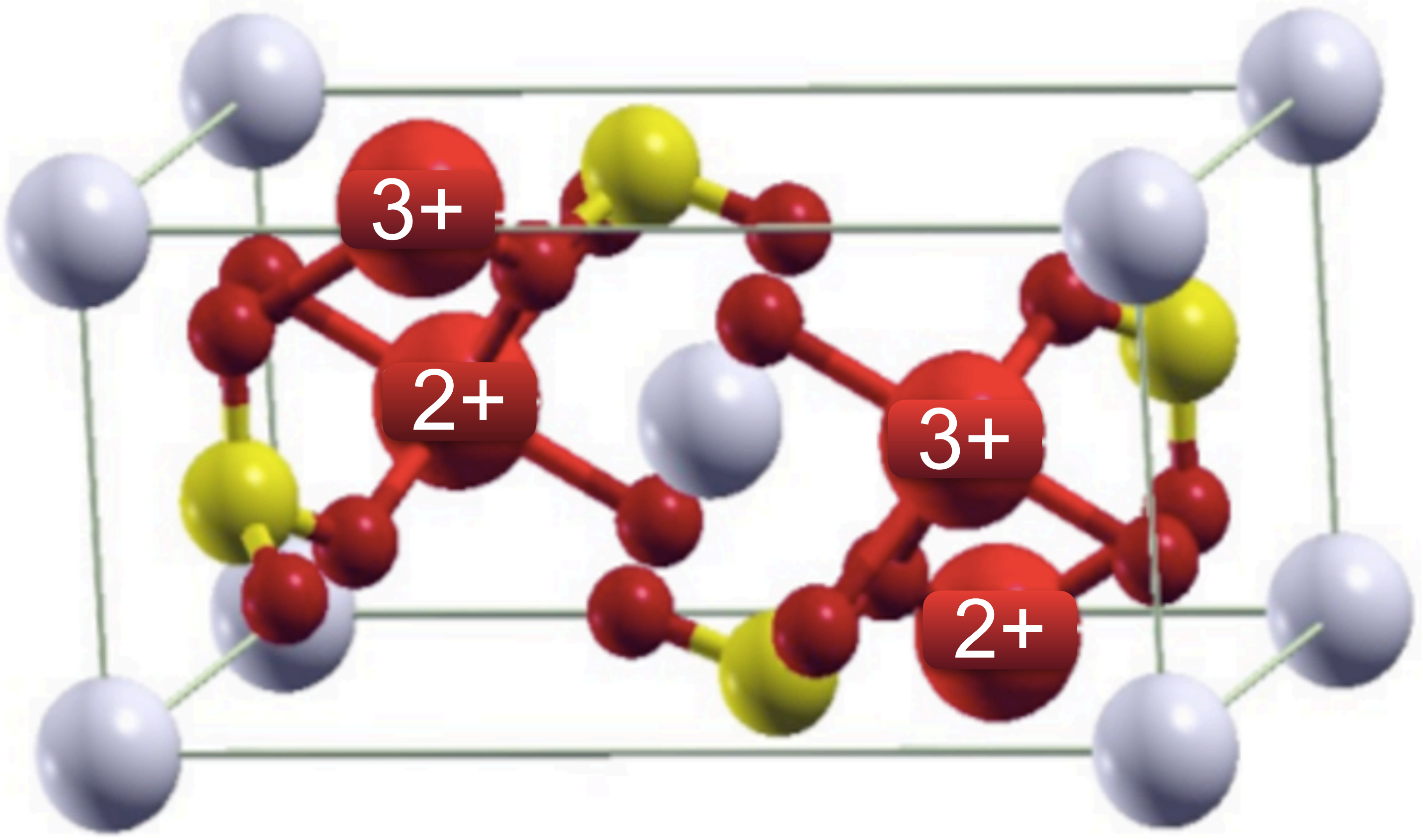

$LiFePO_4$

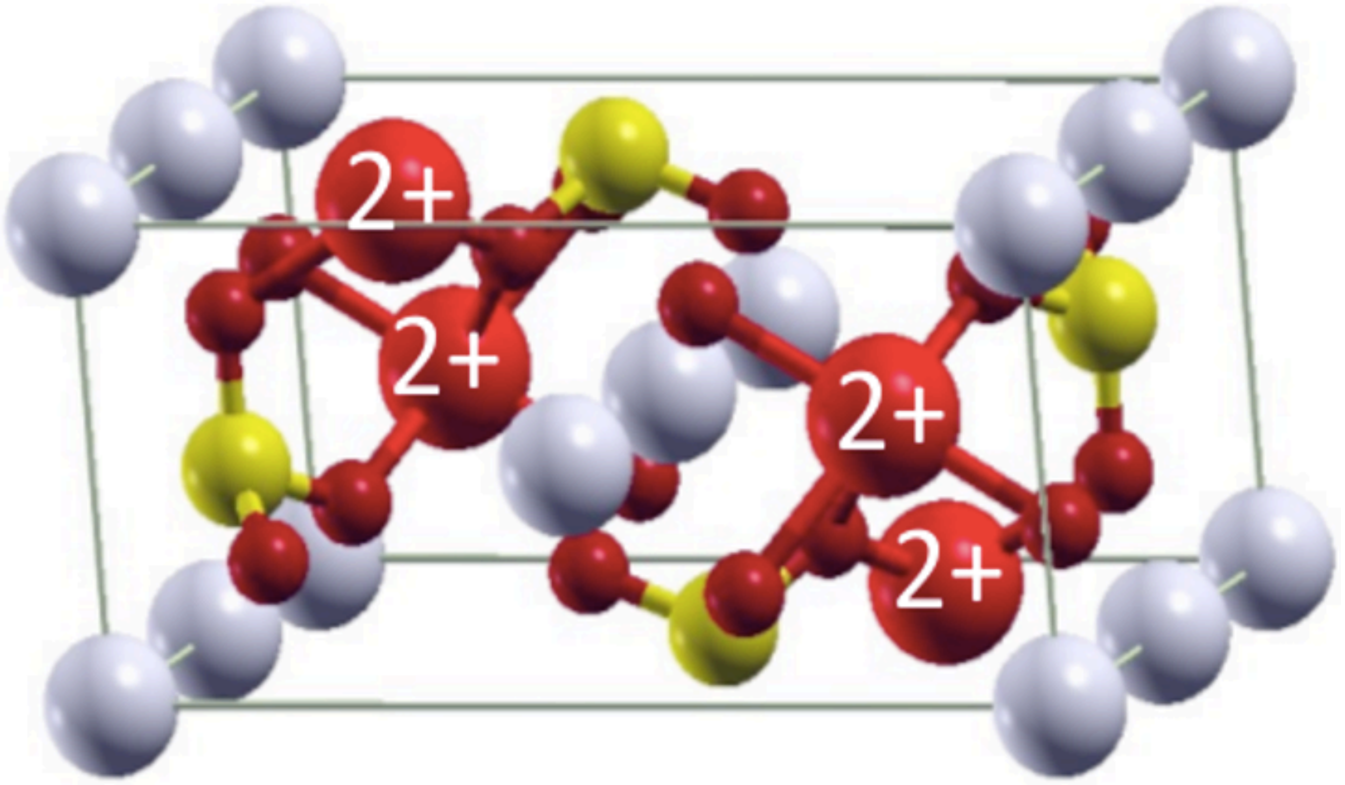

Correct description of change in oxidation state upon lithiation

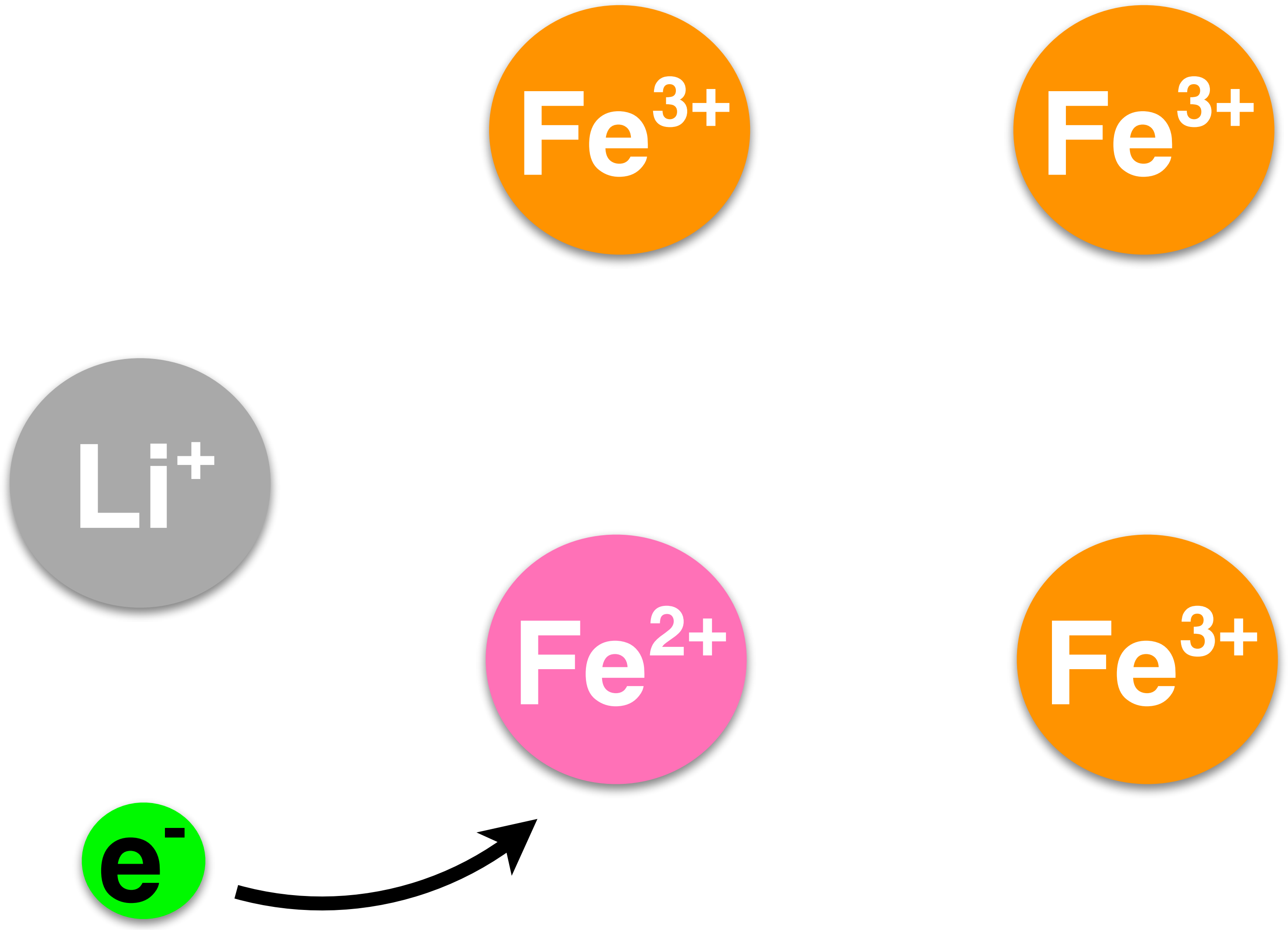

Change in the oxidation state
due to accomodation of an
extra electron

Correct description of change in oxidation state upon lithiation

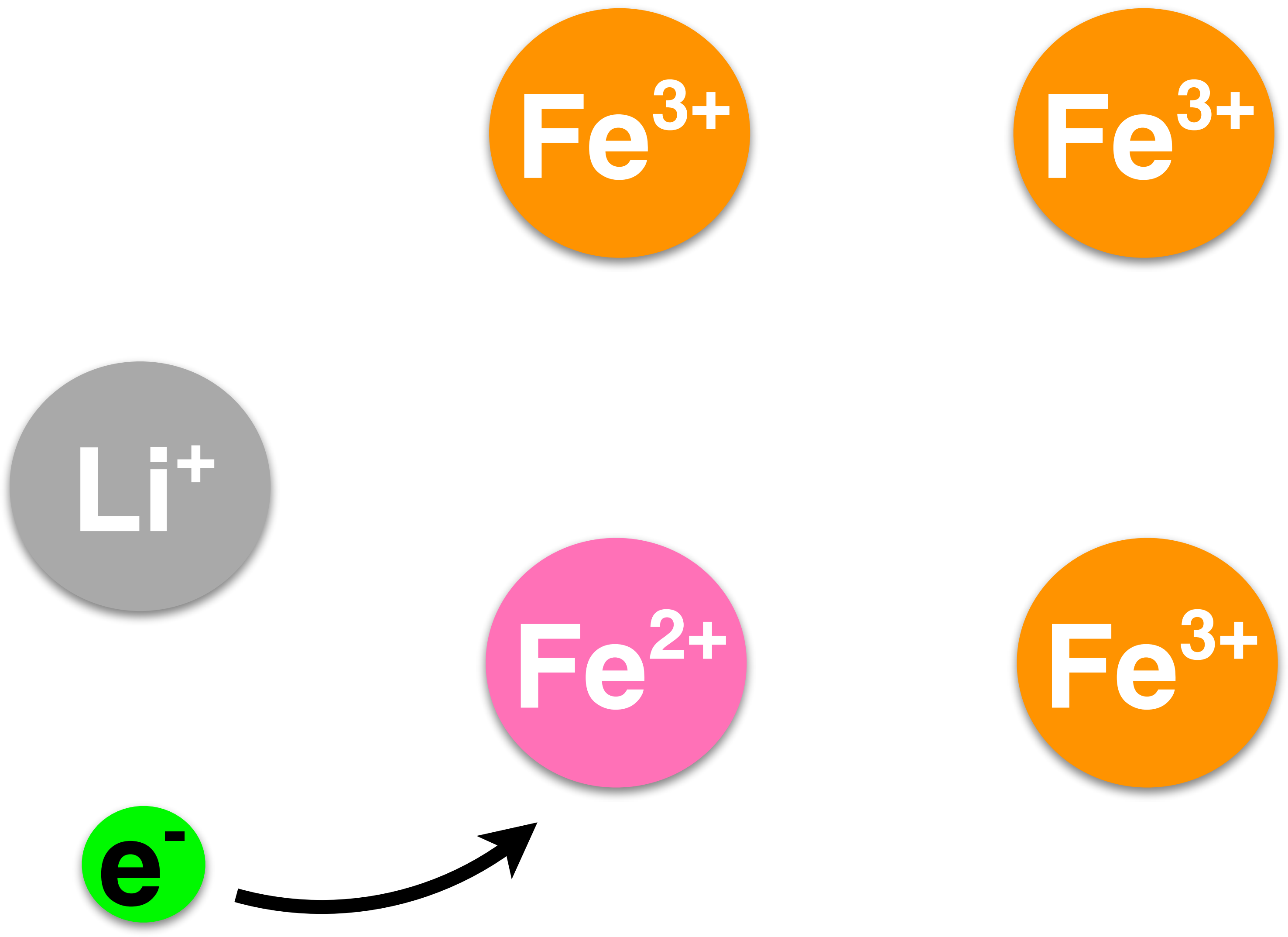

Change in the oxidation state due to accomodation of an extra electron

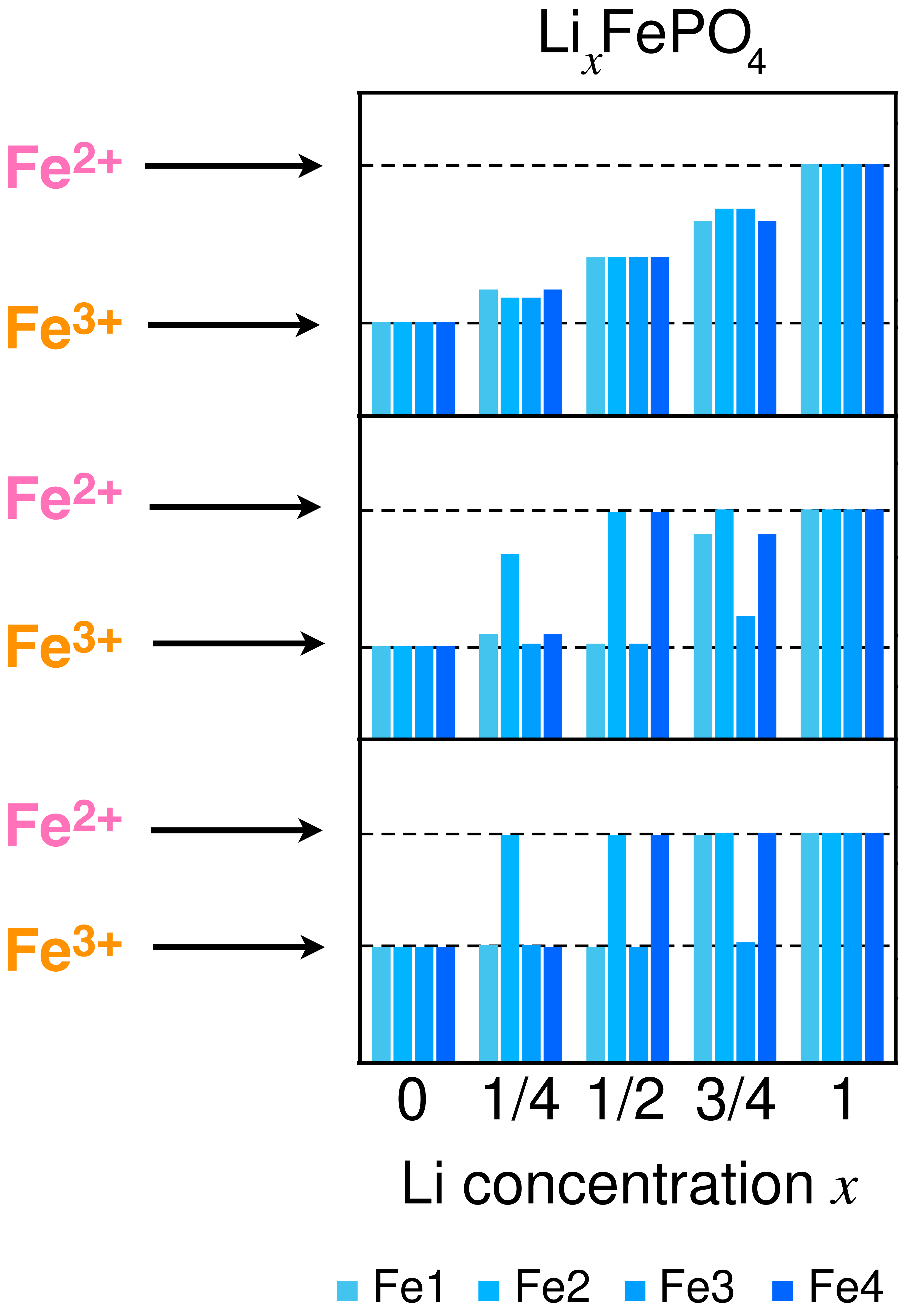

DFT (PBEsol) ✗

Hybrid functional (HSE06) ✗

Extended Hubbard (DFT+U+V) ✓

Li intercalation voltages

$$\Phi = -\frac{E(\mathrm{Li}_{x_2}\mathrm{S}) - E(\mathrm{Li}_{x_1}\mathrm{S}) - (x_2 - x_1)E(\mathrm{Li})}{(x_2 - x_1)e}$$

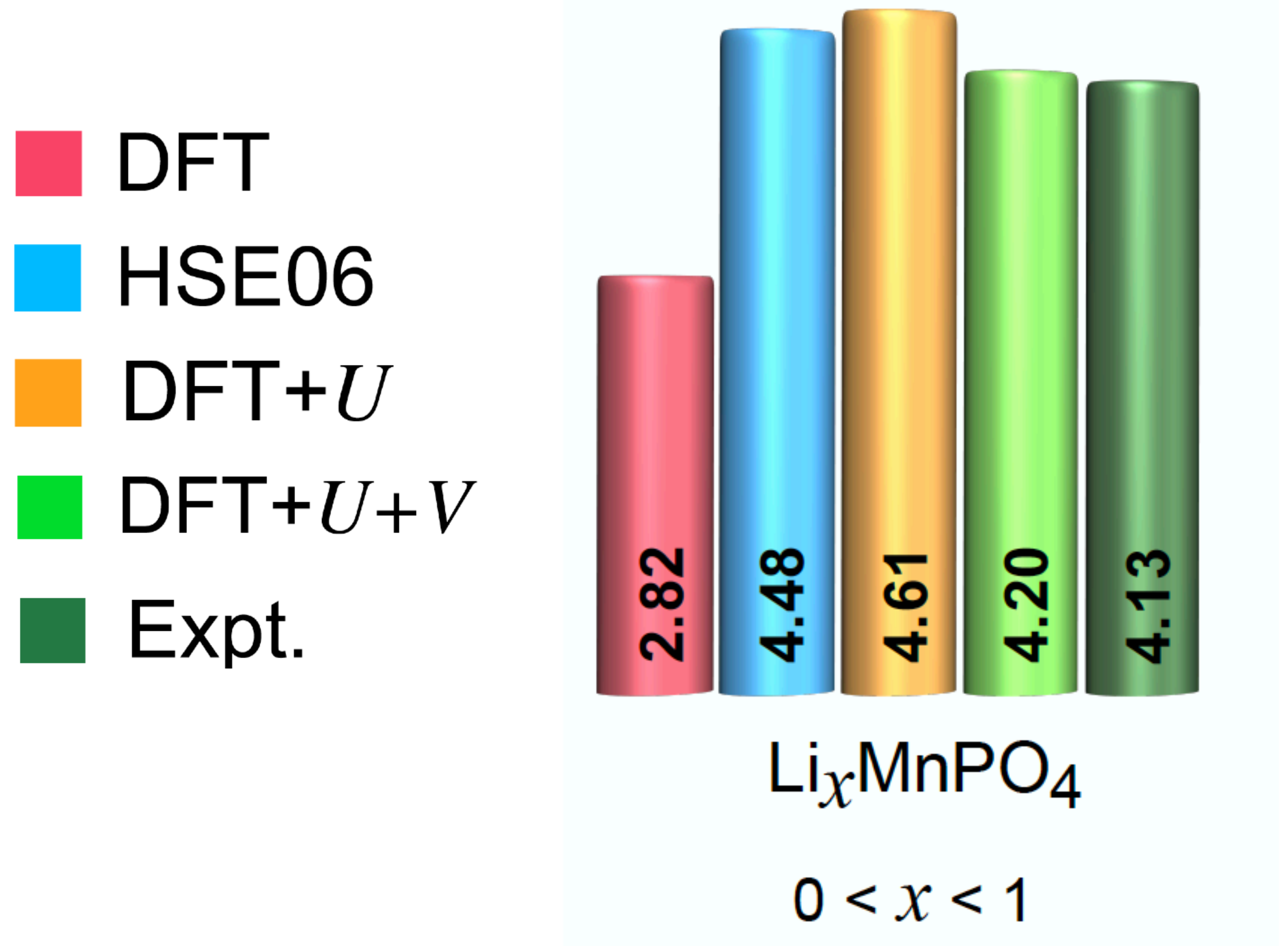

Cococcioni and Marzari, PRM (2019).

Timrov, Aquilante, Cococcioni, Marzari, PRX Energy (2022).

Li intercalation voltages

$$\Phi = -\frac{E(\mathrm{Li}_{x_2}\mathrm{S}) - E(\mathrm{Li}_{x_1}\mathrm{S}) - (x_2 - x_1)E(\mathrm{Li})}{(x_2 - x_1)e}$$

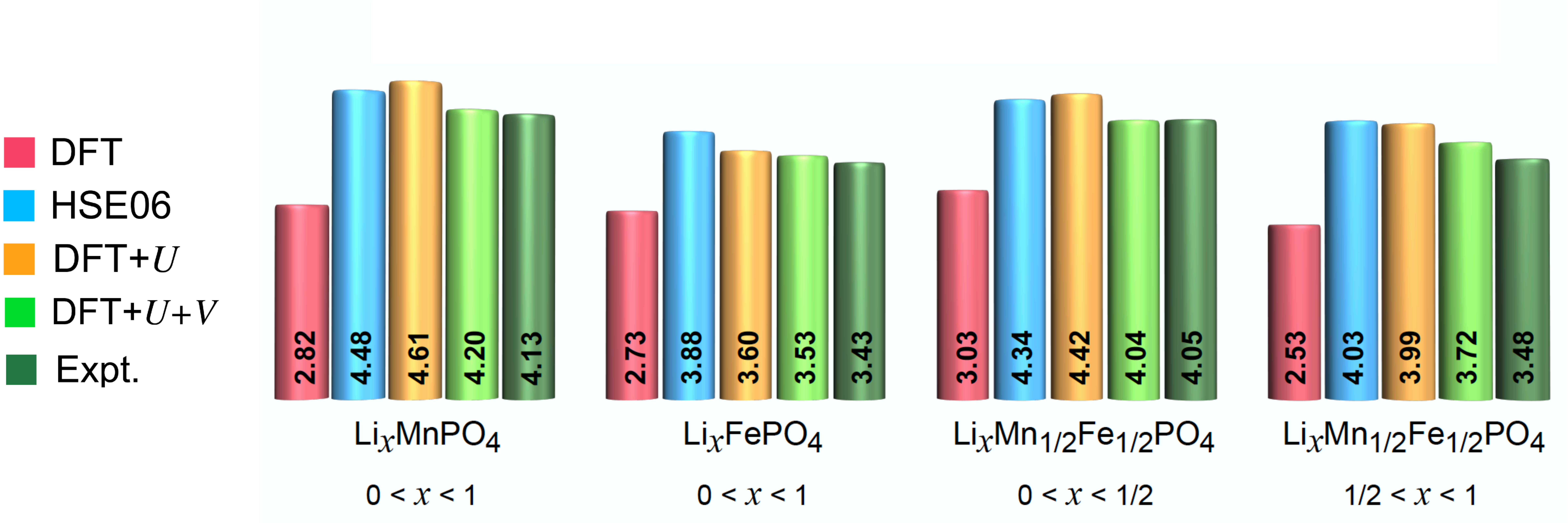

Cococcioni and Marzari, PRM (2019).

Timrov, Aquilante, Cococcioni, Marzari, PRX Energy (2022).

Self-consistent *U* and *V* from linear-response theory

Li_xMnPO_4

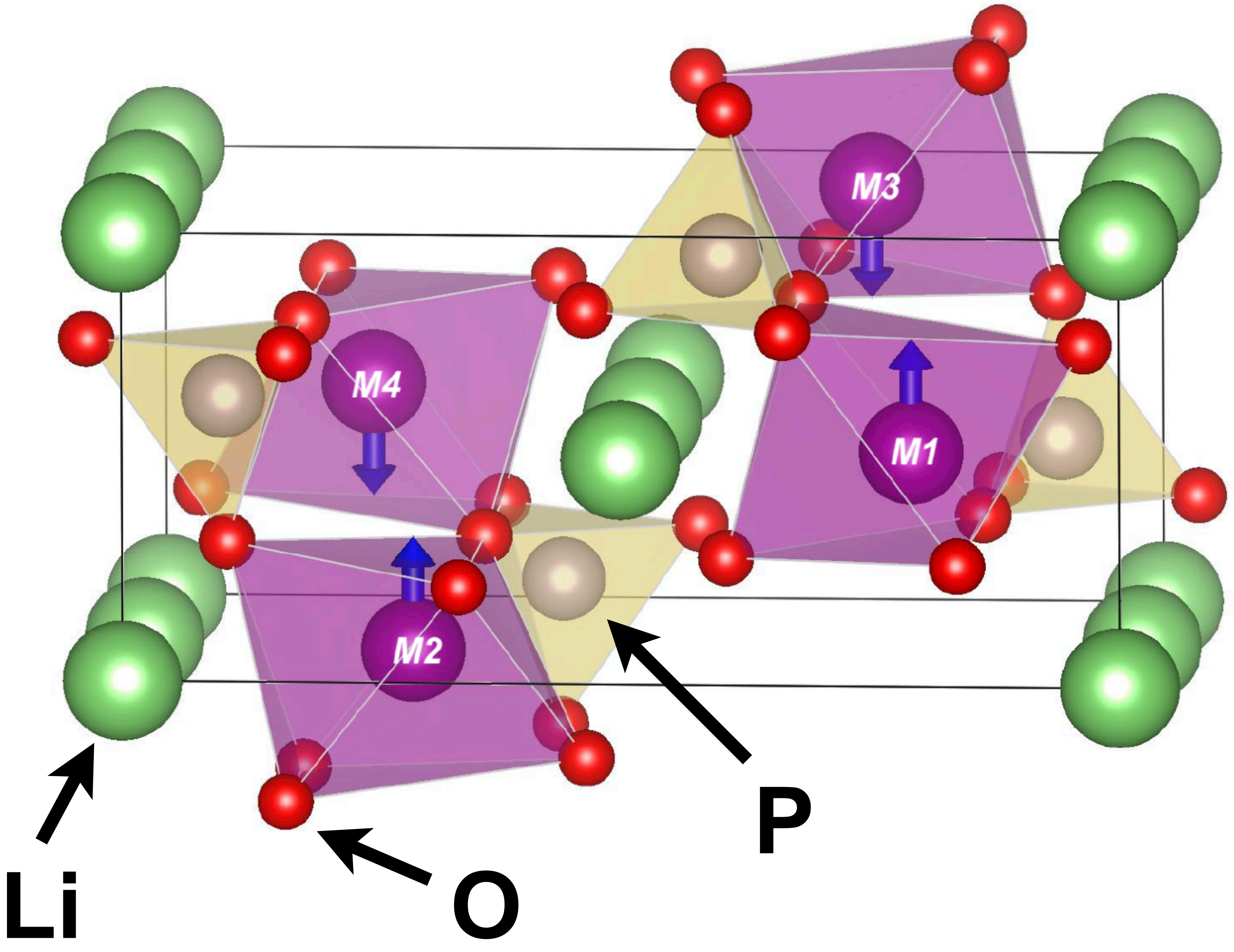

$M1$ - $M4$ = Mn1 - Mn4

x	HP	Mn1	Mn2	Mn3	Mn4
0	U	6.26	6.26	6.26	6.26
	V	0.54-1.07	0.54-1.07	0.54-1.07	0.54-1.07

Self-consistent *U* and *V* from linear-response theory

Li_xMnPO_4

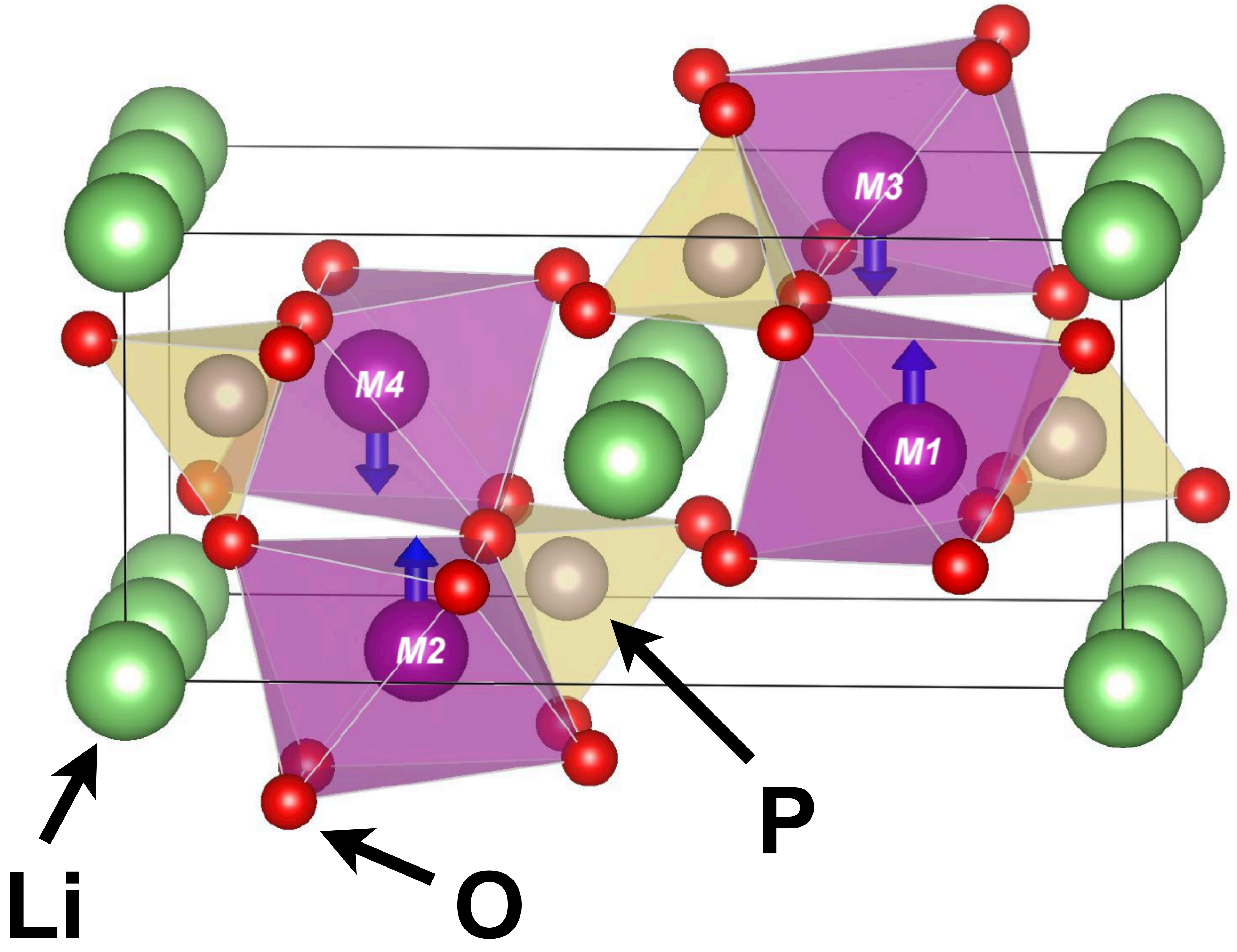

***M1* - *M4* = Mn1 - Mn4**

x	HP	Mn1	Mn2	Mn3	Mn4
0	U	6.26	6.26	6.26	6.26
	V	0.54-1.07	0.54-1.07	0.54-1.07	0.54-1.07
1/4	U	6.26	6.25	6.67	5.44
	V	0.40-1.01	0.46-1.05	0.54-1.11	0.39-1.08

Self-consistent *U* and *V* from linear-response theory

$\mathrm{Li}_x\mathrm{MnPO}_4$

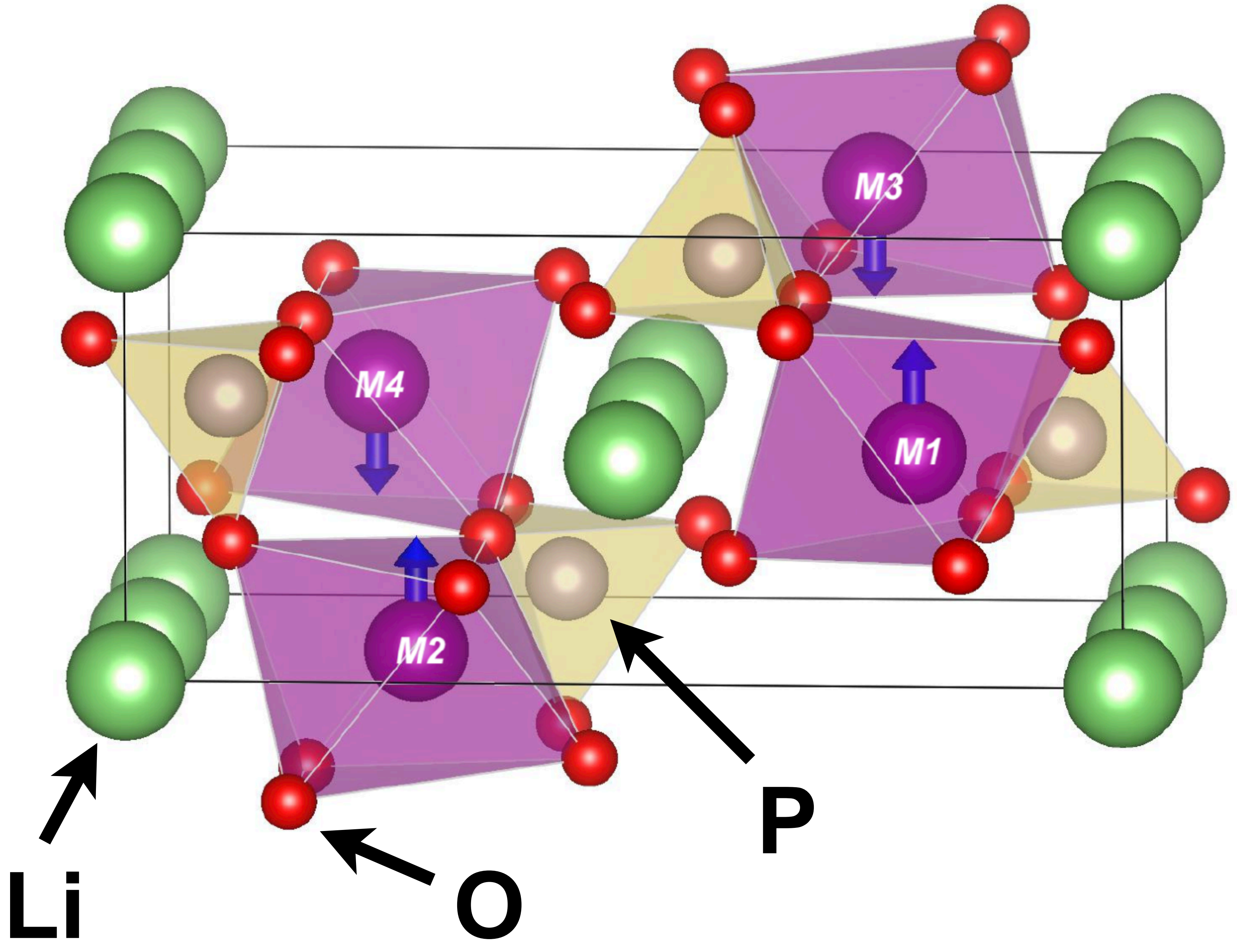

***M1* - *M4* = Mn1 - Mn4**

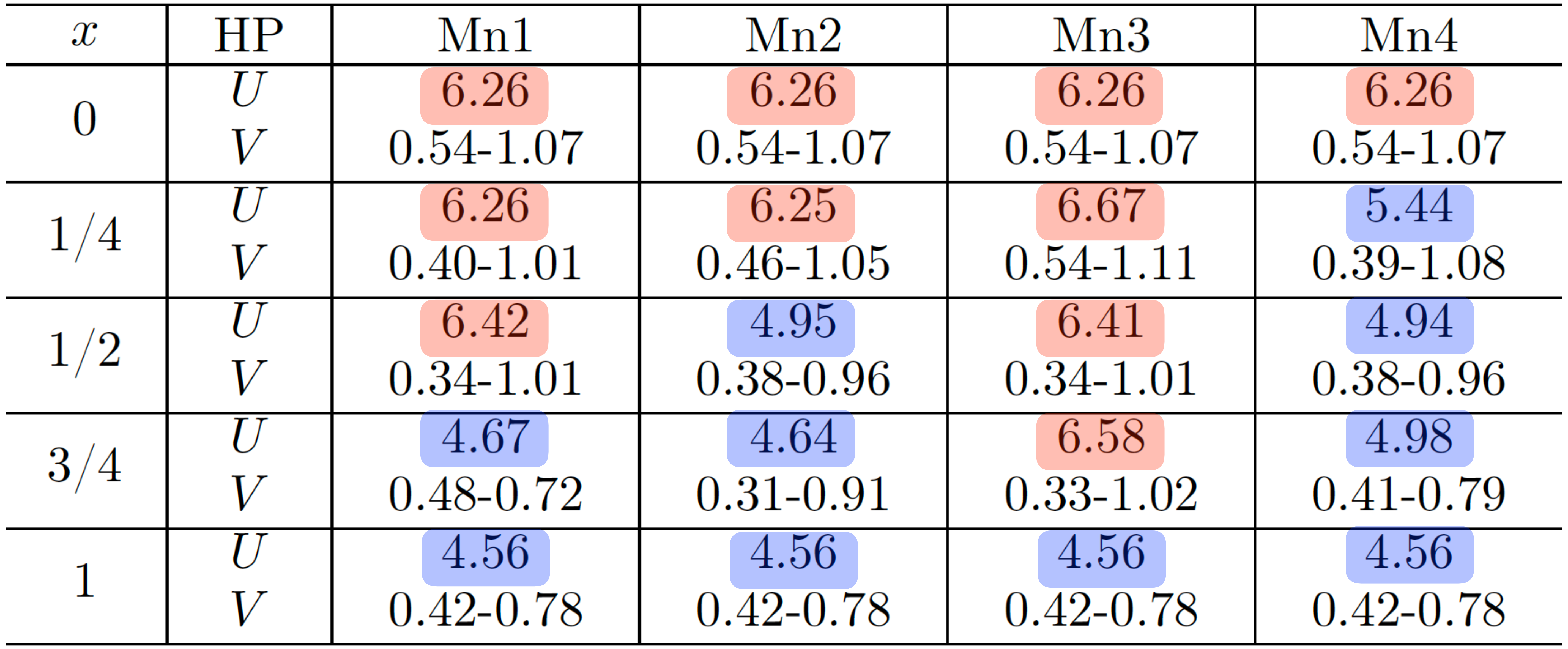

x	HP	Mn1	Mn2	Mn3	Mn4
0	U	6.26	6.26	6.26	6.26
	V	0.54-1.07	0.54-1.07	0.54-1.07	0.54-1.07
1/4	U	6.26	6.25	6.67	5.44
	V	0.40-1.01	0.46-1.05	0.54-1.11	0.39-1.08
1/2	U	6.42	4.95	6.41	4.94
	V	0.34-1.01	0.38-0.96	0.34-1.01	0.38-0.96
3/4	U	4.67	4.64	6.58	4.98
	V	0.48-0.72	0.31-0.91	0.33-1.02	0.41-0.79
1	U	4.56	4.56	4.56	4.56
	V	0.42-0.78	0.42-0.78	0.42-0.78	0.42-0.78

Hubbard parameters are site-dependent and change upon the (de)lithiation

How one would describe the change in *U*&*V* empirically?

Spinel cathodes: large systems with complex magnetism

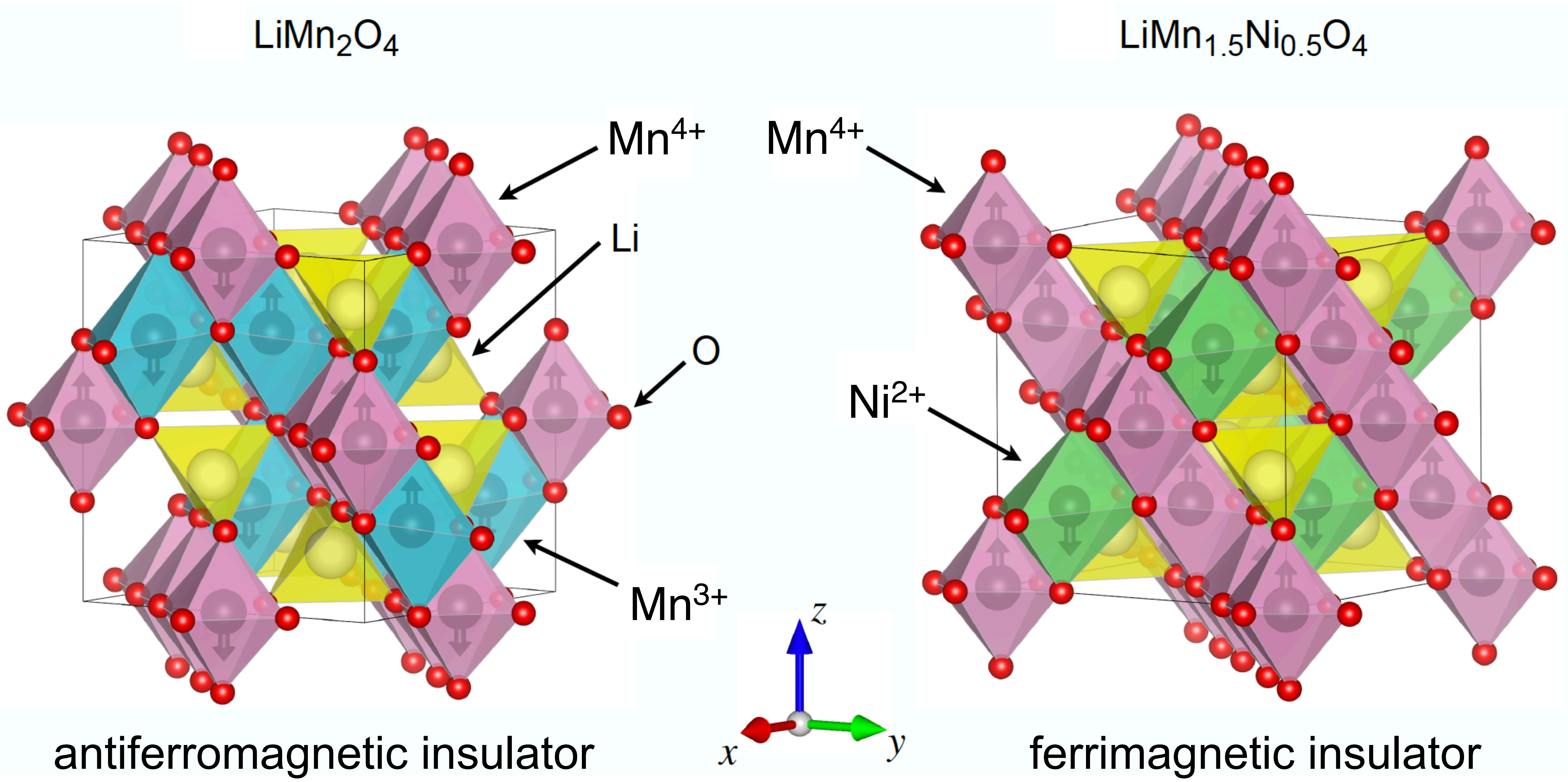

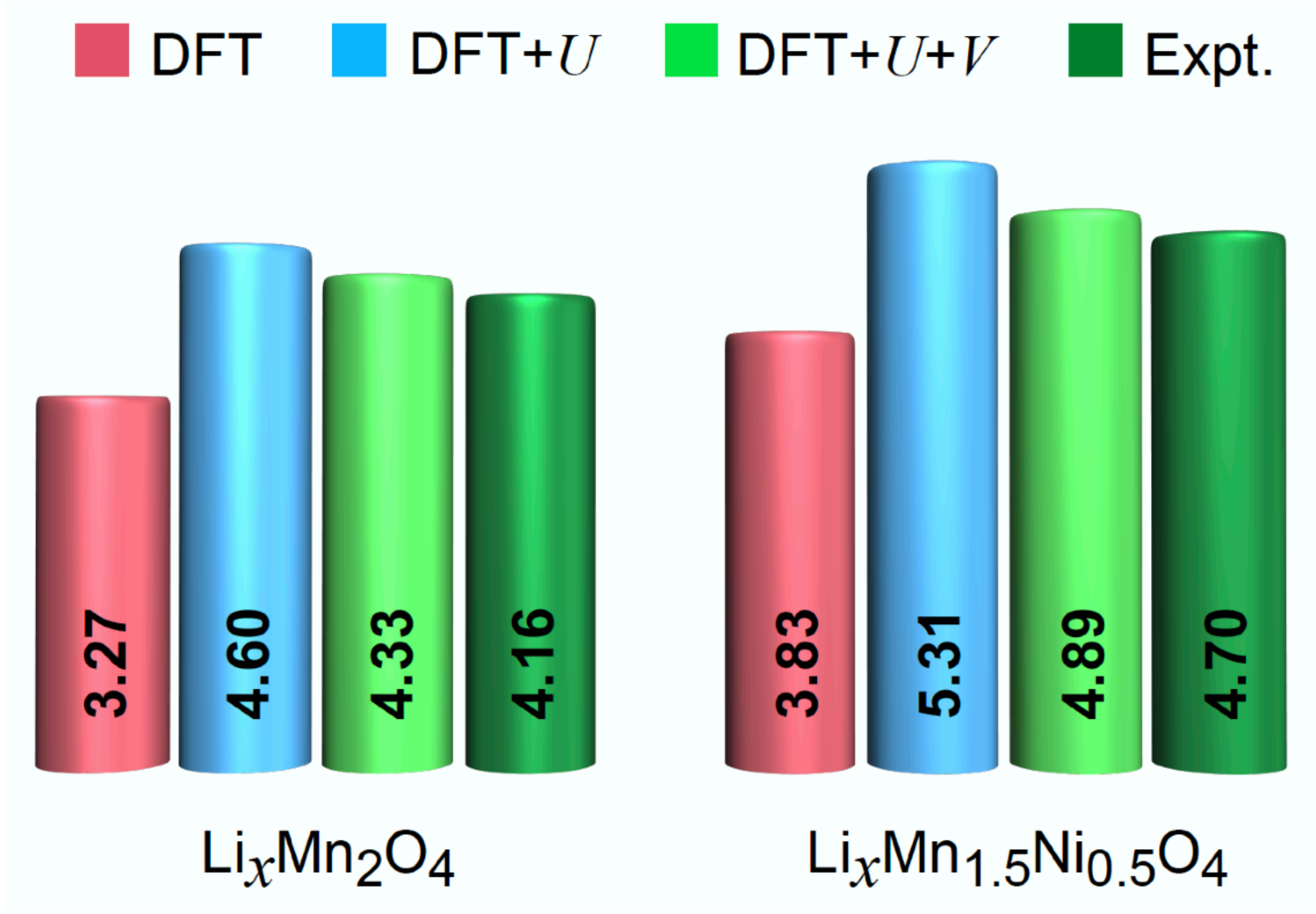

The electronic properties and voltages of spinel cathode materials are well described

Timrov, Kotiuga, and Marzari, PCCP (2023).

Accelerating Hubbard functionals through machine learning

Distribution of Hubbard *U* values for
Mn, Fe, Co, and Ni in various compounds

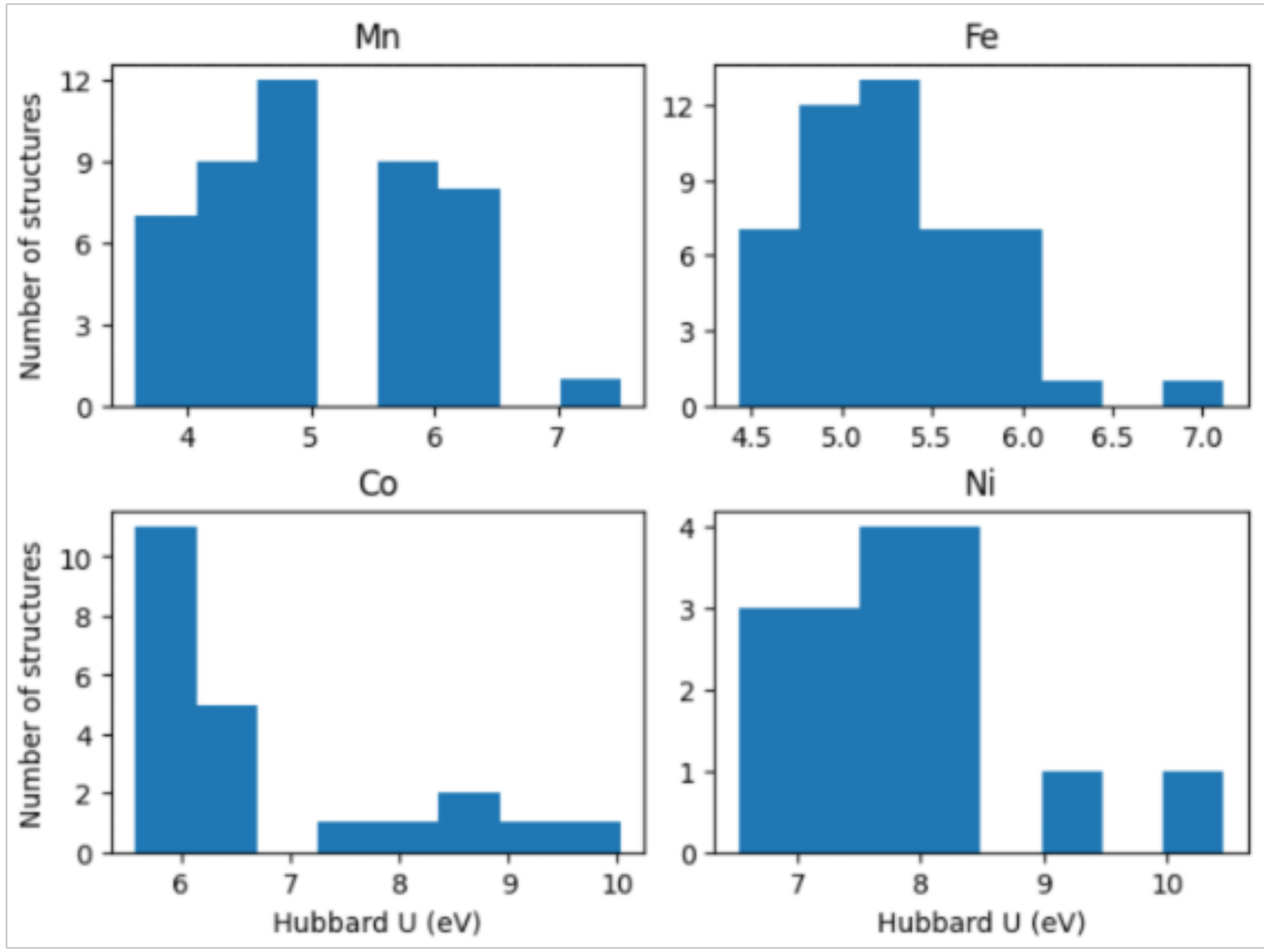

Uhrin, Zadoks, Binci, Marzari, Timrov, npj Comput. Mater (2025).

Accelerating Hubbard functionals through machine learning

Distribution of Hubbard *U* values for
Mn, Fe, Co, and Ni in various compounds

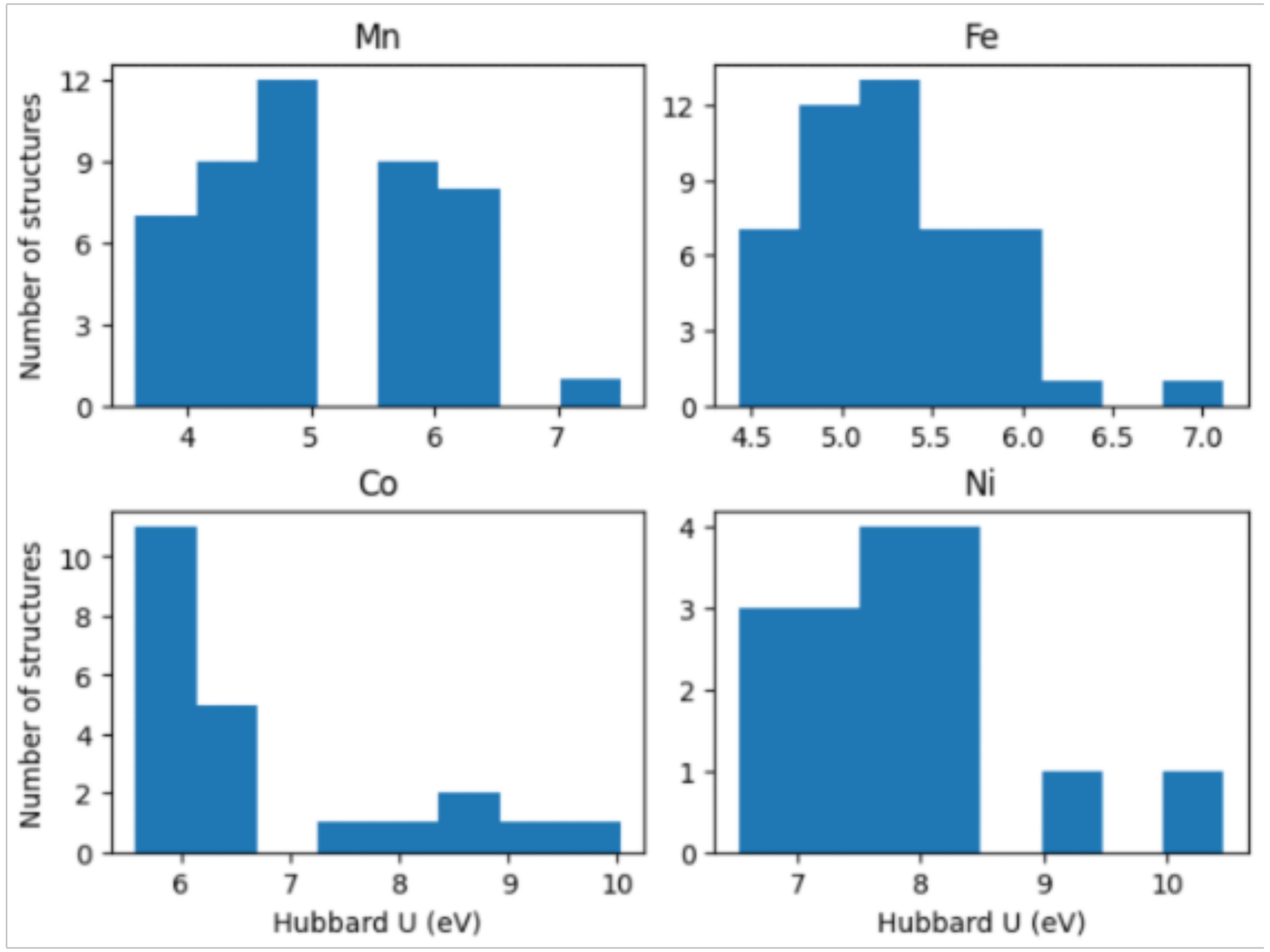

Machine learning
(equivariant neural networks)

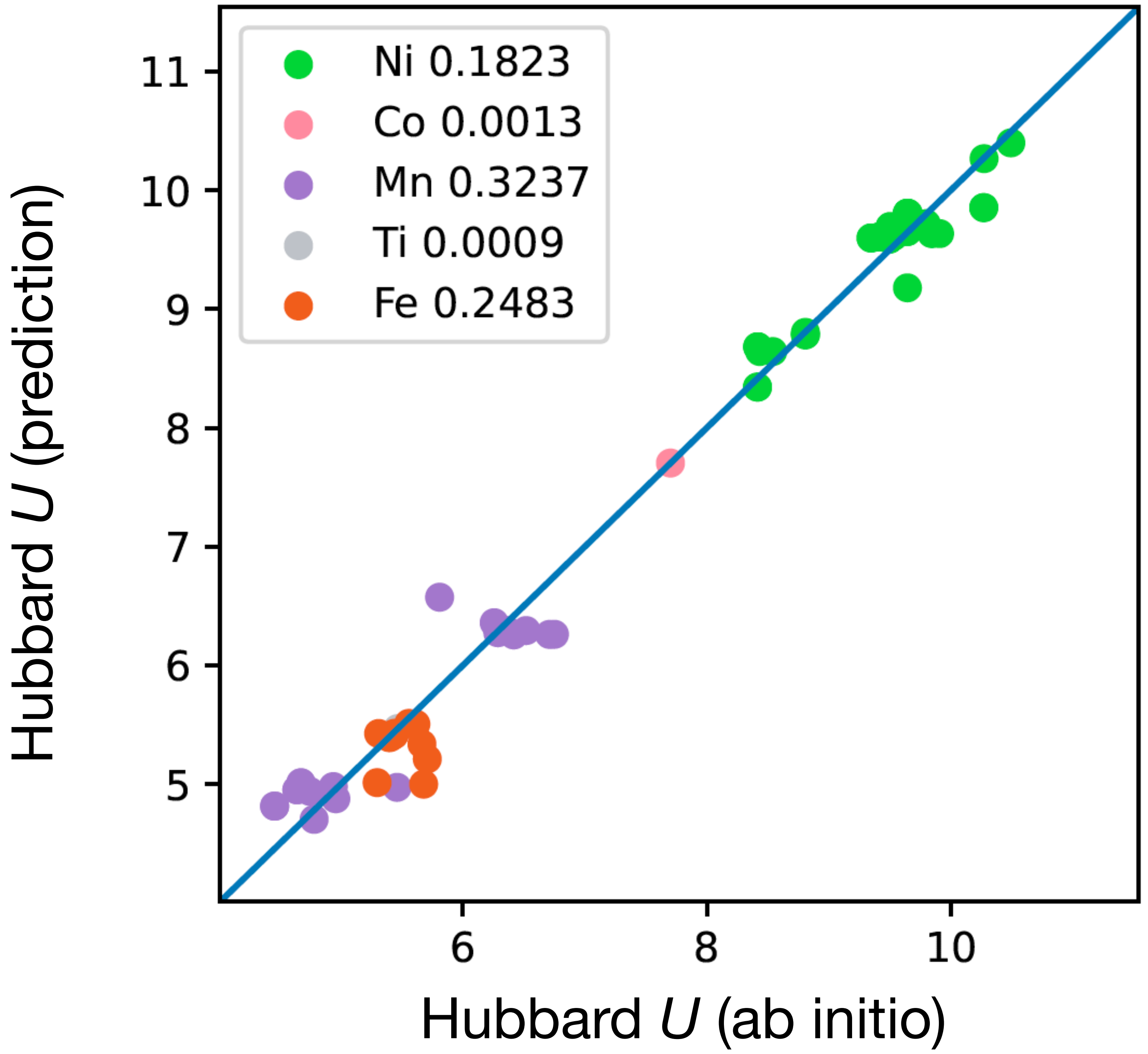

Uhrin, Zadoks, Binci, Marzari, Timrov, npj Comput. Mater (2025).

Perovskites: Oxygen vacancies

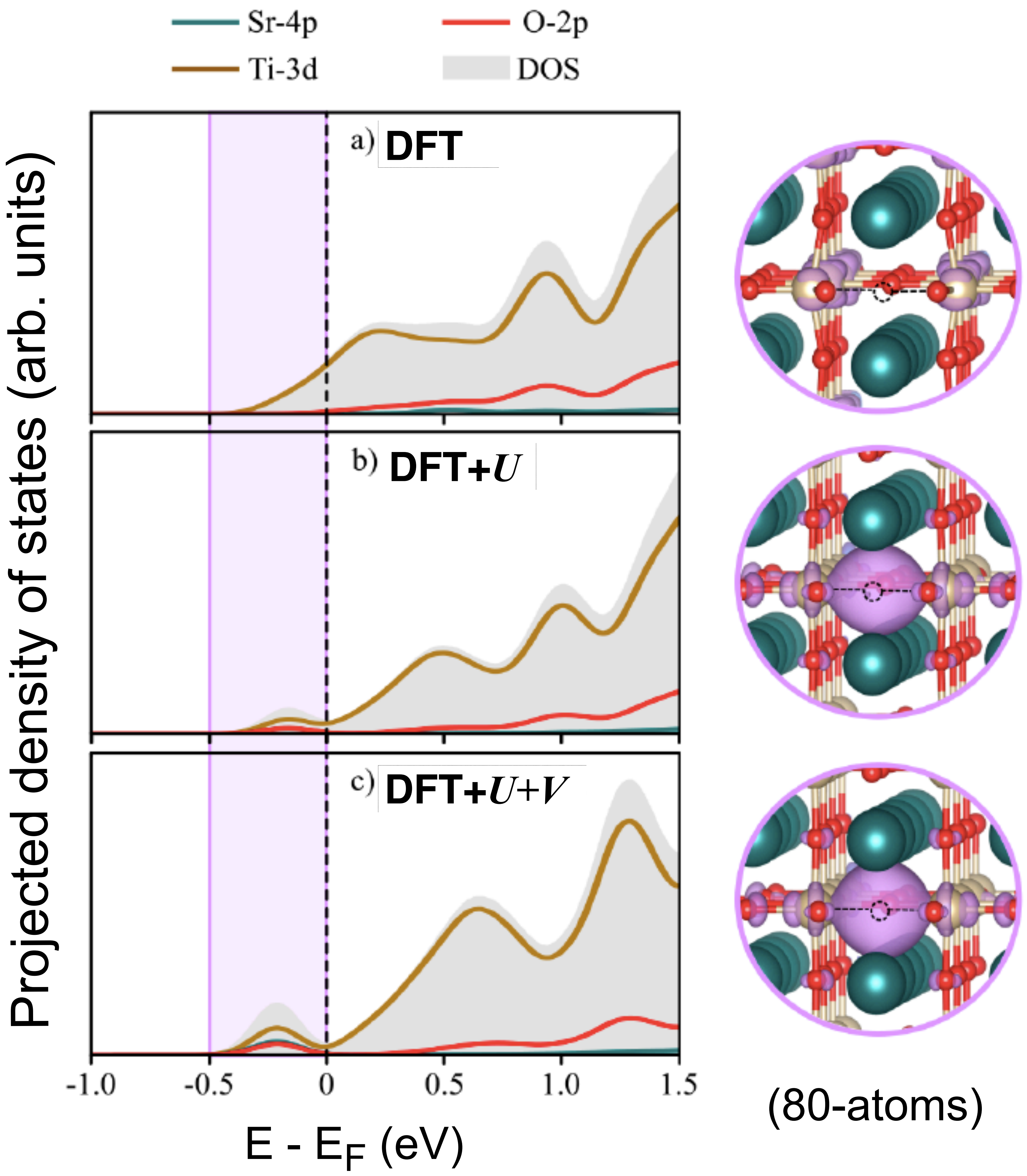

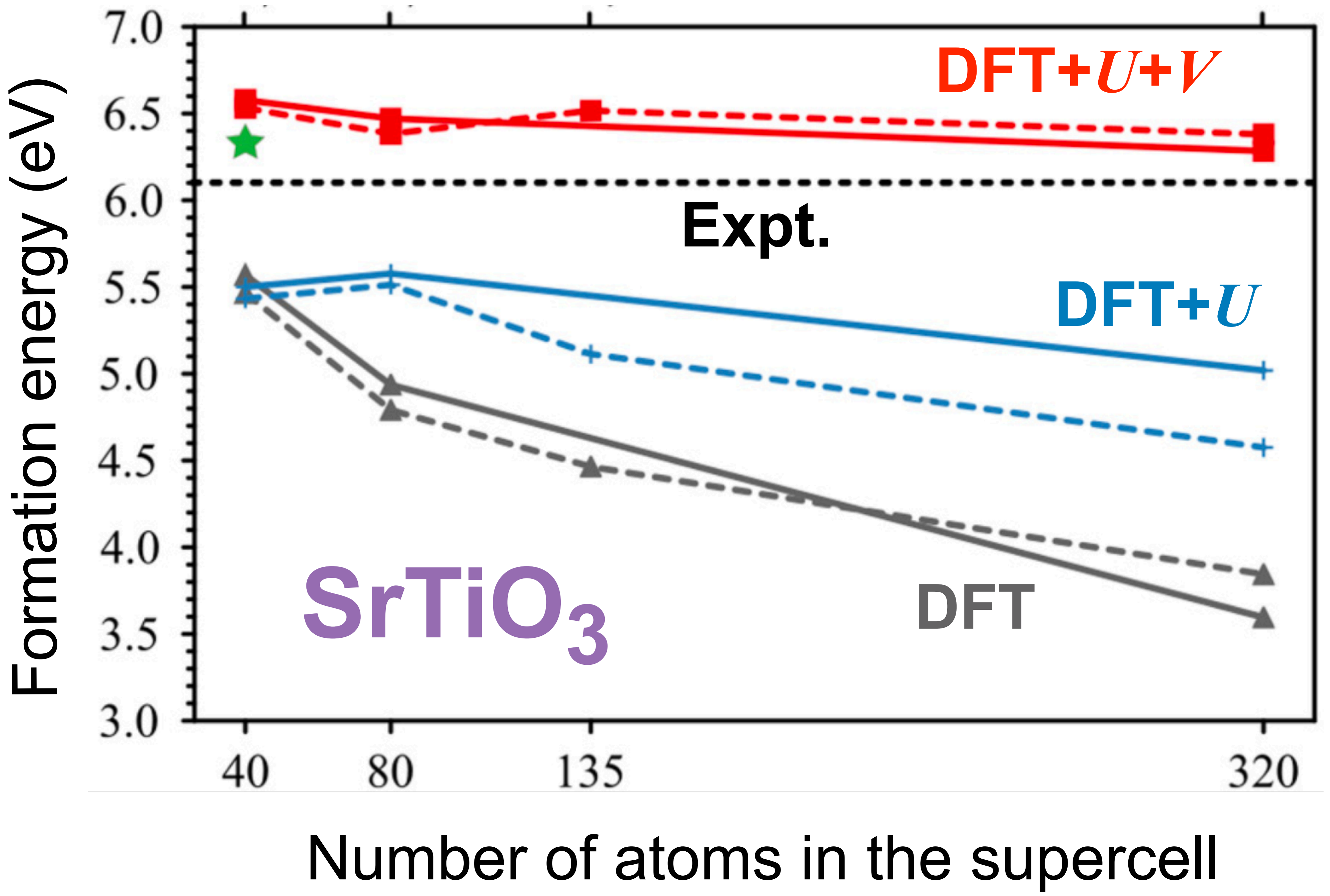

DFT+U+V remarkably predicts the correct formation energies of O vacancies in perovskite materials

Ricca, Timrov, Cococcioni, Marzari, and Aschauer, PRB (2019), PRR (2020).

Perovskites: Phase stability

High T phase　　Low T phase

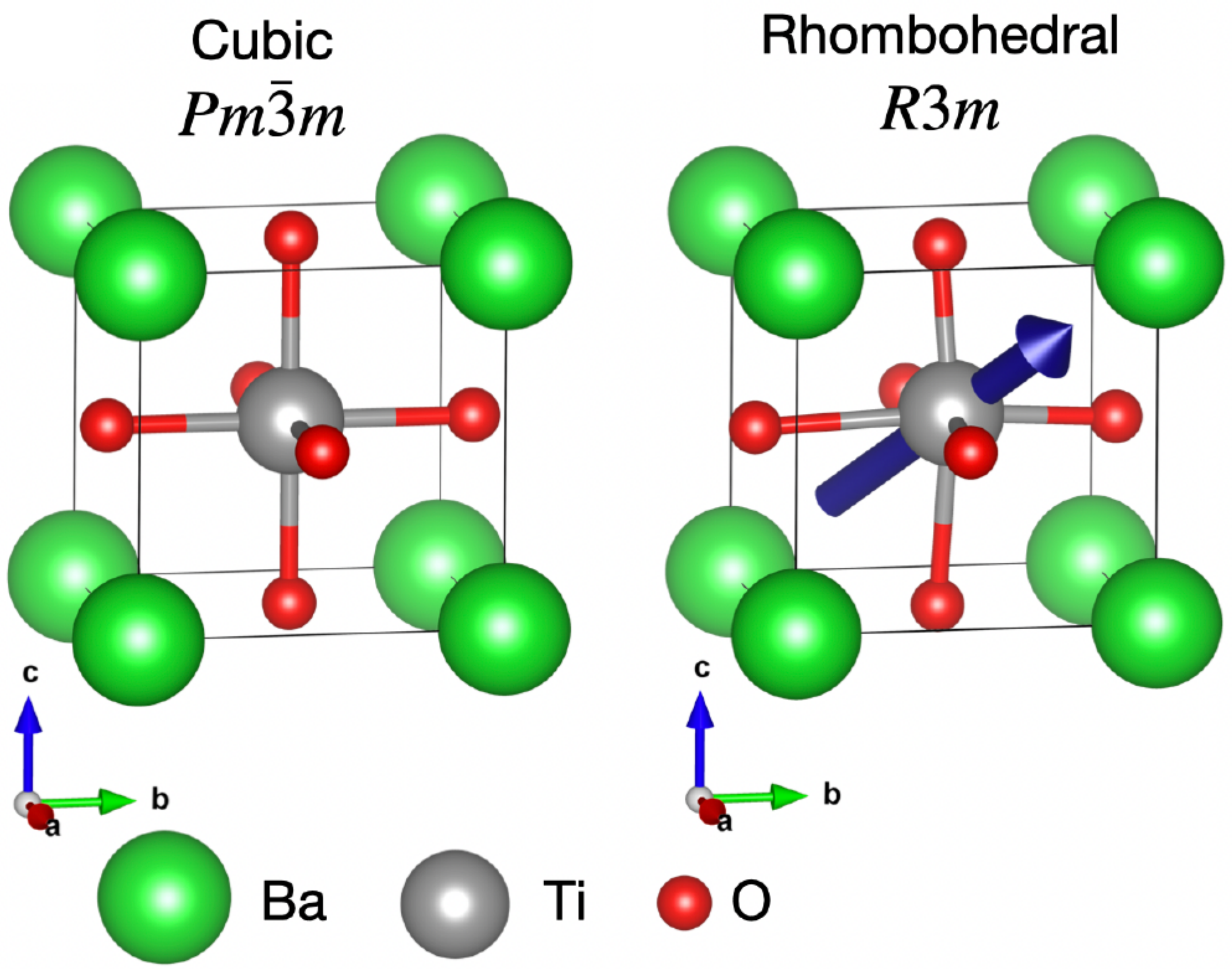

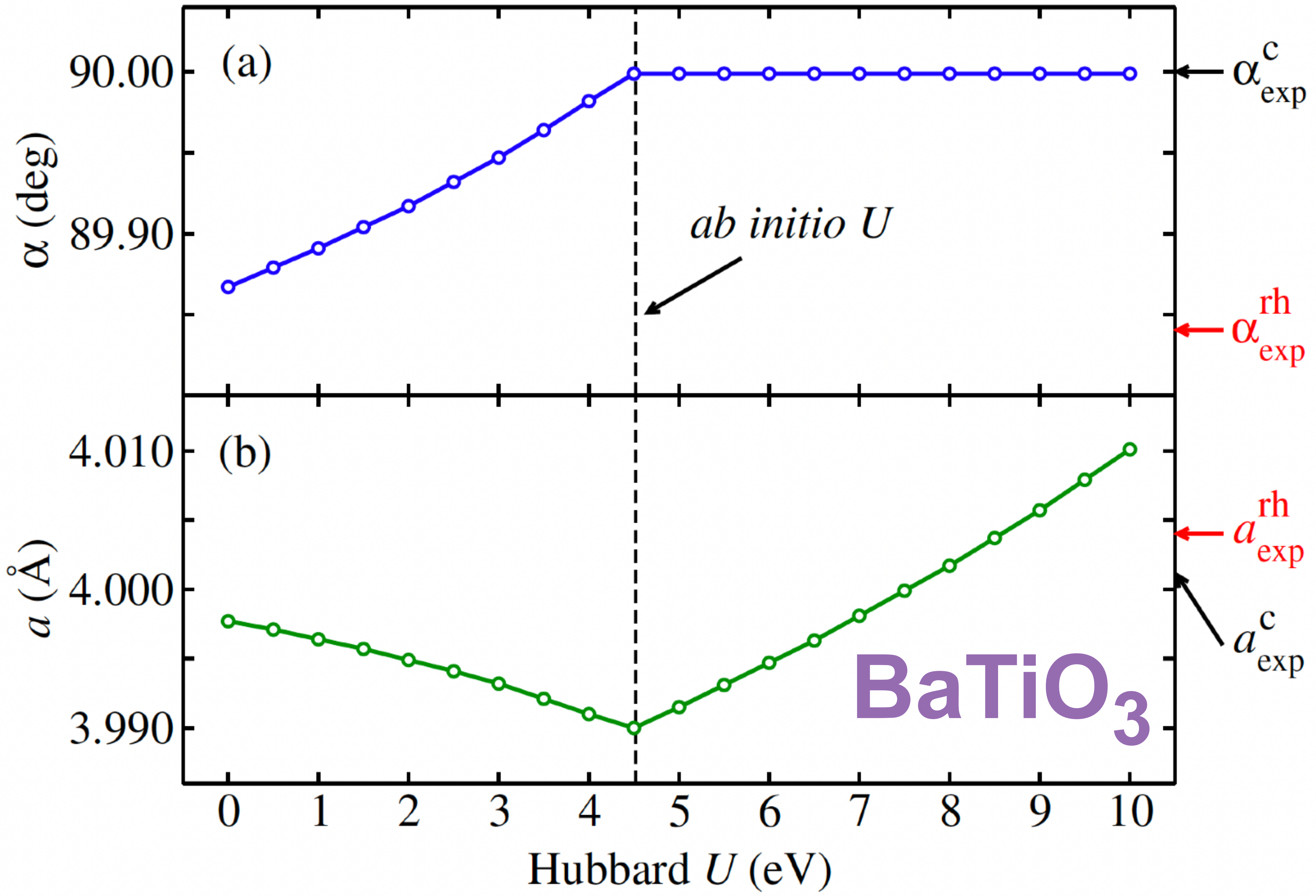

	a (Å)	α (deg)	Δ_{Ti}	Δ_{O}	$\Delta_{\mathrm{O'}}$
PBEsol	3.998	89.87	−0.012	0.011	0.018
PBEsol+U	3.990	90.00	0.000	0.000	0.000
PBEsol+U+V	4.017	89.77	−0.014	0.012	0.020
Expt.	4.004	89.84	−0.013	0.011	0.019

At $T = 0$ K, DFT+*U* incorrectly stabilizes the cubic phase, while DFT+*U*+*V* correctly retains the rhombohedral phase

Gebreyesus, Bastonero, Kotiuga, Marzari, Timrov, PRB (2023).

Phonons in Mott-Hubbard insulators

Electronic band structure of CoO

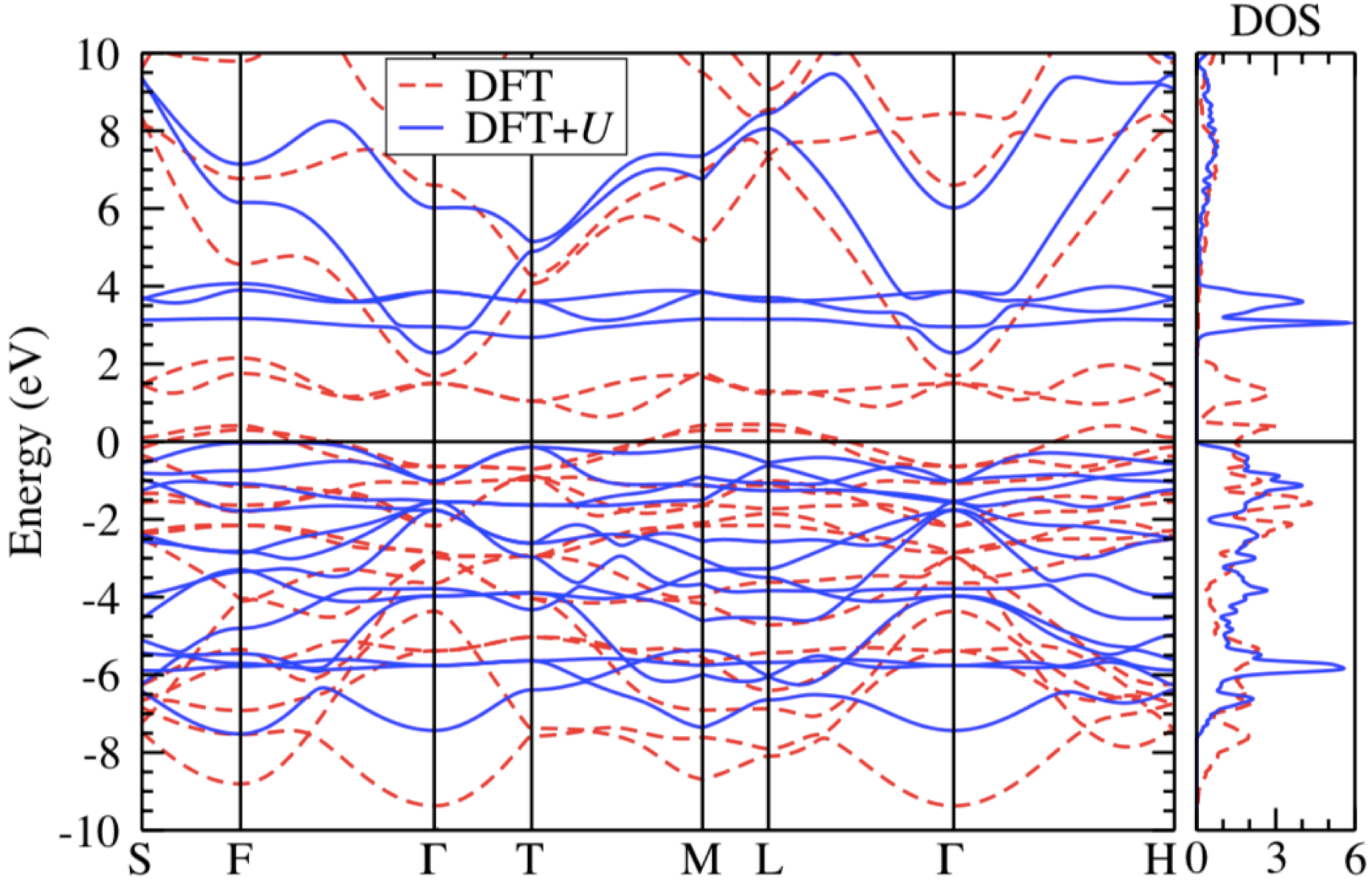

Phonon dispersion of CoO

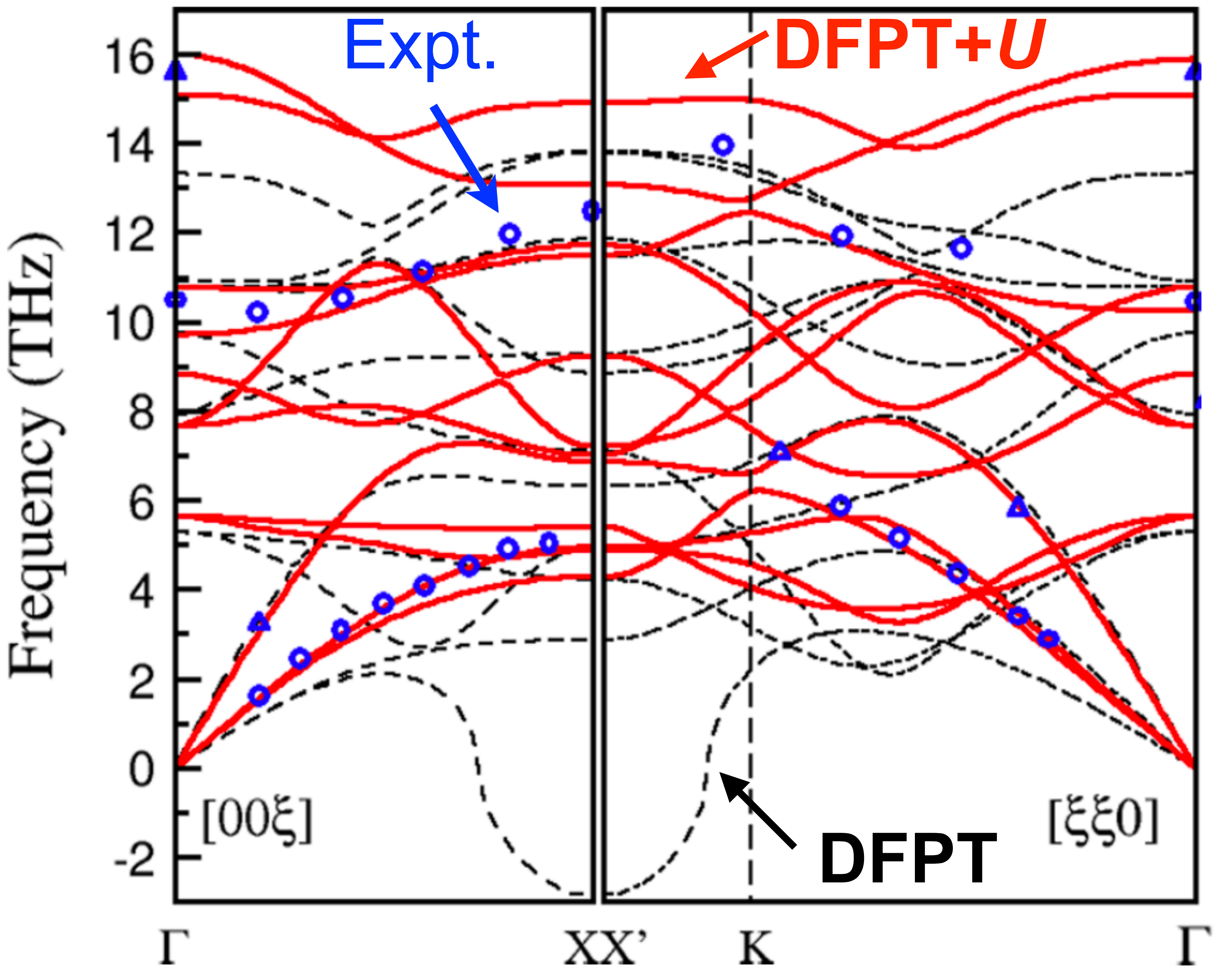

$$U_{\text{eff}} = 4.55\ (\text{eV}) \qquad E_{\text{GAP}}^{\text{DFT}+U} = 2.3\ (\text{eV}) \qquad E_{\text{GAP}}^{expt} = 2.5 - 2.8\ (\text{eV})$$

Dynamical stability of the structure
due to the Hubbard *U* correction

Floris, Timrov, Himmetoglu, Marzari, de Gironcoli, and Cococcioni, PRB (2020).

Electron-phonon coupling in Mott-Hubbard insulators

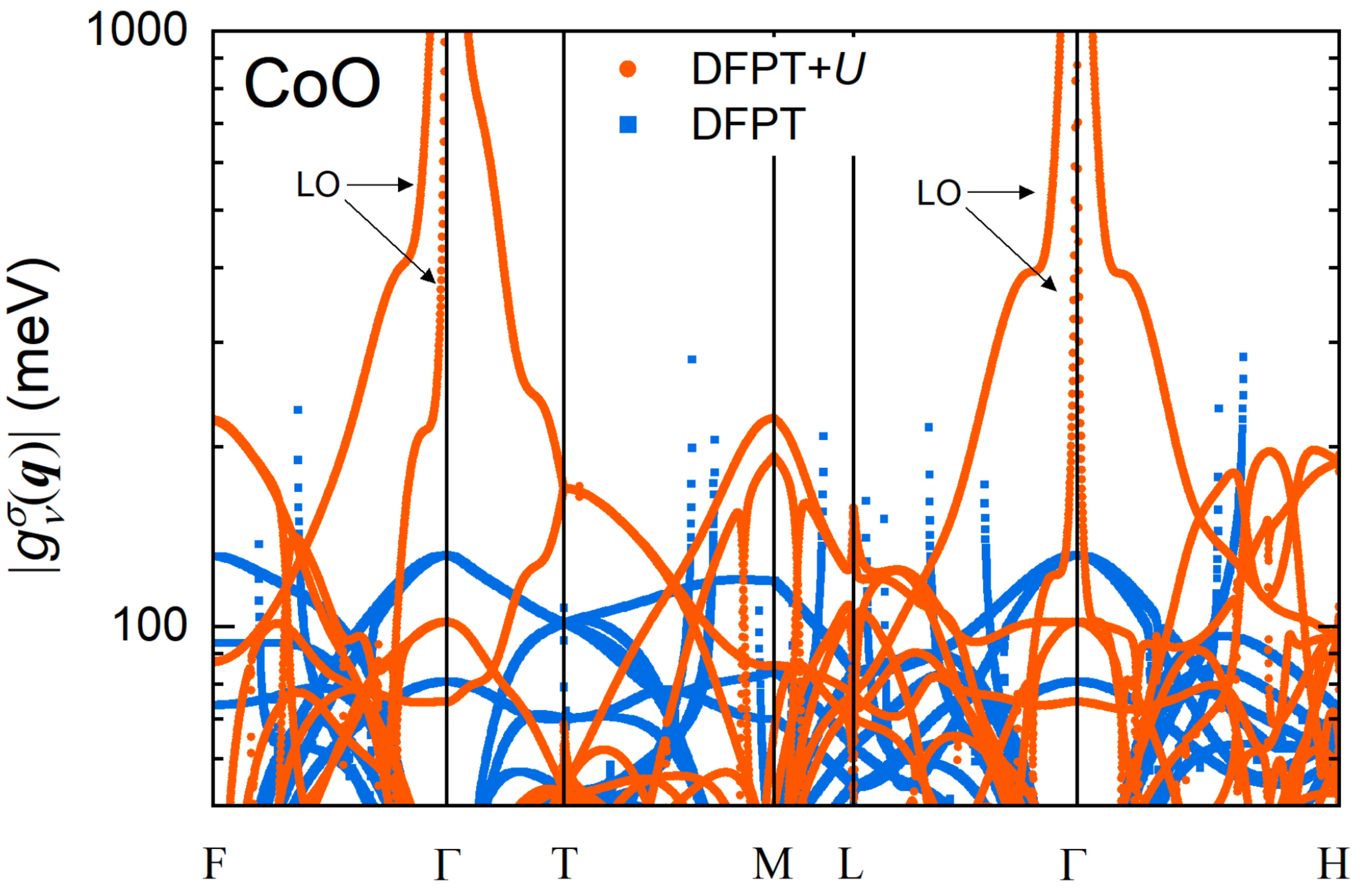

$$|g^{\sigma}_{\nu}(\boldsymbol{q})| \equiv \left(\sum_{mn} |g^{\sigma}_{mn\nu}(\boldsymbol{k}=0,\boldsymbol{q})|^2/N_b\right)^{1/2}$$

Hubbard *U* correction is crucial for the correct description of the electron-phonon coupling in Mott-Hubbard inssulators

Zhou, Park, Timrov, Floris, Cococcioni, Marzari, Bernardi, PRL (2021).

Parent (undoped) cuprate La_2CuO_4

DFT+*U* band structure

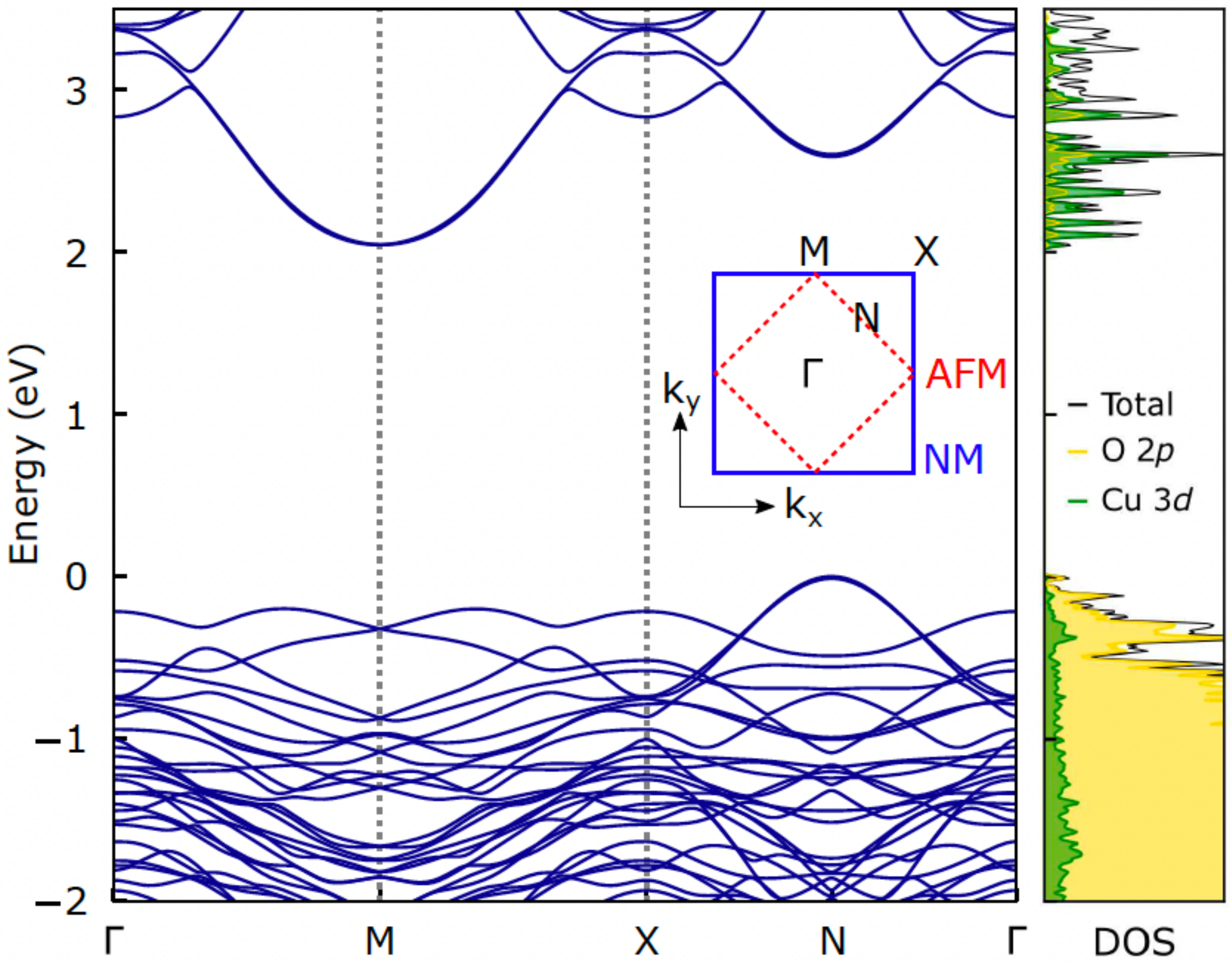

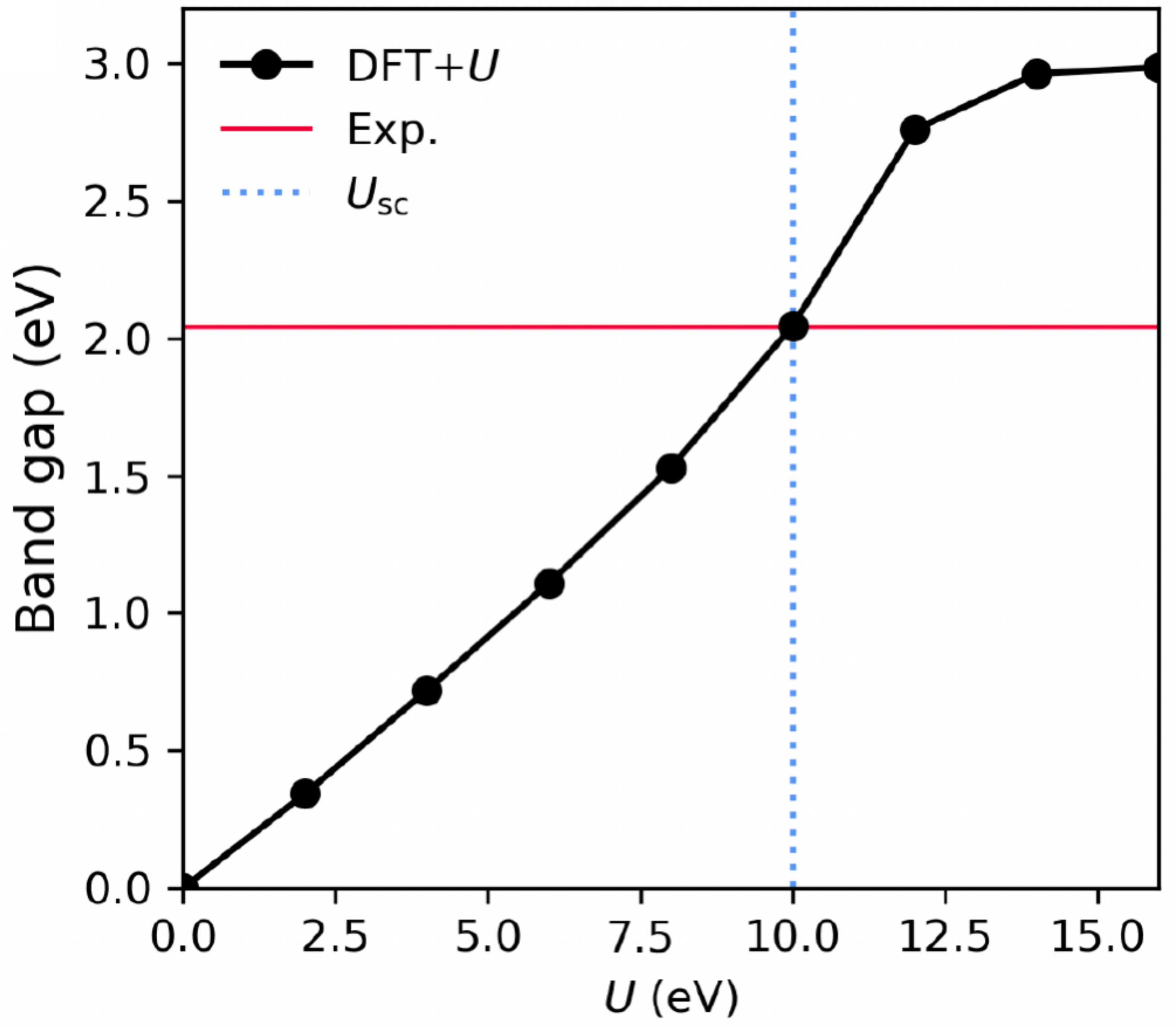

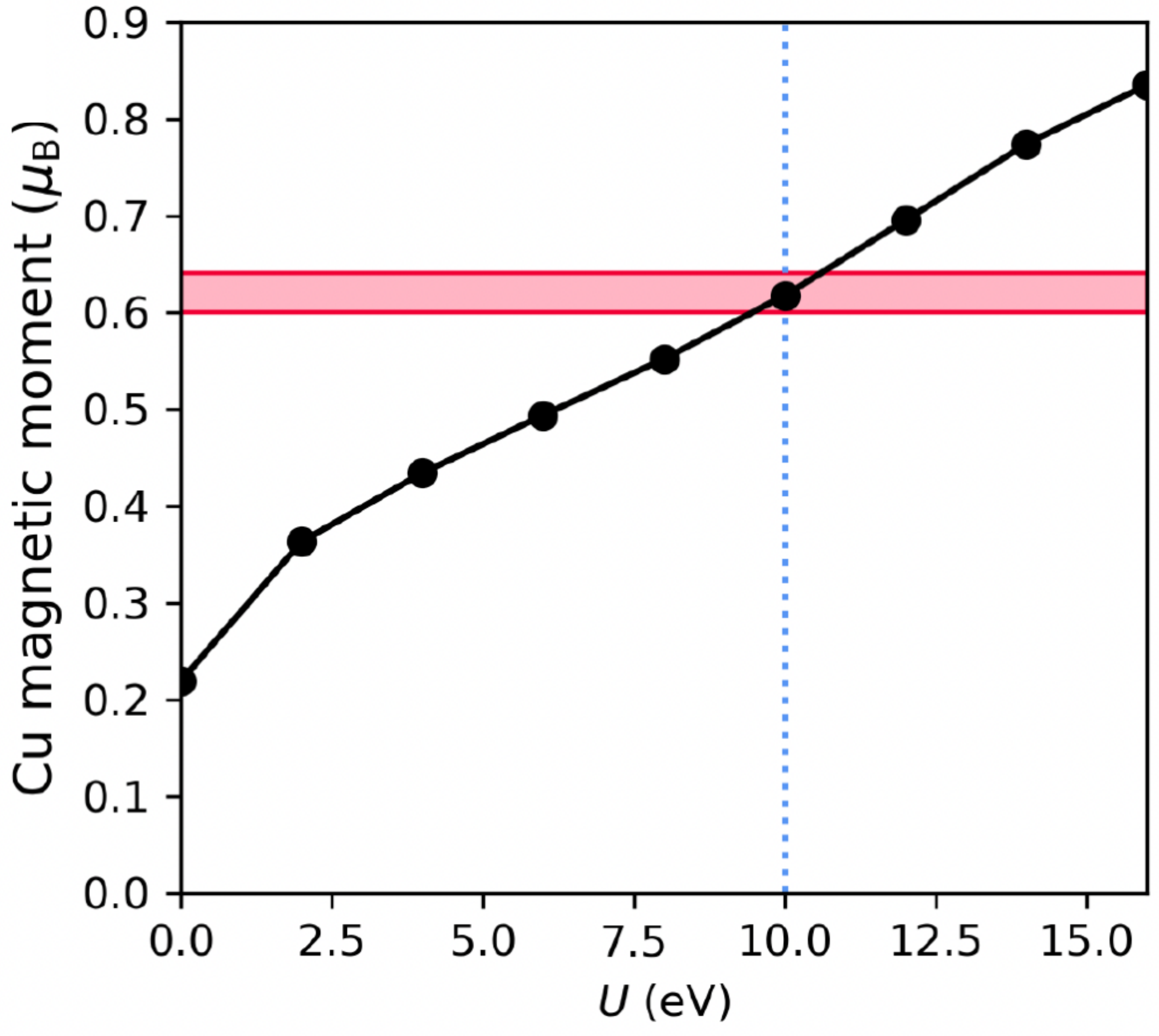

Accurate ground-state properties using the first-principles *U*

Chang, Timrov, Park, Zhou, Marzari, Bernardi, Phys. Rev. Research (2025).

Electron-phonon coupling in La_2CuO_4

Phonons

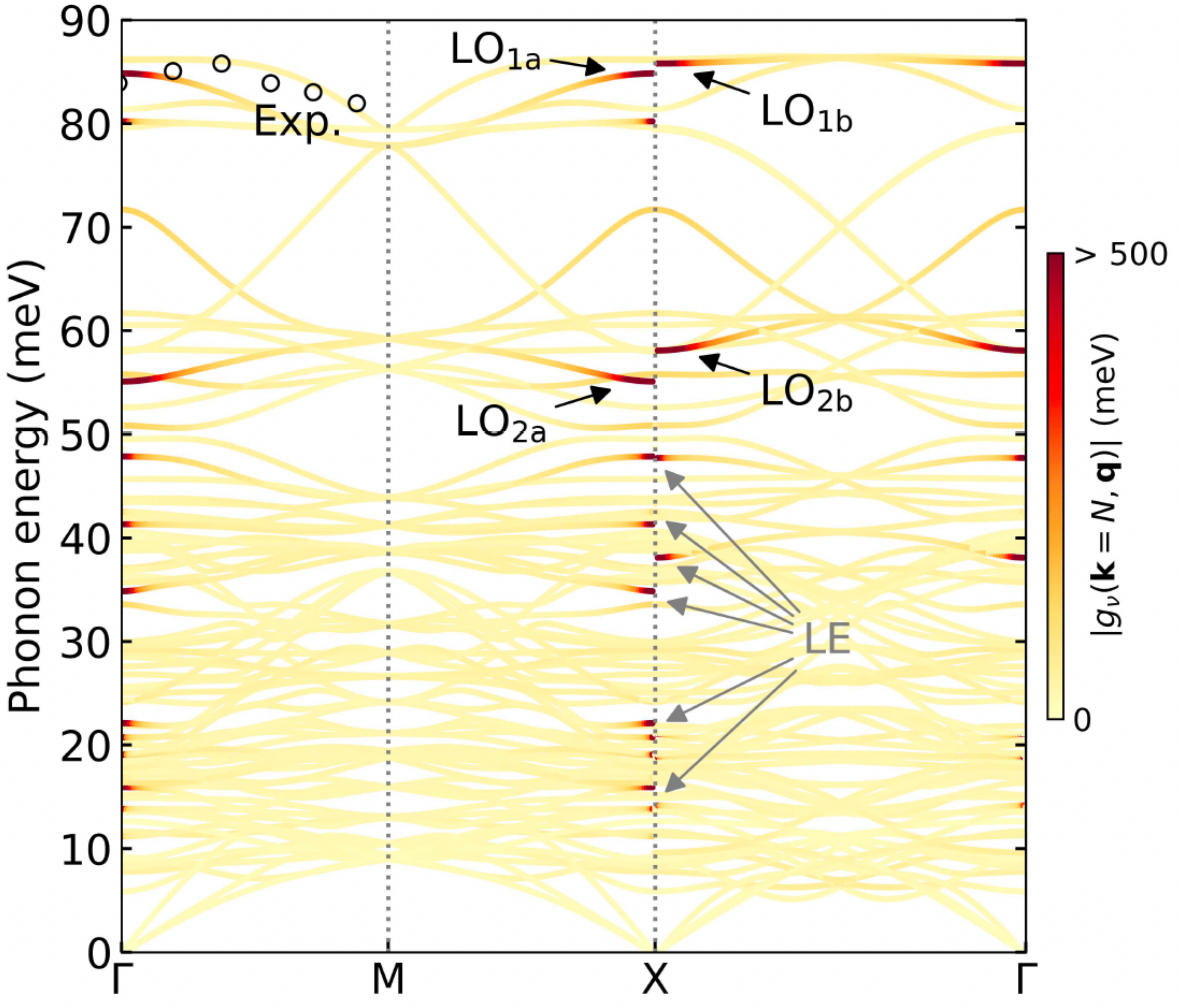

Electron-phonon coupling distribution function

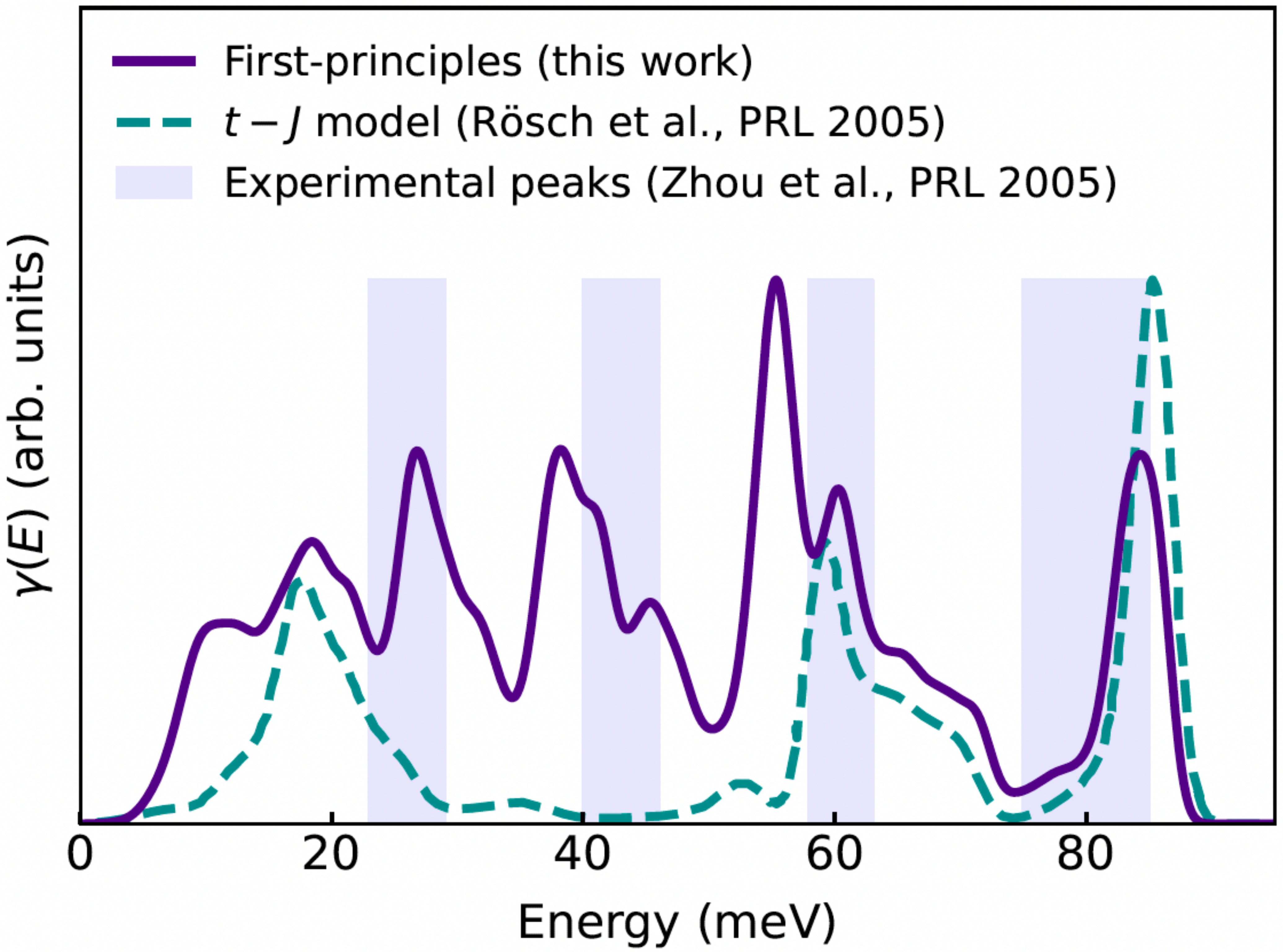

Accurate description of the e-ph coupling to understand the microscopic origin of the high Tc superconductivity

Chang, Timrov, Park, Zhou, Marzari, Bernardi, Phys. Rev. Research (2025).

TDDFPT+U magnon dispersions

Dynamical spin susceptibility

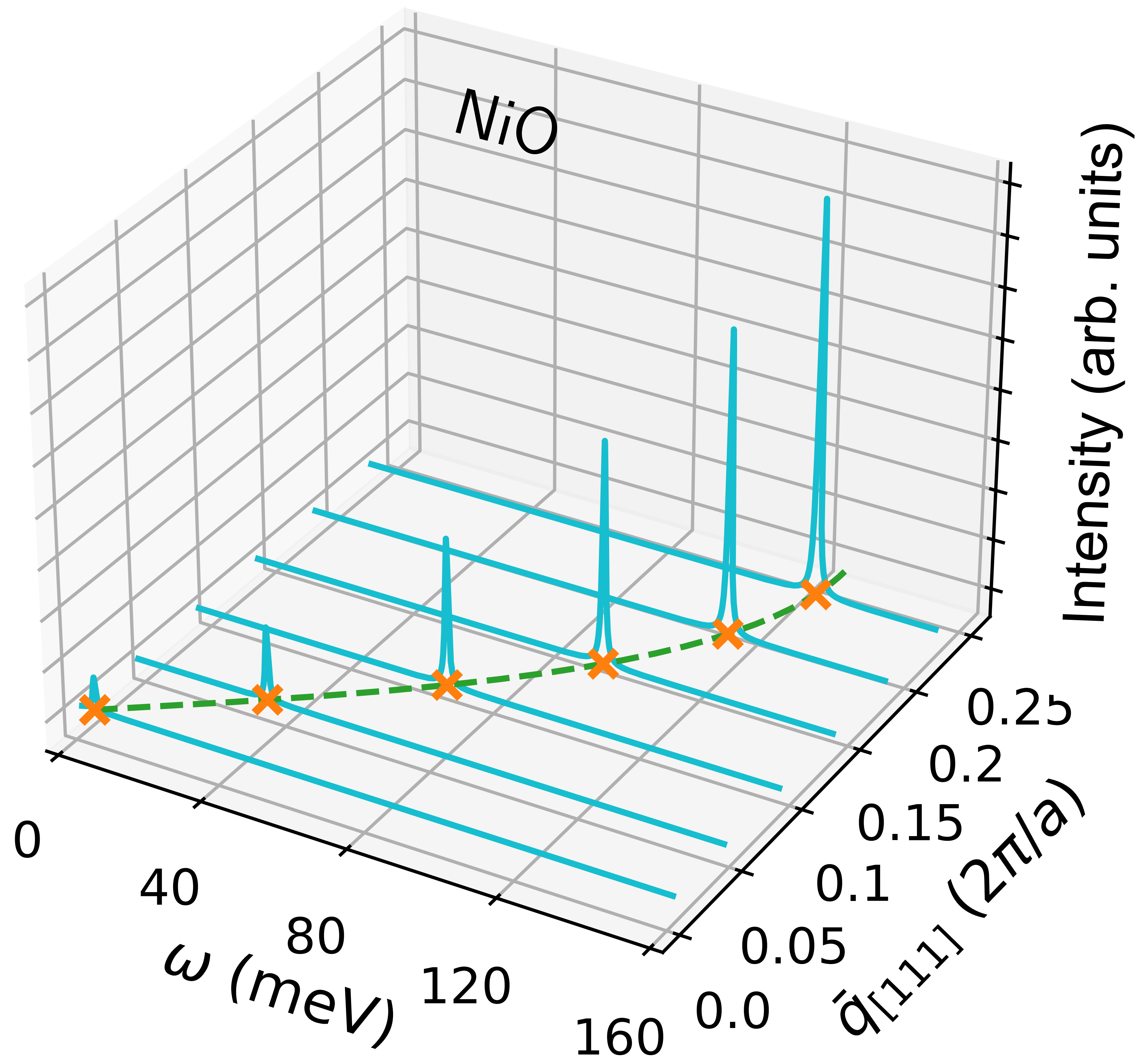

Binci, Marzari, Timrov, npj Comput. Mater. (2025).

TDDFPT+U magnon dispersions

Dynamical spin susceptibility

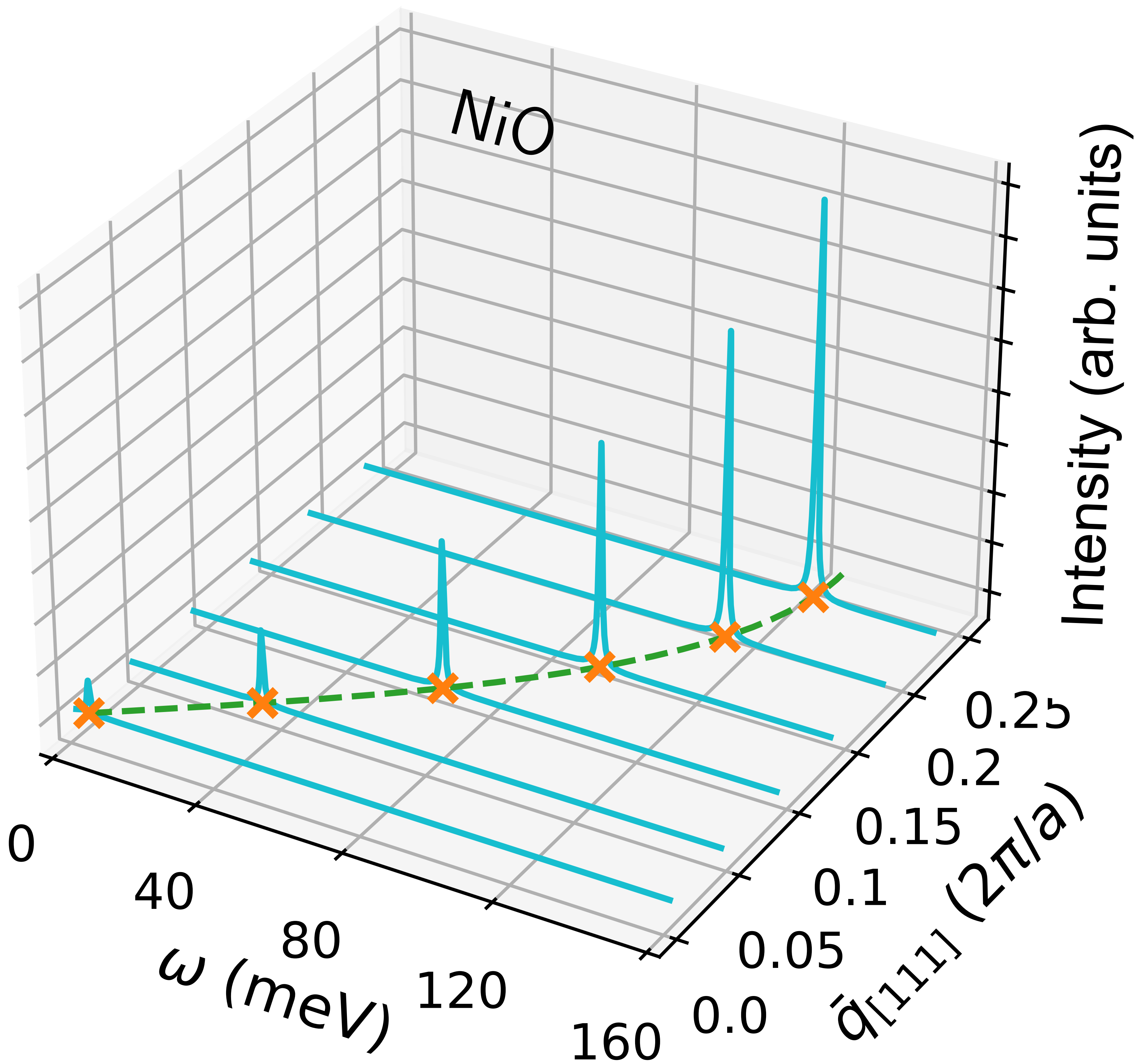

Magnon dispersions

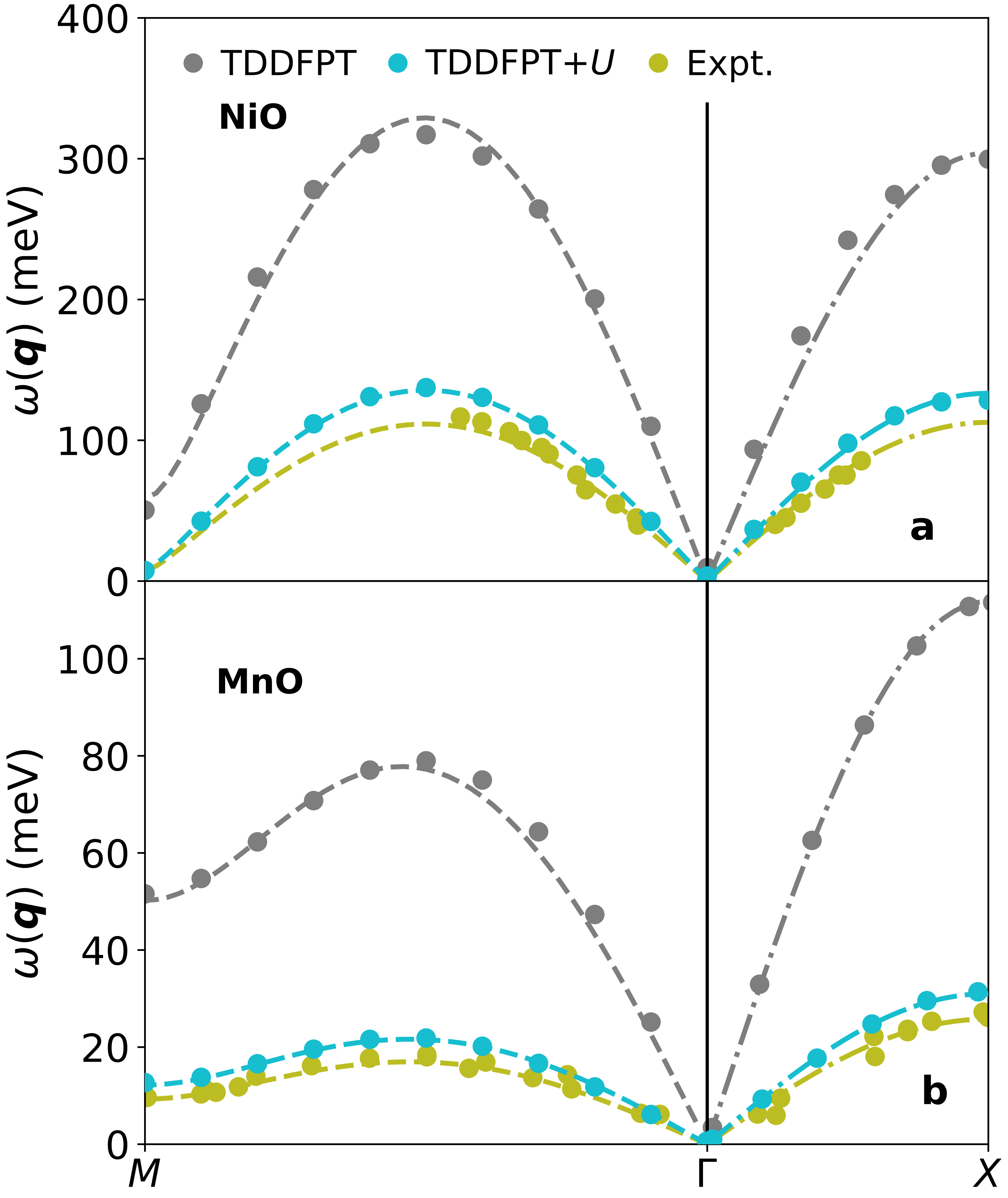

Binci, Marzari, Timrov, npj Comput. Mater. (2025).

U from first principles (6.26 eV for Ni, 4.29 eV for Mn)

Muon spin spectroscopy

Muon asymmetry $A(t)$ Fourier transform of $A(t)$

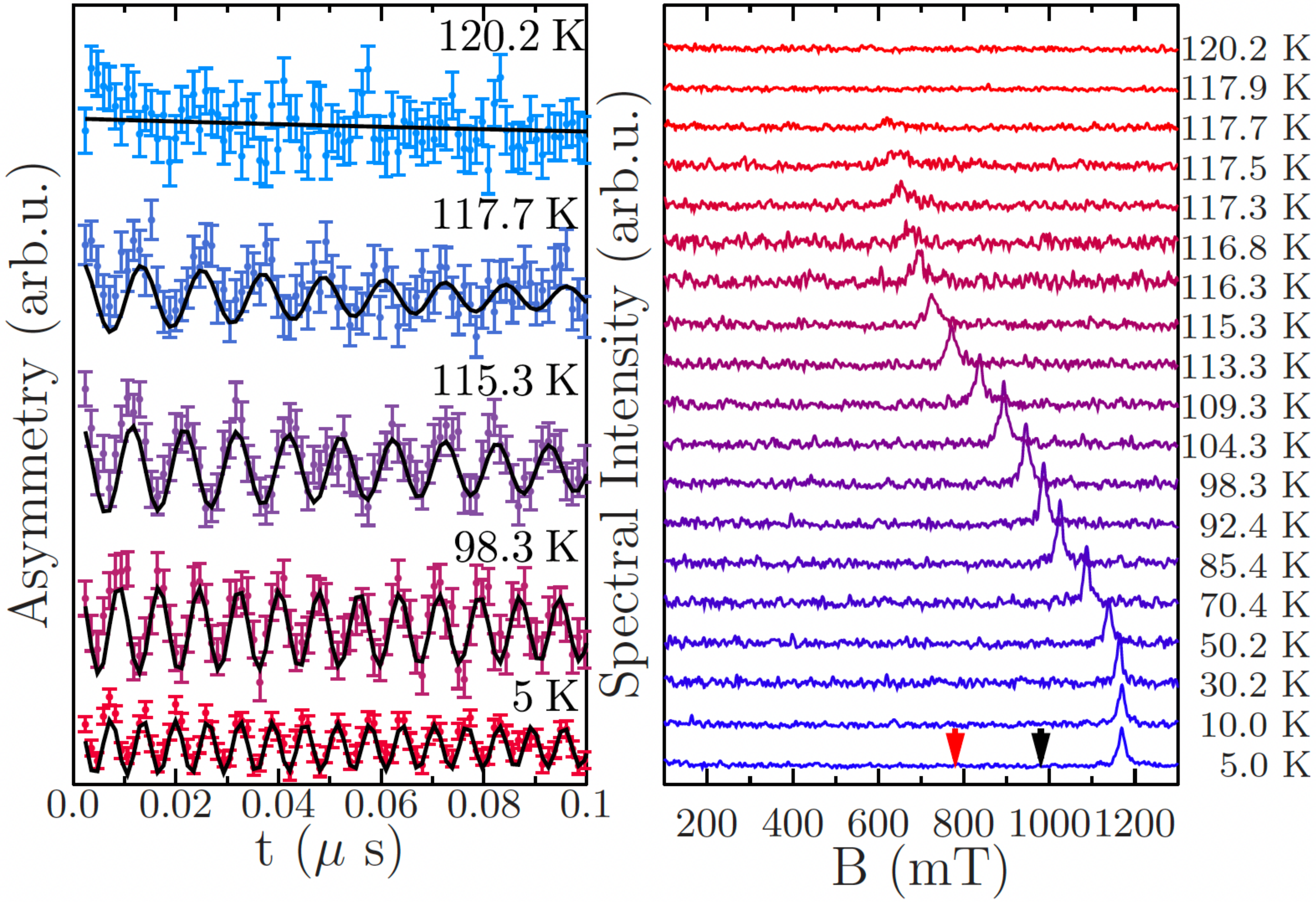

MnO

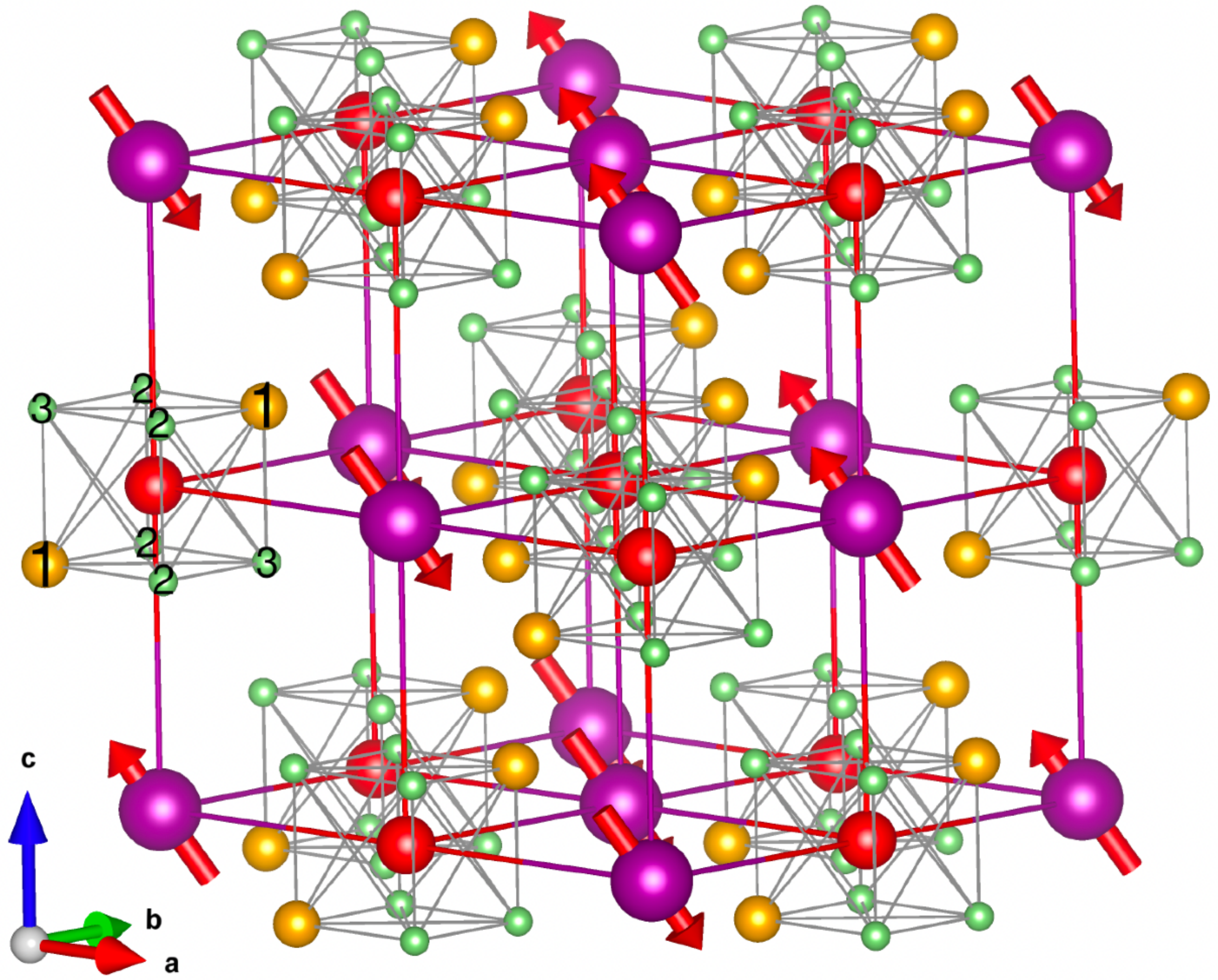

DFT+U+V reveals that the implanted muon is *localized* close to an O atom

Bonfa, Onuorah, Lang, Timrov et al., PRL (2024).

Limitations/open questions of linear-response theory (LRT) for *U* and *V*

- For closed shells (i.e. fully occupied manifolds) the *U* values from LRT are too large
- *U* and *V* are position-dependent $\longrightarrow$ $dU/dR \neq 0$, $dV/dR \neq 0$ $\longrightarrow$ extra terms in forces
- Hubbard functionals are not variational w.r.t. *U* and *V* (no theorem/proof)
- DFT+*U*(+*V*) is a mean-field single-determinant approach (no strong correlations)
- Piece-wise linearity in the Hubbard manifold is heuristic (no proof)

Hybrid functionals

Main idea

Mixing the Fock energy (of the Hartree-Fock method) with the (semi-)local exchange-correlation functionals

$$E_{\mathrm{x}}^{\mathrm{Fock}} = -\frac{1}{2} \underbrace{\sum_{\mathbf{k}} \sum_{\mathbf{k}'}}_{\text{double sum over k points}} \underbrace{\sum_{v} \sum_{v'}}_{\text{double sum over bands}} \int \int \frac{\psi^{*}_{v,\mathbf{k}}(\mathbf{r}) \psi_{v',\mathbf{k}'}(\mathbf{r}) \psi^{*}_{v',\mathbf{k}'}(\mathbf{r}') \psi_{v,\mathbf{k}}(\mathbf{r}')}{|\mathbf{r} - \mathbf{r}'|} \, d\mathbf{r} \, d\mathbf{r}'$$

E_{Fock} is computationally very expensive in the plane-wave basis set

PBE0 hybrid functional

$$\boxed{E_{\mathrm{xc}}^{\mathrm{PBE0}} = \alpha E_{\mathrm{x}}^{\mathrm{Fock}} + (1-\alpha) E_{\mathrm{x}}^{\mathrm{PBE}} + E_{\mathrm{c}}^{\mathrm{PBE}}}$$

25% of the (non-local) exact-exchange (Fock) energy

75% of the (semi-local) exchange GGA-PBE energy

100% of the (semi-local) correlation GGA-PBE energy

C. Adamo and V. Barone, JCP 110, 6158 (1999).

PBE0 hybrid functional

$$\boxed{\alpha = 0.25}$$

$$\boxed{E_{\mathrm{xc}}^{\mathrm{PBE0}} = \alpha E_{\mathrm{x}}^{\mathrm{Fock}} + (1-\alpha) E_{\mathrm{x}}^{\mathrm{PBE}} + E_{\mathrm{c}}^{\mathrm{PBE}}}$$

25% of the (non-local) exact-exchange (Fock) energy

75% of the (semi-local) exchange GGA-PBE energy

100% of the (semi-local) correlation GGA-PBE energy

C. Adamo and V. Barone, JCP 110, 6158 (1999).

Molecules

Electronic atomization energies (i.e. energy required to completely separate a molecule into its constituent atoms) in kcal/mol

Molecule	PBE	PBE0	Expt.
N_2	244	225	227
O_2	143	124	118
SO	142	128	122

PBE0 hybrid functional gives much more accurate results than PBE compared to experiments on simple molecules

J. Paier, R. Hirschl, M. Marsman, G. Kresse, JCP 122, 234102 (2005).

Solids

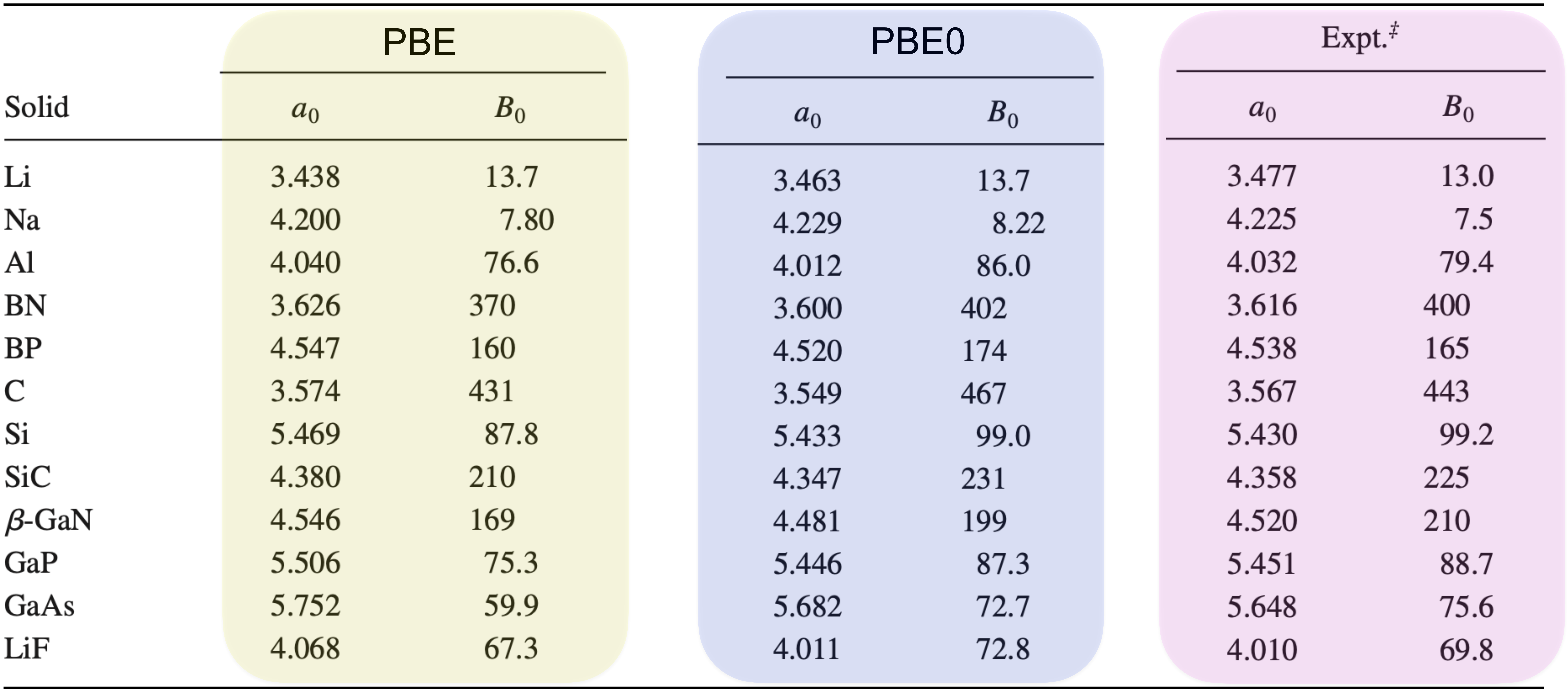

	PBE		PBE0		Expt.‡	
Solid	a_0	B_0	a_0	B_0	a_0	B_0
Li	3.438	13.7	3.463	13.7	3.477	13.0
Na	4.200	7.80	4.229	8.22	4.225	7.5
Al	4.040	76.6	4.012	86.0	4.032	79.4
BN	3.626	370	3.600	402	3.616	400
BP	4.547	160	4.520	174	4.538	165
C	3.574	431	3.549	467	3.567	443
Si	5.469	87.8	5.433	99.0	5.430	99.2
SiC	4.380	210	4.347	231	4.358	225
β-GaN	4.546	169	4.481	199	4.520	210
GaP	5.506	75.3	5.446	87.3	5.451	88.7
GaAs	5.752	59.9	5.682	72.7	5.648	75.6
LiF	4.068	67.3	4.011	72.8	4.010	69.8

PBE0 provides more accurate results than PBE for the lattice parameters and bulk modulus of solids

J. Paier, M. Marsman, K. Hummer, G. Kresse, I.C. Gerber, J.G. Angyan, JCP 124, 154709 (2006).

Solids

Direct and indirect band gaps

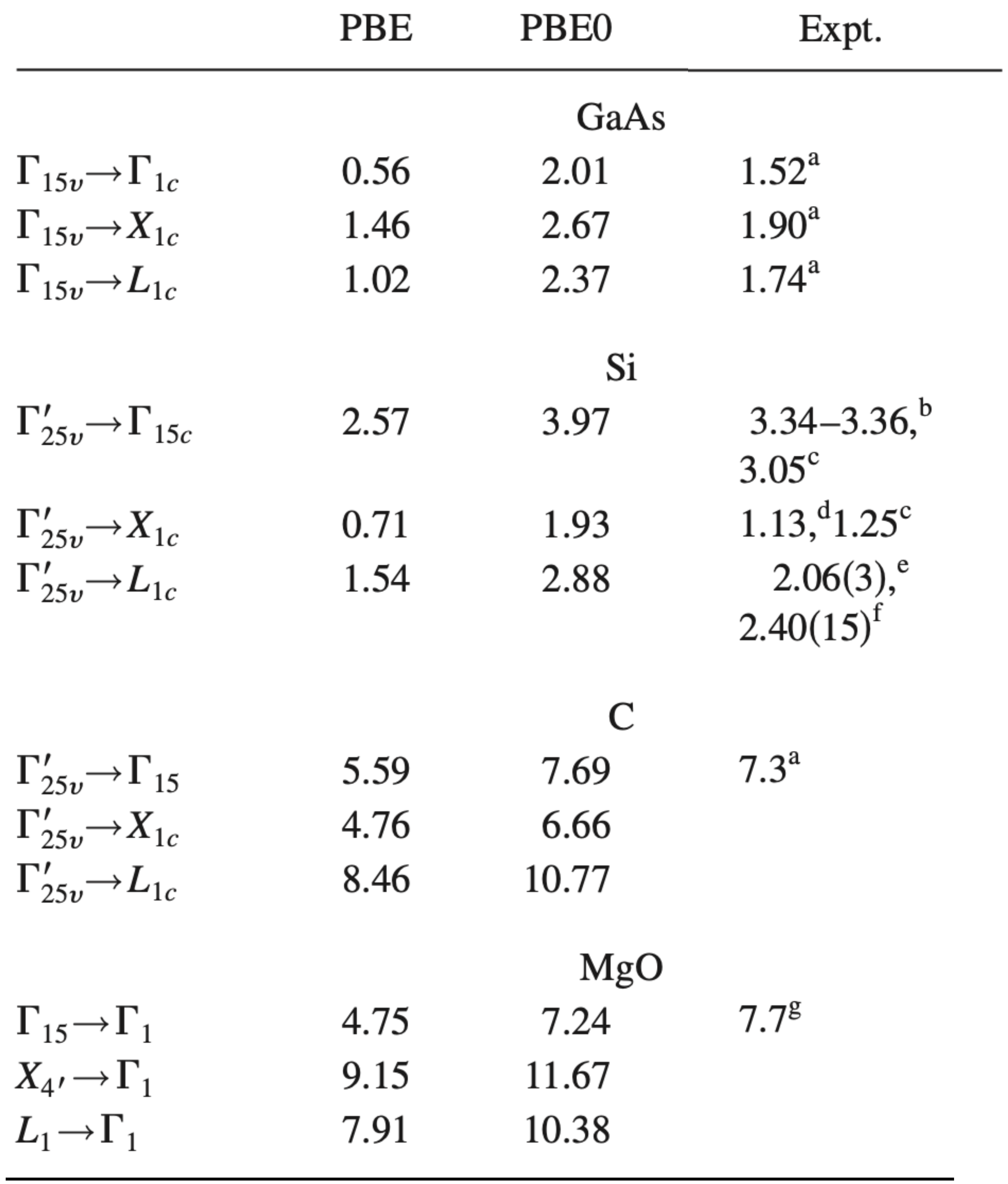

	PBE	PBE0	Expt.
		GaAs	
$\Gamma_{15v}\rightarrow\Gamma_{1c}$	0.56	2.01	1.52[a]
$\Gamma_{15v}\rightarrow X_{1c}$	1.46	2.67	1.90[a]
$\Gamma_{15v}\rightarrow L_{1c}$	1.02	2.37	1.74[a]
		Si	
$\Gamma'_{25v}\rightarrow\Gamma_{15c}$	2.57	3.97	3.34–3.36,[b] 3.05[c]
$\Gamma'_{25v}\rightarrow X_{1c}$	0.71	1.93	1.13,[d] 1.25[c]
$\Gamma'_{25v}\rightarrow L_{1c}$	1.54	2.88	2.06(3),[e] 2.40(15)[f]
		C	
$\Gamma'_{25v}\rightarrow\Gamma_{15}$	5.59	7.69	7.3[a]
$\Gamma'_{25v}\rightarrow X_{1c}$	4.76	6.66	
$\Gamma'_{25v}\rightarrow L_{1c}$	8.46	10.77	
		MgO	
$\Gamma_{15}\rightarrow\Gamma_{1}$	4.75	7.24	7.7[g]
$X_{4'}\rightarrow\Gamma_{1}$	9.15	11.67	
$L_{1}\rightarrow\Gamma_{1}$	7.91	10.38	

- PBE underestimates band gaps
- PBE0 predicts more accurate band gaps, but this is not systematic and there are overestimations
- Overestimation of band gaps in PBE0 is related to the non-optimal fraction of the Fock exchange (see next slides)

J. Paier, M. Marsman, K. Hummer, G. Kresse, I.C. Gerber, J.G. Angyan, JCP 124, 154709 (2006).

B3LYP hybrid functional

$$\boxed{\alpha = 0.20, \beta = 0.72, \gamma = 0.81}$$

$$\boxed{E_{\mathrm{xc}}^{\mathrm{B3LYP}} = \alpha E_{\mathrm{x}}^{\mathrm{Fock}} + (1-\alpha) E_{\mathrm{x}}^{\mathrm{LDA}} + \beta \Delta E_{\mathrm{x}}^{\mathrm{B88}} + \gamma E_{\mathrm{c}}^{\mathrm{LYP}} + (1-\gamma) E_{\mathrm{c}}^{\mathrm{LDA}}}$$

20% of the (non-local) exact-exchange (Fock) energy

80% of the (local) exchange LDA energy

Becke's gradient correction to the exchange functional

81% of the (local) correlation GGA-LYP energy

19% of the (local) correlation LDA energy

A.D. Becke, JCP 98, 1372 (1993).

P.J. Stephens, F.J. Devlin, C.F. Chabalowski, M.J. Frisch, JPC 98, 11623 (1994).

Molecules

Frequencies (ν), dipole strengths (D), rotational strengths (R) of 4-methyl-2-oxetanone

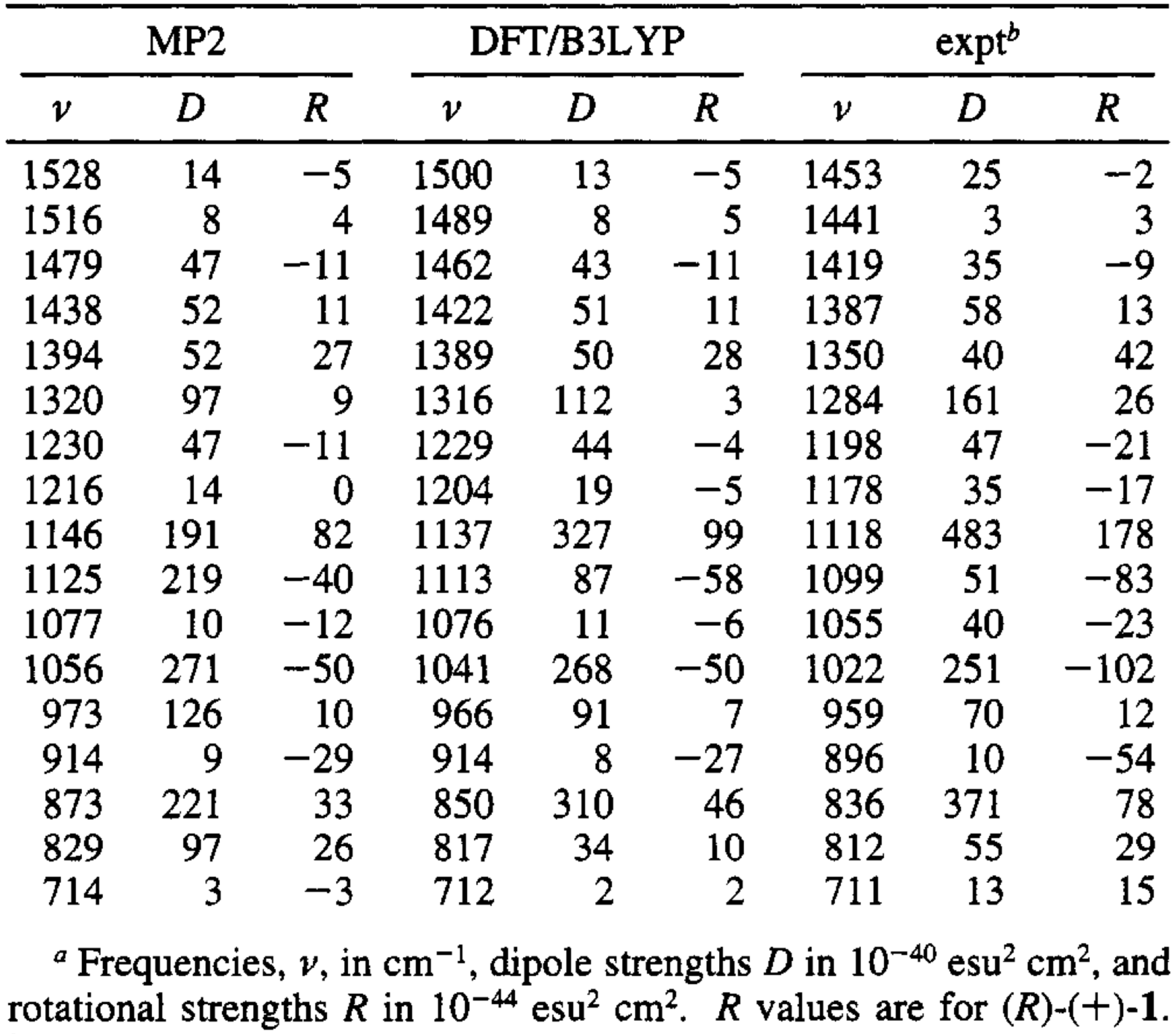

MP2			DFT/B3LYP			expt[b]		
ν	D	R	ν	D	R	ν	D	R
1528	14	−5	1500	13	−5	1453	25	−2
1516	8	4	1489	8	5	1441	3	3
1479	47	−11	1462	43	−11	1419	35	−9
1438	52	11	1422	51	11	1387	58	13
1394	52	27	1389	50	28	1350	40	42
1320	97	9	1316	112	3	1284	161	26
1230	47	−11	1229	44	−4	1198	47	−21
1216	14	0	1204	19	−5	1178	35	−17
1146	191	82	1137	327	99	1118	483	178
1125	219	−40	1113	87	−58	1099	51	−83
1077	10	−12	1076	11	−6	1055	40	−23
1056	271	−50	1041	268	−50	1022	251	−102
973	126	10	966	91	7	959	70	12
914	9	−29	914	8	−27	896	10	−54
873	221	33	850	310	46	836	371	78
829	97	26	817	34	10	812	55	29
714	3	−3	712	2	2	711	13	15

[a] Frequencies, ν, in cm^{-1}, dipole strengths D in 10^{-40} esu^2 cm^2, and rotational strengths R in 10^{-44} esu^2 cm^2. R values are for (R)-(+)-**1**.

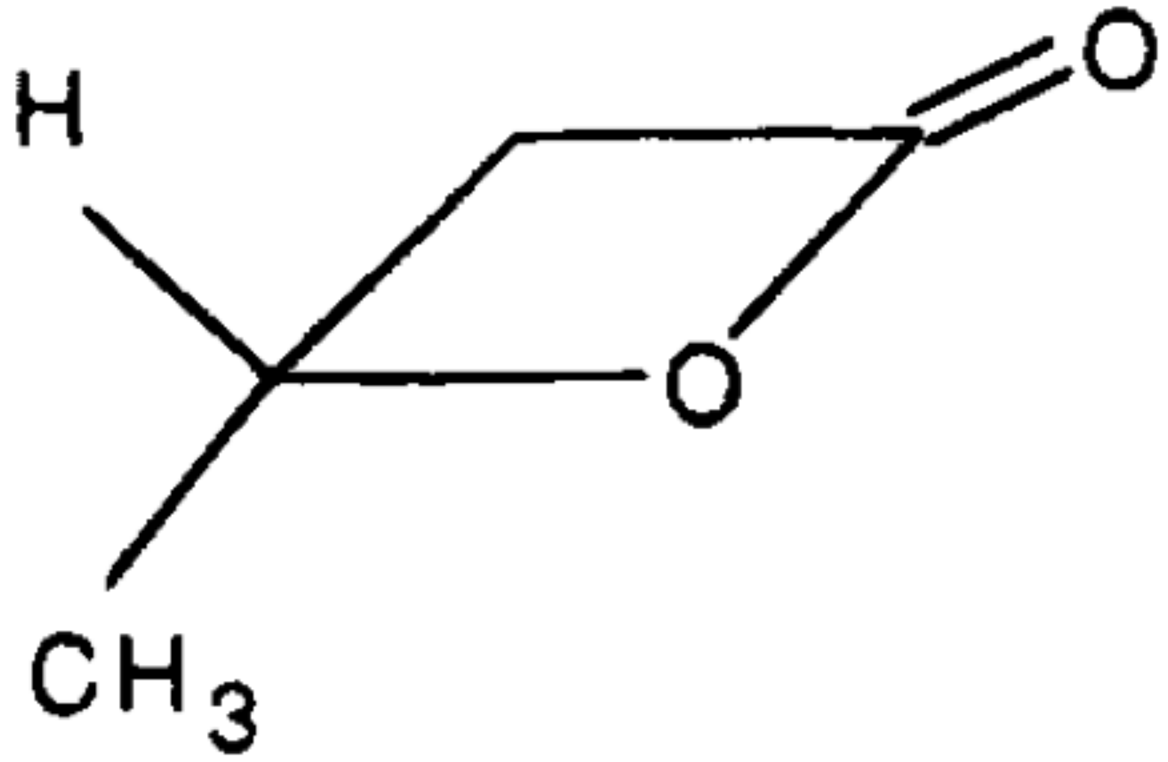

MP2 = second-order Møller-Plesset perturbation theory

B3LYP is very popular in the quantum chemistry community (study of molecules)

P.J. Stephens, F.J. Devlin, C.F. Chabalowski, M.J. Frisch, JPC 98, 11623 (1994).

Range separation

The Coulomb potential is partitioned as a sum of the short-range (SR) and long-range (LR) parts:

$$\frac{1}{|\mathbf{r}-\mathbf{r}'|} = \frac{\operatorname{erfc}(\omega|\mathbf{r}-\mathbf{r}'|)}{|\mathbf{r}-\mathbf{r}'|} + \frac{\operatorname{erf}(\omega|\mathbf{r}-\mathbf{r}'|)}{|\mathbf{r}-\mathbf{r}'|}$$

Range-separated hybrid functional

From PBE0 to HSE hybrid functional

$$\boxed{\alpha = 0.25}$$

$$\boxed{E_{\mathrm{xc}}^{\mathrm{PBE0}} = \alpha E_{\mathrm{x}}^{\mathrm{Fock}} + (1-\alpha)E_{\mathrm{x}}^{\mathrm{PBE}} + E_{\mathrm{c}}^{\mathrm{PBE}}}$$

$$\boxed{E_{\mathrm{xc}}^{\mathrm{HSE06}} = \alpha E_{\mathrm{x}}^{\mathrm{Fock,SR}} + (1-\alpha)E_{\mathrm{x}}^{\mathrm{PBE,SR}} + E_{\mathrm{x}}^{\mathrm{PBE,LR}} + E_{\mathrm{c}}^{\mathrm{PBE}}}$$

J. Heyd, G.E. Scuseria, M. Ernzerhof, JCP 118, 8207 (2003); JCP 124, 219906 (2006).

HSE03 → HSE06

Solids

Direct and indirect band gaps

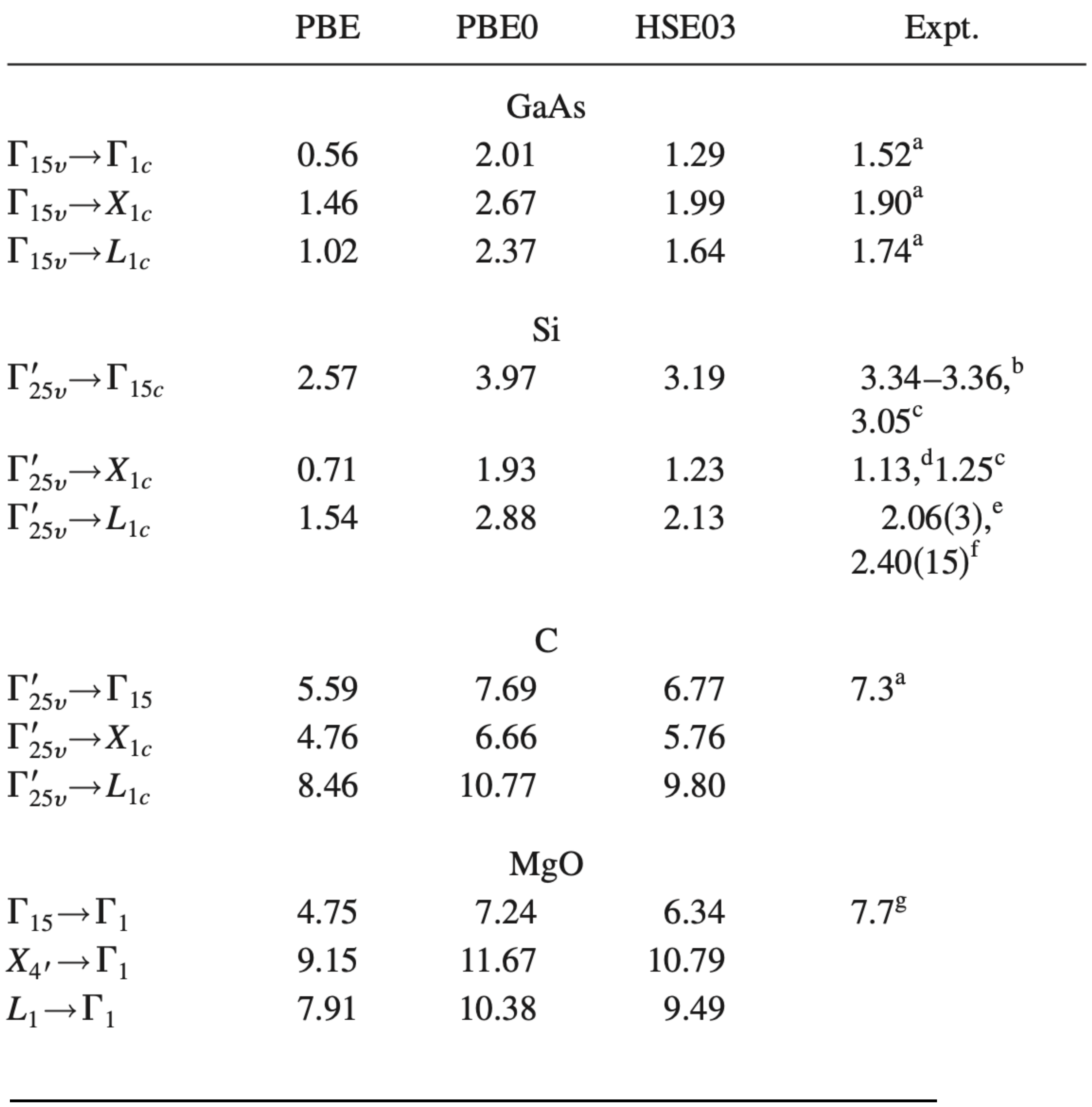

	PBE	PBE0	HSE03	Expt.
GaAs				
$\Gamma_{15v}\rightarrow\Gamma_{1c}$	0.56	2.01	1.29	1.52^{a}
$\Gamma_{15v}\rightarrow X_{1c}$	1.46	2.67	1.99	1.90^{a}
$\Gamma_{15v}\rightarrow L_{1c}$	1.02	2.37	1.64	1.74^{a}
Si				
$\Gamma'_{25v}\rightarrow\Gamma_{15c}$	2.57	3.97	3.19	$3.34–3.36,^{b}$ 3.05^{c}
$\Gamma'_{25v}\rightarrow X_{1c}$	0.71	1.93	1.23	$1.13,^{d}1.25^{c}$
$\Gamma'_{25v}\rightarrow L_{1c}$	1.54	2.88	2.13	$2.06(3),^{e}$ $2.40(15)^{f}$
C				
$\Gamma'_{25v}\rightarrow\Gamma_{15}$	5.59	7.69	6.77	7.3^{a}
$\Gamma'_{25v}\rightarrow X_{1c}$	4.76	6.66	5.76	
$\Gamma'_{25v}\rightarrow L_{1c}$	8.46	10.77	9.80	
MgO				
$\Gamma_{15}\rightarrow\Gamma_{1}$	4.75	7.24	6.34	7.7^{g}
$X_{4'}\rightarrow\Gamma_{1}$	9.15	11.67	10.79	
$L_{1}\rightarrow\Gamma_{1}$	7.91	10.38	9.49	

J. Paier, M. Marsman, K. Hummer, G. Kresse, I.C. Gerber, J.G. Angyan, JCP 124, 154709 (2006).

What fraction of Fock exchange to use in solids (α parameter)?

From the analogy with the many-body perturbation theory, one can realize that:

$$\cancel{\alpha = 0.25} \quad \rightarrow \quad \alpha = \frac{1}{\epsilon_\infty}$$

ϵ_∞ is the electronic dielectric constant of a material

J.H. Skone, M. Govoni, G. Galli, PRB 89, 195112 (2014).

Dielectric constant ϵ_∞ of solids

Material	ϵ_∞
Ge	15.9
Si	11.9
AlP	7.54
SiC	6.52
TiO_2	6.34
NiO	5.76
C	5.70
CoO	5.35
GaN	5.30
ZnS	5.13
MnO	4.95
WO_3	4.81

Material	ϵ_∞
BN	4.50
HfO_2	4.41
AlN	4.18
ZnO	3.74
Al_2O_3	3.10
MgO	2.96
LiCl	2.70
NaCl	2.40
LiF	1.90
H_2O	1.72
Ar	1.66
Ne	1.23

J.H. Skone, M. Govoni, G. Galli, PRB 89, 195112 (2014).

Band gaps of solids

Material	PBE	PBE0 ($\alpha = 0.25$)	PBE0 modified ($\alpha = 1/\epsilon_\infty$)	Expt.
Ge	0.00	1.53	0.77	0.74
Si	0.62	1.75	1.03	1.17
AlP	1.64	2.98	2.41	2.51
SiC	1.37	2.91	2.33	2.39
TiO_2	1.81	3.92	3.18	3.3
NiO	0.97	5.28	4.61	4.3
C	4.15	5.95	5.44	5.48
CoO	0.00	4.53	4.01	2.5
GaN	1.88	3.68	3.30	3.29
ZnS	2.36	4.18	3.85	3.91
MnO	1.12	3.87	3.66	3.9
WO_3	1.92	3.79	3.50	3.38

J.H. Skone, M. Govoni, G. Galli, PRB 89, 195112 (2014).

J.H. Skone, M. Govoni, G. Galli, PRB 93, 235106 (2016).

Calculation of the Fock energy in practice

$$E_{\mathrm{x}}^{\mathrm{Fock}} = -\frac{1}{2}\sum_{\mathbf{k}}\sum_{\mathbf{k}'}\sum_{v}\sum_{v'}\int\int\frac{\psi^{*}_{v,\mathbf{k}}(\mathbf{r})\psi_{v',\mathbf{k}'}(\mathbf{r})\psi^{*}_{v',\mathbf{k}'}(\mathbf{r}')\psi_{v,\mathbf{k}}(\mathbf{r}')}{|\mathbf{r}-\mathbf{r}'|}\,d\mathbf{r}\,d\mathbf{r}'$$

$$\sum_{\mathbf{k}'} \longleftrightarrow \sum_{\mathbf{q}}$$

auxiliary q point grid ($\mathbf{q} = \mathbf{k} - \mathbf{k}'$)

Replace one sum over k points with a sum over q points ($N_{\mathbf{q}} \leq N_{\mathbf{k}}$)

This allows us to speed up significantly the calculation of $E_{\mathrm{x}}^{\mathrm{Fock}}$

From real to reciprocal space

$$E_{\mathrm{x}}^{\mathrm{Fock}} = -\frac{1}{2}\sum_{\mathbf{k}}\sum_{\mathbf{k}'}\sum_{v}\sum_{v'}\int\int \frac{\psi^{*}_{v,\mathbf{k}}(\mathbf{r})\psi_{v',\mathbf{k}'}(\mathbf{r})\psi^{*}_{v',\mathbf{k}'}(\mathbf{r}')\psi_{v,\mathbf{k}}(\mathbf{r}')}{|\mathbf{r}-\mathbf{r}'|}\,d\mathbf{r}\,d\mathbf{r}'$$

From real to reciprocal space

$$\boxed{E_{\mathrm{x}}^{\mathrm{Fock}}} = -\frac{1}{2}\sum_{\mathbf{k}}\sum_{\mathbf{k}'}\sum_{v}\sum_{v'}\int\int \frac{\psi^{*}_{v,\mathbf{k}}(\mathbf{r})\psi_{v',\mathbf{k}'}(\mathbf{r})\psi^{*}_{v',\mathbf{k}'}(\mathbf{r}')\psi_{v,\mathbf{k}}(\mathbf{r}')}{|\mathbf{r}-\mathbf{r}'|}\,d\mathbf{r}\,d\mathbf{r}'$$

$$\boxed{E_{\mathrm{x}}^{\mathrm{Fock}}} = -\frac{2\pi}{\Omega}\frac{1}{N_{\mathbf{q}}}\sum_{\mathbf{q}}\sum_{\mathbf{G}}\frac{A(\mathbf{q}+\mathbf{G})}{|\mathbf{q}+\mathbf{G}|^{2}}, \qquad A(\mathbf{q}+\mathbf{G}) = \frac{1}{N_{\mathbf{k}}}\sum_{\mathbf{k}}\sum_{v,v'}|\rho^{v',\mathbf{k}-\mathbf{q}}_{v,\mathbf{k}}(\mathbf{q}+\mathbf{G})|^{2}$$

From real to reciprocal space

$$E_{\mathrm{x}}^{\mathrm{Fock}} = -\frac{1}{2}\sum_{\mathbf{k}}\sum_{\mathbf{k}'}\sum_{v}\sum_{v'}\int\int \frac{\psi^{*}_{v,\mathbf{k}}(\mathbf{r})\psi_{v',\mathbf{k}'}(\mathbf{r})\psi^{*}_{v',\mathbf{k}'}(\mathbf{r}')\psi_{v,\mathbf{k}}(\mathbf{r}')}{|\mathbf{r}-\mathbf{r}'|}\, d\mathbf{r}\, d\mathbf{r}'$$

$$\Downarrow$$

$$E_{\mathrm{x}}^{\mathrm{Fock}} = -\frac{2\pi}{\Omega}\frac{1}{N_{\mathbf{q}}}\sum_{\mathbf{q}}\sum_{\mathbf{G}}\frac{A(\mathbf{q}+\mathbf{G})}{|\mathbf{q}+\mathbf{G}|^2},$$

$$A(\mathbf{q}+\mathbf{G}) = \frac{1}{N_{\mathbf{k}}}\sum_{\mathbf{k}}\sum_{v,v'}|\rho_{v,\mathbf{k}}^{v',\mathbf{k}-\mathbf{q}}(\mathbf{q}+\mathbf{G})|^2$$

$$\rho_{v,\mathbf{k}}^{v',\mathbf{k}-\mathbf{q}}(\mathbf{r}) = u^{*}_{v',\mathbf{k}-\mathbf{q}}(\mathbf{r})\, u_{v,\mathbf{k}}(\mathbf{r})$$

From real to reciprocal space

$$E_{\mathrm{x}}^{\mathrm{Fock}} = -\frac{1}{2}\sum_{\mathbf{k}}\sum_{\mathbf{k}'}\sum_{v}\sum_{v'}\int\int \frac{\psi^*_{v,\mathbf{k}}(\mathbf{r})\psi_{v',\mathbf{k}'}(\mathbf{r})\psi^*_{v',\mathbf{k}'}(\mathbf{r}')\psi_{v,\mathbf{k}}(\mathbf{r}')}{|\mathbf{r}-\mathbf{r}'|}\, d\mathbf{r}\, d\mathbf{r}'$$

$$\Downarrow$$

$$E_{\mathrm{x}}^{\mathrm{Fock}} = -\frac{2\pi}{\Omega}\frac{1}{N_{\mathbf{q}}}\sum_{\mathbf{q}}\sum_{\mathbf{G}}\frac{A(\mathbf{q}+\mathbf{G})}{|\mathbf{q}+\mathbf{G}|^2},$$

$$A(\mathbf{q}+\mathbf{G}) = \frac{1}{N_{\mathbf{k}}}\sum_{\mathbf{k}}\sum_{v,v'}|\rho_{v,\mathbf{k}}^{v',\mathbf{k}-\mathbf{q}}(\mathbf{q}+\mathbf{G})|^2$$

$$\rho_{v,\mathbf{k}}^{v',\mathbf{k}-\mathbf{q}}(\mathbf{r}) = u^*_{v',\mathbf{k}-\mathbf{q}}(\mathbf{r})\, u_{v,\mathbf{k}}(\mathbf{r})$$

$$\psi_{v,\mathbf{k}}(\mathbf{r}) = \frac{1}{\sqrt{N_{\mathbf{k}}}}e^{i\mathbf{k}\cdot\mathbf{r}}u_{v,\mathbf{k}}(\mathbf{r})$$

From real to reciprocal space

$$E_{\mathrm{x}}^{\mathrm{Fock}} = -\frac{1}{2}\sum_{\mathbf{k}}\sum_{\mathbf{k}'}\sum_{v}\sum_{v'}\int\int \frac{\psi^*_{v,\mathbf{k}}(\mathbf{r})\psi_{v',\mathbf{k}'}(\mathbf{r})\psi^*_{v',\mathbf{k}'}(\mathbf{r}')\psi_{v,\mathbf{k}}(\mathbf{r}')}{|\mathbf{r}-\mathbf{r}'|}\,d\mathbf{r}\,d\mathbf{r}'$$

$$E_{\mathrm{x}}^{\mathrm{Fock}} = -\frac{2\pi}{\Omega}\frac{1}{N_{\mathbf{q}}}\sum_{\mathbf{q}}\sum_{\mathbf{G}}\frac{A(\mathbf{q}+\mathbf{G})}{|\mathbf{q}+\mathbf{G}|^2},$$

$$A(\mathbf{q}+\mathbf{G}) = \frac{1}{N_{\mathbf{k}}}\sum_{\mathbf{k}}\sum_{v,v'}|\rho_{v,\mathbf{k}}^{v',\mathbf{k}-\mathbf{q}}(\mathbf{q}+\mathbf{G})|^2$$

singularity when
$\mathbf{q}+\mathbf{G}=0$

$$\rho_{v,\mathbf{k}}^{v',\mathbf{k}-\mathbf{q}}(\mathbf{r}) = u^*_{v',\mathbf{k}-\mathbf{q}}(\mathbf{r})\,u_{v,\mathbf{k}}(\mathbf{r})$$

$$\psi_{v,\mathbf{k}}(\mathbf{r}) = \frac{1}{\sqrt{N_{\mathbf{k}}}}e^{i\mathbf{k}\cdot\mathbf{r}}u_{v,\mathbf{k}}(\mathbf{r})$$

Gygi-Baldereschi method to treat the q+G=0 singulatiry

$$E_{\mathbf{x}}^{\mathrm{Fock}} \quad = \quad -\frac{2\pi}{\Omega}\frac{1}{N_{\mathbf{q}}}\sum_{\mathbf{q}}\sum_{\mathbf{G}}\frac{A(\mathbf{q}+\mathbf{G})}{|\mathbf{q}+\mathbf{G}|^2}$$

F. Gygi and A. Baldereschi, PRB 34, 4405 (1986).

H.-V. Nguyen and S. de Gironcoli, PRB 79, 205114 (2009).

Gygi-Baldereschi method to treat the q+G=0 singulatiry

$$
\begin{aligned}
E_{\mathbf{x}}^{\mathrm{Fock}} &= -\frac{2\pi}{\Omega}\frac{1}{N_{\mathbf{q}}}\sum_{\mathbf{q}}\sum_{\mathbf{G}}\frac{A(\mathbf{q}+\mathbf{G})}{|\mathbf{q}+\mathbf{G}|^2} \\
&= -\frac{2\pi}{\Omega}\left\{\frac{1}{N_{\mathbf{q}}}\sum_{\mathbf{q},\mathbf{G}}\frac{A(\mathbf{q}+\mathbf{G})-A(0)e^{-\alpha|\mathbf{q}+\mathbf{G}|^2}}{|\mathbf{q}+\mathbf{G}|^2}+\frac{1}{N_{\mathbf{q}}}\sum_{\mathbf{q},\mathbf{G}}\frac{e^{-\alpha|\mathbf{q}+\mathbf{G}|^2}}{|\mathbf{q}+\mathbf{G}|^2}A(0)\right\}
\end{aligned}
$$

We are adding and subtracting exactly the same term (in red)

F. Gygi and A. Baldereschi, PRB 34, 4405 (1986).

H.-V. Nguyen and S. de Gironcoli, PRB 79, 205114 (2009).

Gygi-Baldereschi method to treat the q+G=0 singulatiry

$$
\begin{aligned}
E_{\mathbf{x}}^{\text{Fock}} &= -\frac{2\pi}{\Omega}\frac{1}{N_{\mathbf{q}}}\sum_{\mathbf{q}}\sum_{\mathbf{G}}\frac{A(\mathbf{q}+\mathbf{G})}{|\mathbf{q}+\mathbf{G}|^2} \\
&= -\frac{2\pi}{\Omega}\left\{\frac{1}{N_{\mathbf{q}}}\sum_{\mathbf{q},\mathbf{G}}\frac{A(\mathbf{q}+\mathbf{G})-A(0)e^{-\alpha|\mathbf{q}+\mathbf{G}|^2}}{|\mathbf{q}+\mathbf{G}|^2}+\frac{1}{N_{\mathbf{q}}}\sum_{\mathbf{q},\mathbf{G}}\frac{e^{-\alpha|\mathbf{q}+\mathbf{G}|^2}}{|\mathbf{q}+\mathbf{G}|^2}A(0)\right\} \\
&= -\frac{2\pi}{\Omega}\left\{\frac{1}{N_{\mathbf{q}}}\left[\sum_{\mathbf{q},\mathbf{G}}{}^{\prime}\frac{A(\mathbf{q}+\mathbf{G})}{|\mathbf{q}+\mathbf{G}|^2}+\lim_{\mathbf{q}\to 0}\frac{A(\mathbf{q})-A(0)}{\mathbf{q}^2}\right]+D\times A(0)\right\}
\end{aligned}
$$

$$
D=\frac{1}{N_{\mathbf{q}}}\left[-\sum_{\mathbf{q},\mathbf{G}}{}^{\prime}\frac{e^{-\alpha|\mathbf{q}+\mathbf{G}|^2}}{|\mathbf{q}+\mathbf{G}|^2}+\alpha\right]+\frac{\Omega}{(2\pi)^3}\sqrt{\frac{\pi}{\alpha}}
$$

F. Gygi and A. Baldereschi, PRB 34, 4405 (1986).

H.-V. Nguyen and S. de Gironcoli, PRB 79, 205114 (2009).

Gygi-Baldereschi method to treat the q+G=0 singulatiry

$$
\begin{aligned}
E_{\mathbf{x}}^{\text{Fock}} &= -\frac{2\pi}{\Omega}\frac{1}{N_{\mathbf{q}}}\sum_{\mathbf{q}}\sum_{\mathbf{G}}\frac{A(\mathbf{q}+\mathbf{G})}{|\mathbf{q}+\mathbf{G}|^2} \\
&= -\frac{2\pi}{\Omega}\left\{\frac{1}{N_{\mathbf{q}}}\sum_{\mathbf{q},\mathbf{G}}\frac{A(\mathbf{q}+\mathbf{G})-A(0)e^{-\alpha|\mathbf{q}+\mathbf{G}|^2}}{|\mathbf{q}+\mathbf{G}|^2}+\frac{1}{N_{\mathbf{q}}}\sum_{\mathbf{q},\mathbf{G}}\frac{e^{-\alpha|\mathbf{q}+\mathbf{G}|^2}}{|\mathbf{q}+\mathbf{G}|^2}A(0)\right\} \\
&= -\frac{2\pi}{\Omega}\left\{\frac{1}{N_{\mathbf{q}}}\left[\sum_{\mathbf{q},\mathbf{G}}{}^{'}\frac{A(\mathbf{q}+\mathbf{G})}{|\mathbf{q}+\mathbf{G}|^2}+\lim_{\mathbf{q}\to 0}\frac{A(\mathbf{q})-A(0)}{\mathbf{q}^2}\right]+D\times A(0)\right\}
\end{aligned}
$$

no $\mathbf{q}+\mathbf{G}=0$ singularity, straightforward to compute

non-analytic limit 0/0 can be dealt with using different techniques (e.g. extrapolation)

computed analytically

F. Gygi and A. Baldereschi, PRB 34, 4405 (1986).

H.-V. Nguyen and S. de Gironcoli, PRB 79, 205114 (2009).

meta-GGA functionals

Main idea

$$E_{\mathrm{xc}}[n_\uparrow, n_\downarrow] = \int d^3r\, n(\mathbf{r})\, \varepsilon_{\mathrm{xc}}\Big(n_\uparrow(\mathbf{r}), n_\downarrow(\mathbf{r}), \nabla n_\uparrow(\mathbf{r}), \nabla n_\downarrow(\mathbf{r}), \nabla^2 n_\uparrow(\mathbf{r}), \nabla^2 n_\downarrow(\mathbf{r}), \tau_\uparrow(\mathbf{r}), \tau_\downarrow(\mathbf{r})\Big)$$

$$n(\mathbf{r}) = \sum_\sigma n_\sigma(\mathbf{r})$$ total charge density

$$n_\sigma(\mathbf{r}) = \sum_{v,\mathbf{k}} |\psi^\sigma_{v,\mathbf{k}}(\mathbf{r})|^2$$ spin-charge density

$$\sigma = \{\uparrow, \downarrow\}$$

$$\tau_\sigma(\mathbf{r}) = \frac{1}{2}\sum_{v,\mathbf{k}} |\nabla\psi^\sigma_{v,\mathbf{k}}(\mathbf{r})|^2$$ kinetic energy density

Different meta-GGA functionals

BR89

r^{2}SCAN

MVS

TPSS

SCAN

rSCAN

MGGA_MS2

TASK

revTPSS

HLE17

TM

SCAN-L

SCAN, rSCAN, r²SCAN

$$E_{\mathrm{xc}}[n_\uparrow, n_\downarrow] = \int d^3r\, n(\mathbf{r})\, \varepsilon_{\mathrm{xc}}\Big(n_\uparrow(\mathbf{r}), n_\downarrow(\mathbf{r}), \nabla n_\uparrow(\mathbf{r}), \nabla n_\downarrow(\mathbf{r}), \xcancel{\nabla^2 n_\uparrow}(\mathbf{r}), \xcancel{\nabla^2 n_\downarrow}(\mathbf{r}), \tau_\uparrow(\mathbf{r}), \tau_\downarrow(\mathbf{r})\Big)$$

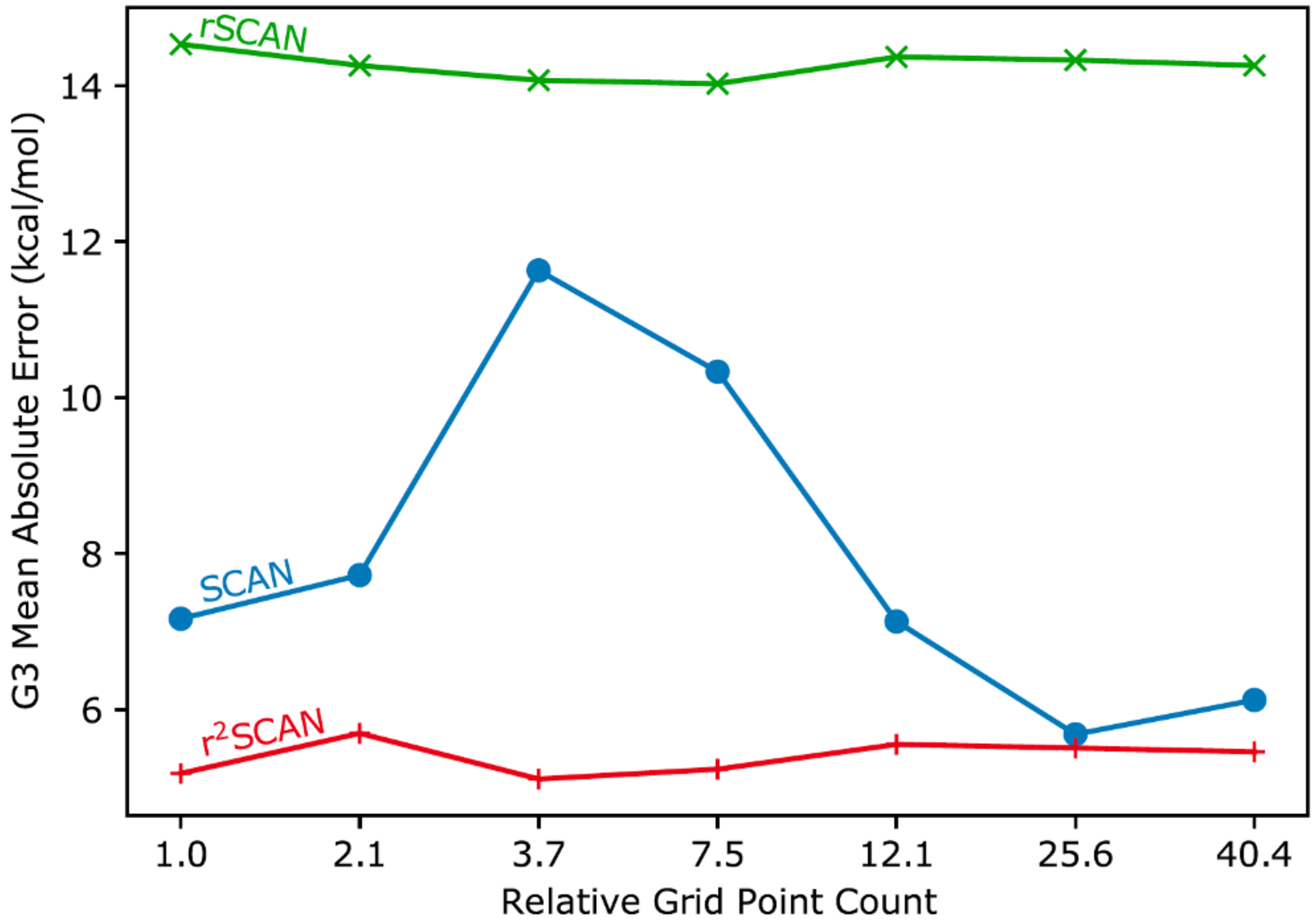

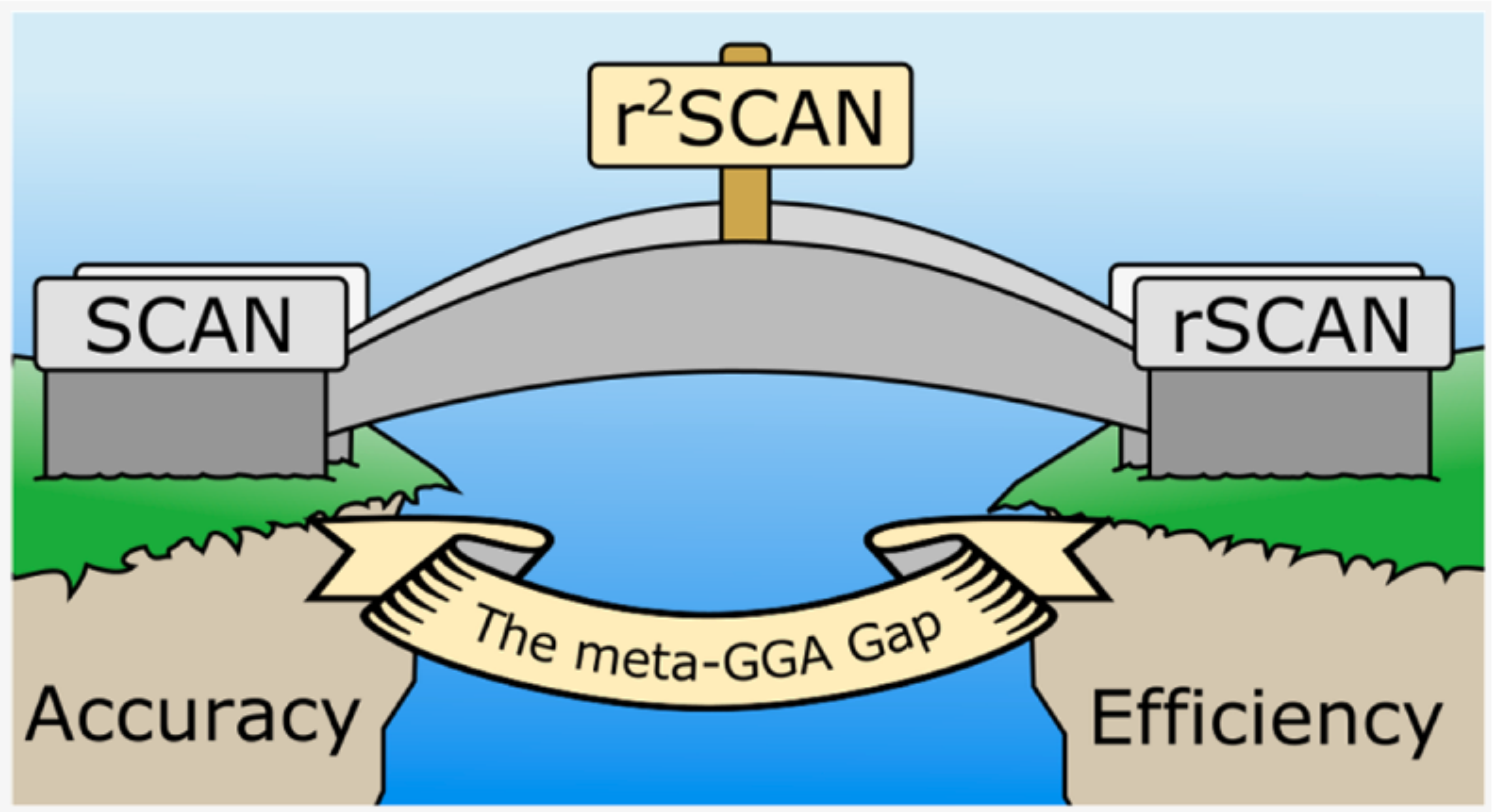

SCAN: J. Sun et al., Phys. Rev. Lett. ***115****, 036402 (2015).*

rSCAN: A. Bartok et al., J. Chem. Phys. ***150****, 161101 (2019).*

r²SCAN: J. Furness et al., J. Phys. Chem. Lett. ***11****, 8208 (2020).*

Accuracy of the SCAN meta-GGA functional

"SCAN" stands for Strongly Constrained and Appropriately Normed functional

SCAN obeys all 17 known exact constraints

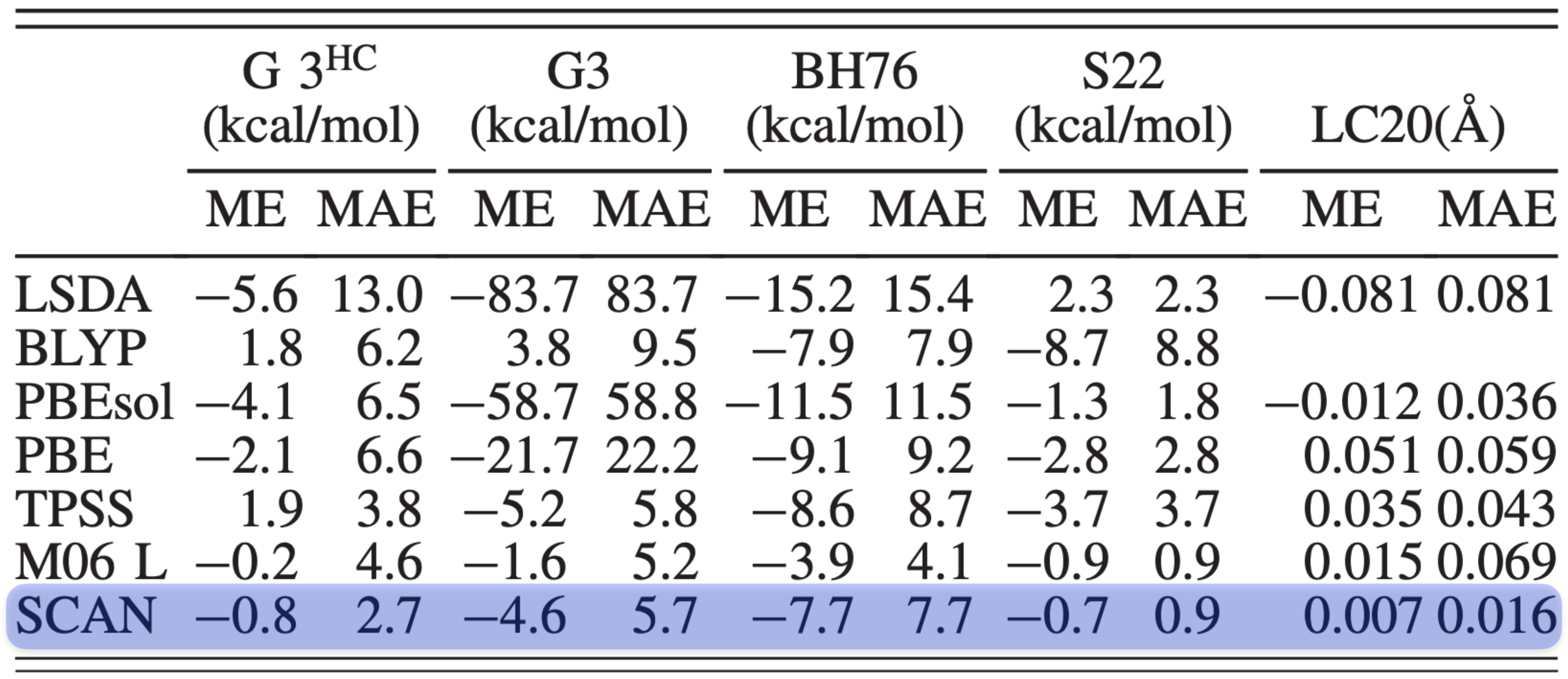

	G 3^{HC} (kcal/mol)		G3 (kcal/mol)		BH76 (kcal/mol)		S22 (kcal/mol)		LC20(Å)	
	ME	MAE	ME	MAE	ME	MAE	ME	MAE	ME	MAE
LSDA	−5.6	13.0	−83.7	83.7	−15.2	15.4	2.3	2.3	−0.081	0.081
BLYP	1.8	6.2	3.8	9.5	−7.9	7.9	−8.7	8.8		
PBEsol	−4.1	6.5	−58.7	58.8	−11.5	11.5	−1.3	1.8	−0.012	0.036
PBE	−2.1	6.6	−21.7	22.2	−9.1	9.2	−2.8	2.8	0.051	0.059
TPSS	1.9	3.8	−5.2	5.8	−8.6	8.7	−3.7	3.7	0.035	0.043
M06 L	−0.2	4.6	−1.6	5.2	−3.9	4.1	−0.9	0.9	0.015	0.069
SCAN	−0.8	2.7	−4.6	5.7	−7.7	7.7	−0.7	0.9	0.007	0.016

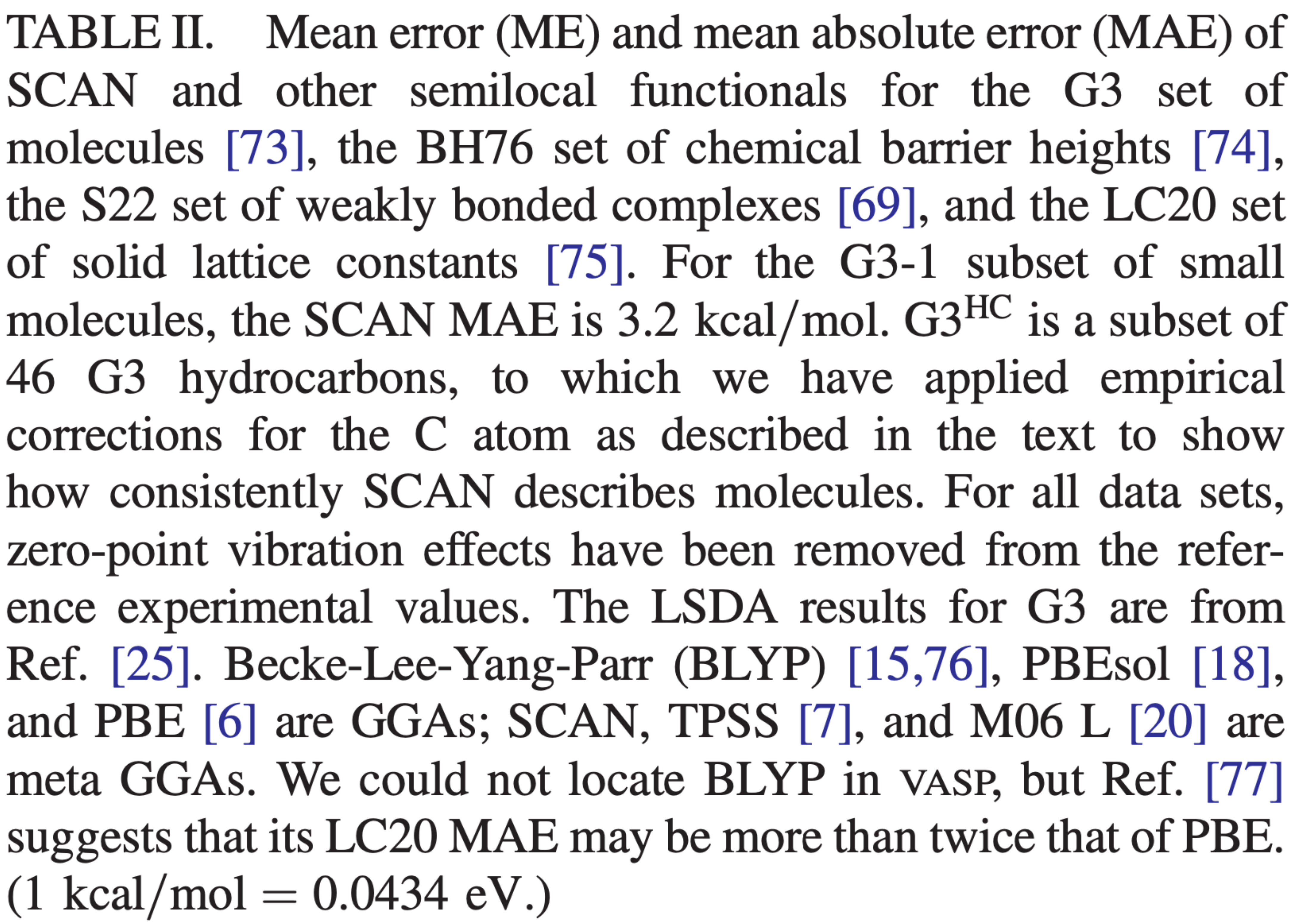

TABLE II. Mean error (ME) and mean absolute error (MAE) of SCAN and other semilocal functionals for the G3 set of molecules [73], the BH76 set of chemical barrier heights [74], the S22 set of weakly bonded complexes [69], and the LC20 set of solid lattice constants [75]. For the G3-1 subset of small molecules, the SCAN MAE is 3.2 kcal/mol. $G3^{HC}$ is a subset of 46 G3 hydrocarbons, to which we have applied empirical corrections for the C atom as described in the text to show how consistently SCAN describes molecules. For all data sets, zero-point vibration effects have been removed from the reference experimental values. The LSDA results for G3 are from Ref. [25]. Becke-Lee-Yang-Parr (BLYP) [15,76], PBEsol [18], and PBE [6] are GGAs; SCAN, TPSS [7], and M06 L [20] are meta GGAs. We could not locate BLYP in VASP, but Ref. [77] suggests that its LC20 MAE may be more than twice that of PBE. (1 kcal/mol = 0.0434 eV.)

J. Sun, A. Ruzsinszky, J. P. Perdew, PRL 115, 036402 (2015).

Regularized SCAN (rSCAN)

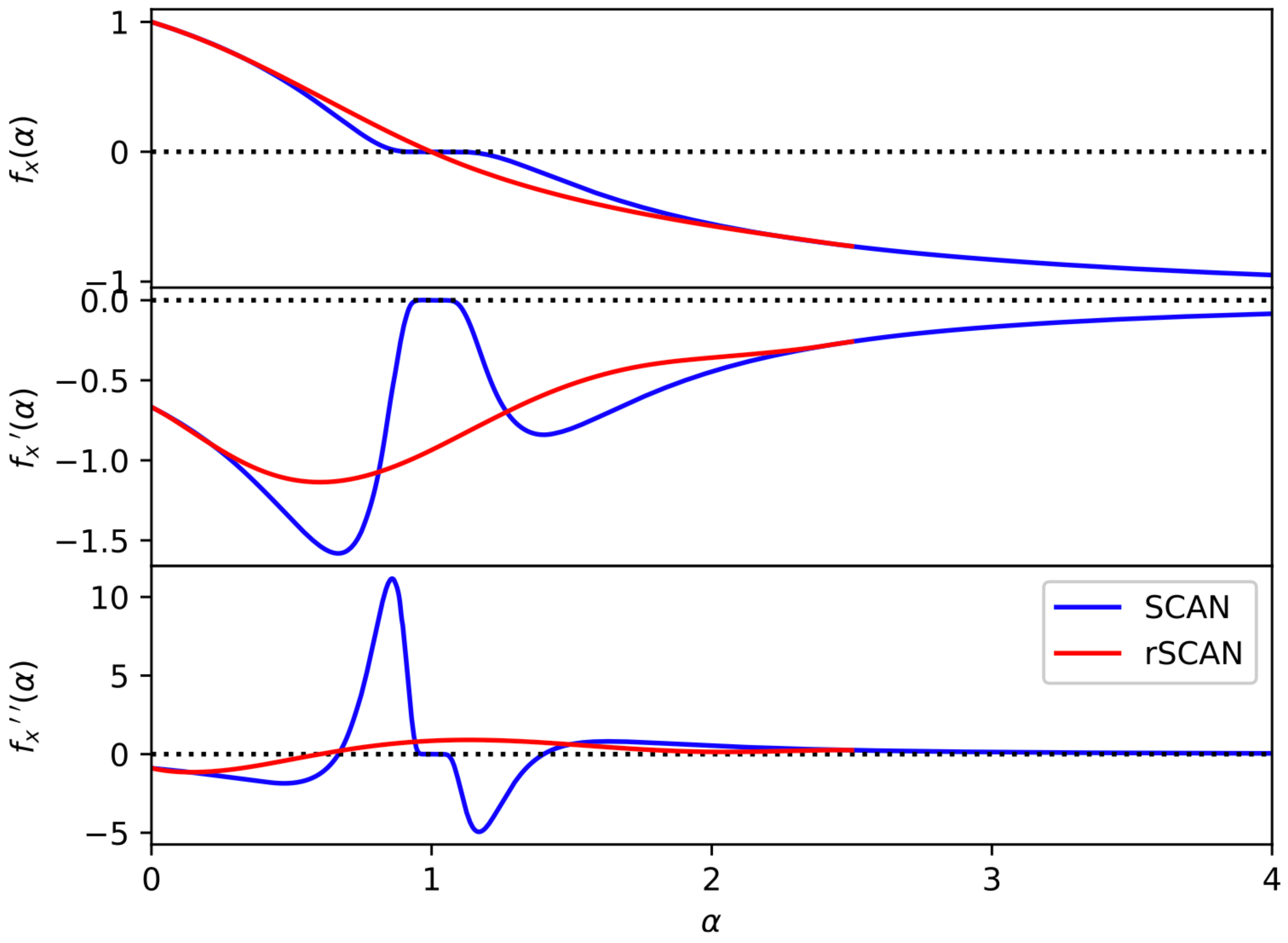

α is the isoorbital indicator function

$f_x,\ f_x',\ f_x''$ are the switching functions

rSCAN has better numerical behavior than SCAN, but it is less accurate than SCAN

A.P. Bartok and J.R. Yates, JCP 150, 161101 (2019).

SCAN vs rSCAN vs r^{2}SCAN

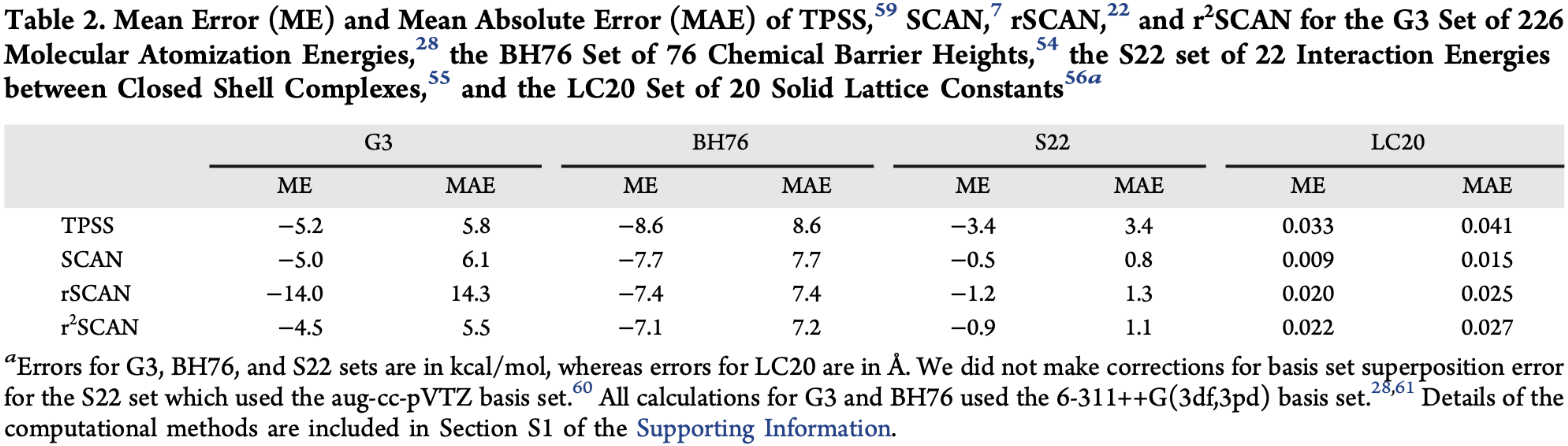

Table 2. Mean Error (ME) and Mean Absolute Error (MAE) of TPSS,[59] SCAN,[7] rSCAN,[22] and r^{2}SCAN for the G3 Set of 226 Molecular Atomization Energies,[28] the BH76 Set of 76 Chemical Barrier Heights,[54] the S22 set of 22 Interaction Energies between Closed Shell Complexes,[55] and the LC20 Set of 20 Solid Lattice Constants[56][a]

	G3		BH76		S22		LC20	
	ME	MAE	ME	MAE	ME	MAE	ME	MAE
TPSS	−5.2	5.8	−8.6	8.6	−3.4	3.4	0.033	0.041
SCAN	−5.0	6.1	−7.7	7.7	−0.5	0.8	0.009	0.015
rSCAN	−14.0	14.3	−7.4	7.4	−1.2	1.3	0.020	0.025
r^{2}SCAN	−4.5	5.5	−7.1	7.2	−0.9	1.1	0.022	0.027

[a] Errors for G3, BH76, and S22 sets are in kcal/mol, whereas errors for LC20 are in Å. We did not make corrections for basis set superposition error for the S22 set which used the aug-cc-pVTZ basis set.[60] All calculations for G3 and BH76 used the 6-311++G(3df,3pd) basis set.[28,61] Details of the computational methods are included in Section S1 of the Supporting Information.

J.W. Furness, A.D. Kaplan, J. Ning, J.P. Perdew, and J. Sun, JPCL 11, 8208 (2020).

Success stories of SCAN

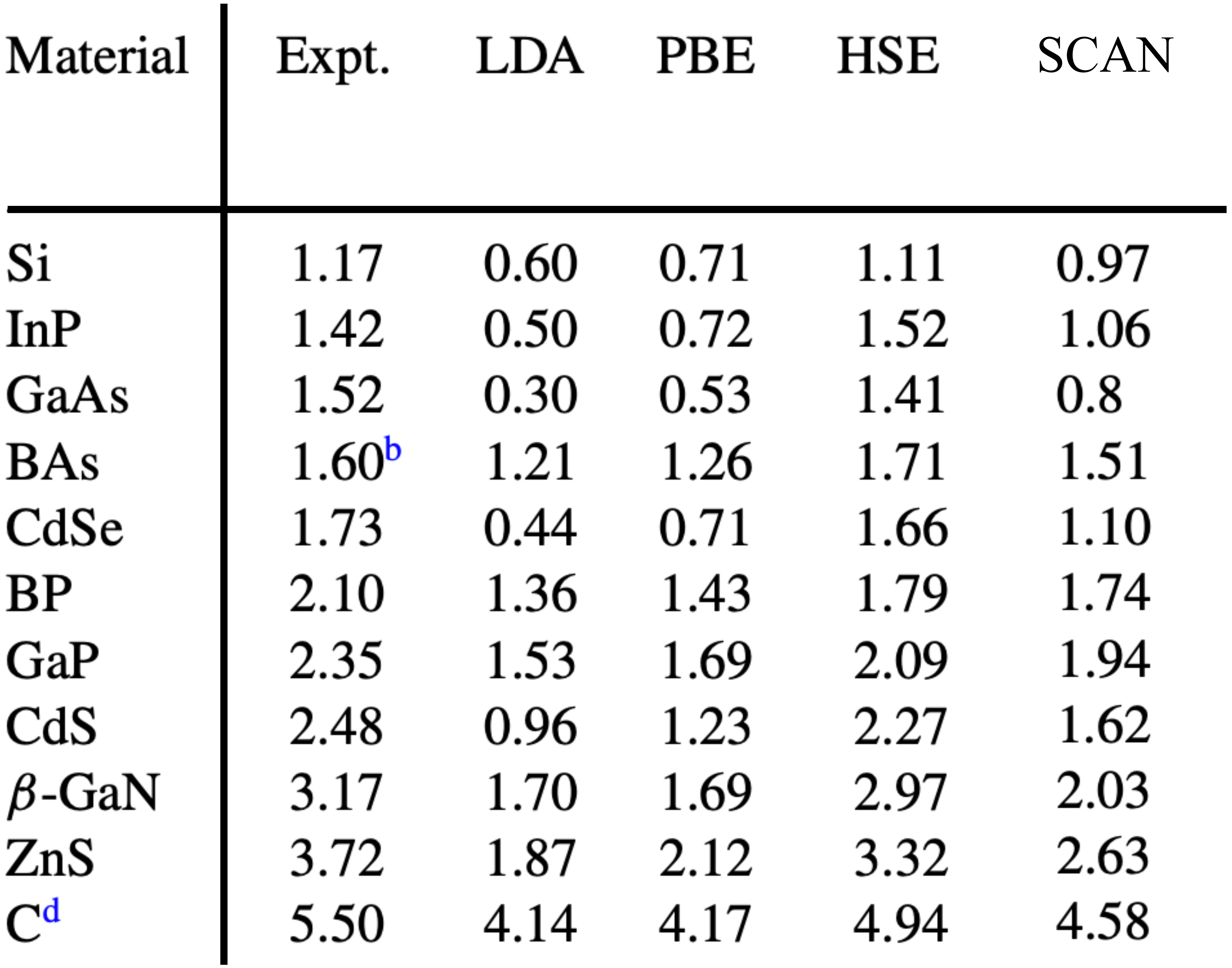

Material	Expt.	LDA	PBE	HSE	SCAN
Si	1.17	0.60	0.71	1.11	0.97
InP	1.42	0.50	0.72	1.52	1.06
GaAs	1.52	0.30	0.53	1.41	0.8
BAs	1.60[b]	1.21	1.26	1.71	1.51
CdSe	1.73	0.44	0.71	1.66	1.10
BP	2.10	1.36	1.43	1.79	1.74
GaP	2.35	1.53	1.69	2.09	1.94
CdS	2.48	0.96	1.23	2.27	1.62
β-GaN	3.17	1.70	1.69	2.97	2.03
ZnS	3.72	1.87	2.12	3.32	2.63
C[d]	5.50	4.14	4.17	4.94	4.58

SCAN provides more accurate band gaps than LDA and PBE, but less accurate than HSE

Z.-H. Yang, H. Peng, J. Sun, and J. P. Perdew, PRB 93, 205205 (2016).

Success stories of SCAN

Six polymorphs of MnO_2

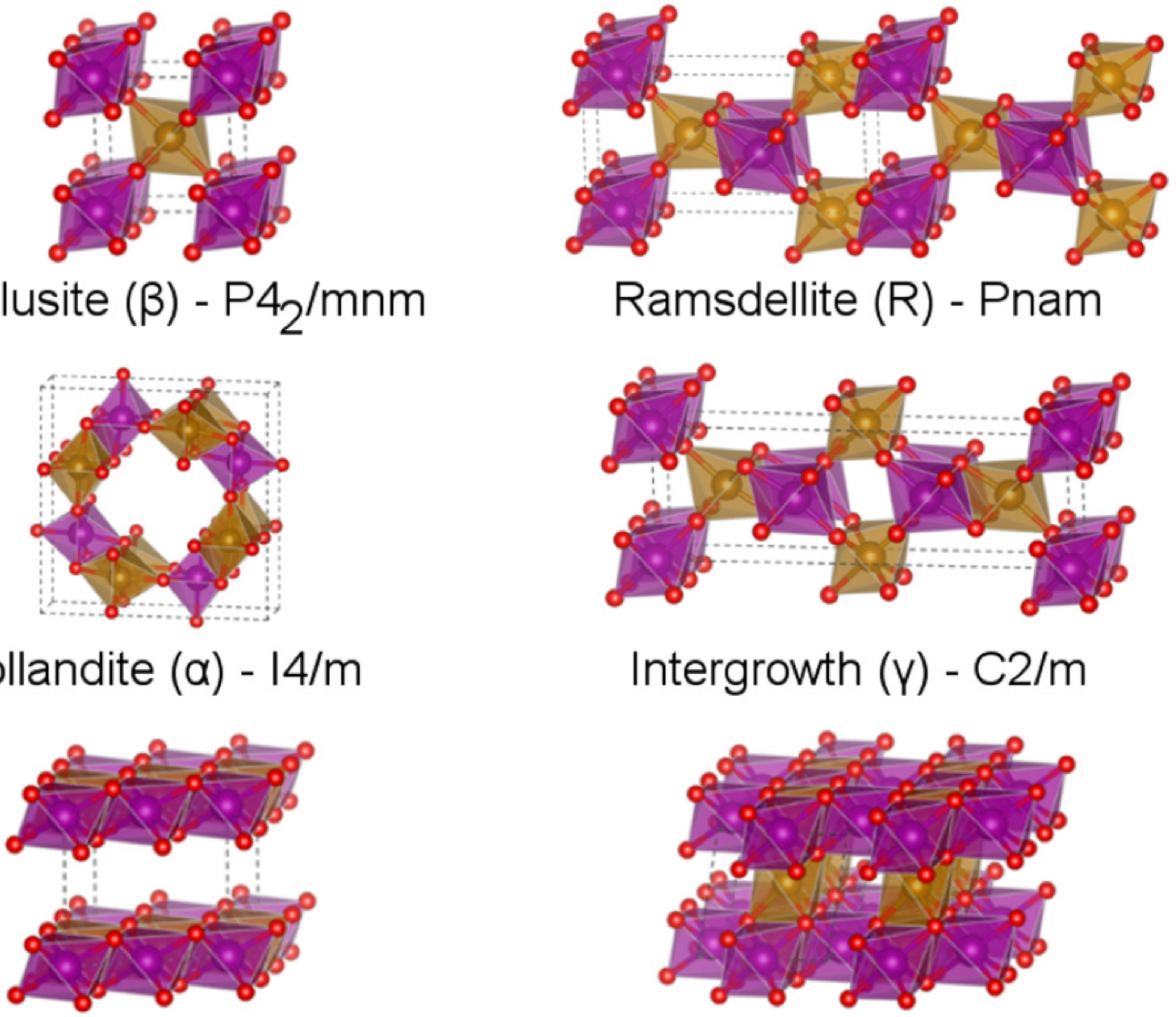

Pyrolusite (β) - $P4_2/mnm$

Ramsdellite (R) - Pnam

Hollandite (α) - I4/m

Intergrowth (γ) - C2/m

Layered (δ) - $R\bar{3}m$

Spinel (λ) - $Fd\bar{3}m$

Formation energies relative to the β phase

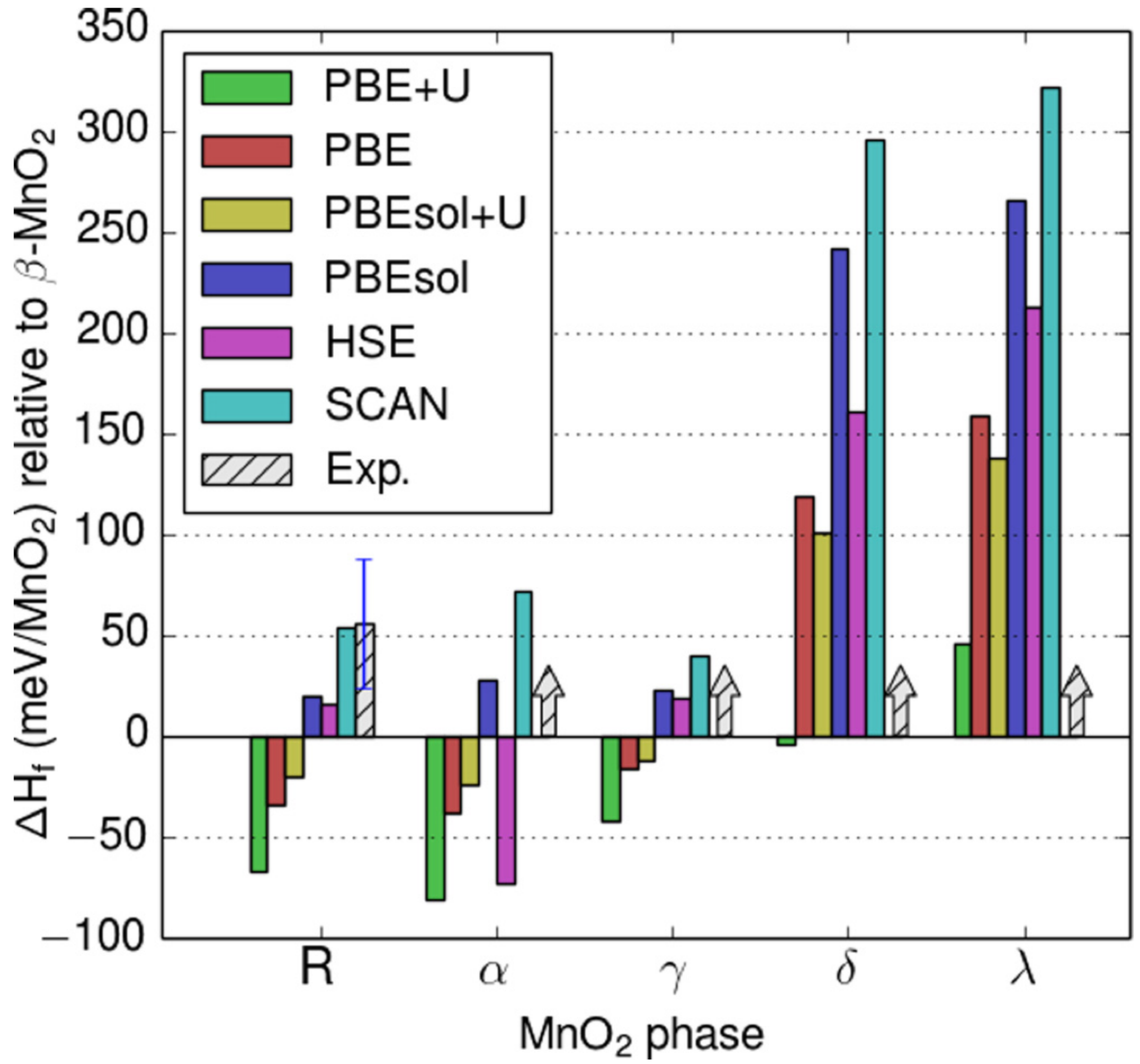

SCAN correctly predicts that the β phase is the lowest-energy phase

D. A. Kitchaev, H. Peng, Y. Liu, J. Sun, J.P. Perdew, and G. Ceder, PRB 93, 045132 (2016).

One of failures of SCAN

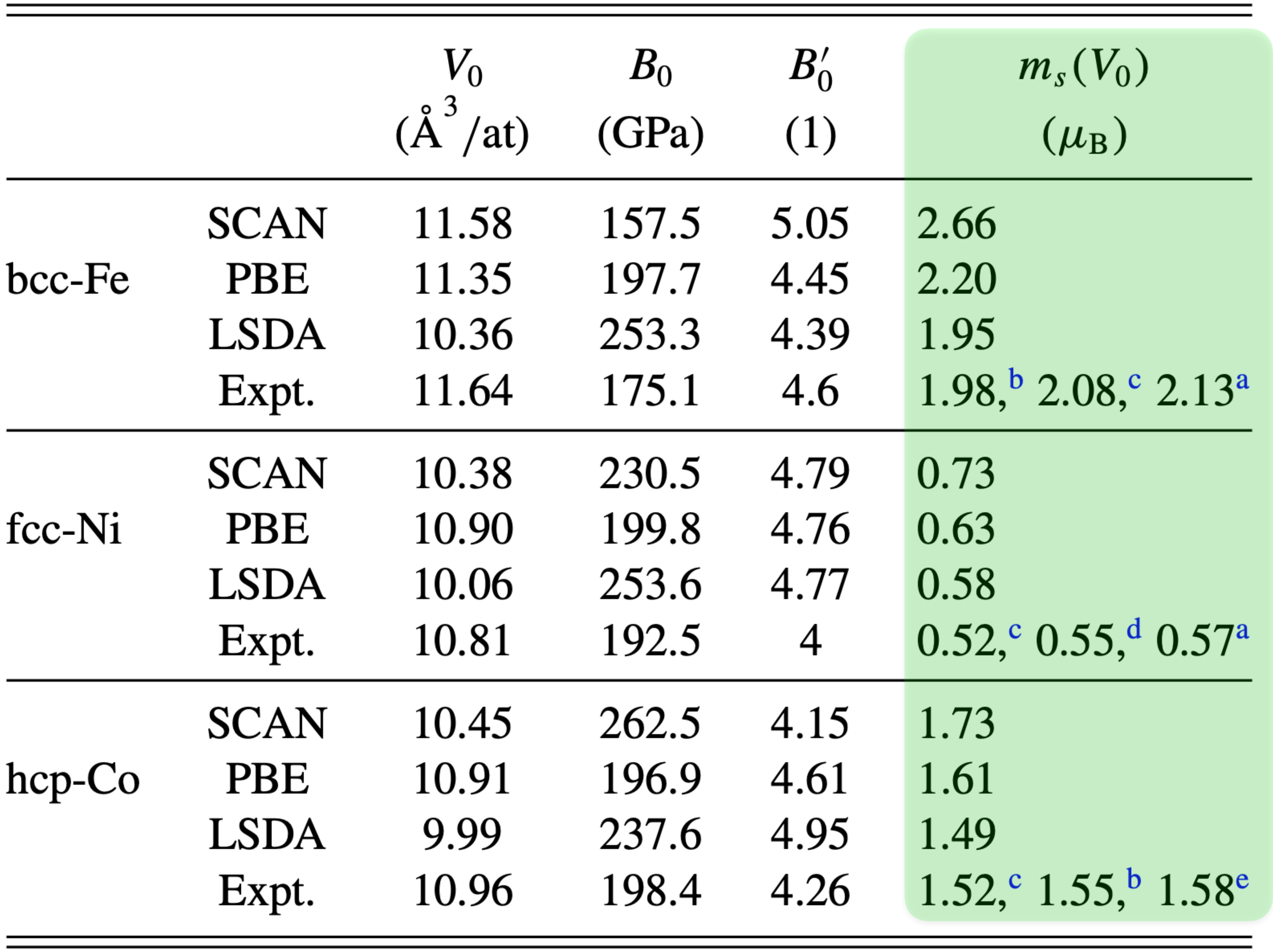

		V_0 (Å^3/at)	B_0 (GPa)	B_0' (1)	$m_s(V_0)$ (μ_B)
bcc-Fe	SCAN	11.58	157.5	5.05	2.66
	PBE	11.35	197.7	4.45	2.20
	LSDA	10.36	253.3	4.39	1.95
	Expt.	11.64	175.1	4.6	1.98,[b] 2.08,[c] 2.13[a]
fcc-Ni	SCAN	10.38	230.5	4.79	0.73
	PBE	10.90	199.8	4.76	0.63
	LSDA	10.06	253.6	4.77	0.58
	Expt.	10.81	192.5	4	0.52,[c] 0.55,[d] 0.57[a]
hcp-Co	SCAN	10.45	262.5	4.15	1.73
	PBE	10.91	196.9	4.61	1.61
	LSDA	9.99	237.6	4.95	1.49
	Expt.	10.96	198.4	4.26	1.52,[c] 1.55,[b] 1.58[e]

SCAN overestimates magnetic moments in itinerant ferromagnets

M. Ekholm, D. Gambino, H. J. M. Jönsson, F. Tasnádi, B. Alling, and I. A. Abrikosov, PRB 98, 094413 (2018).

van der Waals functionals

van der Waals (vdW) force

- vdW is a distance-dependent interaction between atoms or molecules
- vdW is weak, and it is different from ionic and covalent bonding
- vdW originate from correlations between charge fluctuations in different parts of an extended system (different fragments)
- vdW interactions are non-local
- vdW are not captured by LDA, GGA, meta-GGA (except SCAN for short-range part of vdW), DFT+U, and hybrids.

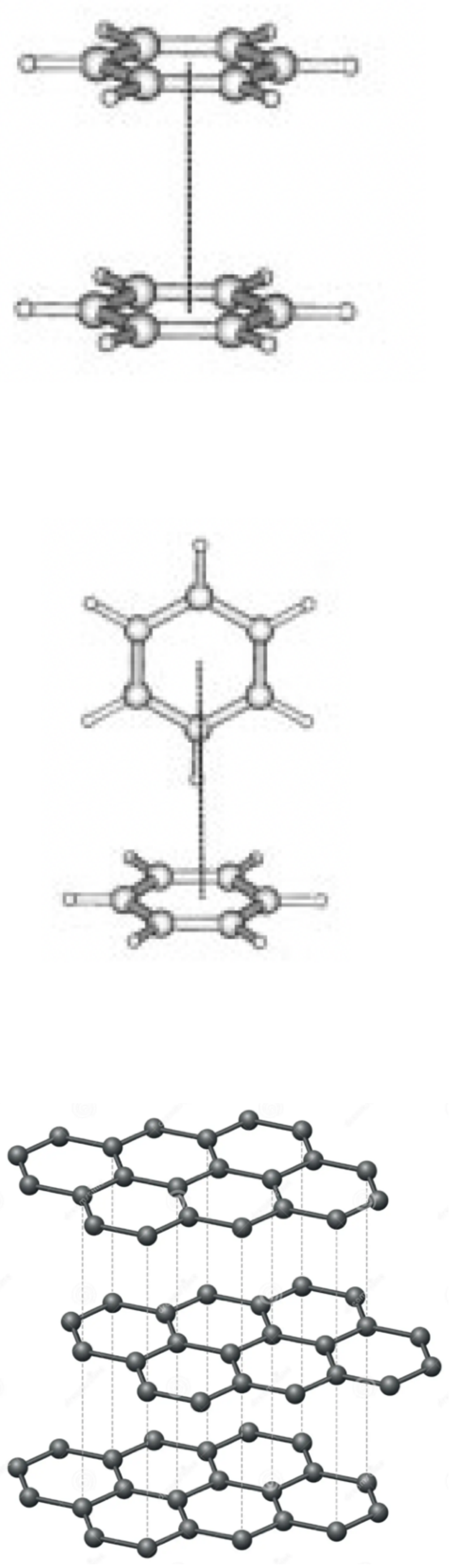

Two types of vdW functionals

vdW functionals

Empirical (or *ab initio*) corrections

$$C_6 R^{-6}$$

Fully nonlocal functionals

$$\frac{1}{2}\int\int n(\mathbf{r})\,\Phi(\mathbf{r},\mathbf{r}')\,n(\mathbf{r}')\,d\mathbf{r}\,d\mathbf{r}'$$

Two types of vdW functionals

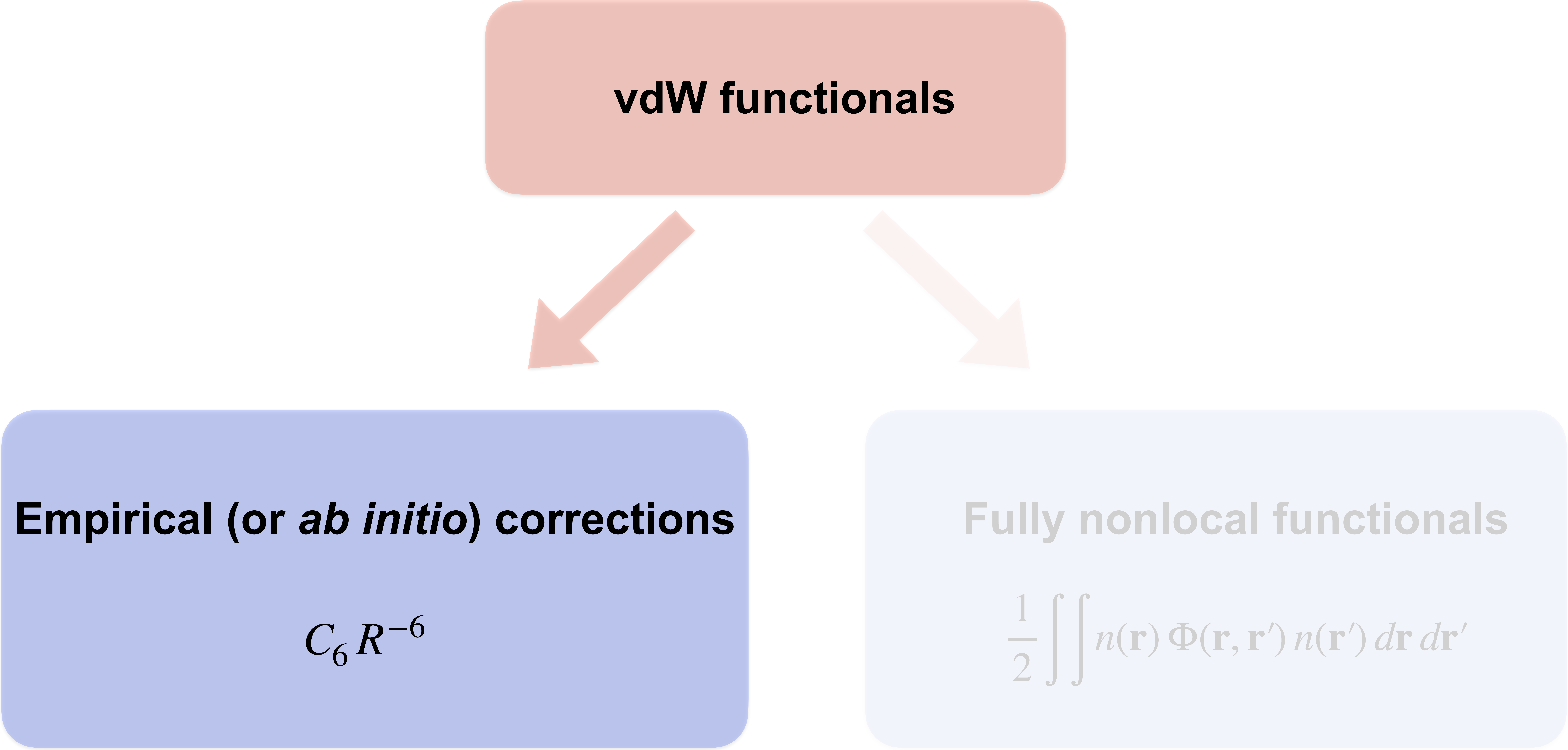

vdW functionals

Empirical (or *ab initio*) corrections

$C_6 R^{-6}$

Fully nonlocal functionals

$$\frac{1}{2}\int\int n(\mathbf{r})\,\Phi(\mathbf{r},\mathbf{r}')\,n(\mathbf{r}')\,d\mathbf{r}\,d\mathbf{r}'$$

Lennard-Jones potential

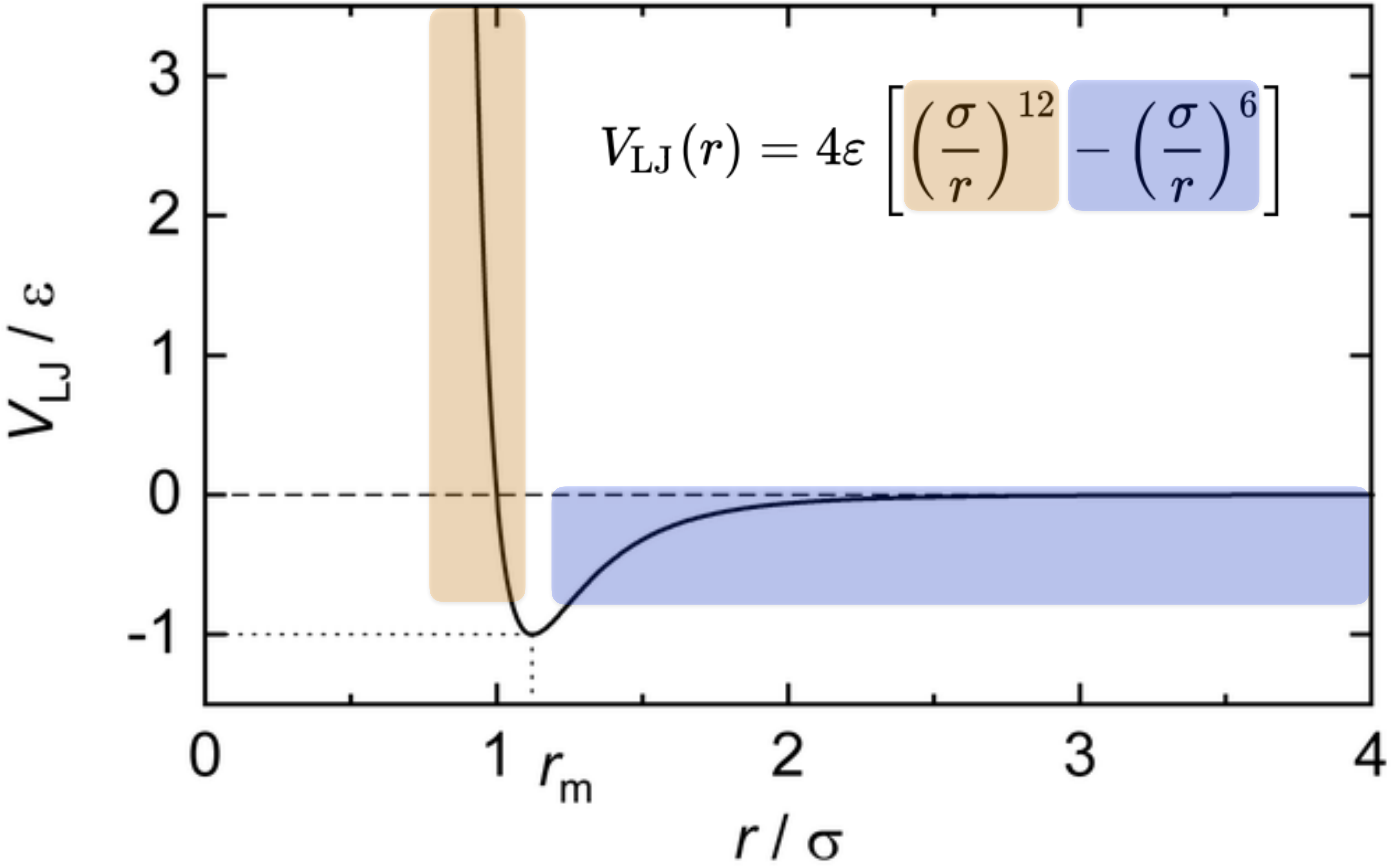

$$V_{\mathrm{LJ}}(r) = 4\varepsilon\left[\left(\frac{\sigma}{r}\right)^{12} - \left(\frac{\sigma}{r}\right)^{6}\right]$$

DFT-D functional

$$E_{\mathrm{DFT-D}} = E_{\mathrm{DFT}} + E_{\mathrm{vdW}}, \qquad E_{\mathrm{vdW}} = -s_6 \sum_{i=1}^{N_{\mathrm{at}}-1} \sum_{j=i+1}^{N_{\mathrm{at}}} \frac{C_6^{ij}}{R_{ij}^6} f_{\mathrm{dmp}}(R_{ij}), \qquad f_{\mathrm{dmp}}(R_{ij}) = \frac{1}{1+e^{-d(R_{ij}/R_r-1)}}$$

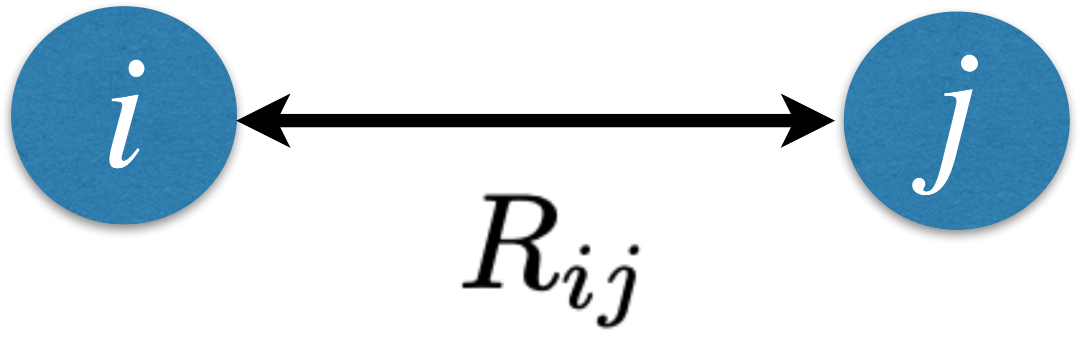

- Dispersion coefficients C_6^{ij} are determined empirically
- f_{dmp} is a damping function to avoid near-singularities for small R_{ij}

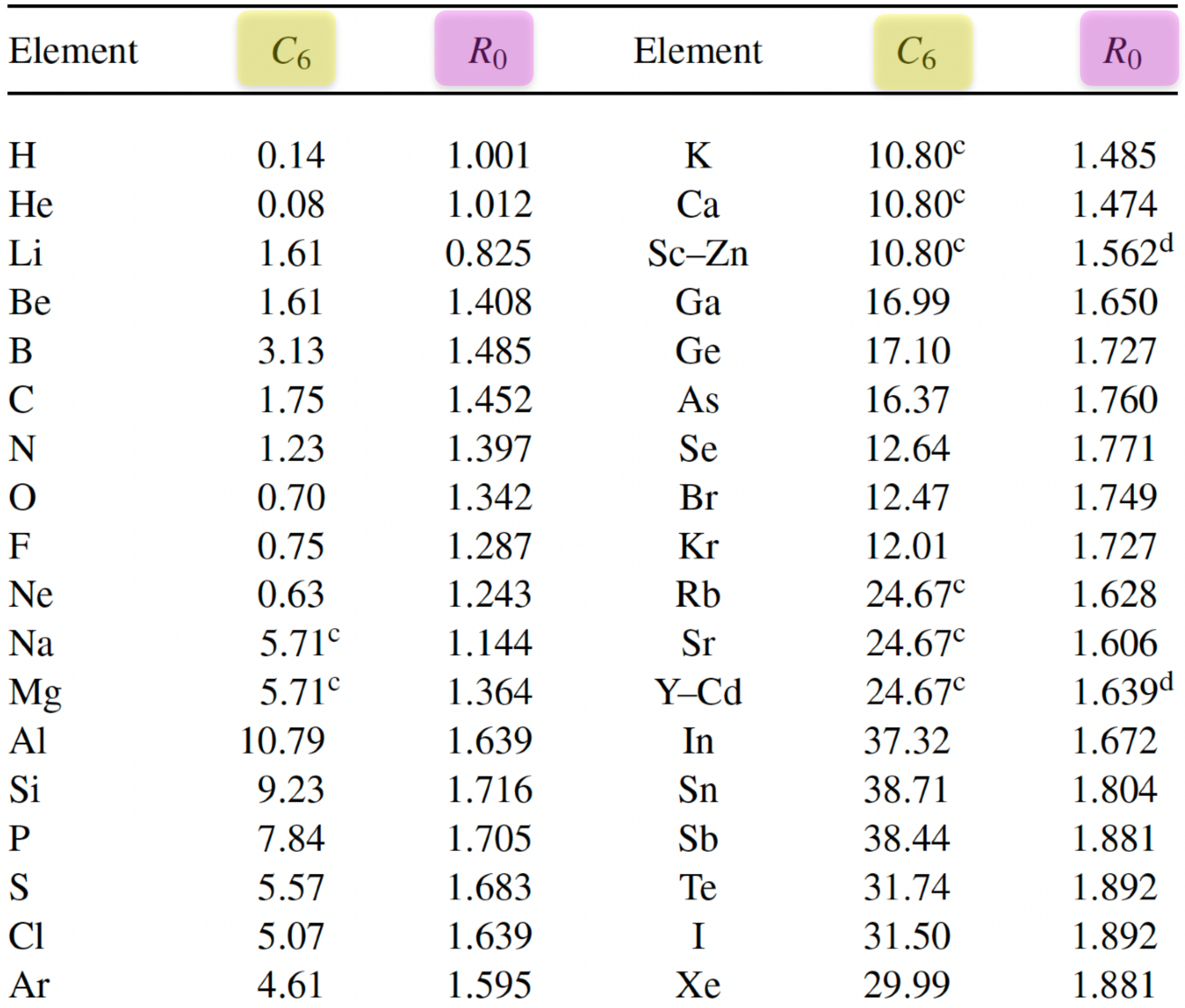

Element	C_6	R_0	Element	C_6	R_0
H	0.14	1.001	K	10.80[c]	1.485
He	0.08	1.012	Ca	10.80[c]	1.474
Li	1.61	0.825	Sc–Zn	10.80[c]	1.562[d]
Be	1.61	1.408	Ga	16.99	1.650
B	3.13	1.485	Ge	17.10	1.727
C	1.75	1.452	As	16.37	1.760
N	1.23	1.397	Se	12.64	1.771
O	0.70	1.342	Br	12.47	1.749
F	0.75	1.287	Kr	12.01	1.727
Ne	0.63	1.243	Rb	24.67[c]	1.628
Na	5.71[c]	1.144	Sr	24.67[c]	1.606
Mg	5.71[c]	1.364	Y–Cd	24.67[c]	1.639[d]
Al	10.79	1.639	In	37.32	1.672
Si	9.23	1.716	Sn	38.71	1.804
P	7.84	1.705	Sb	38.44	1.881
S	5.57	1.683	Te	31.74	1.892
Cl	5.07	1.639	I	31.50	1.892
Ar	4.61	1.595	Xe	29.99	1.881

S. Grimme, J. Comput. Chem. 27, 1787 (2006).

V. Barone et al., J. Comput. Chem. 30, 934 (2008).

DFT-D3 functional

$$E_{\text{DFT-D3}} = E_{\text{KS-DFT}} - E_{\text{vdW}}$$

$$E_{\text{vdW}} = E^{(2)} + E^{(3)}$$

S. Grimme, J. Antony, S. Ehrlich, H. Krieg, JCP 132, 154104 (2010).

DFT-D3 functional

$$E_{\text{DFT-D3}} = E_{\text{KS-DFT}} - E_{\text{vdW}}$$

$$E_{\text{vdW}} = E^{(2)} + E^{(3)}$$

Two-body term:

$$E^{(2)} = \sum_{AB} \sum_{n=6,8,10,\ldots} s_n \frac{C_n^{AB}}{r_{AB}^n} f_{d,n}(r_{AB})$$

$$f_{d,n}(r_{AB}) = \frac{1}{1 + 6(r_{AB}/(s_{r,n}R_0^{AB}))^{-\alpha_n}}$$

S. Grimme, J. Antony, S. Ehrlich, H. Krieg, JCP 132, 154104 (2010).

DFT-D3 functional

$$E_{\mathrm{DFT\text{-}D3}} = E_{\mathrm{KS\text{-}DFT}} - \boxed{E_{\mathrm{vdW}}}$$

$$\boxed{E_{\mathrm{vdW}}} = \boxed{E^{(2)}} + \boxed{E^{(3)}}$$

Two-body term:

$$\boxed{E^{(2)}} = \sum_{AB} \sum_{n=6,8,10,\ldots} s_n \frac{C_n^{AB}}{r_{AB}^n} f_{d,n}(r_{AB})$$

$$f_{d,n}(r_{AB}) = \frac{1}{1 + 6(r_{AB}/(s_{r,n} R_0^{AB}))^{-\alpha_n}}$$

Three-body term:

$$\boxed{E^{(3)}} = \sum_{ABC} f_{d,(3)}(\bar{r}_{ABC}) E^{ABC}$$

$$E^{ABC} = \frac{C_9^{ABC}(3 \cos \theta_a \cos \theta_b \cos \theta_c + 1)}{(r_{AB} r_{BC} r_{CA})^3}$$

S. Grimme, J. Antony, S. Ehrlich, H. Krieg, JCP 132, 154104 (2010).

Tkatchenko-Scheffler (TS) functional

$$E_{\mathrm{vdW}} = -\frac{1}{2}\sum_{A,B} f_{\mathrm{damp}}(R_{AB}, R_A^0, R_B^0)\, C_{6AB} R_{AB}^{-6}$$

Dispersion coefficients are computed from first principles using the electronic charge density

A. Tkatchenko and M. Scheffler, PRL 102, 073005 (2009).

Tkatchenko-Scheffler (TS) functional

$$E_{\mathrm{vdW}} = -\frac{1}{2}\sum_{A,B} f_{\mathrm{damp}}(R_{AB}, R_A^0, R_B^0)\,C_{6AB}\,R_{AB}^{-6}$$

Dispersion coefficients are computed from first principles using the electronic charge density

$$C_{6AB} = \frac{2C_{6AA}C_{6BB}}{\left[\frac{\alpha_B^0}{\alpha_A^0}C_{6AA} + \frac{\alpha_A^0}{\alpha_B^0}C_{6BB}\right]}$$

$$C_{6AA}^{\mathrm{eff}} = \frac{\eta_A^{\mathrm{eff}}}{\eta_A^{\mathrm{free}}}\left(\frac{\kappa_A^{\mathrm{free}}}{\kappa_A^{\mathrm{eff}}}\right)^2\left(\frac{V_A^{\mathrm{eff}}}{V_A^{\mathrm{free}}}\right)^2 C_{6AA}^{\mathrm{free}}$$

A. Tkatchenko and M. Scheffler, PRL 102, 073005 (2009).

Tkatchenko-Scheffler (TS) functional

$$E_{\mathrm{vdW}} = -\frac{1}{2}\sum_{A,B} f_{\mathrm{damp}}(R_{AB}, R_A^0, R_B^0)\, C_{6AB} R_{AB}^{-6}$$

Dispersion coefficients are computed from first principles using the electronic charge density

$$C_{6AB} = \frac{2C_{6AA}C_{6BB}}{\left[\frac{\alpha_B^0}{\alpha_A^0}C_{6AA} + \frac{\alpha_A^0}{\alpha_B^0}C_{6BB}\right]}$$

$$C_{6AA}^{\mathrm{eff}} = \frac{\eta_A^{\mathrm{eff}}}{\eta_A^{\mathrm{free}}}\left(\frac{\kappa_A^{\mathrm{free}}}{\kappa_A^{\mathrm{eff}}}\right)^2\left(\frac{V_A^{\mathrm{eff}}}{V_A^{\mathrm{free}}}\right)^2 C_{6AA}^{\mathrm{free}}$$

Hirshfeld partitioning of the electronic charge density:

$$\frac{\kappa_A^{\mathrm{eff}}}{\kappa_A^{\mathrm{free}}}\frac{\alpha_A^{\mathrm{eff}}}{\alpha_A^{\mathrm{free}}} = \frac{V_A^{\mathrm{eff}}}{V_A^{\mathrm{free}}} = \left(\frac{\int r^3 w_A(\mathbf{r})n(\mathbf{r})d^3\mathbf{r}}{\int r^3 n_A^{\mathrm{free}}(\mathbf{r})d^3\mathbf{r}}\right),$$

$$w_A(\mathbf{r}) = \frac{n_A^{\mathrm{free}}(\mathbf{r})}{\sum_B n_B^{\mathrm{free}}(\mathbf{r})},$$

A. Tkatchenko and M. Scheffler, PRL 102, 073005 (2009).

Two types of vdW functionals

vdW functionals

Empirical (or *ab initio*) corrections

$$C_6 R^{-6}$$

Fully nonlocal functionals

$$\frac{1}{2}\int\int n(\mathbf{r})\,\Phi(\mathbf{r},\mathbf{r}')\,n(\mathbf{r}')\,d\mathbf{r}\,d\mathbf{r}'$$

Fully nonlocal vdW functionals

Nonlocal correlation energy: $E_c[n] = E_c^0[n] + \boxed{E_c^{nl}[n]}$

$E_c^{nl}[n]$ is defined to include the longest ranged or most nonlocal terms that give the vdW interaction and to approach zero in the limit of a slowly varying density. The term $E_c^0[n]$ is also nonlocal, but approaches the LDA in this limit.

$$\boxed{E_c^{nl}} = \frac{1}{2}\int\int n(\mathbf{r}) \underbrace{\Phi\Big(n(\mathbf{r}), n(\mathbf{r}'), |\nabla n(\mathbf{r})|, |\nabla n(\mathbf{r}')|, |\mathbf{r}-\mathbf{r}'|\Big)}_{\text{nonlocal kernel}} n(\mathbf{r}')\, d\mathbf{r}\, d\mathbf{r}'$$

There are different numerical methods and approximations how to compute $E_c^{nl}[n]$

Fully nonlocal vdW functionals

vdW-DF	M. Dion et al., PRL 92, 246401 (2004).
vdW-DF2	K. Lee et al., PRB 82, 081101(R) (2010).
VV10	O.A. Vydrov and T. Van Voorhis, JCP 133, 244103 (2010).
rVV10	R. Sabatini, T. Gorni, S. de Gironcoli, PRB 87, 041108(R) (2013).

Examples

Binding energy curves for the Ar dimer

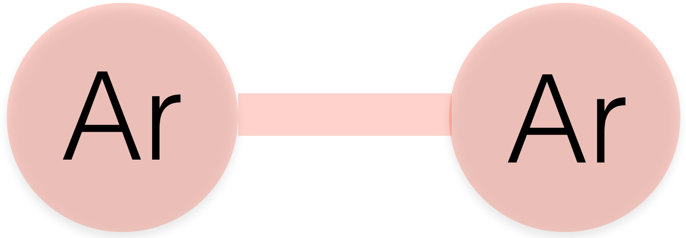

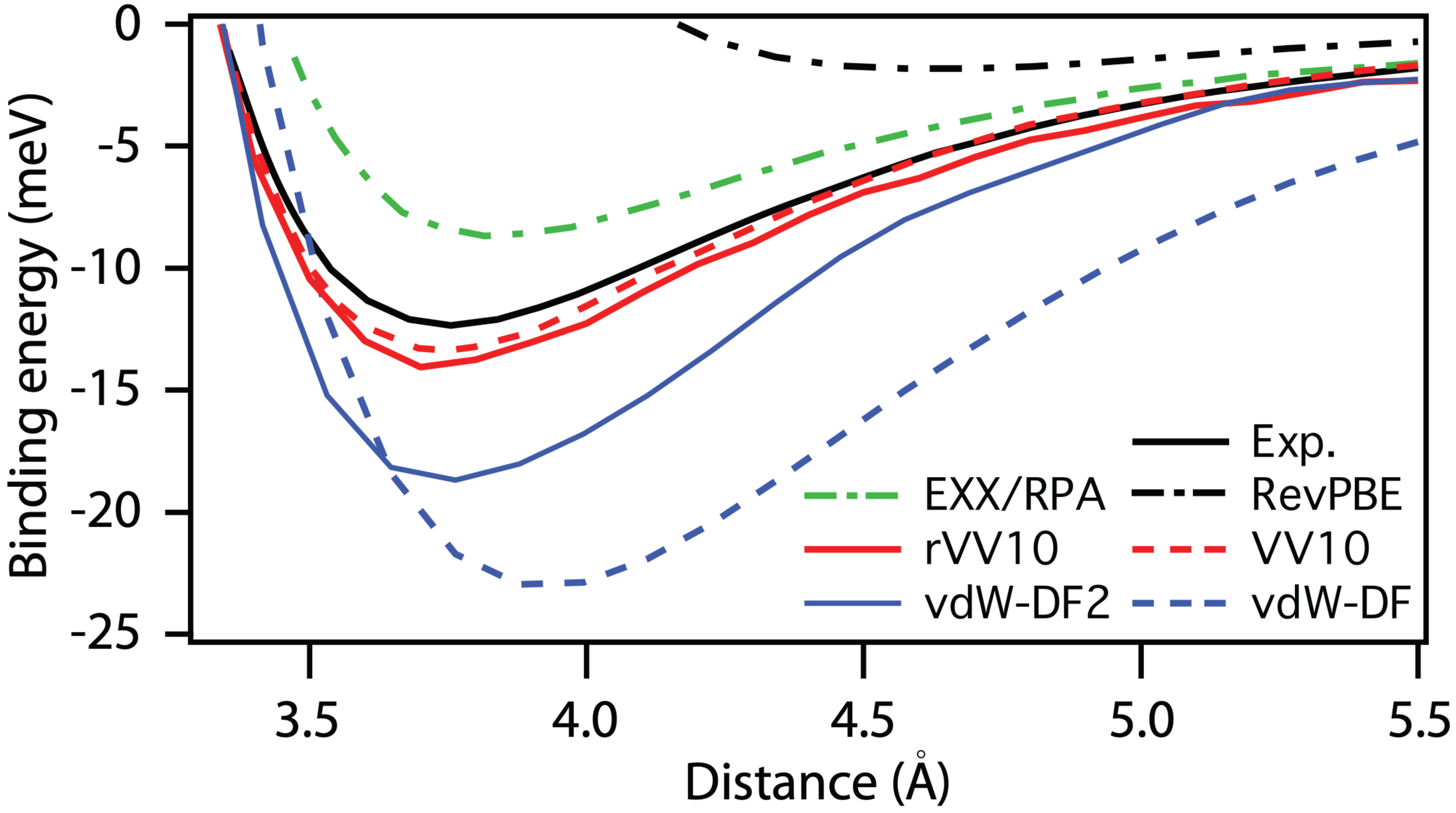

R. Sabatini, T. Gorni, S. De Gironcoli, PRB 87, 041108(R) (2013).

Examples

X = Ar, H_2, CO, H_2O

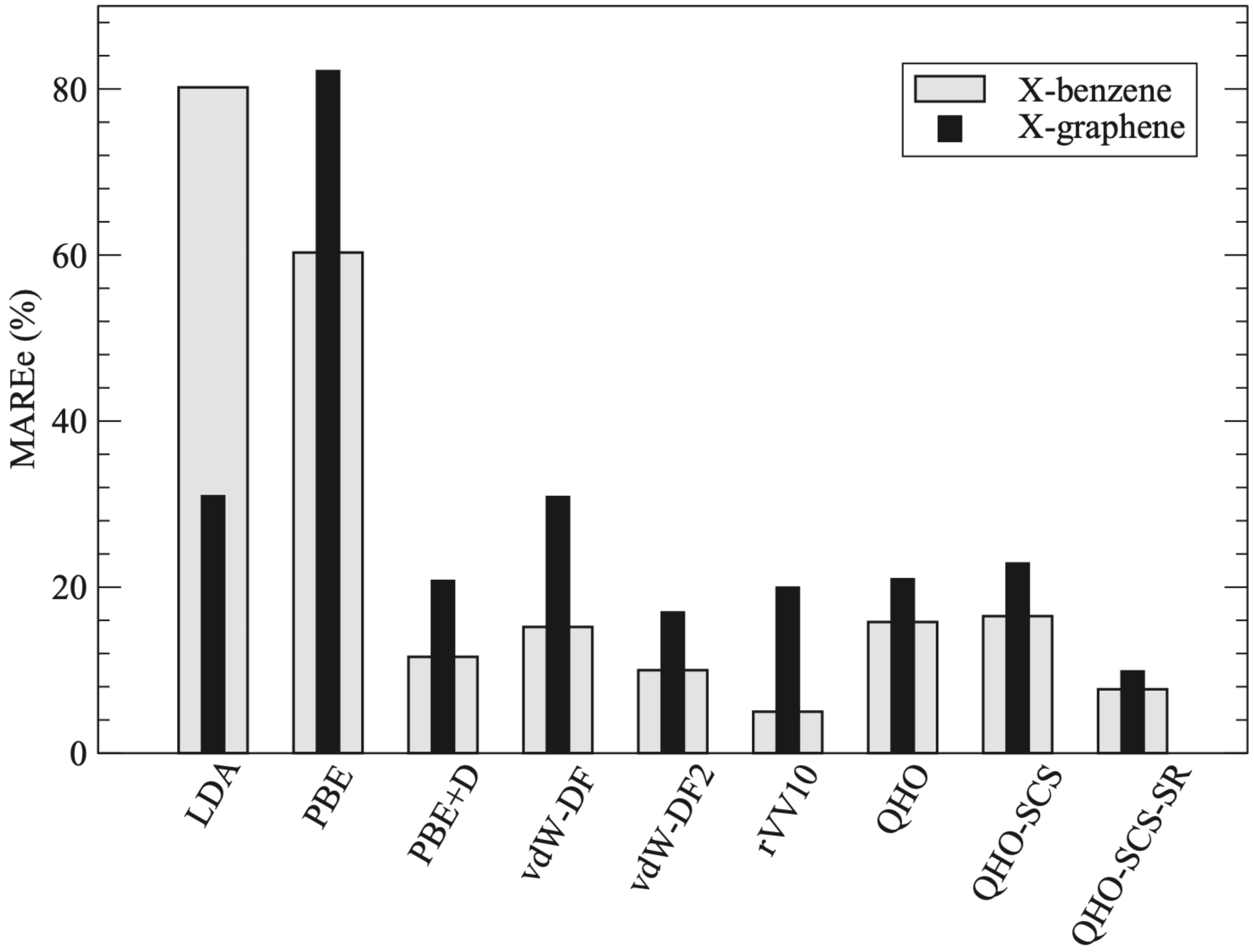

CO molecule

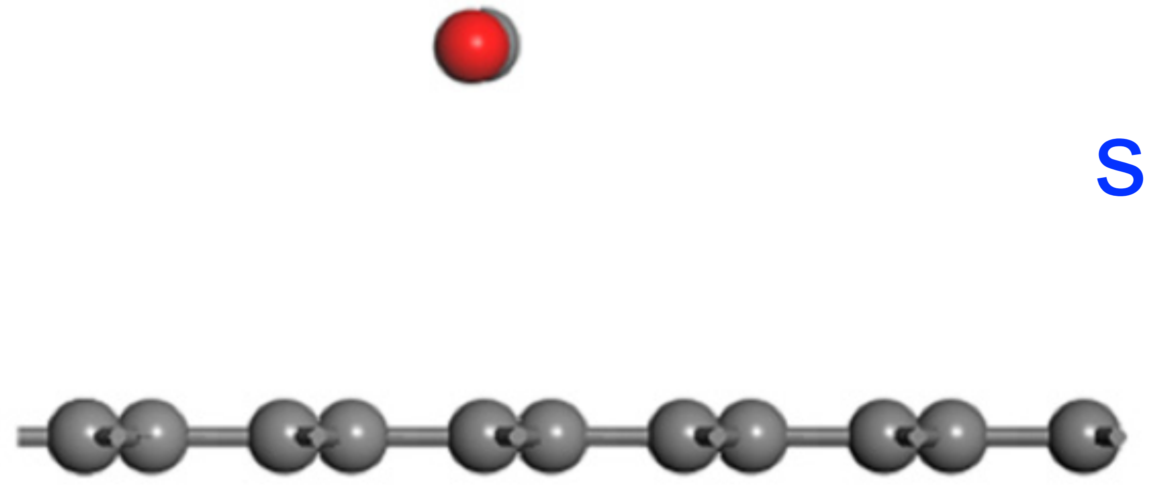

side view

graphene

top view

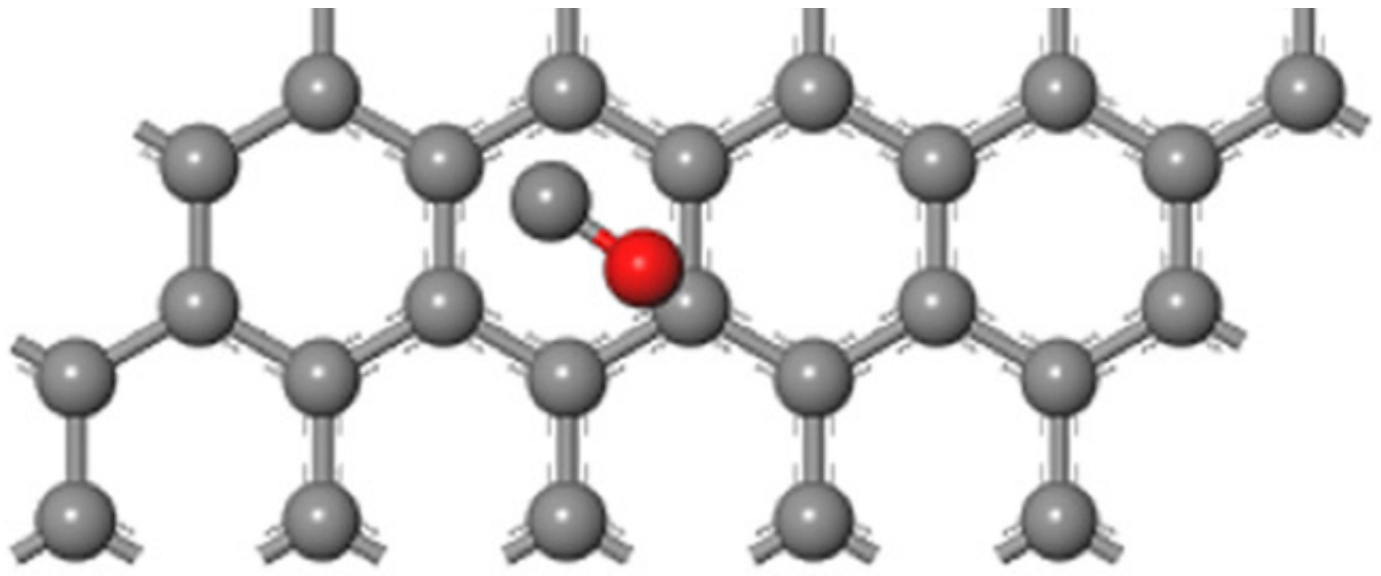

P.L. Silvestrelli and A. Ambrosetti, JCP 140, 124107 (2014).

Can we mix advanced functionals?

(meta-GGA) + (van der Waals) + (Hubbard *U*)

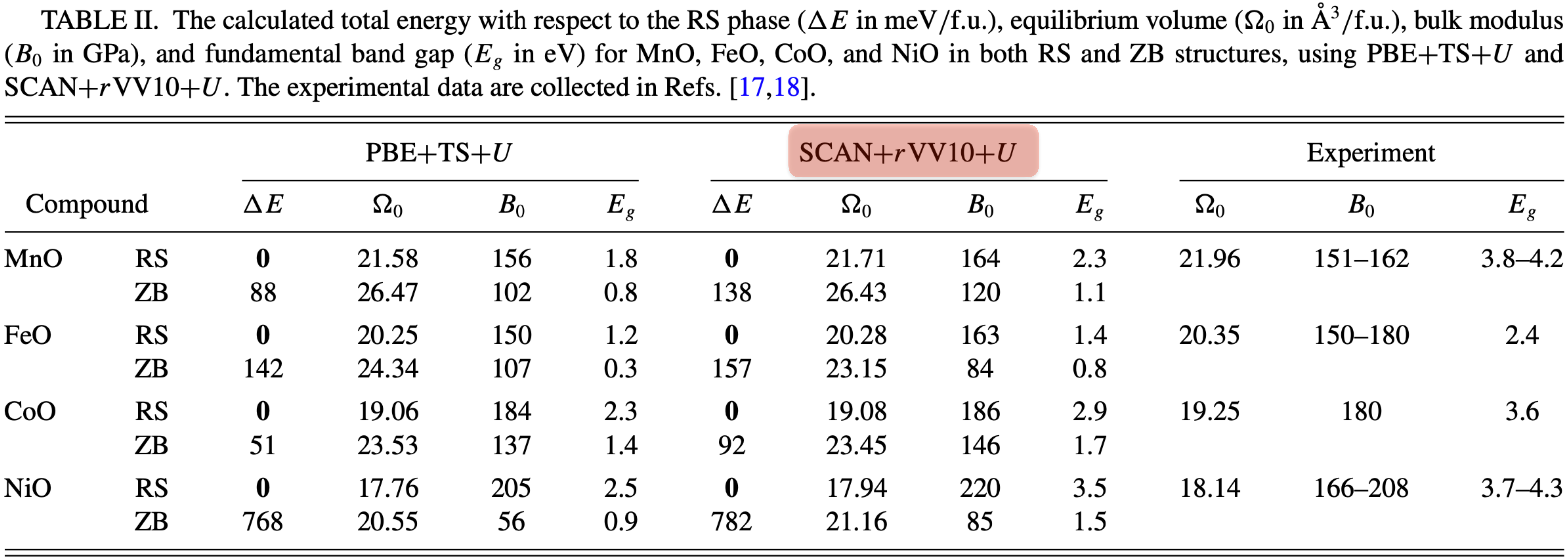

TABLE II. The calculated total energy with respect to the RS phase (ΔE in meV/f.u.), equilibrium volume (Ω_0 in Å^3/f.u.), bulk modulus (B_0 in GPa), and fundamental band gap (E_g in eV) for MnO, FeO, CoO, and NiO in both RS and ZB structures, using PBE+TS+U and SCAN+rVV10+U. The experimental data are collected in Refs. [17,18].

Compound		PBE+TS+U				SCAN+rVV10+U				Experiment		
		ΔE	Ω_0	B_0	E_g	ΔE	Ω_0	B_0	E_g	Ω_0	B_0	E_g
MnO	RS	**0**	21.58	156	1.8	**0**	21.71	164	2.3	21.96	151–162	3.8–4.2
	ZB	88	26.47	102	0.8	138	26.43	120	1.1			
FeO	RS	**0**	20.25	150	1.2	**0**	20.28	163	1.4	20.35	150–180	2.4
	ZB	142	24.34	107	0.3	157	23.15	84	0.8			
CoO	RS	**0**	19.06	184	2.3	**0**	19.08	186	2.9	19.25	180	3.6
	ZB	51	23.53	137	1.4	92	23.45	146	1.7			
NiO	RS	**0**	17.76	205	2.5	**0**	17.94	220	3.5	18.14	166–208	3.7–4.3
	ZB	768	20.55	56	0.9	782	21.16	85	1.5			

H. Peng and J. P. Perdew, PRB 96, 100101(R) (2017).